Functional analysis of DNA replication initiation

Marta Barbon

A thesis submitted to Imperial College London

for the degree of Doctor of Philosophy 2018

DNA replication group

Medical Research Council, London Institute of Medical Sciences

Imperial College London

Declaration of originality

I, Marta Barbon, declare that the work presented in this thesis is my own, unless indicated explicitly. Information derived from unpublished material or collaborations with colleagues are acknowledged in the text and a full bibliography of published data is provided.

Copyright Declaration

The copyright of this thesis rests with the author and is made available under a Creative Commons Attribution Non-Commercial No Derivatives licence. Researchers are free to copy, distribute or transmit the thesis on the condition that they attribute it, that they do not use it for commercial purposes and that they do not alter, transform or build upon it. For any reuse or redistribution, researchers must make clear to others the licence terms of this work.

Abstract

Initiation of DNA replication is highly conserved from yeast to human. A crucial factor during this process is the replicative helicase MCM2-7, a ring-shaped hetero-hexameric protein assembly, which unwinds DNA at the replication fork. In a multi-step process, ORC, Cdc6 and Cdt1 promote the loading of two MCM2-7 hexamer into a head-to-head double hexamer around double stranded DNA.

The recent cryo-EM structure of an ORC/Cdc6/Cdt1/MCM2-7 (OCCM) intermediate has revealed that the MCM2-7 hexamer and ORC/Cdc6 are connected by C-terminal winged helix domains (WHDs). However, how these WHDs function for helicase loading and MCM2-7 double-hexamer formation has been largely unknown. Using a combination of biochemical and structural approaches, we have investigated the function of the different Mcm C-termini during pre-RC formation.

In this study, we developed a new concept, explaining how distinct functions of the individual WHDs drive the multi-step pre-RC formation process. In particular, we discovered that the Mcm5 WHD serves as a key factor in order to signal helicase loading defects and to induce quality control during pre-RC formation. In addition, it was found that the Mcm5 WHD is also required for the OCCM to double hexamer transition. While exploring the Mcm7 WHD, we discovered new rules and requirements for ATP hydrolysis dependent Cdt1 release. Finally, we identified novel mechanism in CDK dependent control of helicase loading, which are important for genome stability. The work performed as part of this thesis has resulted in the discovery of several new mechanisms, which together provide fundamental insights into the function and regulation of the highly complex eukaryotic helicase loading process.

Table of Contents

Copyright Declaration 3

Abstract 4

Table of Contents 5

List of Figures 10

List of Tables 13

List of abbreviations 14

Acknowledgments 18

Chapter 1 - Introduction 20

1.1. Eukaryotic cell cycle and DNA regulation 21

1.2. Origin licensing: the pre-replicative complex formation 22

1.2.1. ORC/Cdc6 24

1.2.2. MCM2-7/Cdt1 24

1.2.3. ORC/Cdc6/Cdt1/MCM2-7 (OCCM) 25

1.2.4. ORC/Cdc6/MCM2-7 (OCM) 27

1.2.5. Double hexamer 28

1.3. ATP hydrolysis during pre-RC formation 30

1.3.1. MCM2-7 ATP hydrolysis 30

1.3.2. Orc1 and Cdc6 ATP hydrolysis 31

1.4. Regulation of pre-RC formation 33

1.5. Activation of the replicative helicase 34

1.6. Origin firing 36

1.7. Termination of DNA replication 37

1.8. Proteins involved in pre-RC formation 38

1.8.1. AAA+ proteins: structural architecture 38

1.8.2. The winged helix domain 40

1.8.3. ORC 42

1.8.4. Cdc6 44

1.8.5. Cdt1 45

1.8.6. MCM2-7 47

1.9. Origins of replication: the ARS element 53
1.10. Comparison of helicase loading in *E. coli* and eukaryotes 54
1.11. DNA replication and relevance for human health 55
1.11.1. Cancer diagnosis 55
1.11.2. MCM2-7 as a target for cancer therapy 56
1.11.3. Meier-Gorlin syndrome (MGS) 57
1.12. Summary and project aims 58

Chapter 2 - Materials and Methods 60
2.1. Materials 60
2.1.1. Solutions 60
2.1.2. Reagents 60
2.1.3. Plasmids 63
2.1.4. Yeast strains 65
2.1.5. Chromatography resins, columns and beads 71
2.1.6. Antibodies 72
2.1.7. Oligonucleotides 72
2.1.8. Yeast media 73
2.1.9. Bacterial competent cells 74
2.2. Molecular biology 74
2.2.1. Cloning 74
2.2.2. Mutagenesis 74
2.2.3. DNA precipitation 75
2.2.4. Phenol-chloroform DNA extraction 75
2.2.5. Plasmid DNA preparation 75
2.2.6. Agarose gel electrophoresis 76
2.3. Bacterial manipulations 76
2.3.1. Competent cells 76
2.3.2. Transformation 76
2.3.3. Cultures 77
2.3.4. Protein expression 77
2.4. Yeast manipulations 77
2.4.1. Competent cells 77
2.4.2. Strain construction 77
2.4.3. Transformation 77

2.4.4. Cultures and yeast growth 78
2.4.5. Dominant lethality assay (spotting assay) 78
2.4.6. Protein expression 78
2.4.7. Cell lysis 79
2.5. Protein purifications 79
2.6. Protein analysis 80
2.6.1. SDS-PAGE 80
2.6.2. Protein staining 81
2.6.3. Western blotting 81
2.6.4. ^{32}P visualisation 82
2.7. Bead-based helicase loading assay 82
2.7.1. Origin DNA amplification 82
2.7.2. Conjugation of origin DNA to magnetic beads 82
2.7.3. *In vitro* reconstitution of MCM loading (pre-RC assay) 83
2.8. Immuno-precipitations 85
2.9. MCM2-7 immuno-precipitation assay 85
2.10. ATPase assay 86
2.11. Single particle Electron Microscopy 87
2.11.1. Samples preparation 87
2.11.2. Grids preparation (negative staining) 87
2.12. Statistical analysis 87

Chapter 3 - Function of the Mcm5 carboxyl-terminus during pre-RC 88
3.1. Introduction 88
3.2. The Mcm5 C-terminus is essential for double hexamer formation and for cell viability 89
3.3. Cdt1 is required for OCM complex assembly with MCM2-7ΔC5 93
3.4. Both hexamers require a functional Mcm5 C-terminus 94
3.5. The MCM5 C-terminus is not required for insertion of DNA into the MCM2-7 ring 96
3.6. The MCM5 C-terminus role in the transition from OCCM to OCM 99
3.7. The MCM5 C-terminus in the transition from OCM to double hexamer 101
3.8. WT and MCM2-7ΔC5 complexes exhibit similar pre-RC induced ATPase activity 103

3.9. Generation of an MCM2-7 construct with protease-inducible C-terminus cleavage 107
3.10. Discussion 117

Chapter 4 - Understanding the mechanism of the Mcm5 carboxyl-terminal domain 121
4.1. Introduction 121
4.2. Mcm5C contains a winged helix domain 124
4.3. Domain swap mutants 127
4.4. ATPase activity of domain swapped complexes 131
4.5. Double deletion mutants 133
4.6. Mutation of the linker region in the Mcm5C 137
4.7. Rationale for the design of point mutant constructs 143
4.8. Point mutations in Mcm5C affects helicase loading 147
4.9. ATPase activity of the point mutants 155
4.10. CDK regulation of the helicase loading 161
4.11. Discussion 164

Chapter 5 - Understanding the role of the C-termini of Mcm2, Mcm4 and Mcm7 173
5.1. Introduction 173
5.2. *In vivo* characterisation of the Mcm C-termini 174
5.3. *In vitro* functional analysis of the deletion mutants 176
5.4. MCM2-7ΔC2 181
5.5. MCM2-7ΔC7 183
5.6. OCCM WT and OCCMΔC7 187
5.6.1. WT OCCM 187
5.6.2. OCCMΔC7 192
5.7. MCM2-7ΔC6-ΔC7 196
5.8. Discussion 199

Chapter 6 - Progresses towards the high resolution structure of OCM 203
6.1. Electron microscopy 203
6.2. Introduction 208
6.3. The OCM is a short-living intermediate 210
6.4. The OCM can be assembled at low temperatures 214

6.5. An OCM can be assembled on short DNA 218
6.6. Negative stain analysis of the OCM on a short DNA 224
6.7. Discussion 227

Chapter 7 - Discussion and conclusions 230
7.1. The function of the Mcm5C during initiation of DNA replication 231
7.2. The role of the other MCM2-7 C-termini 237
7.3. The C-termini in S phase 242
7.4. A new concept for the MCM2-7 WHDs 243
7.5. CDK as a negative regulator of DNA replication 247
7.6. The role of MCM C-termini beyond DNA replication 250
7.7. The OCM 251
7.8. Final remarks 252

References 254

List of Figures

Figure 1.1. Schematic representation of MCM2-7 helicase loading 23

Figure 1.2. MCM2-7 protein interactions in the context of OCCM 27

Figure 1.3. The cell cycle regulation of replication initiation 36

Figure 1.4. The organisation of AAA+ domain. 40

Figure 1.5. Schematic representation of the winged helix domain 42

Figure 1.6. Schematic representation of S. cerevisiae and H. sapiens Cdt1 47

Figure 1.7. The MCM2-7 replicative helicase 48

Figure 1.8. MCM2-7 protein interactions 49

Figure 1.9. Comparison of the overall structures of the Mcm2-7 in different replication complexes. 53

Figure 2.1. Schematic representation of *in vitro* reconstitution of pre-RC 85

Figure 2.2. ATPase assay 87

Figure 3.1. Purification MCM2-7ΔC5 from *S.cerevisiae* 90

Figure 3.2. In *vitro* and *in vivo* test of MCM2-7ΔC5 activity 92

Figure 3.3. Analysis of the effect of Cdt1 on pre-RC formation in the presence of MCM2-7ΔC5 93

Figure 3.4. Analysis of pre-RC assembly in the presence of MCM2-7 WT and soluble Mcm5 C-terminus 95

Figure 3.5. DNA is inserted into the MCM2-7ΔC5 ring 96

Figure 3.6. MCM2-7ΔC5 mutant does not affect helicase loading 99

Figure 3.7. MCM2-7ΔC5 forms a stable OCM complex 100

Figure 3.8. MCM7ΔC5 is not able to recruit a second hexamer 103

Figure 3.9. The ATP-hydrolysis produced by MCM2-7ΔC5 is similar to the MCM2-7 wild type 104

Figure 3.10. Down-regulation of Cdc6-induced ATP hydrolysis is required for OCM stability in MCM2-7ΔC5 107

Figure 3.11. Design of cleavable MCM2-7 constructs 109

Figure 3.12. *In vivo* and *in vitro* activity of the cleavable MCM2-7 proteins ... 112

Figure 3.13. Test the accessibility of the cleavage sites 112

Figure 3.14. Test the accessibility of the cleavage sites in the contest of MCM2-7, OCCM and OCM using the cleavable MCM2-7-3XPreScission construct. 114

Figure 3.15. Test the accessibility of the cleavage site in the double hexamer complex. 116

Figure 3.16. Model for the Mcm5C-induced quality control mechanism during pre-RC formation 120

Figure 4.1. The C-terminus of Mcm5 contains a winged helix domain..... 123

Figure 4.2. The Mcm5-Mcm2 gate 123

Figure 4.3. The C-terminus of Mcm5 contains a winged helix domain..... 127

Figure 4.4. Sequence alignment and structural representation of the Mcm5 domain swap mutants..... 128

Figure 4.5. Test for in vivo dominant lethality and in vitro preRC activity of the Mcm5-domain swap..... 130

Figure 4.6. Analysis of the ATPase activity of the Mcm2-7 domain swapped. 132

Figure 4.7. In vivo assay of the double deletion mutants 133

Figure 4.8. Purifications of MCM2-7ΔC5-ΔC4, MCM2-7ΔC5-ΔC6, MCM2-7ΔC5-ΔC7..... 136

Figure 4.9. *In vitro* activity of the double deletion mutants of MCM2-7 136

Figure 4.10. Design of the Mcm5C linker mutants 138

Figure 4.11. Analysis of the linker mutants *in vivo* and *in vitro*..... 140

Figure 4.12. Analysis of ATPase activity of the linker mutants in Mcm5C 142

Figure 4.13. Position of WHD5 and Orc3 in the context of the OCCM..... 143

Figure 4.14. Double and triple point mutations in Mcm5 C-terminus 145

Figure 4.15. Combination of point mutations in Mcm5 C-terminus 146

Figure 4.16. *In vivo* dominant lethality test of the point mutants 148

Figure 4.17. Purification of Mcm5C point mutants 150

Figure 4.18. Purified Mcm5C point mutants..... 150

Figure 4.19. *In vitro* assay to test the activity of the mutants 153

Figure 4.20. *In vitro* assay to test the activity of the mutants Mcm5-8 and Mcm5-9..... 154

Figure 4.21. ATPase activity of Mcm5-1, Mcm5-2, Mcm5-3 159

Figure 4.22. Analysis of ATPase activity of the mutants Mcm5-8 and Mcm5-9 160

Figure 4.23. CDK regulation of helicase loading. 164
Figure 4.24. Model for Mcm5C-induced quality control pathway. 171
Figure 4.25. Model for the mechanisms of CDK-phosphorylated ORC during pre-RC formation 172
Figure 5.1. Design of the MCM2-7 deletion mutants 174
Figure 5.2. In vivo analysis of the MCM2-7 deletion mutants 175
Figure 5.3. Purification of MCM2-7ΔC2 and MCM2-7ΔC7 from *S. cerevisiae* 177
Figure 5.4. *In vitro* test of MCM2-7ΔC activity 179
Figure 5.5. *In vitro* activity of the deletion mutants in the absence of Cdt1 180
Figure 5.6. MCM2-7ΔC2 182
Figure 5.7. *In vitro* activity of MCM2-7ΔC7 183
Figure 5.8. MCM2-7ΔC7 form a stable complex in the presence of ORC, Cdc6 and Cdt1. 185
Figure 5.9. Cdt1 binds to the ORC-Cdc6-MCM2-7ΔC7 complex 186
Figure 5.10. Structure of the ORC/Cdc6/MCM2-7/Cdt1 complex. 188
Figure 5.11. Effect of different salts on pre-RC formation 189
Figure 5.12. Cross-linking mass spectrometry 191
Figure 5.13. OCCMΔC7 194
Figure 5.14. ORC/Cdc6/MCM2-7ΔC7 in ATPγS. 196
Figure 5.15. MCM2-7ΔC6ΔC7 197
Figure 5.16. *In vitro* activity of the MCM2-7ΔC6ΔC7 199
Figure 6.1. A schematic workflow of the structure determination using single-particle EM. 204
Figure 6.2. Negative stain grid preparation 206
Figure 6.3. Cryo-EM grid preparation 207
Figure 6.4. Eukaryotic initiation of DNA replication 210
Figure 6.5. The OCM is a short-living intermediate. 211
Figure 6.6: Cross-linked reaction before the elution from the beads 213
Figure 6.7. OCM is formed at low temperatures 215
Figure 6.8 Temperature might help in increasing the homogeneity of the sample 216
Figure 6.9. DNaseI dilutions affect the length of the exposed DNA 218

Figure 6.10. Design of a new DNA containing replication origin 219
Figure 6.11. An OCM complex is formed on the 10XAB1 DNA 221
Figure 6.12. Cryo-EM analysis of OCM..... 222
Figure 6.13. 3D classification procedure 223
Figure 6.14 EM negative staining of the OCM complex assembled on 10XAB1 DNA 225
Figure 6.15. OCM in 10XAB1 cross-linked on beads..... 227
Figure 7.1. Model for Mcm5C-induced quality control pathway. 237
Figure 7.2. Model for Mcm5C-induced quality control pathway. 241
Figure 7.3. Molecular events mediated by the Mcm C-termini during the loading of the first Cdt1-bound Mcm2-7 hexamer by the ORC-Cdc6. 247

List of Tables

Table 2.1 List of Reagents 60
Table 2.2. List of pre-existing and new plasmid used in experiments described in the text. 63
Table 2.3. List of pre-existing and new yeast strains used in experiments 65
Table 2.4. List of columns used in the experiments described in this study..... 71
Table 2.5. List of antibodies used in the experiments described in this study... 72
Table 2.6. List of oligonucleotides used for PCR 72
Table 2.7. List of yeast media and their components used in this study 73
Table 4.1. Summary of the Mcm5C point mutants 154

List of abbreviations

A	Alanine
Abf1	ARS binding factor1
ACS	ARS1 consensus sequence
ARS1	Autonomous replication sequence
AAA+	ATPases associated with various cellular activities
ATP	Adenosine triphosphate
ATP γ S	Adenosine 5′-[γ-thio]triphosphate
ATR	Serine/threonine-protein kinase
BAH	Bromo adjacent homology
Bp	Base pairs
BS3	Bis(sulfosuccinimidyl)suberate
ChIP	Chromatin immunoprecipitation
Ci	Curie
CLMS	Cross-linking mass spectrometry
C-terminus	Carboxyl-terminus
Cdc45	Cell division cycle 45
Cdc6	Cell division cycle protein 6
CDK	Cyclin-dependent kinase
Cdt1	Cdc10-dependent transcription factor 1
CMG	Cdc45/MCM2-7/GINS complex
DDK	Dbf4-dependent kinase
DH	Double hexamer
DMSO	Dimethyl sulfoxide

DNA	Deoxyribonucleic acid
DNaseI	Deoxyribonuclease
Dpb11	DNA polymerase B possible subunit 11
dsDNA	Double stranded DNA
DTT	Dithiothreitol
D	Aspartic acid
E	Glutamic acid
E. coli	*Escherichia coli*
EDTA	Ethylenediaminetetraacetic acid
EM	Electron microscope
Fen1	Flap endonuclease 1
FRB	FKBP12-Rapamycin Binding domain of mTOR
FRET	Fluorescence Resonance Energy Transfer
G	Glycine
G1, G2	Gap (phase of the cell cycle)
GINS	Go ichi ni san
GST	Glutathione S-transferase
GTP	Guanosine-5'-triphosphate
HA	Haemagglutinin
HP1	Hetereochromatin protein 1
HS	High salt
IP	Immunoprecipitation
IPTG	Isopropyl β-D-1-thiogalactopyranoside
LB	Luria-Bertani broth
Leu	Leucine

LS	Low salt
µ	Micro
m	Milli or meter
M	Molar or Mitosis
MBP	Maltose-binding protein
MCM	Mini chromosome maintenance protein
MGS	Meyer-Gorlin syndrome
n	Nano
N	Asparagine
NaCl	Sodium chloride
N-terminus	Ammino-terminus
NMR	nuclear magnetic resonance
OCCM	ORC/Cdc6/Cdt1/MCM2-7
OCM	ORC/Cdc6 /MCM2-7
OD600	Optical density at 600 nm
ORC	Origin recognition complex
PAGE	Polyacrylamide gel electrophoresis
PCNA	Proliferating cell nuclear antigen
PCR	Polymerase chain reaction
P-ORC	Phosphorylated ORC
PEG	Polyethylene glycol
Pre-RC	Pre-Replication complex
Q	Glutamine
R	Arginine
RFC	Replication factor C

Rpm	Revolutions per minute
SDS	Sodium dodecyl sulphate
S	Synthesis (phase of the cell cycle)
S. cerevisiae	*Saccharomyces cerevisiae*
S. pombe	*Saccharomyces pombe*
SC	Synthetic complete
ssDNA	Single stranded DNA
T	Thymine
TBS-T	Tris-buffered saline with Tween 20
TEV	Tobacco Etch Virus
Trp	Tryptophan
Ura	Uracil
v/v	Volume in volume
w/v	Weight in volume
wt	Wild type
WHD	Winged helix domain

Acknowledgments

I would like to thank my supervisor, Prof Christian Speck for allowing me to do my PhD in his group. Thank you for your support and guidance in all aspects of this work. Thank you for your patience and for your encouragements throughout these exciting and challenging four years.

I would also like to thank Indiana, for efficient technical assistance. Thanks to all present and former members of the DNA replication group, for interesting discussions and technical support. A special thanks to Noelia, for being a good friend and good colleague: thank you for your constant support, critical discussions and good laughs.

I would like to thank the collaborating groups, especially the lab of Dr Huilin Li for the cryo-EM analysis of the OCCM variants. A big thank you also to Dr Ricardo Aramayo, EM facility manager at the LMS, for the amazing help with image acquisition and data analysis of the OCM.

I would like to thank my academic mentors, Dr Till Bartke, Dr Naveenan Navaratnam and Prof David Rueda for support, discussions and for the assessment of this work throughout the four years.

Thank you to Dr Wayne Mitchell, for introducing me to teaching at the university as a graduate teaching assistant.

Thank you to Raquel and Theresa for being the best housemates one could ever wish to have and very good friends. It has been a great adventure and I am glad I have shared it with you.

Il mio piu grande grazie và a Mamma e Papà, perchè senza di voi nulla sarebbe stato possible. Grazie per il vostro costante supporto, pazienza e amore, e infine per il vostro aiuto durante la scrittura di questa tesi. Grazie anche ai miei fratelli Emanuela e Stefano e loro famiglie, ai miei zii e zie che mi han sostenuto lungo questo percorso, nonostante la distanza.

(My biggest thanks goes to my parents, because without you none of the achievements of my life would have been possible. Thanks for the constant support, love and patience and for ultimately helping during the writing of this

work. Thanks to my brother and sister and their families, my aunts and uncles, you all have been for me a great support during these years, despite the distances.)

A really huge thanks to Robin, for the wonderful support and for the critical discussions and revisions.

This thesis is dedicated to the loving memory of my grandparents, especially to my grandmother Emma, who suddenly passed away only few months ago.

Nonna, you have been and will always be my strength.

Questa tesi è dedicata alla memoria dei miei nonni, in particolare a mia nonna Emma, che è improvvisamente mancata pochi mesi fa.

Nonna, sei sempre stata e sempre sarai la mia forza.

Chapter 1 - Introduction

All living cells need to replicate their genetic material prior to their division in order to maintain genomic stability. This is a sophisticated process, which is under the control of many different proteins and enzymes. The multi-protein apparatus, called replisome, includes a helicase to unwind the double-stranded DNA, a polymerases to synthesise new strands of DNA and a clamp loader to recruit the sliding clamp on DNA. These machines have the role of ensuring that every piece of the genome becomes replicated only once per cell cycle. The replisome is assembled in a controlled manner at specific chromosomal regions called origins of DNA replication (Leonard and Mechali, 2013). It proceeds in three enzymatically catalysed and coordinated steps: initiation, elongation and termination. The basic mechanisms are conserved among the three domains of life (bacteria, archaea, eukaryotes) (O'Donnell et al., 2013).

The following introduction will focus on the mechanisms of the helicase loading onto origins of replication in the budding yeast *Saccharomyces cerevisiae (S. cerevisiae)*, which has been used as a model in the field of eukaryotic DNA replication for many reasons. First of all, unlike other species, its origin of replication has been isolated, the sequence identified and genetically characterised (Marahrens and Stillman, 1992; Stinchcomb et al., 1979; Struhl et al., 1979). Secondly, the well understood cell cycle and the easy genetic manipulation of the organism facilitated a large number of *in vivo* studies. More recently, the *in vitro* reconstitution of the budding yeast helicase loading using purified proteins has allowed the mechanistic and structural analysis of this process (Evrin et al., 2009; Remus et al., 2009; Yeeles et al., 2015; Yeeles et al., 2017). In parallel, single molecule and structural biology have started to provide an important contribution towards the understanding of DNA replication (Georgescu et al., 2017; Li et al., 2018; Li et al., 2015; Noguchi et al., 2017; Sun et al., 2013; Sun et al., 2014; Ticau et al., 2017; Ticau et al., 2015; Yeeles et al., 2015; Yeeles et al., 2017; Yuan et al., 2017; Zhai et al., 2017a).

1.1. Eukaryotic cell cycle and DNA regulation

Two of the most important characteristics of eukaryotic cells are bidirectional DNA replication and multiple origins on chromosomes (Cairns, 1966; Huberman and Riggs, 1966, 1968). Eukaryotic genomes are larger than prokaryotic ones but their replication rate is still very high. The reason of that is the high number of origins that are equally distributed over the chromosomes. Budding yeast starts the replication of its DNA from 250-400 origins (Mechali, 2001) distributed over 16 chromosomes, whereas *Escherichia coli* (*E. coli)* contains only a single origin which is responsible for the replication of the whole genome.

The first model of DNA replication was suggested by Jacob, Brenner and Cuzin (Jacob and Brenner, 1963) with the "replicon model", based on *E. coli* studies. They suggested that a DNA sequence ("the replicator") is the target for a protein ("the initiator") to start the replication. However, we now know that the replication of DNA is a much more complex process, involving several proteins and many biochemical events. In addition, replication origins are tightly regulated to ensure a faithful process. Indeed, the stability of the genome is dependent upon each origin being fired once and only once per cell cycle (Siddiqui et al., 2013). Re-replication of the same origin has been reported to be responsible for gene amplification ultimately associated with cancers (Green et al., 2010).

The eukaryotic cell cycle is composed of four phases: G1, S, G2 and mitosis. The cells replicate their genome during the S phase and they divide during mitosis. The G1 and G2 are phases in which the cell produces proteins needed for replication and mitosis, respectively. The cell cycle progression is under a control of checkpoints, ensuring a mechanism of quality control of its genetic material. The duration of the cell cycle varies among cells, and in budding yeast lasts approximately 90 minutes.

Initiation of DNA replication is divided into two temporally distinct steps (Diffley et al., 1994; Siddiqui et al., 2013). First, in the G1 phase of the cell cycle, the core of the replicative helicase Mini chromosome maintenance protein 2-7 (MCM2-7) is loaded onto DNA forming the pre-replicative complex (pre-RC). This step is referred as "origin licensing" (Blow and Laskey, 1988) and MCM2-7

is encircling double stranded (ds) DNA (Evrin et al., 2009; Remus et al., 2009). Unlike bacteria, where the helicase is loaded in an active form, the MCM2-7 complex at this stage is inactive. In S phase, “origin firing” involves the activation of MCM2-7 by a number of factors and two S-phase kinases. Thus, the helicase undergoes a structural rearrangement that promotes the assembly of Cdc45-MCM2-7-GINS complex (CMG), which represents the active helicase (Gambus et al., 2006; Moyer et al., 2006). In this complex, MCM2-7 is encircling single stranded (ss) DNA. In the S-phase, helicases are activated but pre-RC assembly is inhibited preventing re-replication and ensuring that each origin is used only once per cell cycle. Importantly, at each cell cycle a large number of MCM2-7 become loaded on DNA but only few of them become activated. The excess of inactive MCMs functions as a “dormant origins” representing a pool of backup helicases that can become activated in the case of stalling of the replication fork under DNA replication damage (Ibarra et al., 2008; Woodward et al., 2006).

1.2. Origin licensing: the pre-replicative complex formation

Eukaryotic replication licensing is completed when the helicase MCM2-7 is loaded onto dsDNA in a stable head-to-head double hexamer (Evrin et al., 2009; Gambus et al., 2011; Remus et al., 2009; Riera et al., 2014). This is achieved when single MCM2-7 hexamer chaperoned by Cdt1 is loaded onto DNA complexed with the origin recognition complex (ORC) and Cdc6. Pre-RC formation requires the repeated loading of single MCM2-7 at each origin (Bowers et al., 2004; Edwards et al., 2002). Structural characterisation of multiple intermediates are revealing the stepwise process that involves several pre-RC factors (Figure 1.1). Furthermore, the recent *in vitro* reconstitution of budding yeast DNA replication initiation (Yeeles et al., 2015) has made the analysis of the steps after pre-RC formation possible.

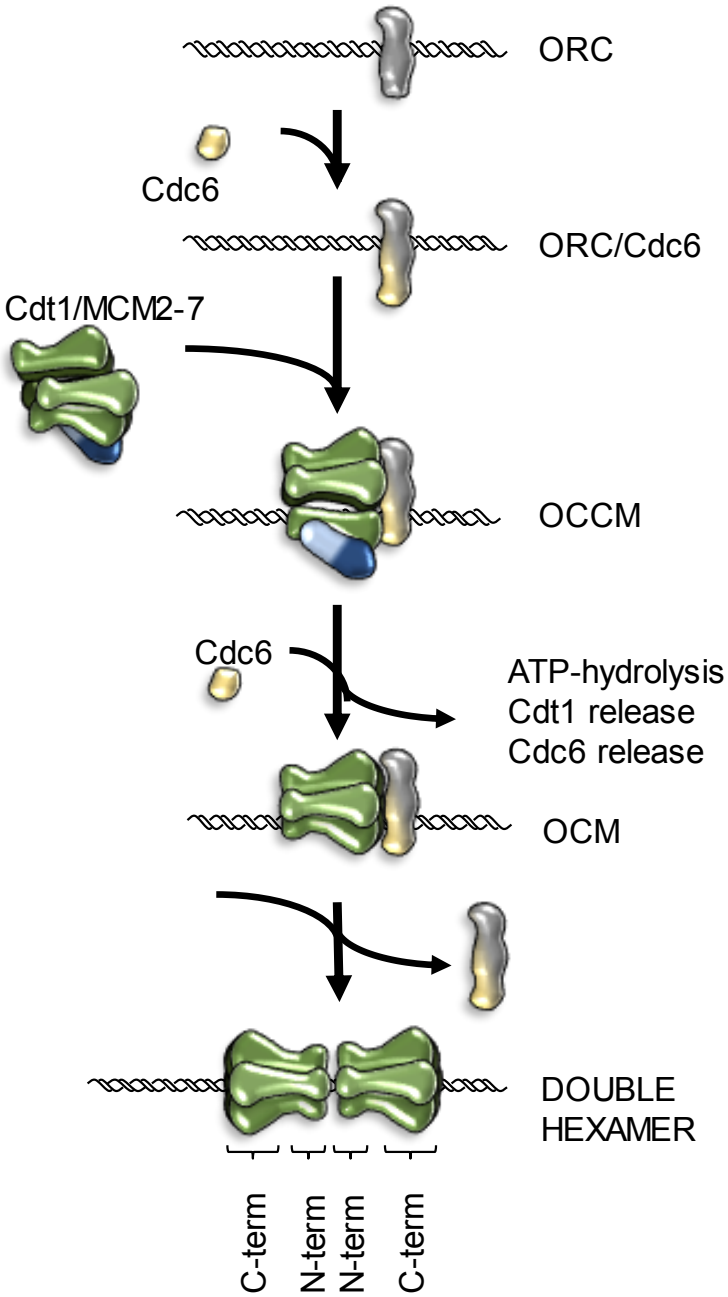


Figure 1.1. Schematic representation of MCM2-7 helicase loading

ORC binds to replication origin and recruits Cdc6 forming a ring-shape complex around the DNA (ORC/Cdc6). The spiral open ring MCM2-7/Cdt1 bind ORC/Cdc6 and form the intermediate ORC/Cdc6/Cdt1/MCM2-7 (OCCM). Upon ATP hydrolysis, Cdc6 and Cdt1 are released, and a second Cdc6 molecule binds ORC and MCM2-7 forming a complex called ORC/Cdc6/MCM2-7 (OCM). The binding of a second MCM2-7 conformation generates a head-to-head double hexamer loaded on DNA. Adapted from (Riera et al., 2014).

1.2.1. ORC/Cdc6

The first step in helicase loading is binding of ORC to origin DNA. Several low resolution structures of *Drosophila* ORC (Bleichert et al., 2013) and *S. cerevisiae* ORC (Speck et al., 2005) were reported but they showed different conformations. Recently, high resolution structures of apoORC (no DNA) from *Drosophila* (Bleichert et al., 2015) and *S. cerevisiae* DNA-ORC (Li et al., 2018) become available. Both structures showed a subunit order of Orc1-Orc4-Orc5-Orc3-Orc2 arranged in a ring with a gap between Orc1 and Orc2. This is consistent with the direct interaction observed between Cdc6 and Orc1 (Sun et al., 2013; Sun et al., 2012; Wang et al., 1999).

ORC/Cdc6 represents the initiator of DNA replication at origins. In the absence of DNA, ORC-Cdc6 complex formation can only be observed in the presence of a slowly hydrolysable ATP analogue (ATPγS) but not with ATP suggesting that ATP hydrolysis regulates complex stability (Speck et al., 2005). In the same study, a low resolution electron microscopy structure of ORC/Cdc6 in the presence of ATPγS was reported. The binding of Cdc6 to ORC produced a closed ring shape with a large central cavity. More recent work showed a 2D cryo - electron microscope (cryo-EM) classification of a *Drosophila* ORC/Cdc6 complex in the presence of DNA, where DNA appears to be bent (Bleichert et al., 2018).

1.2.2. MCM2-7/Cdt1

Biochemical and structural analysis have revealed that in the absence of ATP, the six subunits MCM2-7 complex adopts an “open-ring” architecture with a “gate” between the Mcm2 and Mcm5 subunits (Bochman and Schwacha, 2008; Costa et al., 2011). A recent high resolution structure of the MCM2-7/Cdt1 heptamer confirmed the six MCM2-7 subunits arrangement in a left-handed helical conformation with a gap between Mcm2 and Mcm5 (Zhai et al., 2017a). Interestingly, the size of the gap is too narrow (10-15 Å) to allow dsDNA entry, which suggests that further conformational changes need to take place in order to widen the Mcm2/5 gate and allow DNA insertion. Furthermore, the winged helix domains (WHD) of Mcm5 and Mcm4 are located in the central

channel blocking DNA entry (further discussed in 1.8.6). Indeed, MCM2-7/Cdt1 does not bind DNA on its own (Bowers et al., 2004; Coster et al., 2014; Evrin et al., 2009; Frigola et al., 2013; Kang et al., 2014; Remus et al., 2009). Even though only part of Cdt1 was resolved in this complex, it was suggested that Cdt1 might contribute to the stabilisation of inter-subunit interactions within the MCM2-7. Cdt1 embraces half of the ring, making contacts with the N-terminal regions of Mcm2, Mcm6 and Mcm4, and forming a tight complex, which helps in maintaining the structural integrity of the MCM2-7 complex (Frigola et al., 2013; Liu et al., 2012). Importantly, MCM2-7 cannot be recruited by ORC/Cdc6/DNA in the absence of Cdt1 (Evrin et al., 2009; Fernandez-Cid et al., 2013; Randell et al., 2006).

1.2.3. ORC/Cdc6/Cdt1/MCM2-7 (OCCM)

The first step of the loading reaction is the recruitment of the helicase MCM2-7 onto DNA origins. Cdt1 escorts the open MCM2-7 ring to the ORC/Cdc6 bound to origin DNA in order to form an ORC/Cdc6/Cdt1/MCM2-7 (OCCM) complex. In the absence of Cdt1, MCM2-7 hexamers fail to load on DNA (Chen and Bell, 2011). *In vitro* experiments provided the molecular mechanism for this observation (Fernandez-Cid et al., 2013). This is due to the presence of an auto-inhibitory domain in the Mcm6 C-terminus (Mcm6C) that prevents binding of MCM2-7 to ORC/Cdc6. Indeed, Cdt1 binding to MCM2-7 releases this inhibition. Moreover, in budding yeast it was shown that the same Mcm6C-Cdt1 interaction is essential for the nuclear import of the helicase. Mutations that prevent the formation of this interaction block MCM2-7 binding to chromatin (Tanaka and Diffley, 2002; Wu et al., 2012). *In vitro* studies of *S. cerevisiae* showed that MCM2-7 lacking Mcm6C (MCM2-7ΔC6) supported Cdt1 independent ORC/Cdc6 interaction with MCM2-7ΔC6, demonstrating that the Mcm6C contains an auto-inhibitory domain (Fernandez-Cid et al., 2013). However, this MCM2-7 variant did not support the formation of salt-stable double hexamer, since ATP hydrolysis is not induced and Cdt1 not released. Thus, Mcm6C plays three roles, one for nuclear import, one to regulate auto inhibition and one to induce ATP-hydrolysis.

A direct interaction between Cdt1 and Orc6 was also reported and it was suggested that dynamic binding of Cdt1 with ORC is important for repetitive MCM2-7 loading at origins. Orc6 contains two binding sites for Cdt1 (Chen et al., 2007) and cyclin-dependent kinase (CDK) phosphorylation of the N-terminus of Orc6 inhibits pre-RC formation (Chen and Bell, 2011; Nguyen et al., 2001).

Employing purified proteins in an *in vitro* pre-RC assembly system, ORC/Cdc6 and MCM2-7/Cdt1 were shown to rapidly assemble on DNA in an ATP hydrolysis independent manner forming an OCCM complex (Evrin et al., 2013; Fernandez-Cid et al., 2013; Sun et al., 2013; Yuan et al., 2017). This protein complex is a short-living intermediate but can be isolated in the presence of ATPγS. The strategy has been used to obtain cryo-EM structures of this 14 proteins complex (Sun et al., 2013; Yuan et al., 2017). Structural information and biochemical experiments showed that in the OCCM only one MCM2-7 hexamer is present and that the MCM2-7 spiral becomes transformed into a nearly closed planar ring (Ticau et al., 2015; Yuan et al., 2017). Importantly, dsDNA is already inside the central channel of MCM2-7, although the Mcm2/5 interface remains partially open (Sun et al., 2013; Yuan et al., 2017). Within the OCCM, Cdt1 interactions with the Mcm2, Mcm4 and Mcm6 subunits may keep Mcm2/5 at the N-terminal interface open. Indeed, from cryo-EM and Fluorescence Resonance Energy Transfer (FRET) studies, it was suggested that the helicase ring is only partially closed in the OCCM, since the sealing of the Mcm2/5 gate requires ATP hydrolysis and Cdt1 release (Ticau et al., 2017). The cryo-EM structure of the OCCM revealed that ORC/Cdc6 and MCM2-7/Cdt1 are tethered together using flexible links. Major players in these connections are the Mcm C-termini which contain flexible linkers and WHDs, which latch onto ORC/Cdc6. Importantly, the C-termini of Mcm2, Mcm6 and Mcm4 are connected directly to the WHDs of Orc5, Orc4 and Orc1, respectively. Although the functional relevance of these interactions has not been elucidated yet, a role in DNA loading has been suggested (Yuan et al., 2017) (Figure 1.2).

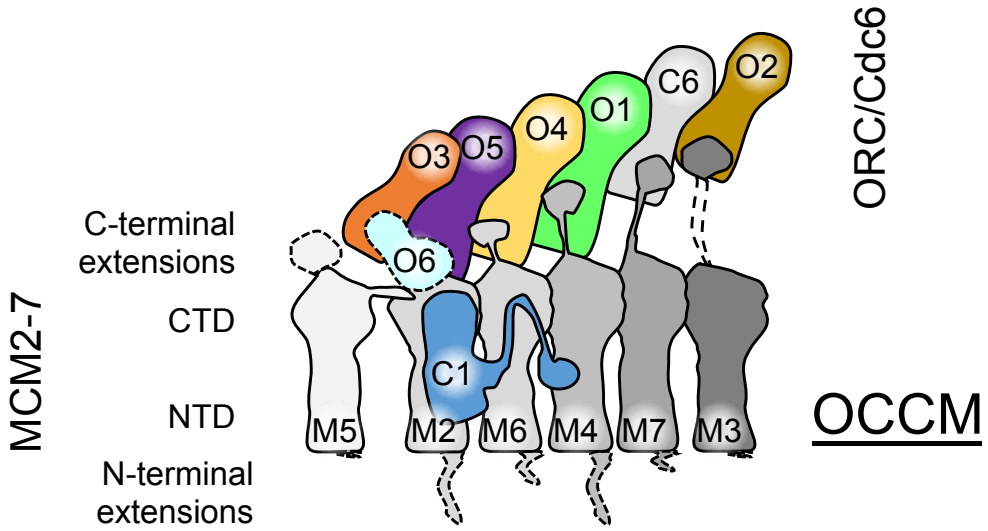


Figure 1.2. MCM2-7 protein interactions in the context of OCCM

Schematic representation of the protein-protein interactions between the Mcm subunits (in grey) and Orc subunits (Orc1 in green Orc2 in brown, Orc3 in salmon, Orc4 in cyan, Orc5 in purple, Orc6 in dark grey), Cdc6 (in pink) and Cdt1 (in blue) in the context of OCCM). The dot lines represents the regions of the structure that are not visible by cryo-EM (from Riera et al, 2017).

1.2.4. ORC/Cdc6/MCM2-7 (OCM)

After OCCM formation, ATP hydrolysis induces the release of Cdt1 and the formation of a complex containing a single copy of ORC, Cdc6 and MCM2-7 resulting in an ORC/Cdc6/MCM2-7 (OCM) (Fernandez-Cid et al., 2013; Randell et al., 2006). Recent single-molecule experiments showed that ATP hydrolysis is responsible also for Cdc6 release, which occurs prior to Cdt1 release (Ticau et al., 2015). The same study showed that another Cdc6 molecule is recruited to ORC/MCM2-7 forming a short-living OCM with the consequent full closure of the MCM2-7 ring. The rapid exchange between the bound and soluble states of both proteins suggests that they could be involved in multiple origin licensing events. The levels of Cdt1 and Cdc6 are tightly controlled during the cell cycle, perhaps to prevent inappropriate origin licensing.

Importantly, it was shown that Orc6, the smallest ORC subunit, is essential for OCM formation, since the Orc1-5 complex is able to support OCCM formation but fails during OCM formation (Fernandez-Cid et al., 2013; Frigola et al., 2013). Isolating the OCM complex has revealed to be challenging, since biochemical and EM experiments showed that after 7 minutes of ORC, Cdc6, MCM2-7/Cdt1 incubation with DNA, 75% of the particles appeared to be in the double hexameric state (Sun et al., 2014). Consequently, to date no 3D structures of this pre-RC intermediate have been obtained.

This transient and salt-sensitive pre-RC intermediate was shown to be competent for the recruitment of the second MCM2-7/Cdt1 heptamer (Fernandez-Cid et al., 2013). At present, the mechanism of binding of the second hexamer remains unknown. Several models have been suggested (Coster and Diffley, 2017; Riera et al., 2014; Zhai et al., 2017b). Here we describe the current state of knowledge. It was shown that both hexamers require an intact Mcm3 C-terminus (Mcm3C) for loading on DNA (Abid Ali et al., 2017; Frigola et al., 2013; Sun et al., 2013). Both hexamers are recruited in a Cdt1-dependent manner (Fernandez-Cid et al., 2013) in a head-to-head orientation to a single ORC. EM studies identified particles containing two hexamers bound to one ORC (Sun et al., 2014) and recent single molecule experiments demonstrated that one stable ORC is sufficient to load a double hexamer (Duzdevich et al., 2015; Ticau et al., 2015). Other evidence supports a model in which two ORC molecules are loading the two hexamers with the same mechanism explained above (Coster and Diffley, 2017). It remains to be established whether just one of these models applies to all origins or whether both mechanisms can function. It should be noted that different ORC concentration and different replication origins were used in both studies, parameters that could in part explain the divergent results.

1.2.5. Double hexamer

Although the mechanism of the second hexamer recruitment is not entirely clear, the final product of the loading reaction is the salt-resistant double hexamer. Ticau et al. showed that after recruitment of the double hexamers, ORC, Cdc6 and Cdt1 become sequentially released. Furthermore, ORC release

from the origin DNA is coordinated with the closure of the second MCM2-7 ring (Ticau et al., 2017). Recent high resolution cryo-EM structures of this stable complex confirmed previous observations related to the double hexamer conformation. These showed that the head-to-head hexamers interact via their N-termini, with the C-terminal domains of each MCM2-7 located at the opposite ends (Abid Ali et al., 2017; Li et al., 2015; Noguchi et al., 2017). Here, the MCM2-7 ring is arranged in a plane conformation with the Mcm2/5 gate closed around the dsDNA that passes through the central channel (Evrin et al., 2009; Remus et al., 2009). The cryo-EM structures showed that the two hexamers are tightly interconnected via their N-terminal zinc fingers domain. Interestingly, each of the six zinc fingers interacts in different ways generating a visible tilt and twist between the two hexamers (Abid Ali et al., 2017; Li et al., 2015; Noguchi et al., 2017; Remus et al., 2009). The tilted conformation of the MCM2-7 subunits resulted in structural changes in the arginine fingers of adjacent subunits. Indeed, the ATPase rate of the double hexamer is strongly reduced when compared with the single hexamer (Sun et al., 2014). In the apo-double hexamer (no DNA) all six sites of adenosine-nucleotide binding sites are occupied with ATP (Li et al., 2015). In contrast, in the dsDNA-double hexamer structures, the nucleotide was found only in two (Noguchi et al., 2017) or four (Abid Ali et al., 2017) ATP sites. These differences might be due to the different concentrations of ATP present in the buffers used in the three systems and different purification protocols.

Noguchi et al. showed that dsDNA is pressed against the N-tier of Mcm2 and Mcm5. They suggested that the interface between these two subunits, where the DNA passes through during helicase loading, might also be the site of DNA extrusion during helicase activation. Double hexamer bound to dsDNA revealed that DNA has a zig-zag conformation through the channel formed by the two hexamers, but it is not unwound (Abid Ali et al., 2017; Noguchi et al., 2017).

The MCM2-7 double hexamer has also been observed at licensed origins in *Xenopus* egg extracts (Gambus et al., 2011). It appears to be a stable complex since it tolerates gel filtration, DNaseI treatment or concentration steps (Evrin et al., 2009; Gambus et al., 2011; Noguchi et al., 2017). This complex can slide on DNA (Remus et al., 2009) but it unwinds DNA only after its activation in S-phase, with the recruitment of other factors.

1.3. ATP hydrolysis during pre-RC formation

1.3.1. MCM2-7 ATP hydrolysis

The use of MCM2-7 ATP binding and hydrolysis mutants has suggested that MCM2-7 binds and hydrolyses ATP during the pre-RC formation (Coster et al., 2014; Kang et al., 2014). The active ATPase sites are located at the interface between neighbouring subunits and ATPase activity is generated by the contribution of residues from both subunits (Davey et al., 2003). The inter-subunit nature of the active sites together with the ring shape allow cooperative interactions between ATP hydrolysis and DNA unwinding activities. According to this model, the introduction of a single ATP binding mutation into the MCM2-7 complex results in reduction of the ATPase activity of the entire protein and causes lethality in yeast (Coster et al., 2014; Schwacha and Bell, 2001). However, mutations in the different motifs of the ATPase domain (Walker A and B motif and arginine fingers) showed that individual ATPase sites of MCM subunits contribute differently to the overall MCM2-7 activity (Bochman and Schwacha, 2008, 2010). Mutations in the Walker A were reported to be lethal *in vivo* in yeast and failed to promote a salt resistant double hexamer *in vitro*. Only two mutations in the arginine finger were viable under restricted temperature conditions, but all of them showed defects in pre-RC assembly. The most severe defects were observed with Mcm5 and Mcm6 ATPase mutants, which blocked double hexamer formation or Cdt1 release *in vitro* (Coster et al., 2014; Kang et al., 2014). Additionally, mutations in the arginine fingers of Mcm2 and Mcm5 affected Cdt1 release (Coster et al., 2014), while in Mcm3 caused a reduction of the overall ATPase activity but supported a salt-stable double hexamer formation *in vitro* (Fernandez-Cid et al., 2013). These results suggested that different MCM subunits play different roles in ATP binding and hydrolysis.

MCM2-7 exhibits *in vitro* a low but robust ATP hydrolysis activity, which is suppressed when the double hexamer is assembled (Sun et al., 2014). Due to the inter-subunit location of the ATPase sites, it is possible that mutations in these regions affect the structural organisation of MCM2-7. Importantly, in the transition from the spiral-to-ring conformation, these mutations could interfere with the correct closing of the gate or with the ATP hydrolysis-dependent Cdt1

release. The cryo-EM of OCCM has provided further insights into the role of MCM2-7 ATP binding and hydrolysis during pre-RC formation. The ATP is present between the subunits Mcm3/7, Mcm7/4, Mcm4/6 and Mcm6/2, but was not found in the Mcm2/5 interface, consistent with the idea that it represents the gate for DNA entry and is partially open (Yuan et al., 2017). Interestingly, ATP can be found at all of the Mcm subunit interfaces in the double hexamer. However, a rearrangement in the arginine fingers is present as a consequence of the tilted conformation (Li et al., 2015; Noguchi et al., 2017). Furthermore, the ATPase activity was minimal in this protein complex (Sun et al., 2014).

1.3.2. Orc1 and Cdc6 ATP hydrolysis

In addition to MCM2-7, Orc1 and Cdc6 are active ATPases (Klemm et al., 1997; Perkins and Diffley, 1998; Randell et al., 2006). Mutational analysis of the ATPase motifs in both proteins have shown that these domains are essential for origin licensing in the *S. cerevisiae* ORC and Cdc6 (Bowers et al., 2004; Klemm and Bell, 2001; Perkins and Diffley, 1998; Weinreich and Stillman, 1999). Early studies of Orc1 and Cdc6 Walker B mutants caused dominant lethality in yeast and MCM2-7 loading defects (Klemm et al., 1997; Perkins and Diffley, 1998).

In budding yeast, ORC binds DNA in the presence of ATP (Bell and Dutta, 2002; Bell and Stillman, 1992; Klemm et al., 1997). Whilst Orc1-5 subunits belong to the AAA+ family (described in 4.1), only Orc1, Orc4 and Orc5 contain functional ATPase motifs but only Orc1 can hydrolyse the nucleotide (Klemm et al., 1997; Randell et al., 2006; Speck and Stillman, 2007). Orc1 ATPase activity is regulated in a DNA sequence specific manner, activated by an arginine residue of the adjacent Orc4 subunit (Klemm et al., 1997). A mutation in the Walker A motif of Orc1 that blocks ATP binding also affect ORC ability to bind DNA. An ORC complex containing a mutation in the arginine finger of Orc4 blocks Orc1 ATPase activity in the context of origin DNA and caused lethality in budding yeast (Bowers et al., 2004). Yet, this mutant can bind DNA and load MCM2-7 but cannot support repetitive rounds of helicase loading. An Orc1 Walker B mutant reduced pre-RC ATP hydrolysis and affected Cdt1 release and double hexamer formation. In summary, Orc1 ATP hydrolysis is dispensable for

the loading reaction (Coster et al., 2014; Evrin et al., 2013; Fernandez-Cid et al., 2013) and is required for the repeated MCM2-7 loading on origins (Bowers et al., 2004).

Cdc6 binds to ORC in the presence of DNA and ATP (Randell et al., 2006; Speck et al., 2005; Wang et al., 1999). A mutation of the conserved lysine 114 in the Walker A motif of human Cdc6 causes ATP binding and hydrolysis defects (Herbig et al., 1999). The corresponding mutant in *S. cerevisiae* is lethal *in vivo*, fails to load MCM2-7 onto chromatin (Perkins and Diffley, 1998; Speck et al., 2005) and cannot recruit or load MCM2-7 *in vitro* (Evrin et al., 2013). Cdc6 containing a mutation in the conserved glutamic acid in the Walker B (E224G) is lethal when overexpressed and failed in origin licensing *in vivo* (Perkins and Diffley, 1998). This mutant binds ATP but shows defect in hydrolysing it, which causes reduction in both Cdt1 release and MCM2-7 loading *in vitro* (Randell et al., 2006). The Cdc6-E224Q cause a stronger effect in yeast cell viability and also promoted MCM binding at origins *in vivo* but cells remained blocked in G1-phase (Chang et al., 2015).

Additionally, mutations in the Sensor 1 (N263A) and Sensor 2 (R332E) are associated with failure in MCM2-7 loading *in vivo* (Schepers and Diffley, 2001; Takahashi et al., 2002). Specifically, the sensor 1 mutant has a defect in ATP hydrolysis in complex with ORC (Speck and Stillman, 2007).

In the context of pre-RC, *S. cerevisiae* Cdc6 ATP hydrolysis was associated with functional assembly of MCM2-7 double hexamer. A point mutation in the Mcm3C activates ORC/Cdc6 ATPase activity, which promotes MCM2-7 release in the absence of Cdt1 (Frigola et al., 2013) suggesting a mechanism of quality control driven by ORC and Cdc6 ATP hydrolysis in the presence of unsuccessful loading reactions.

ATPase measurements showed that Cdc6 Sensor 1 and Walker B mutants reduced ATP hydrolysis significantly. These mutants interacted with ORC but led to poor MCM2-7 loading, since they affect the ability of Cdc6 to bind with ORC and therefore fail to promote efficient MCM2-7 loading (Evrin et al., 2013).

Cdc6 has been demonstrated to be responsible for ATP hydrolysis-dependent clearance of unsuccessfully loaded intermediates (Coster et al., 2014; Frigola et al., 2013; Kang et al., 2014). Although the removal mechanism is not yet

identified, Cdc6 ATPase activity is shown to be induced during pre-RC formation (Fernandez-Cid et al., 2013). In the presence of Cdc6 ATPase mutants, a mild Cdt1 release defect was observed (Fernandez-Cid et al., 2013; Kang et al., 2014; Randell et al., 2006). Furthermore, Cdc6 appears to be involved in the releasing of successfully loaded double hexamers from ORC, an event that is essential for the helicase activation (Chang et al., 2015). Cdc6 ATP hydrolysis is therefore required for disengagements from the pre-RC (OCM) after helicase loading to advance the progression in helicase activation.

A combination of Orc1 and Cdc6 ATPase mutants blocked Cdt1 release and MCM2-7 loading *in vitro* but these mutations on their own caused only a reduction in pre-RC induced ATP hydrolysis (Fernandez-Cid et al., 2013). From the results in this work, it was suggested that the pre-RC induced ATPase activity was generated by the combined activity of Orc1 and Cdc6. In light of the recent studies, the Cdc6 dependent part could reflect quality control occurring during the *in vitro* pre-RC reaction e.g. when pre-RC assembly occurs on the wrong DNA template.

The requirement for ATP binding by ORC and Cdc6 is believed to be conserved in metazoans. In *Xenopus* extract, ATP supports Cdc6 loading and Cdc6 induced ATP hydrolysis appears to be important for helicase loading (Frolova et al., 2002; Gillespie et al., 2001).

1.4. Regulation of pre-RC formation

Origin licensing and helicase loading is restricted to late M/G1 phase of the cell cycle, thus ensuring the genome duplication only occurs once per cell cycle (Arias and Walter, 2007; Symeonidou et al., 2012). It is essential that origin licensing does not occur in S phase, since this would result in re-replication events that destabilise the genome integrity. Helicase loading can be blocked in S phase by several mechanisms that vary among organisms.

In *S. cerevisiae,* a major way that a cell prevents re-replication is CDK-mediated phosphorylation of pre-RC components. CDK phosphorylation of Orc2 and Orc6 (Nguyen et al., 2001) is thought to prevent the interaction between Cdt1 and Orc6 (Chen and Bell, 2011), with consequent nuclear export of Cdt1 in G1 (Tanaka and Diffley, 2002) and inhibition of MCM2-7 loading. Cdc6

phosphorylated by CDK becomes degraded by the SCF-Cdc4 complex (Drury et al., 2000). CDK targets MCM2-7/Cdt1, which is exported from the nucleus, preventing its interactions with chromatin bound ORC/Cdc6 (Labib et al., 1999; Liku et al., 2005; Nguyen et al., 2001; Tanaka and Diffley, 2002).

In higher eukaryotes, the main target for regulation of origin licensing is Cdt1. In S and G2 phase, Cdt1 is bound by geminin, a nuclear protein present in high levels in S phase, inhibiting its binding with MCM2-7 and preventing re-replication in S-phase (Wohlschlegel et al., 2000). In *Saccharomyces pombe (S. pombe)* and other metazoan, Cdt1 levels are cell cycle-dependent and this protein is degraded during S-phase in two ways: (1) CDK phosphorylation, (2) Cullin4-based ubiquitin ligase and proliferating cell nuclear antigen (PCNA), a eukaryotic sliding clamp stimulating replicative DNA polymerases (Fujita, 2006). CDK phosphorylation of pre-RC components prevents re-replication in different ways. Cdc6 phosphorylated is exported from the nucleus (Saha et al., 1998) while ORC phosphorylated cannot bind to origin DNA during the G2 and M phases of the cell cycle (Siddiqui et al., 2013). Additionally, ubiquitylation and degradation of p21, a CDK inhibitor, prevents re-replication, since S-phase CDK phosphorylates Cdc6 which is exported from the nucleus (Kim and Kipreos, 2008). Finally, the checkpoint proteins Serine/Threonine protein kinase ATR and checkpoint kinase 1 also repress re-replication in normal cells (Liu et al., 2007).

1.5. Activation of the replicative helicase

The MCM2-7 double hexamer formed in the G1 phase of the cell cycle is inactive. In S phase, a small proportion of MCM2-7 becomes activated, while the remaining double hexamers serve as “dormant origins”, which are activated only in the case of replication stress (McIntosh and Blow, 2012). The activation of MCM2-7 helicase is dependent on the combined action of two protein kinases, Ddf4-depended kinase Cdc7 (DDK) and CDK (Figure 1.3).

In yeast, CDK phosphorylates Sld2 and Sld3, which then generates binding sites for Dpb11 (Tanaka et al., 2007; Zegerman and Diffley, 2007). The DDK phosphorylated double hexamer recruits Sld3 with its binding partner Sld7 (Tanaka et al., 2011) and Cdc45 to replication origins (Bruck and Kaplan, 2015;

Deegan and Diffley, 2016; Fang et al., 2016; Herrera et al., 2015). Mcm2, Mcm4 and Mcm6 contain specific Serine/Threonine at their N-terminal extensions that are phosphorylated by DDK once they are loaded on chromatin (Francis et al., 2009), promoting S-phase progression (Randell et al., 2010; Sheu and Stillman, 2006, 2010). Sld2, Dbp11 and the GINS (Go, Ichi, Nii, San: five, one, two, and three in Japanese) hetero-tetramer binds to Cdc45/Sld3/MCM2-7 with consequent release of Sld2, Sld3 and Dbp11. The resulting complex is called CMG and refers to the 11-subunit helicase (Cdc45/MCM2-7/GINS) (Ilves et al., 2010; Kanemaki and Labib, 2006; Yeeles et al., 2015).

Recent cryo-EM structures of *Drosophila* CMG (Abid Ali et al., 2016; Costa et al., 2011) and *S. cerevisiae* CMG (Georgescu et al., 2017; Sun et al., 2015; Yuan et al., 2016) have revealed the organisation of the proteins involved in the complex. However, how the double hexamer encircling dsDNA becomes rearranged into two CMG complexes encircling ssDNA is largely unknown. For the focus of this thesis, it is important to note that in the “apo” structure of CMG (without DNA) (Yuan et al., 2016), the WHD of Mcm5 (WHD5) is located in the central channel, pinned by the WHD of Mcm6 (WHD6). The central pore is occluded by these domains and is not wide enough to insert DNA. On the other hand, in the ssDNA-CMG structure, the WHD5 is no longer visible indicating its repositioning out of the central channel. The WHD6 moves away and the WHD of Mcm4 (WHD4) is now partially closing the channel. A comparison between the two different conformations revealed that in the presence of ssDNA, the C-tier ring of MCM2-7 undergo a horizontal movement towards the Cdc45 site of MCM2-7, while the N-tier and GINS/Cdc45 are in the same position.

MCM2-7 in complex with Cdc45 and GINS translocates along ssDNA (leading strand) but its orientation was initially uncertain. Recent studies of a reconstituted CMG using purified proteins suggested that the CMG translocates with the N tier ahead of the C tier (Douglas et al., 2018; Georgescu et al., 2017).

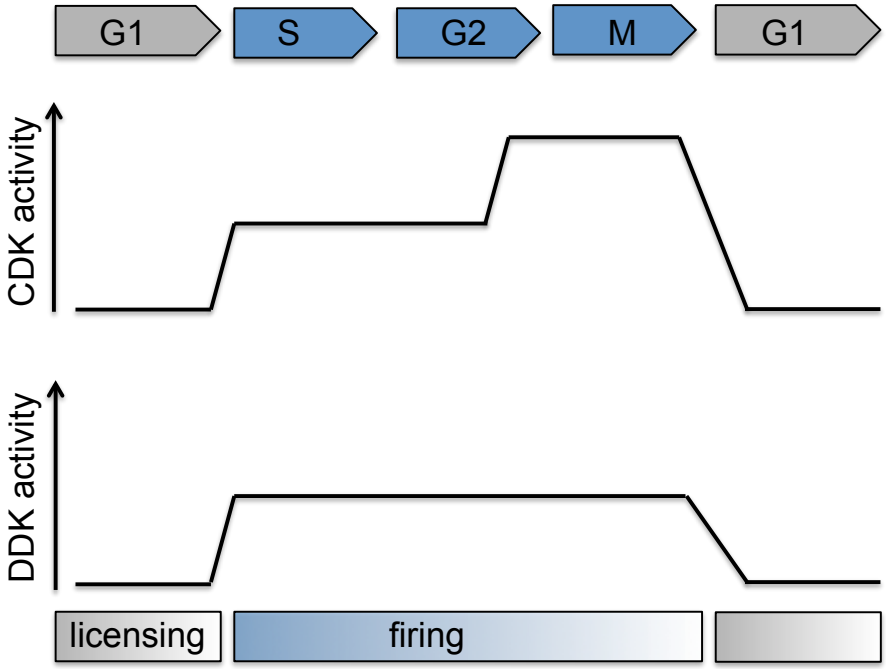


Figure 1.3. The cell cycle regulation of replication initiation

The two temporally distinct phases of the cell cycle, origin licensing and origin firing, are tightly linked to the cell cycle. Origin licensing occurs during late M/G1 phase, when the levels of CDK and DDK are low. The levels of both kinases rise from S phase to mitosis, when origins are fired.

1.6. Origin firing

Once the CMG is assembled, many other factors are recruited to origins to form the replisome (Gambus et al., 2006). Three polymerases participate in the eukaryotic DNA replication: polymerase α, ε and δ. Initial priming of DNA synthesis requires polymerase α, which generates short RNA primers that are required for DNA synthesis. Polymerase ε and δ are thought to be responsible for the leading and lagging strand, respectively (Burgers et al., 2016; Nick McElhinny et al., 2008; Pursell et al., 2007). However, polymerase δ also participates to the synthesis of the leading strand (Johnson et al., 2015), particularly during initiation of DNA replication and under replication stress in budding yeast (Pavlov et al., 2001; Yeeles et al., 2017). The EM structure of the CMG/polymerase ε complex showed that the polymerase is located on top of

the CMG, at the C-terminal AAA+ domains of Mcm2, Mcm5, Cdc45 and GINS ideally located to carry our leading strand synthesis (Sun et al., 2015).

Mcm10 is required for the recruitment of polymerase α and is important for CMG activation and DNA elongation travelling with the replisome, as a mutation in its C-terminus results in shorter replication products without affecting origin firing (Gambus et al., 2006; Looke et al., 2017).

A clamp loader, the pentameric replication factor C (RFC), binds to the RNA/DNA primer generated by the polymerase α and recruits the sliding clamp PCNA (proliferating cell nuclear antigen) (Moldovan et al., 2007; Yao and O'Donnell, 2012). The RCF-PCNA binding is ATP-dependent and ATP hydrolysis by RCF results in its release and in the closing of the PCNA rings loaded on DNA (Bowman et al., 2004). This process is reminiscent of the MCM2-7 recruitment by ORC/Cdc6, which binds in an ATP-dependent manner followed by ATP hydrolysis-dependent helicase loading. The CMG complex interacts directly with polymerase ε to enhance its activity, and this polymerase only uses a few sliding clamps since the synthesis of the leading strand occurs in a processive and uninterrupted manner (Pursell et al., 2007). On the other hand, polymerase δ does not interact directly with CMG, and uses several sliding clamps to synthesise multiple Okazaki fragments. Recent work showed that polymerase δ stimulated leading strand synthesis and could begin its synthesis before the faster CMG-polymerase ε takes over (Yeeles et al., 2017).

Once the synthesis of discontinuous Okazaki fragments is completed, polymerase δ exhibits a strand displacement synthesis activity, generating a 5' flap structure that is targeted by the sequential action of the flap endonuclease 1 (Fen1) and the nuclease/helicase Dna2 for the removal of the RNA/DNA primer downstream generated by polymerase α (Kang et al., 2000). The removal of these segments is essential for genome stability since polymerase α is not a high fidelity enzyme and does not have proofread activity. Finally, Okazaki fragments are joint together by ligase I.

1.7. Termination of DNA replication

The replication forks move on the chromatin and when two forks meet each other replication terminates. The replisome needs to disassemble from

chromatin to prevent the recruitment of further replication factors and to ensure cell cycle progression. While the correct mechanism of unloading of active helicase remains to be elucidated, experiments performed in *Xenopus* egg extracts showed that CMG complexes were released from the DNA once DNA replication is completed (Dewar et al., 2015).

The disassembly of the active CMG from chromatin is ubiquitylation-dependent (Bell, 2014; Maric et al., 2014; Moreno et al., 2014). Specifically, in budding yeast and frog, Mcm7 subunit was found to be poly-ubiquitylated with lysine 48 linked chains at the end of DNA replication. However, Mcm7 was not degraded by the proteasomes, but was extracted from chromatin by the p97/VCP/Cdc48 segregase. P97 is a ring-shaped protein, member of the AAA+ family and conserved among species (Maric et al., 2014; Moreno et al., 2014).

PCNA, the other ring shaped molecule bound to chromatin, should also be removed once DNA replication is terminated. Several studies suggest that a RFC-like complex is responsible for PCNA unloading (Kang et al., 2018). Importantly, the removal of PCNA is essential to ensure progression to G2/M phase. Delays in cell cycle progression are caused by inappropriate recruitment of replication proteins to PCNA, which is not being removed.

1.8. Proteins involved in pre-RC formation

1.8.1. AAA+ proteins: structural architecture

ORC, Cdc6 and MCM2-7 are part of the family of the ATPases associated with various cellular activities (AAA+) (Neuwald et al., 1999). The structural architecture of the ATP sites have common features. They contain a highly conserved 200-250 amino acid ATP-binding domain, with key elements essential for ATP binding and hydrolysis (Figure 1.4). One side of the active site contains the Walker A and B motifs, the sensor 1 and the arginine fingers, while the other side contains the sensor 2. The Walker A motif - GXXXXGK(T/S) where X stands for any amino acid – is responsible for the direct interaction with the β and γ phosphates of ATP. The Walker B motif is characterised by the sequence hhhD(D/E), where h stands for a hydrophobic amino acid followed by an aspartate or glutamate as terminal residue. The conserved glutamate

represents the catalytic site to activate a water molecule for nucleophilic attack on the γ phosphates of ATP during hydrolysis (Iyer et al., 2004). Through the coordination of Mg^{2+} and water molecules, this domain facilitates ATP hydrolysis. Mutations in the Walker B motif block ATP hydrolysis, but not its binding. Sensor 1, physically located between the Walker A and B motifs, is involved in ATP hydrolysis since mutations of residues in this domain impair the ATPase activity (Karata et al., 1999; Neuwald et al., 1999). At the other end of the Walker B are the arginine fingers, so named because of an analogous arginine first discovered in the Ras GTPase-activating proteins that are inserted into GTP-binding sites to promote hydrolysis (Scheffzek et al., 1997). Mutations of key residues in the arginine fingers are involved in arresting the ATP hydrolysis (Ogura et al., 2004). The sensor 2 motif is located on the "AAA+ lid" and is involved in binding and hydrolysis of ATP (Ogura et al., 2004). A hexameric architecture is often associated with AAA+ proteins, with the ATP-binding sites at the interface between subunits. Arginine fingers act *in trans*, which means that arginine fingers from one subunit constitute part of the nucleotide binding site of the adjacent subunit. This conformation allows interactions between the nucleotide-binding sites of adjacent subunits and coordination of ATP hydrolysis. Since most AAA+ proteins have a ring shape, structural changes in the ring can have profound impact on the overall ATPase activity of the entire complex. The ATP binding and/or hydrolysis leads to conformational changes in the AAA+ proteins, that are transmitted to the domains that are interacting with AAA+ domains. Therefore, a single non-functional ATPase site blocks the overall ATPase rate of the entire protein. These rearrangements seem to be responsible for the function of this class of proteins which are involved in assembly, movement or disassembly of protein machines (Neuwald et al., 1999).

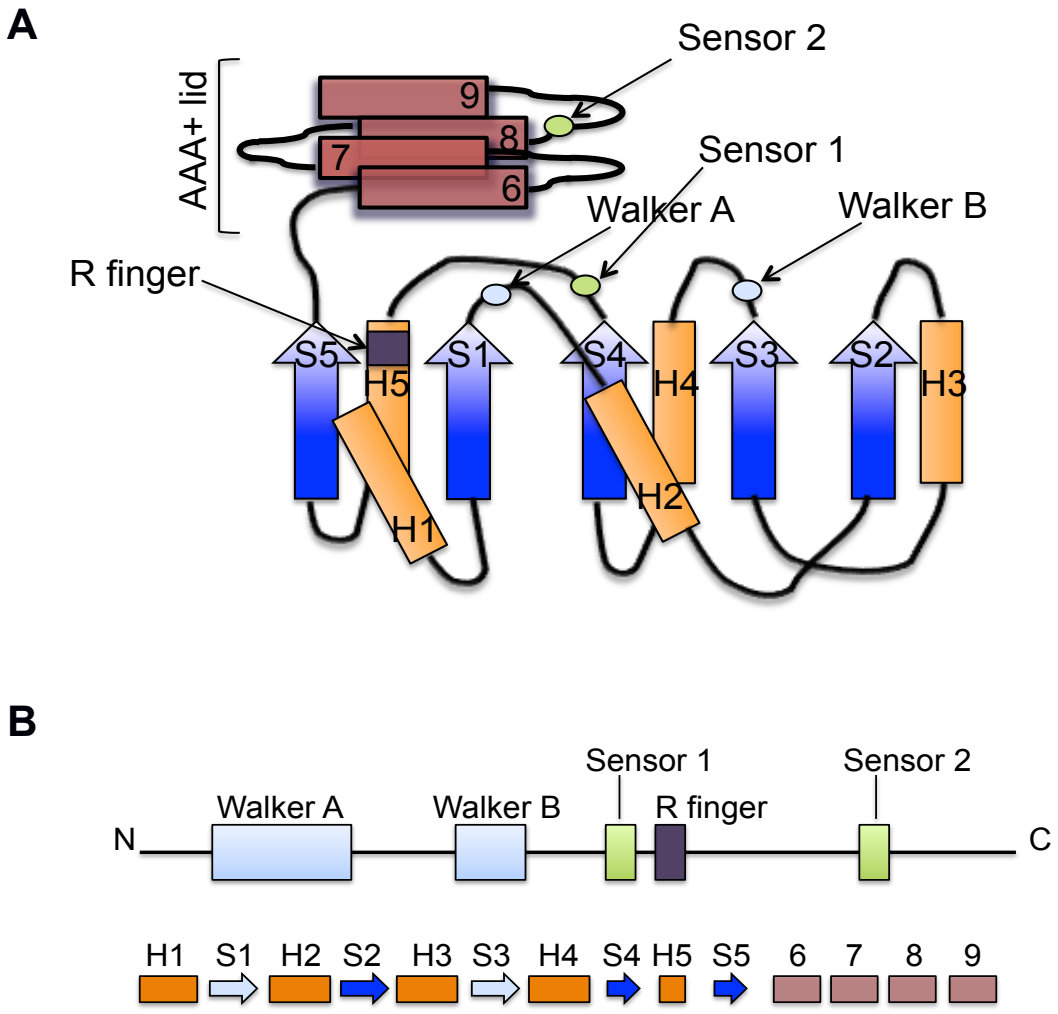


Figure 1.4. The organisation of AAA+ domain.

A) Topological arrangement of a classic AAA+ protein. The colouring of the secondary strucuture elements is consistent with the lower panel. Walker A and Walker B: light blue; Sensor 1 and Sensor 2: green; arginine finger: purple; α-helices are coloured in orange and β-strands in blue; AAA+ lid: red. **B**) The secondary structure and key elements of an AAA+ protein are shown in a linear diagram. The approximate position of α-helices and β-strands are represented by the orange and blue bars respectively. In red the AAA+ lid.

1.8.2. The winged helix domain

The WHD belongs to the helix-turn-helix motif family, which was first identified in transcription regulatory proteins from bacteriophage λ and *E. coli*

(Brennan and Matthews, 1989). Many other proteins containing a WHD were identified based on their sequence and/or structural similarity. Although the overall structure of the WHD is conserved, variations from the canonical arrangement are common.

Initially, the winged helix motif was defined as a dsDNA-binding motif, present in one third of the DNA-binding proteins (Aravind et al., 2005). However, a more recent structural analysis has shown that this domain is also responsible for protein-protein interactions (Gajiwala and Burley, 2000).

Topologically, the winged helix domain consists of three alpha helices (H1, H2, H3), three β strands (S1, S2, S3) and two wings (W1, W2) organised in order H1-S1-H2-H3-S2-W1-S3-W2 (Figure 1.5).

The biological functions of this domain range from dsDNA sequence recognition by transcription factors, DNA unwinding (helicases) to protein-protein interactions (Harami et al., 2013). Winged helix domains are present in many proteins involved in DNA replication, associated in both DNA-binding and protein-protein interactions. The functions of each individual protein will be described in the following paragraphs.

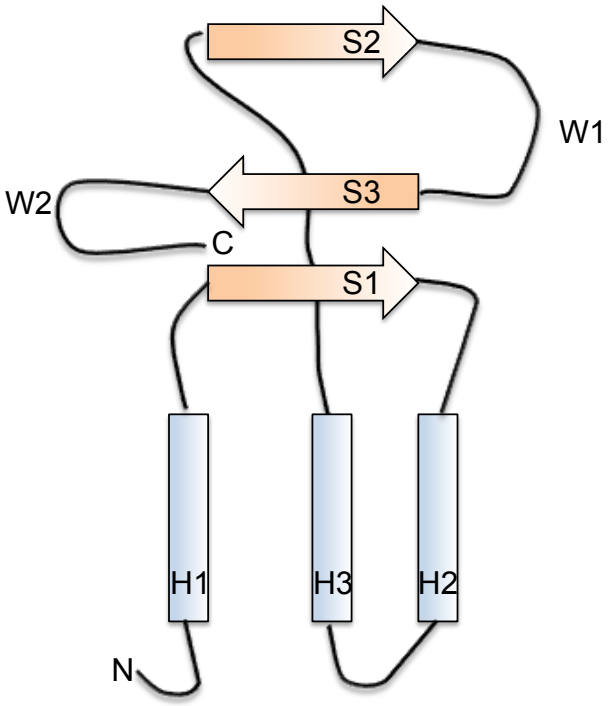


Figure 1.5. Schematic representation of the winged helix domain

The three α-helices (H1, H2, H3), three β strands (S1, S2, S3) and two wings (W1, W2) are organised in order H1-S1-H2-H3-S2-W1-S3-W2.

1.8.3. ORC

The six-subunit ORC was first identified and purified from yeast in 1992, through its ATP-dependent ability to bind specifically to the budding yeast origin autonomous replication sequence ARS1 (Bell and Stillman, 1992). The mechanism of ORC function has been investigated in several model organisms, revealing that the core components are conserved. The 400 kDa *S. cerevisiae* ORC is arranged in a subunit conformation of Orc1-Orc4-Orc5-Orc3-Orc2 forming a open ring. DNaseI footprinting assays were used to identify the binding elements of ARS1 recognised by *S. cerevisiae* ORC (Bell et al., 1995) while ChIP showed that over 300 DNA replication origin sequences are recognised by this protein complex (Wyrick et al., 2001). However, in higher eukaryotes, ORC consensus sequences were not identified. ORC is well conserved from yeast to human (Li and Stillman, 2012) where it essentially functions for DNA licensing (Mendez and Stillman, 2000; Romanowski et al.,

1996). Orc1-5 are structurally related, containing a AAA+ domain in the N-terminus and a WHD in the C-terminus (Bleichert et al., 2015; Speck et al., 2005; Tocilj et al., 2017). Orc6 is not an AAA+ protein and structural analysis showed that *Homo sapiens* Orc6 has shown homology with transcription factor TFIIB (Liu et al., 2011). Orc1-5 forms a notched ring and Orc6 interacts with Orc3 via a short C-terminal alpha-helix (Bleichert et al., 2013; Bleichert et al., 2015). Orc6 assembly with the other ORC subunits differs among species (Duncker et al., 2009). It strongly interacts with *Drosophila* and *S. cerevisiae* Orc1-5, but only weakly with human Orc1-5 and not at all with *Xenopus* Orc1-5 (Gillespie and Blow, 2000; Thomae et al., 2011). Importantly, Orc6 is the only ORC subunit not required for ORC binding to DNA (Lee and Bell, 1997), but it is essential for MCM2-7/Cdt1 association with origin DNA (Chen et al., 2007). Negative staining EM of the *S. cerevisiae* ORC was initially performed to identify the rough shape of the complex and through systematic maltose-binding protein (MBP) fusion to each individual subunit the basic subunits arrangement was revealed to be Orc1, Orc4, Orc5, Orc2, Orc3, Orc6 (Chen et al., 2008). A crystal structure of *Drosophila* ORC at 3.5 Å resolution confirmed the subunits arrangement even though this *Drosophila* structure adopts in contrast to *S. cerevisiae* an auto-inhibited conformation (Bleichert et al., 2015). A recent cryo-EM structure of the *S. cerevisiae* ORC bound to origin DNA was obtained at 3 Å resolution revealing bending of the DNA in the ARS consensus sequence and the B1 element (Li et al., 2018).

Although Orc1-5 encircles DNA, using the AAA+ and WHD (Bleichert et al., 2017; Li et al., 2018; Tocilj et al., 2017; Yuan et al., 2017), only Orc1 is able to hydrolyse ATP (Chesnokov et al., 2001; Giordano-Coltart et al., 2005; Klemm et al., 1997). Orc4 and Orc5 are able to bind but not to hydrolyse ATP. Despite containing the AAA+ features, Orc2 and Orc3 seem to have lost the ability to bind and hydrolyse ATP (Bleichert et al., 2015; Speck et al., 2005). ORC's ability to recognise and bind DNA is ATP-dependent (Bell and Stillman, 1992), whereas binding of ORC to origin DNA down-regulates its ATPase activity (Klemm et al., 1997). It was shown that *Drosophila* ORC exists as an auto-inhibited complex in solution in the absence of ATP and DNA (Bleichert et al., 2015), a conformation recently shown to be true also for the human ORC (Bleichert et al., 2018).

ORC has been reported to interact not only with DNA but also with chromatin or histones. Orc1 contains a bromo adjacent homology (BAH) domain, which in metazoan directly interacts with histone H4 dimethylated at lysine 20 (Callebaut et al., 1999; Kuo et al., 2012). However, no specific Orc1-histone interactions have been reported in *S. cerevisiae*.

1.8.4. Cdc6

Cell division cycle 6 (Cdc6) was first identified during a genetic screen aimed at identifying mutants that arrested the budding yeast cell cycle (Hartwell, 1973). It was found that Cdc6 was structurally related to ORC (Muzi-Falconi and Kelly, 1995). Indeed, it belongs to the AAA+ protein family and during the late M-phase of the cell cycle, it becomes recruited to chromatin in an ORC-dependent way. The binding of ORC and Cdc6 is ATP dependent (Evrin et al., 2013; Kang et al., 2014; Perkins and Diffley, 1998; Speck et al., 2005; Ticau et al., 2015) and it involves interactions between Cdc6 and the Orc1 and Orc3 subunits (Wang et al., 1999; Yuan et al., 2017) generating an extended protein-DNA interface (Speck and Stillman, 2007). The first high resolution crystal structure of Cdc6 was obtained from an archaeal homolog and revealed the structural architecture of the ATPase protein and the presence of a WHD, typically found in proteins involved in DNA binding (Liu et al., 2000). A recent high resolution structure of the DNA bound ORC/Cdc6 in complex with MCM2-7/Cdt1 revealed DNA contacts inside the ORC/Cdc6 ring (Yuan et al., 2017). The ATPase core allows Cdc6 to integrate into Orc1-5 forming a hexameric ring around dsDNA ideally suited to recruit the ring-shaped MCM2-7 (Bleichert et al., 2015; Iyer et al., 2004; Speck et al., 2005; Yuan et al., 2017). The C-terminal extension of Cdc6 contains a WHD that interacts with DNA (Clarey et al., 2006; Speck et al., 2005; Speck and Stillman, 2007), whereas the N-terminal extension is a target for CDK phosphorylation regulating its stability (Perkins et al., 2001). Cdc6 is a key factor during origin licensing since it was demonstrated that it is essential for the recruitment of the MCM2-7 helicase onto origins of replication (Cocker et al., 1996; Donovan et al., 1997; Liang and Stillman, 1997; Tanaka et al., 1997). Indeed, as budding yeast ORC is chromatin bound throughout the cell cycle, Cdc6 binding to ORC is the initiation point for pre-RC

formation in budding yeast. Importantly, Cdc6 can bind and hydrolyse ATP, which allows sequence specific DNA binding and induces conformational changes essential for pre-RC formation (Randell et al., 2006; Speck et al., 2005).

1.8.5. Cdt1

The Cdt1 protein (Cdc10-dependent transcript 1) was so called because it was initially identified in *S. pombe*, where its transcription was shown to be regulated by Cdc10, the fission yeast homolog of budding yeast Swi6 (Hofmann and Beach, 1994). Work in *Xenopus*, fission yeast and human demonstrated that this protein is essential for MCM2-7 loading since MCMs are not recruited to DNA without Cdt1 (Maiorano et al., 2000; Nishitani et al., 2000; Rialland et al., 2002). In budding yeast, Cdt1 interacts directly with MCM2-7 in solution (Liu et al., 2012; Tanaka and Diffley, 2002) and it is not released until MCM2-7 is successfully loaded (Fernandez-Cid et al., 2013; Randell et al., 2006). Unlike other essential proteins involved in the licensing reaction, Cdt1 does not have enzymatic activity and shares little similarity with other proteins of known molecular function. Despite the fact that *S. cerevisiae* and human Cdt1 show low sequence similarity, several well-conserved regions among species are conserved (Figure 1.6). The N-terminal domain is a short sequence, which contains phosphorylation sites. In budding yeast, the N-terminus of Cdt1 was found to interact with MCM2-7 but is not sufficient for MCM2-7 recruitment to DNA origins *in vitro* (Fernandez-Cid et al., 2013; Takara and Bell, 2011). The central and C-terminal domains contain WHDs, which have been crystallised from *Mus musculus* Cdt1 (Khayrutdinov et al., 2009; Lee et al., 2004). In budding yeast both WHDs are involved in the MCM2-7 recruitment to replication origins and ORC/Cdc6 induced ATP hydrolysis during pre-RC formation (Fernandez-Cid et al., 2013; Takara and Bell, 2011). In *H. sapiens*, the central WHD contains binding site for geminin, a Cdt1 inhibitor present in higher eukaryotes but not in fission and budding yeast (Tada et al., 2001; Wohlschlegel et al., 2000). The C-terminal WHD of Cdt1 interacts with MCM2-7 and nuclear magnetic resonance (NMR) analysis of the human and budding yeast proteins identified the structure of its interaction with Mcm6C (Jee et al.,

2010; Liu et al., 2012; Wei et al., 2010). Canonical WHDs bind DNA, but it is unlikely that the WHDs of Cdt1 have this function. Indeed, key amino acids in Cdt1 are incompatible with DNA binding when compared to WHDs of DNA-binding proteins. Moreover, Cdt1 cannot associate to chromatin in cells in the absence of ORC (Chen and Bell, 2011; Maiorano et al., 2000) and purified yeast Cdt1 does not bind origin DNA without ORC, Cdc6 and MCM2-7 (Evrin et al., 2009; Remus et al., 2009). Consistently with these observations, the C-terminal WHD of Cdt1 is involved in protein-protein interactions rather than protein-DNA interactions. This is also confirmed by mutational analysis in the C-terminal domain of Cdt1 which prevented binding to MCM2-7 *in vitro* (Jee et al., 2010; Liu et al., 2012) and affected cell growth *in vivo* (Jee et al., 2010). These biochemical data supported structural studies, which showed a direct interaction between Cdt1 C-terminus and Mcm6C (Khayrutdinov et al., 2009).

The structure of Cdt1 has been difficult to obtain for many years, because of its high degree of flexibility. However, recent high resolution structures obtained by cryo-EM revealed insights into the interactions between Cdt1 and MCM2-7 when bound together in solution (Zhai et al., 2017a) and in the DNA-bound licensing intermediate OCCM (Yuan et al., 2017). Both structures visualised a three domain architecture of Cdt1. In addition to the already described interaction with the C-terminus of Mcm6, Cdt1 appeared to contact other subunits of MCM2-7. Mcm2, Mcm6 and Mcm4 are embraced by Cdt1 in the OCCM suggesting a role of this protein in stabilisation of the MCM inter-subunits interactions. Because of the proximity to the Mcm5-Mcm2 gate through which the DNA in inserted during helicase loading, Cdt1 is in a suitable position to affect MCM2-7 conformation during the loading reaction (Bochman and Schwacha, 2010; Samel et al., 2014). Multiple studies have identified Mcm6 as the primary Cdt1 binding site on MCM2-7 (Ferenbach et al., 2005; Liu et al., 2012). However, the interaction Mcm6C-Cdt1 is not observed in the MCM2-7/Cdt1 structure (Zhai et al., 2017a) suggesting that upon ORC/Cdc6 interaction with Cdt1/MCM2-7 a structural rearrangement affects Cdt1 binding to the helicase. Indeed, this interaction is altering the WHD6 conformation; thus Cdt1 creates the ORC/Cdc6 binding surface for the C-termini of MCM2-7.

An interaction between Cdt1 and Orc6 has been described (Chen and Bell, 2011; Heller et al., 2011) and identified by cross-linking mass spectrometry

(CLMS) in the context of OCCM, but not visualised in the cryo-EM map due to the flexibility of Orc6 (Yuan et al., 2017).

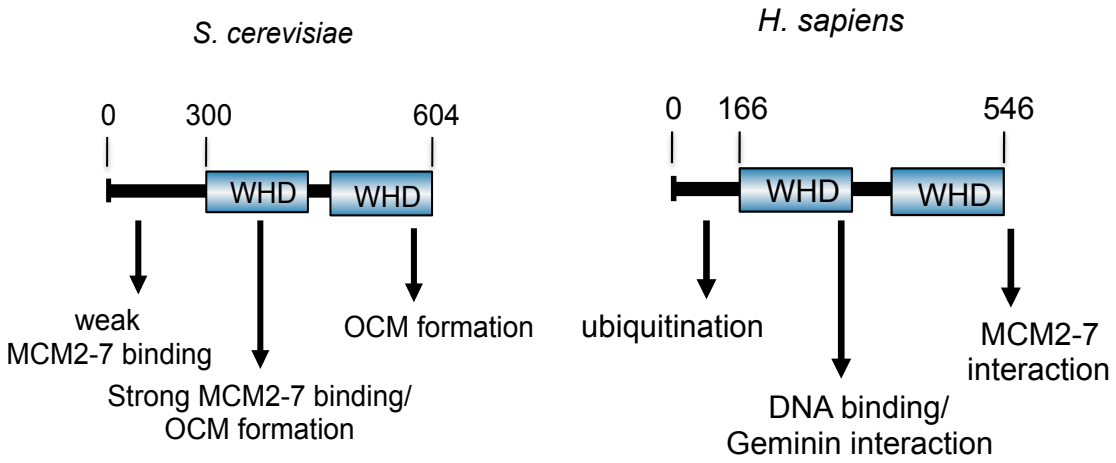


Figure 1.6. Schematic representation of S. cerevisiae and H. sapiens Cdt1

The S. cerevisiae Cdt1 has an N-terminal domain involved in MCM2-7 binding and two winged helix domains (WHD), mainly thought to be involved in OCM formation. The human Cdt1 has a shorter N-terminal extension, which is ubiquitinated, and contains two WHDs in the central and C-terminal regions, with specific functions (Figure adapted from Riera and Speck, 2015).

1.8.6. MCM2-7

The heterohexameric MCM2-7 proteins form the core of the eukaryotic replicative helicase (Bochman and Schwacha, 2009; Forsburg, 2004; Tye, 1999). Initially identified during a genetic screening for yeast mutants that affected plasmid maintenance (Maine et al., 1984), these proteins share conserved structural organisation from yeast to human (Figure 1.7).



Figure 1.7. The MCM2-7 replicative helicase

The diagram is showing the structural domains present in the six subunits of the *S. cerevisiae* MCM2-7 in comparison with an archaeal MCM (*Sulfolobus solfataricus)*. The central domain (AAA+ domain) is conserved between eukaryotes and archaeal MCMs, containing the canonical domains of the AAA+ proteins: the Zinc finger (purple), the Walker A and B motifs (blue) and the arginine finger (pink) are shown. The length of the N-terminal extension varies among subunits, while it is absent in archaea. A winged helix domain (WHD) is present in the C-terminal extension of all subunits, besides Mcm2.

Highly related homologs are present in archaea, in which the hexamer is usually constituted by a single homo-hexamer (Costa and Onesti, 2009). Like Orc1-5 and Cdc6, MCM2-7 proteins belong to the AAA+ family and all of the six subunits support ATP hydrolysis. The most conserved region is the central AAA+ domain, which contains the key features of the ATPase proteins: the Walker A and B motifs and the arginine finger. The N-terminus contains two subdomains. (1) A conserved zinc finger, which is involved in the formation of the head-to-head double-hexamer conformation, granting it stability when exposed to high salt (Abid Ali et al., 2017; Noguchi et al., 2017; Zhai et al., 2017a). (2) An oligonucleotide/olidosaccharide binding fold (OB-fold) which establishes contacts with the ssDNA, possibly involved in the initial unwinding during double hexamer activation, as described in *Pyrococcus furious* (Froelich et al., 2014). This domain is also involved in the assembly of MCM2-7 into the hexameric conformation establishing hydrophobic interactions (Bochman and Schwacha, 2009). Eukaryotic MCM2-7 are characterised by long N-terminal extensions, not present in archaea. These regions in Mcm2, Mcm4 and Mcm6 are flexible and contain phosphorylation sites for DDK (Randell et al., 2010).

The Mcm4 N-terminus contains an auto-inhibitory domain that is alleviated by DDK dependent phosphorylation, essential for progressing into S-phase (Sheu and Stillman, 2006, 2010), while the Mcm2 N-terminus is important for replication-coupled assembly of chromatin (Huang et al., 2015; Richet et al., 2015). The MCM2-7 C-terminal domains contain extensions of different length, which are composed of WHDs (Li et al., 2015; Yuan et al., 2016; Yuan et al., 2017; Zhai et al., 2017a) (Figure 1.8). Recent structural and biochemical studies revealed the locations and functions of the WHDs. The *S. solfataricus* MCM WHD can bind single-stranded DNA weakly (Pucci et al., 2007) and the majority of the data obtained in archaea showed that the function of this domain is to allosterically modulate the ATP hydrolysis rate of the AAA+ domain (Jenkinson and Chong, 2006; Wiedemann et al., 2015). Furthermore, in *S. solfataricus* the WHD was found to be required for MCM recruitment to origins (Samson et al., 2016). The WHDs of eukaryotic Mcm3 and Mcm6 have been shown to be important for MCM2-7/Cdt1 recruitment to ORC/Cdc6. Mcm3C binds ORC/Cdc6 (Frigola et al., 2013; Sun et al., 2013), while Cdt1 binding to Mcm6C alleviates the auto-inhibitory activity in Mcm6 (Fernandez-Cid et al., 2013).

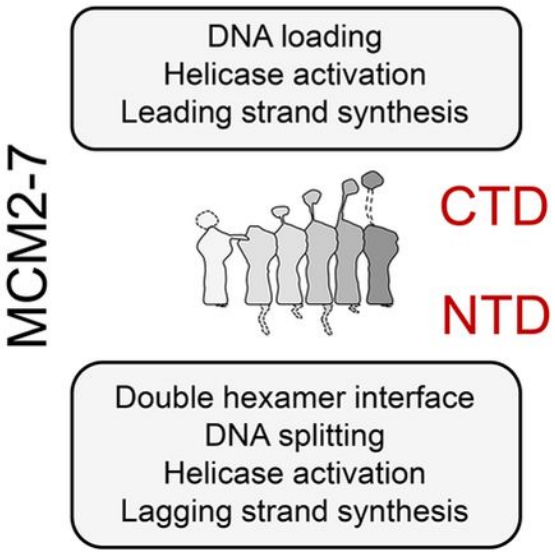


Figure 1.8. MCM2-7 protein interactions

Summary of the different functions in which the MCM2-7 helicase is involved through different interactions via its C- and N- terminal extensions with other proteins during DNA replication (from Riera et al, 2017).

Previous studies observed MCM2-7 in different conformations. The *S. cerevisiae* MCM2-7 was imaged by low-resolution negative stain EM and reported to be in a closed ring conformation (Bochman and Schwacha, 2007; Samel et al., 2014), similarly to the archaeal and bacterial helicases (Enemark and Joshua-Tor, 2008; Miller et al., 2014). On the other hand, *Drosophila* MCM2-7 and the *Encephalitozoon cuniculii* MCM adopted a spiral or open ring conformations (Costa et al., 2011; Lyubimov et al., 2012).

Recent cryo-EM structures of four complexes containing MCM2-7 revealed the conformational changes of each subunit of the MCM2-7 during the DNA replication loading process (Figure 1.9). For the interest of this thesis, a focused analysis on the C-terminal domains of MCM2-7 will be described, highlighting the main changes that affect these regions, in the following structures: the hexamer MCM2-7 at 7.3 Å (Zhai et al., 2017a), the heptamer MCM2-7/Cdt1 at 7.1 Å (Zhai et al., 2017a), the 14-protein OCCM at 3.9 Å, the double hexamer without DNA at 3.8 Å (Li et al., 2015) and with DNA at 3.9 Å (Noguchi et al., 2017) and at 4.7 Å (Abid Ali et al., 2017).

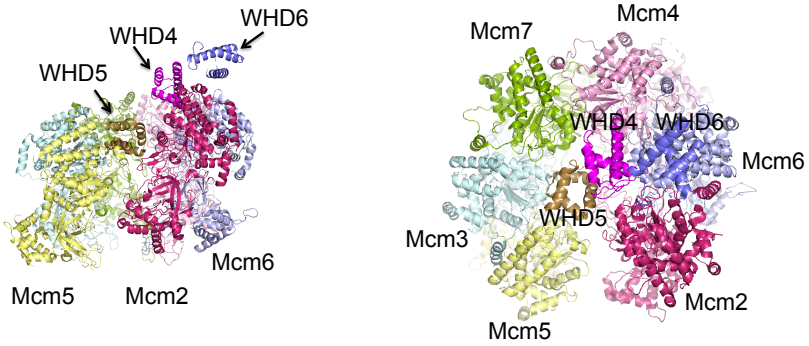
The six MCM subunits in MCM2-7 alone or in combination with Cdt1 are arranged in a spiral structure with a gap of 10-15 Å between Mcm5 and Mcm2, which is not wide enough to allow dsDNA entry. In this conformation, only the WHDs of Mcm5, Mcm4 and Mcm6 were visible, with the first one located in the central channel and the other two forming a pseudo-dimer (Zhai et al., 2017a). The spatial arrangement of the WHD5 and WHD4 partially occludes the central channel preventing dsDNA to enter. This is in line with biochemical data showing that MCM2-7 and MCM2-7/Cdt1 cannot bind DNA spontaneously (Bowers et al., 2004; Coster et al., 2014; Evrin et al., 2009; Frigola et al., 2013; Kang et al., 2014; Remus et al., 2009). Interestingly, similar location of the WHD5 on the central pore was seen in the CMG structure without DNA (inactive helicase) (Yuan et al., 2016). The direct interaction between Mcm6C and the C-terminus of Cdt1 was shown by NMR analysis (Fernandez-Cid et al., 2013; Liu et al., 2012; Wei et al., 2010), but this interaction was not visible in the MCM2-7/Cdt1 structure. In the OCCM structure it is visible, suggesting that this interaction has a role in the OCCM formation (Yuan et al., 2017). Indeed, in the OCCM, the WHDs of Mcm3, Mcm4, Mcm6 and Mcm7 are structurally resolved and they extend onto the ORC/Cdc6 surface establishing interactions. The

Mcm3C interacts with Cdc6. The role of Mcm3C in helicase loading has been biochemically analysed (Frigola et al., 2013). The deletion of this domain from the full length MCM2-7 prevented the loading of the helicase into ORC/Cdc6 precluding any interactions between ORC/Cdc6 and MCM2-7/Cdt1, suggesting that the Mcm3C is essential for the initial contact of the helicase with ORC/Cdc6. The Mcm7C is also visible and binds Orc1 and Cdc6, but its role in pre-RC formation has not been elucidated yet. The only WHD that is not visible in the OCCM is Mcm5 suggesting that this domain has a high degree of flexibility in this helicase loading intermediate. The conformational change observed in the WHD5 between MCM2-7/Cdt1 and OCCM was suggested to be involved in helping the dsDNA to go through the Mcm2-Mcm5 gate and contributing to conformational changes from the MCM2-7 spiral-to-ring transition (Zhai et al., 2017b).

The MCM2-7 double hexamer represents a stable DNA replication intermediate in which the two hexamers are arranged in an head-to-head conformation via their N-termini. The role of the C-terminal domains in double hexamer formation is not known, with the exception of the Mcm3C which was found to be essential for the recruitment of both hexamers to ORC/Cdc6 (Frigola et al., 2013). Once the loading process is complete, the C-termini of MCM2-7 cannot be seen in any of the recent high resolution structures of the double-hexamer, suggesting that they are flexible, and are therefore not visible. The Mcm2-Mcm5 gate is tightly closed and the central channel is wide enough to accommodate dsDNA. However, the double hexamer does not have helicase activity until it becomes activated during the G1/S phase transition (Moyer et al., 2006). Interestingly, the individual subunits of MCM2-7 in the double hexamer are twisted between the N-termini and C-termini (Li et al., 2015; Noguchi et al., 2017). This negatively regulates its ATPase activity. Thus, the double hexamer represents a very stable auto-inhibited conformation, which guarantees that only specific factors in S-phase can activate the complex.

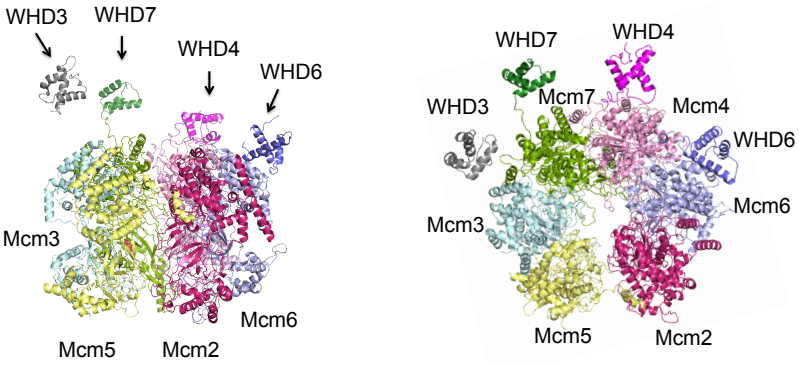
A

Mcm2-7/Cdt1



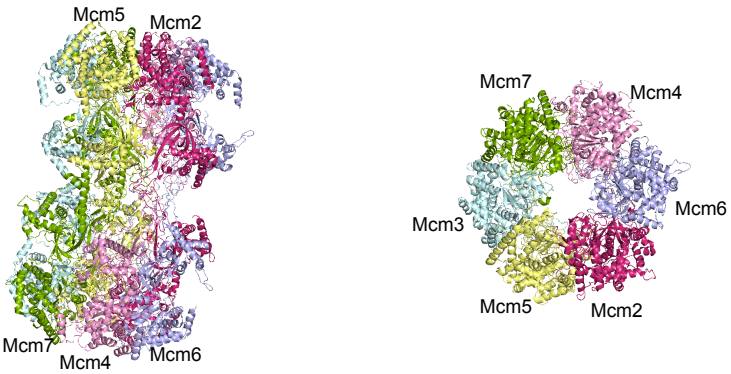
B

OCCM



C

Double hexamer



D

CMG

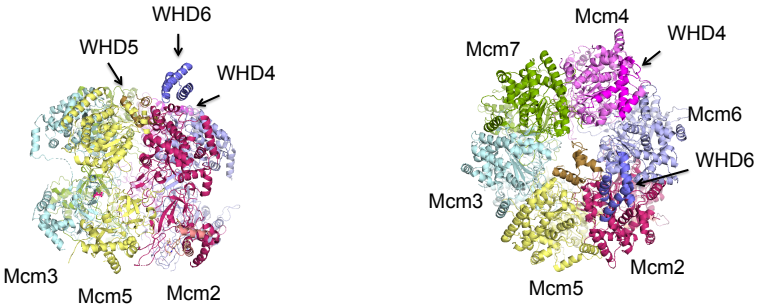


Figure 1.9. Comparison of the overall structures of the Mcm2-7 in different replication complexes.

Cryo-EM structures of MCM2-7 hexamer extracted from different DNA replication complexes, shown in cartoon representation. On the left hand side the structures are presented as front view while on the right hand side of the figure top views are shown. Mcm5 is shown in yellow, Mcm2 in magenta, Mcm6 in blue, Mcm4 in pink, Mcm7 in green, Mcm3 in cyan. The WHDs are highlighted with same colours but darker. **A)** MCM2-7/Cdt1 heptamer (PBD: 5H7I) – Cdt1 was not shown. **B)** MCM2-7 from OCCM (PBD: 5UDB) – ORC, Cdc6 and Cdt1 not shown. **C)** The two MCM2-7 from the double hexamer (5BK4). **D)** MCM2-7 in the context of CMG, but without GINS and Cdc45.

1.9. Origins of replication: the ARS element

The first eukaryotic replication origin was identified more than 30 years ago in *S. cerevisiae* (Chan and Tye, 1980; Stinchcomb et al., 1980). These DNA fragments were called autonomous replication sequence (ARS), because when inserted into a plasmid they showed autonomous ability to transform yeast at high frequency and propagate efficiently (Hsiao and Carbon, 1979; Stinchcomb et al., 1979; Struhl et al., 1979). These AT-rich sequences are around 100-150 base pairs (bp) long and serve to recruit ORC and initiate DNA replication (Bell and Stillman, 1992).

ARS1 is a *S. cerevisiae* replication origin and has an 11-17 bp consensus sequence (ACS) that is essential for its function. In addition to that, ARS1 contains three further elements, B1, B2 and B3 which are important to the origin function. The ACS is also referred to as “A element” and together with B1 represents the recognition site for ORC (Bell and Stillman, 1992; Rao and Stillman, 1995; Rowley et al., 1995; Speck et al., 2005). The B2 element is suggested to have a role in MCM2-7 loading after ORC binding to DNA (Lipford and Bell, 2001; Zou and Stillman, 2000). B3 is the binding site for the transcription factor Abf1 (Diffley and Stillman, 1988; Marahrens and Stillman, 1992). The yeast genome contains over 12000 ACS-like sequences but only around 400 of these are used for DNA replication (Linskens and Huberman, 1988; Nieduszynski et al., 2006; Wyrick et al., 2001). This low usage of origin DNA derives from the influence of other elements close to the ACS motif (Marahrens and Stillman, 1992). In addition, nucleosome occupancy around the ACS defines which origins will be active. The ACS is necessary to confer a nucleosome-free region (around 130 bp) where pre-RC is assembled. If ORC is

depleted, the size of these nucleosome free regions is decreased and the positioning of adjacent nucleosomes is affected, suggesting that ORC binding is required to induce precise nucleosome positioning for replication initiation (Hoggard et al., 2013; Leonard and Mechali, 2013).

Interestingly, in other metazoans there is no such sequence-specificity (Remus et al., 2004), since ORC binds to different regions in the genome (Hyrien and Mechali, 1993; Mechali and Kearsey, 1984). Recent studies have suggested that ORC might show a preference in binding GC-rich regions (Hoshina et al., 2013; Zellner et al., 2007), that are found to form a G-quadruplex structure in metazoan origins (Cayrou et al., 2012a; Cayrou et al., 2011; Cayrou et al., 2012b). A structural feature rather than specific sequence may drive ORC binding to origins. Overall, both yeast and metazoan origins contain conserved DNA elements that are recognised by ORC. Yeast contains specific DNA sequence whereas in metazoan the architecture of DNA seems to be more important than sequence specificity.

1.10. Comparison of helicase loading in *E. coli* and eukaryotes

There are several similarities in the mechanism of DNA replication initiation between *E. coli* and eukaryotes. However, important differences are present. The genome of *E. coli* contains only a single origin where two replication forks assemble and move into opposite directions. The rate of replication is fast, with the entire genome replicated in 30 minutes. On the other hand, eukaryotes have multiple chromosomes and multiple origins, with replication forks that move around 20 times slower than bacterial ones (O'Donnell et al., 2013).

DNA replication in bacteria starts at one specific region of the genome, called origin (OriC), whereas in eukaryotes the DNA sequences of the origins are not defined (with the exception of *S. cerevisiae*). To begin the process, multiple copies of DnaA-origin binding proteins are self-assembled into a helical filament on the origin, in an ATP-dependent manner (Erzberger et al., 2006). The origin melting precedes the helicase recruitment. DnaA unwinds DNA in A/T rich regions, resulting in an ssDNA sequestered by the AAA+ domains mediated

DnaA filament. Two copies of the homo-hexameric helicase (DnaB) are loaded on dsDNA, one in each direction. In eukaryotes, the helicase loader ORC binds origin DNA, but does not unwind DNA (Sun et al., 2012). The hetero-hexamer MCM2-7 is loaded on dsDNA as a double hexamer and no unwinding occurs before S-phase, where the helicase is activated by other factors (Ilves et al., 2010).

An interesting similarity between the two systems is that helicase loading in both *E. coli* and eukaryotes requires at least an additional factor. Before loading, DnaB and MCM2-7 are bound by DnaC and Cdt1 respectively. DnaC binds DnaB in an ATP dependent manner and facilitates its recruitment on the unwound DNA bubble generated by DnaA (Kaguni, 2011). In eukaryotes, Cdc6 and Cdt1 are required for MCM2-7 recruitment onto DNA origins. Cdc6 belongs to the AAA+ family, like DnaC, and has weak ATPase activity on its own. Cdt1 shares with DnaC the property of binding the replicative helicase and facilitating its loading on DNA.

One of the biggest differences between the two systems is the role of the helicase loader. Unlike bacteria where DnaA melts dsDNA, ORC's primary role is to load the double hexamer. ATP also has a crucial role in ORC but different than the ATP in the bacterial loader. ATP hydrolysis by ORC and Cdc6 is required for MCM2-7/Cdt1 recruitment and ATP hydrolysis by DnaA plays a regulatory role by preventing re-replication (Katayama et al., 1998)

1.11. DNA replication and relevance for human health

DNA replication needs to be accurate in order to prevent mistakes and accumulation of mutations that are responsible for genomic instability, growth defects and cancer. Due to the conserved features of DNA replication among species, insight obtained in studying any organism can ultimately be relevant for human health.

1.11.1. Cancer diagnosis

Early diagnosis of most common cancers is essential for efficient treatment. DNA replication factors have demonstrated to be good markers for early detection of many common cancers. In particular, MCM2-7 specific antibodies have been revealed to be more effective than the currently used PCNA (Jackson et al., 2014). Indeed, MCM2-7 proteins are expressed at high levels in proliferating cells but not at all in quiescent and differentiated cells (Madine et al., 2000; Stoeber et al., 2001). Therefore, they have emerged as potential diagnostic pre-cancer markers (Gonzalez et al., 2005). Moreover, MCM2-7 proteins appear to be a better marker than other pre-RC factors because of their nuclear abundance and expression in malignant cells and for the availability of specific antibodies (Gonzalez et al., 2005; Madine et al., 2000). Early diagnosis of cervical cancer (Baldwin et al., 2003), bladder and prostate cancer (Stoeber et al., 2002) are only three examples in which MCMs proteins have been used as a marker.

1.11.2. MCM2-7 as a target for cancer therapy

MCM2-7 is the helicase that unwinds DNA. Helicases of many pathogenic organisms have been studied in order to discover compounds that act as inhibitors for replication of these organisms. Viral helicases such as the herpes simplex or papillomavirus are widely studied as a drug target, since they are essential enzymes for the DNA replication of these human pathogens. In bacteria, the use of high-throughput screenings identified inhibitors against DnaB, that could be used to treat pathogenic strains of *E. coli* (Head et al., 2016). Increased expression of Mcm7, Mcm5 and Mcm2 were reported in several type of tumours twenty years ago (Hiraiwa et al., 1997; Todorov et al., 1998). Recently, high-throughput screening of a range of cancer tissues indicated that the amplification of at least one of the MCMs genes is commonly found. Point mutations of MCM are also found in cancer. For example, a mutation in a conserved amino acid (F345I) in Mcm4 was identified in genetic screen for spontaneous chromosomal instability in mice (Shima et al., 2007a; Shima et al., 2007b). This mutation results in spontaneous mammary tumours in 80% of mice and the same mutation in budding yeast showed reduced viability (Shima et al., 2007a). Deregulation of Mcm7 expression has been

linked to increase in tumour formation in a mouse chemical carcinogenesis model (Honeycutt et al., 2006). To date, a few small molecules have been identified to inhibit helicase activity in budding yeast (Simon and Schwacha, 2014). However, limitations on the identification of therapeutic inhibitors have so far been related to (1) difficulties in purifying high amount of MCM2-7 or CMG needed for high-throughput screening, (2) limited knowledge of structural aspects and mechanisms of action. Currently most strategies for targeting the MCM2-7 helicase are based on the regulation of the proteins expression or control of enzymatic activities by small molecules (reviewed in (Seo and Kang, 2018)).

1.11.3. Meier-Gorlin syndrome (MGS)

MGS is a rare autosomal recessive disorder, but its incidence is unknown. It is considered a form of primordial dwarfism, because the patients affected show intrauterine slow growth. After birth, this syndrome is primarily characterised by short stature, small ears and absence of the patella (Cohen et al., 1991). Despite the small head, patients affected do not have mental retardation (Bicknell et al., 2011a). Although there is no direct correlation to reduced life expectancy, complications such as difficulties in breathing and feeding in early infancy have been reported (Bongers et al., 2001).

Studies of the genetics of MGS have identified mutations in genes that are encoding for proteins involved in pre-RC formation (Bicknell et al., 2011a; Bicknell et al., 2011b; de Munnik et al., 2012). Specifically, mutations in Orc1, Orc4, Orc6, Cdt1 and Cdc6 have been found in patients affected by MGS. It should be noted that many factors involved in pre-RC formation have also other functions in the cell. It is the case of Orc1, which controls centriole and centrosome copy number in human cells (Hemerly et al., 2009). Orc1 and Orc3 bind hetereochromatin protein 1 (HP1), suggesting a function of ORC in gene regulation (Prasanth et al., 2010). Thus, the MGS mutations appear to effect mostly roles outside of DNA replication, consistent with its low impact on genome stability.

1.12. Summary and project aims

In recent years much progress has been made in the field of DNA replication and it has become clear that complex regulatory circuits control the initiation steps of DNA replication. Many of the events involved in the formation of the replisome are now well understood in bacteria. Studies in *E. coli* have served as a useful simplified model for understanding the process of replisome assembly in eukaryotes. The recent *in vitro* reconstitution of the budding yeast pre-RC (Evrin et al., 2009; Remus et al., 2009) and replisome (Yeeles et al., 2017) using purified proteins has provided excellent tools for studying the process of initiation of DNA replication in more complex eukaryotic systems. Furthermore, recent technological advancements in cryo-EM have allowed near atomic resolution structures to be achieved for a number of pre-RC intermediates.

Although extensive biochemistry and structural work has provided insight into the helicase loading, important questions remain and much remains to be discovered. In the last few years we have learnt that ORC, Cdc6, MCM2-7 and Cdt1 promote regulated pre-RC assembly. Although MCM2-7 helicase loading is essential for replication fork assembly and genome stability, the actual roles of Mcm proteins during pre-RC formation remain to be established.

Recent work from the Speck lab reported a 3D structure of the OCCM intermediate, a complex that traps the four proteins (ORC, Cdc6, MCM2-7, Cdt1) together. Despite the low resolution, this model revealed that the C-terminal section of the helicase is oriented towards the helicase loader (Sun et al., 2013). It has been shown that the C-termini of Mcm3 and Mcm6 are required for the recruitment of the first and the second MCM2-7 hexamer, suggesting that each hexamer needs to interact with ORC/Cdc6 (Frigola et al., 2013; Sun et al., 2013). However the role of the other C-terminal regions of MCM2-7 (Mcm2, Mcm4, Mcm5, Mcm7) during pre-RC formation was not known. Preliminary data obtained before the beginning of this project showed that the deletion of the Mcm2, Mcm4 and Mcm5 C-termini did not affect MCM2-7 association with ORC/Cdc6 but that the mutant lacking the Mcm5 C-terminus failed to promote salt stable MCM2-7 double hexamer formation. These results highlighted that the Mcm5 C-terminus is essential for pre-RC formation.

The major aim of this thesis project is to define the molecular mechanisms by which the Mcm C-termini promote regulated helicase loading onto DNA.

The main hypothesis is that the helicase loader ORC/Cdc6 interacts specifically with the C-terminal portion of MCM2-7 subunits promoting structural changes in MCM2-7. The interaction domains will be mapped and then characterised by cryo-EM and cross-linking mass spectrometry.

Employing a combination of biochemistry, genetics and structural analysis we aim to demonstrate the functional role of the Mcm5 C-terminus for the fundamental process of helicase loading onto DNA. To understand how this helicase mutant influence pre-RC formation, it will be important to identify at which point of pre-RC assembly pathway it blocks the reaction. In order to do that, this project took advantage of the *in vitro* reconstitution system and other well established protocols, which allow to identify several stages of the pre-RC assembly pathway.

A role of the C-terminus of Mcm5 in regulating ATP-hydrolysis driven quality control was described during this study. The hypothesis that Mcm5C establishes protein-protein interactions with adjacent ORC subunits in order to down-regulate the quality control pathway led to an extensive mutational analysis of Mcm5C with the attempt to validate the proposed model.

Chapter 2 - Materials and Methods

2.1. Materials

2.1.1. Solutions

TBS: 50 mM Tris-HCl pH 7.5, 150 mM NaCl

TBST: 50 mM Tris-HCl pH 7.5, 150 mM NaCl, 0.1% Tween-20

PBST: 1.37M NaCl, 27 mM KCl, 100 mM Na2HPO4, 18 mM KH2PO4, 0.05% Tween 20

EB: 10 mM Tris-HCl pH 8.5

Western blot transfer buffer (Dunn Carbonate buffer): 10 mM $NaHCO_3$, 3 mM Na_2CO_3, 20% ethanol

MILK+TBST: 5% skim milk powder (Sigma-Aldrich), TBST

TBE 0.5X: 45 mM Tris-borate, 1 mM EDTA

HA beads regeneration buffer: 3 M MgCl2, 50 mM MES pH 5

Laemmli buffer 2X: 4% SDS, 20% glycerol, 100 mM Tris-HCl pH 6.8, 100 mM DTT, 0.02% bromophenol blue

Binding and washing buffer for dynabeads (2X): 10 mM Tris-HCl pH 7.5, 1 mM EDTA, 2 M NaCl

2.1.2. Reagents

Table 2.1 List of Reagents

Category	Name	Company
Agarose gel electrophoresis	Agarose	Invitrogen
Agarose gel electrophoresis	SYBR Safe DNA gel stain	Invitrogen
Agarose gel electrophoresis	1 kb plus DNA ladder	Invitrogen
Antibiotics	Ampicillin disodium salt	Thermo Scientific
Chemicals	Ethanol	Thermo Scientific

Chemicals	Dithiothreitol (DTT)	Thermo Scientific
Chemicals	Bidistilled glycerol	Thermo Scientific
Chemicals	Dimethyl sulfoxide (DMSO)	Sigma
Chemicals	Tween-20	Sigma
Chemicals	Phenol	Sigma
Chemicals	EDTA	Sigma
Chemicals	EGTA	Sigma
Chemicals	KOH	Sigma
Chemicals	NaOH	Sigma
Cloning/mutagenesis	*Long Amp polymerase*	*NEB*
Cloning/mutagenesis	*Long Amp buffer*	*NEB*
Cloning/mutagenesis	Herculase II Fusion DNA polymerase	Agilent Technologies
Cloning/mutagenesis	Herculase II buffer	Agilent Technologies
Cloning/mutagenesis	dNTPs	Roche
Cloning/mutagenesis	Restriction enzymes	NEB
Cloning/mutagenesis	CutSmart buffer	NEB
Competent cells	Codon Plus BL21 –RIL strain	Agilent Technologies
Competent cells	DHα competent cells	Invitrogen
DNA purification	DNA purification kit	Qiagen
DNA purification	Gel extraction kit	Qiagen
DNA purification	Glycogen	Thermo Scientific
EM	Grids quantifoil	Agar scientific
EM	Uranyl acetate	Agar scientific
EM	Gluteraldehyde EM grade	Agar scientific
Media	Yeast extract	ForMedium
Media	Bacto-peptone	ForMedium
Media	Yeast nitrogen base without amino acids	ForMedium
Media	Supplement mix	ForMedium
Media	Adenine	Sigma
Media	Histidine	ForMedium
Media	Glucose	SLS
Media	Bacto-agar	Invitrogen
Media	Lactic acid	Acros
Protein purification	Prescission protease	Speck lab
Protein purification	TEV protease	
Protein purification	Amicon Ultra 15 centrifugal devices 15/5ml	Merck Millipore
Protein purification	Microcon 500ul	Merck Millipore
Protein purification	HA peptide	Genscript

Protein purification	Alpha-factor	Genscript
Protein purification	Complete protease inhibitor cocktail +/- EDTA	Roche
Protein purification	Brafdord reagent	BioRad
Protein purification	Isopropyl β-D-1-thiogalactopyranoside (IPTG)	ThermoFisher
Protein purification	Illustra micro spin G50	GE
Protein staining	Instant blue	Expedeon
Protein staining	Methanol	ThermoFisher
Protein staining	Formaldehyde solution	Sigma
Protein staining	Silver nitrate	Acros
Protein staining	Sodium thiosulfate	VWR
Protein staining	Acetic acid	VWR
Radiolabeled assay	γ-^{32}P-ATP	PerkinElmer
Radiolabeled assay	PEI cellulose TLC plastic sheets	VWR
SDS-PAGE	Tris-Glycine-SDS (10X)	Fisher Bioreagents
SDS-PAGE	MOPS-SDS running buffer 20X	ForMedium
SDS-PAGE	MEPS-SDS running buffer 20X	ForMedium
SDS-PAGE	SDS-PAGE standard broad range protein marker	BioRad
SDS-PAGE	Acrylamide 40% solution	GE Healthcare
SDS-PAGE	Methylenbisacrylamide 2% solution	GE Healthcare
SDS-PAGE	Tetramethylethylenediamine (TEMED)	Sigma
SDS-PAGE	Ammonium persulfate (APS)	Sigma
SDS-PAGE	NuPage Novex 4-12% Bis-Tris Protein gels	Invitrogen
Western blotting	SuperSignal west Pico/Dura/Fempto substrate kits	ThermoFisher
Western blotting	Restore western blot stripping buffer	ThermoFisher
Western blotting	Nitrocellulose blotting membrane	GE Healthcare
Western blotting	CL-X Posure X-ray film	Thermo Scientific
Western blotting	Ponceau S staining solution	Sigma

2.1.3. Plasmids

Table 2.2. List of pre-existing and new plasmid used in experiments described in the text.

Code	Gene	Plasmid backbone	Reference
pCS14	pESC-LEU-MCM2-MCM7	pESC-Leu	Speck lab
pCS232	pESC-URA-HA Nter_MCM3-MCM5	pESC-Ura	Speck lab
pCS15	pESC-TRP-MCM6-MCM4	pESC-Trp	Speck lab
pCS372	ARS1	pUC19	Evrin et al, 2009
pCS735	10XARS1	pUC19	Noguchi and Speck, 2017
pCS736	10Xshort ARS1	pUC19	Speck lab, unpublished
pCS160	Cdc6	pGEX6P-1	Speck et al, 2005
pCS15	pESC-Trp-Mcm6-Mcm4	pESC-Trp	Evrin et al, 2009
pCS525	pGEX-6P1_yMcm2 C-terminal	pGEX	Speck lab unpublished
pCS526	pGEX-6P1_yMcm3 C-terminal	pGEX	Speck lab unpublished
pCS527	pGEX-6P1_yMcm4 C-terminal	pGEX	Speck lab unpublished
pCS528	pGEX-6P1_yMcm5 C-terminal	pGEX	Speck lab unpublished
pCS529	pGEX-6P1_yMcm6 C-terminal	pGEX	Speck lab unpublished
pCS530	pGEX-6P1_yMcm7 C-terminal	pGEX	Speck lab unpublished
pCS491	pESC-LEU_MCM2-MCM7-Mcm2(Δ848-868)	pESC-Leu	Speck lab unpublished
pCS492	pESC-URA_MCM5_MCM3-Mcm3(Δ739-971)	pESC-Ura	Speck lab unpublished
pCS494	pESC-TRP_MCM6_MCM4-Mcm4(Δ837-933)	pESC-Trp	Speck lab unpublished
pCS495	pESC-URA_MCM5_MCM3-Mcm5 (Δ693-775)	pESC-Ura	Speck lab unpublished
pCS496	pESC-TRP_MCM6_MCM4-Mcm6 (Δ839-1017)	pESC-Trp	Speck lab unpublished
pCS497	pESC-LEU_MCM2-MCM7-	pESC-Leu	Speck lab

	Mcm7(Δ727-845)		unpublished
pCS778	pUC57-yMCM5-prescission site	pUC57	This study (Genscript)
pCS779	pUC57-yMCM5-TEV site	pUC57	This study (Genscript)
pCS782	pESC-URA-MCM5prescission-MCM3	pESC-Ura	This study (Genscript)
pCS783	pESC-URA-MCM5_TEV-MCM3	pESC-Ura	This study (Genscript)
pCS784	pESC-URA-MCM5-(R713E,R720E,R735E)-MCM3	pESC-Ura	This study (Genscript)
pCS785	pESC-URA-MCM5-(K757D,R764E,R772E)-MCM3	pESC-Ura	This study (Genscript)
pCS786	pESC-URA-MCM5-(E710R,E717R,E736R) -MCM3	pESC-Ura	This study (Genscript)
pCS787	pESC-URA-MCM5-(D749R,E756R,E759R)-MCM3	pESC-Ura	This study (Genscript)
pCS784	pESC-URA-MCM5-R713E,R720E,R735E -MCM3	pESC-Ura	This study (Genscript)
pCS785	pESC-URA-MCM5-K757D,R764E,R772E -MCM3	pESC-Ura	This study (Genscript)
pCS786	pESC-URA-MCM5-E710R,E717R,E736R -MCM3	pESC-Ura	This study (Genscript)
pCS787	pESC-URA-MCM5-D749R,E756R,E759R -MCM3	pESC-Ura	This study (Genscript)
pCS811	pESC-URA-MCM5-R721E,R736E-MCM3	pESC-Ura	This study (Genscript)
pCS812	pESC-URA-MCM5-R721E,E756R-MCM3	pESC-Ura	This study (Genscript)
pCS813	pESC-URA-MCM5-R721A,R736A-MCM3	pESC-Ura	This study (Genscript)
pCS814	pESC-URA-MCM5-E756R,K532E-MCM3	pESC-Ura	This study (Genscript)
pCS815	pESC-URA-MCM5-E756A,K532A-MCM3	pESC-Ura	This study (Genscript)
pCS816	pESC-URA-MCM5_2prescission sites_MCM3	pESC-Ura	This study (Genscript)
pCS817	pESC-URA-MCM5_3prescission sites_MCM3	pESC-Ura	This study (Genscript)
pCS822	pESC-URA-MCM5-yWHD4-MCM3	pESC-Ura	This study (Genscript)
pCS823	pESC-URA-MCM5-hWHD5-MCM3	pESC-Ura	This study

			(Genscript)
pCS755	GC rich	pBSSK+	Speck lab
pCS818	10XAB1	pUC57	This study
pCS819	10XAB1 in pCS755 (GC rich environment)	pBSSK+	This study
pCS836	pESC-URA-MCM5-linker only-MCM3	pESC-Ura	This study (Genscript)
pCS837	pESC-URA-MCM5-short linker-MCM3	pESC-Ura	This study (Genscript)
pCS838	pESC-URA-MCM5-flexible linker -MCM3	pESC-Ura	This study (Genscript)
pCS839	pESC-URA-MCM5-rigid linker-MCM3	pESC-Ura	This study (Genscript)
pCS840	pESC-URA-MCM5-linker+FRB-MCM3	pESC-Ura	This study (Genscript)
pCS879	pESC-URA_MCM5_E710R,E717R,E736E,E757D,R764E,R772E,MCM3	pESC-Ura	This study (Genscript)
pCS880	pESC-URA_MCM5_E710R,E717R,E736E,K757D,R764E,R772E,R721E,R735E_MCM3	pESC-Ura	This study (Genscript)
pCS881	pESC-URA_MCM5_E710R,E717R,E736E,R721E,R735E_MCM3	pESC-Ura	This study (Genscript)

2.1.4. Yeast strains

The background strain AS499 was available in the lab. All yeast strains used during this study are listed in Table 2.3. All strains were grown in synthetic complete (SC) drop-out medium (-U-L-T) at 30°C.

Table 2.3. List of pre-existing and new yeast strains used in experiments

Code	Name	Genotype	Reference
YC119	WT MCM2-7	MATa bar1Δ leu2-3,112 ura3-52 his3-Δ200 trp1-Δ 63 ade2-1 lys2-801 pep4 pESC-LEU-MCM2-MCM7 pESC-TRP-MCM6-MCM4 pESC-URA-HA_MCM3-MCM5	Evrin et al, 2009

YC388	MCM2-7ΔC2	MATa bar1Δ leu2-3,112 ura3-52 his3-Δ200 trp1-Δ63 ade2-1 lys2-801 pep4 pESC-LEU-MCM2 Δ848-868 -MCM7 pESC-TRP-MCM6-MCM4 pESC-URA-MCM3-MCM5	Winkler and Speck, unpublished
YC389	MCM2-7ΔC3	MATa bar1Δ leu2-3,112 ura3-52 his3-Δ200 trp1-Δ63 ade2-1 lys2-801 pep4 pESC-LEU-MCM2-MCM7 pESC-TRP-MCM6-MCM4 pESC-URA-MCM3 Δ739-971 -MCM5	Winkler and Speck, unpublished
YC391	MCM2-7ΔC4	MATa bar1Δ leu2-3,112 ura3-52 his3-Δ200 trp1-Δ63 ade2-1 lys2-801 pep4 pESC-LEU-MCM2-MCM7 pESC-TRP-MCM6-MCM4 Δ837-933 pESC-URA-MCM3-MCM5	Winkler and Speck, unpublished
YC392	MCM2-7ΔC5	MATa bar1Δ leu2-3,112 ura3-52 his3-Δ200 trp1-Δ63 ade2-1 lys2-801 pep4 pESC-LEU-MCM2-MCM7 pESC-TRP-MCM6-MCM4 pESC-URA-MCM3-MCM5 Δ693-775	Winkler and Speck, unpublished
YC393	MCM2-7ΔC6	MATa bar1Δ leu2-3,112 ura3-52 his3-Δ200 trp1-Δ63 ade2-1 lys2-801 pep4 pESC-LEU-MCM2-MCM7 pESC-TRP-MCM6 Δ838-1017 -MCM4 pESC-URA-MCM3-MCM5	Fernandez-Cid et al, 2013
YC394	MCM2-7ΔC7	MATa bar1Δ leu2-3,112 ura3-52 his3-Δ200 trp1-Δ63 ade2-1 lys2-801 pep4 pESC-LEU-MCM2-MCM7 Δ727-845 pESC-TRP-MCM6-MCM4 pESC-URA-MCM3-MCM5	Winkler and Speck, unpublished
YC507	MCM2-7ΔC6-ΔC7	AS499 (MATa bar1Δ leu2-3,112 ura3-52 his3-Δ200 trp1-Δ 63 ade2-1 lys2-801) + pESC-LEU-MCM2-MCM7Δ727-845+pESC-TRP-MCM6Δ839-1017+pESC-URA-HA-MCM3-MCM5 (497,496,232)	This study

YC600	Mcm5-WHD4	AS499 (MATa bar1Δ leu2-3,112 ura3-52 his3-Δ200 trp1-Δ 63 ade2-1 lys2-801) + pESC-LEU-MCM2-MCM7 +pESC-TRP-MCM6-MCM4 + pESC-URA-HA Nter_MCM3-MCM5_WHD4 (14,15,822)	This study
YC601	Mcm5-hWHD5	AS499 (MATa bar1Δ leu2-3,112 ura3-52 his3-Δ200 trp1-Δ 63 ade2-1 lys2-801) + pESC-LEU-MCM2-MCM7 +pESC-TRP-MCM6-MCM4 + pESC-URA-HA Nter_MCM3-MCM5_hWHD5 (14,15,823)	This study
YC566	Mcm5-1Xprescission+WHD5	AS499 (MATa bar1Δ leu2-3,112 ura3-52 his3-Δ200 trp1-Δ 63 ade2-1 lys2-801) + pESC-LEU-MCM2-MCM7 +pESC-TRP-MCM6-MCM4 + pESC-URA-HA Nter_MCM3-MCM5_prescissionWHD5 (14,15,782)	This study
YC567	Mcm5-1XTEV+WDH5	AS499 (MATa bar1Δ leu2-3,112 ura3-52 his3-Δ200 trp1-Δ 63 ade2-1 lys2-801) + pESC-LEU-MCM2-MCM7 +pESC-TRP-MCM6-MCM4 + pESC-URA-HA Nter_MCM3-MCM5_TEV_WHD5 (14,15,783)	This study
YC568	Mcm5-0	AS499 (MATa bar1Δ leu2-3,112 ura3-52 his3-Δ200 trp1-Δ 63 ade2-1 lys2-801) + pESC-LEU-MCM2-MCM7 +pESC-TRP-MCM6-MCM4 + pESC-URA-HA Nter_MCM3-MCM5_R713E,R720E,R735E (14,15,784)	This study
YC569	Mcm5-1	AS499 (MATa bar1Δ leu2-3,112 ura3-52 his3-Δ200 trp1-Δ 63 ade2-1 lys2-801) + pESC-LEU-MCM2-MCM7 +pESC-TRP-MCM6-MCM4 + pESC-URA-HA Nter_MCM3-MCM5_K757D,R764E,R772E (14,15,785)	This study

YC570	Mcm5-2	AS499 (MATa bar1Δ leu2-3,112 ura3-52 his3-Δ200 trp1-Δ 63 ade2-1 lys2-801) + pESC-LEU-MCM2-MCM7 +pESC-TRP-MCM6-MCM4 + pESC-URA-HA Nter_MCM3-MCM5_E710R,E717R,E736R (14,15,786)	This study
YC608	MCM2-7ΔC4 ΔC5	AS499 (MATa bar1Δ leu2-3,112 ura3-52 his3-Δ200 trp1-Δ 63 ade2-1 lys2-801) + pESC-LEU-MCM2-MCM7 +pESC-TRP-MCM6-MCM4ΔC4 + pESC-URA-HA Nter_MCM3-MCM5_ΔC5 (14,495,494)	This study
YC609	MCM2-7ΔC6 ΔC5	AS499 (MATa bar1Δ leu2-3,112 ura3-52 his3-Δ200 trp1-Δ 63 ade2-1 lys2-801) + pESC-LEU-MCM2-MCM7 +pESC-TRP-MCM6ΔC6-MCM4 + pESC-URA-HA Nter_MCM3-MCM5_ΔC5 (14,495,496)	This study
YC610	MCM2-7ΔC7 ΔC5	AS499 (MATa bar1Δ leu2-3,112 ura3-52 his3-Δ200 trp1-Δ 63 ade2-1 lys2-801) + pESC-LEU-MCM2-MCM7ΔC7 +pESC-TRP-MCM6-MCM4 + pESC-URA-HA Nter_MCM3-MCM5_ΔC5 (15,495,497)	This study
YC611	Mcm5-3	AS499 (MATa bar1Δ leu2-3,112 ura3-52 his3-Δ200 trp1-Δ 63 ade2-1 lys2-801) + pESC-LEU-MCM2-MCM7 +pESC-TRP-MCM6-MCM4 + pESC-URA-HA Nter_MCM3-MCM5_R721E-R736E (14,15,811)	This study
YC612	Mcm5-4	AS499 (MATa bar1Δ leu2-3,112 ura3-52 his3-Δ200 trp1-Δ 63 ade2-1 lys2-801) + pESC-LEU-MCM2-MCM7 +pESC-TRP-MCM6-MCM4 + pESC-URA-HA Nter_MCM3-MCM5_R721E-R756R (14,15,812)	This study

YC613	Mcm5-5	AS499 (MATa bar1Δ leu2-3,112 ura3-52 his3-Δ200 trp1-Δ 63 ade2-1 lys2-801) + pESC-LEU-MCM2-MCM7 +pESC-TRP-MCM6-MCM4 + pESC-URA-HA Nter_MCM3-MCM5_R721A-R735A (14,15,813)	This study
YC614	Mcm5-6	AS499 (MATa bar1Δ leu2-3,112 ura3-52 his3-Δ200 trp1-Δ 63 ade2-1 lys2-801) + pESC-LEU-MCM2-MCM7 +pESC-TRP-MCM6-MCM4 + pESC-URA-HA Nter_MCM3-MCM5_E756R-K532E (14,15,814)	This study
YC615	Mcm5-7	AS499 (MATa bar1Δ leu2-3,112 ura3-52 his3-Δ200 trp1-Δ 63 ade2-1 lys2-801) + pESC-LEU-MCM2-MCM7 +pESC-TRP-MCM6-MCM4 + pESC-URA-HA Nter_MCM3-MCM5_E756A-K532A (14,15,815)	This study
YC616	Mcm5-2XPreScission	AS499 (MATa bar1Δ leu2-3,112 ura3-52 his3-Δ200 trp1-Δ 63 ade2-1 lys2-801) + pESC-LEU-MCM2-MCM7 +pESC-TRP-MCM6-MCM4 + pESC-URA-HA Nter_MCM3-MCM5_2XPreScission (14,15,816)	This study
YC617	Mcm5-3XPreScission	AS499 (MATa bar1Δ leu2-3,112 ura3-52 his3-Δ200 trp1-Δ 63 ade2-1 lys2-801) + pESC-LEU-MCM2-MCM7 +pESC-TRP-MCM6-MCM4 + pESC-URA-HA Nter_MCM3-MCM5_3XPreScission (14,15,817)	This study
YC622	Mcm5- linker only	AS499 (MATa bar1Δ leu2-3,112 ura3-52 his3-Δ200 trp1-Δ 63 ade2-1 lys2-801) + pESC-LEU-MCM2-MCM7 +pESC-TRP-MCM6-MCM4 + pESC-URA-HA Nter_MCM3-MCM5_linker only (14,15,836)	This study

YC623	Mcm5-short linker+C5	AS499 (MATa bar1Δ leu2-3,112 ura3-52 his3-Δ200 trp1-Δ 63 ade2-1 lys2-801) + pESC-LEU-MCM2-MCM7 +pESC-TRP-MCM6-MCM4 + pESC-URA-HA Nter_MCM3-MCM5_short linker (14,15,837)	This study
YC624	Mcm5-flexible linker+C5	AS499 (MATa bar1Δ leu2-3,112 ura3-52 his3-Δ200 trp1-Δ 63 ade2-1 lys2-801) + pESC-LEU-MCM2-MCM7 +pESC-TRP-MCM6-MCM4 + pESC-URA-HA Nter_MCM3-MCM5_flexible linker (14,15,838)	This study
YC625	Mcm5-rigid linker+C5	AS499 (MATa bar1Δ leu2-3,112 ura3-52 his3-Δ200 trp1-Δ 63 ade2-1 lys2-801) + pESC-LEU-MCM2-MCM7 +pESC-TRP-MCM6-MCM4 + pESC-URA-HA Nter_MCM3-MCM5_rigid linker (14,15,839)	This study
YC626	Mcm5-FRB	AS499 (MATa bar1Δ leu2-3,112 ura3-52 his3-Δ200 trp1-Δ 63 ade2-1 lys2-801) + pESC-LEU-MCM2-MCM7 +pESC-TRP-MCM6-MCM4 + pESC-URA-HA Nter_MCM3-MCM5_linker+FRB (14,15,840)	This study
YC651	Mcm5-8	AS499 (MATa bar1Δ leu2-3,112 ura3-52 his3-Δ200 trp1-Δ 63 ade2-1 lys2-801) + pESC-LEU-MCM2-MCM7 +pESC-TRP-MCM6-MCM4 + pESC-URA-HA Nter_MCM3-MCM5_E710R_E717R_E736E_E757D_R764E_R772E (14,15,879)	This study
YC652	Mcm5-10	AS499 (MATa bar1Δ leu2-3,112 ura3-52 his3-Δ200 trp1-Δ 63 ade2-1 lys2-801) + pESC-LEU-MCM2-MCM7 +pESC-TRP-MCM6-MCM4 + pESC-URA-HA Nter_MCM3-MCM5_E710R_E717R_E736E_K757D_R764E_R772E_R721E_R735E (14,15,880)	This study

YC653	MCm5-9	AS499 (MATa bar1Δ leu2-3,112 ura3-52 his3-Δ200 trp1-Δ 63 ade2-1 lys2-801) + pESC-LEU-MCM2-MCM7 +pESC-TRP-MCM6-MCM4 + pESC-URA-HA Nter_MCM3-MCM5_E710R_E717R_E736E_R721E_R735E (14,15,881)	This study

2.1.5. Chromatography resins, columns and beads

All the resins, columns and beads used in the experiments explained in the text are listed in Table 2.4.

Table 2.4. List of columns used in the experiments described in this study

Name	**Company**	**Use**	**Cat. number**
EZview Red Anti-HA affinity Gel	Sigma	MCM2-7 purification	E6779
Glutathione beads GST agarose	Sigma	Cdc6 purification	G4510
Hydroxyapatite HTP beads Macroprep 80µm	Bio-rad	Cdc6 purification	1582000
Superose 6 10/30	GE Healtcare	MCM2-7 purification	29-0915-96
Dynabeads MyOne Streptavidin	Invitrogen	preRC assay	65601
Dynabeads Protein G	Invitrogen	IP for GST/MBP	1004D
Anti GST magnetic beads	Genscript	IP for GST/MBP	customised

2.1.6. Antibodies

Table 2.5. **List of antibodies used in the experiments described in this study**

Name (antigen)	Source	Dilution	Reference	Purpose
MCM2	mouse	1:3000	Zou&Stillman 2000	Western blot
MCM5	mouse	1:5000	Zou&Stillman 2000	Western blot
ORC1	mouse	1:2000	Stillman	Western blot
Cdc6	mouse	1:200	Santa Cruz (sc-53218)	Western blot
Cdt1	rabbit	1:3000	Stillman	Immuno-precipitation
MBP	mouse	1:10000	NEB E8032L	Immuno-precipitation
GST	rat	1:1000	Sigma (SAB4200055)	Immuno-precipitation
HA	mouse	1:1000	Sigma (H3663)	Immuno-precipitation
Anti mouse (IgG)	goat	1:10000	Sigma (A4416)	Western blot
Anti rat	rabbit	1:20000	Sigma (A5795)	Western blot
Anti rabbit	mouse	1:10000	Sigma (R2655)	Western blot

2.1.7. Oligonucleotides

All oligonucleotides used during this study and listed in Table 2.6 were obtained from Sigma.

Table 2.6. **List of oligonucleotides used for PCR**

Number	Name	Sequence	Use	Reference
2292	GC-rich DNA_fw	ATGAGAAAGCGCCACGCT	GC rich DNA (for beads)	This study
2291	GC-rich DNA_rev	biotin-ATAGGCGTATCACGAGGC	GC rich DNA (for beads)	This study
261	GC FWD 90	GATCGGTGCGGGCCTCTTCG	GC rich 90bp	Speck lab
263	ARS1 150	CAAAATAGCAAATTTCG	150 bp	Speck

	FWD	TCAAAAATGC	ARS1	lab
453	ARS1 150 REV	TTTACATCTTGTTATTTTACAGATTTTATGTTTAGATC	150 bp ARS1	Speck lab
475	GC REV 290	GGGAAAACCCTGGCGTTACC	GC rich 90bp	Speck lab
1693	Amp pUC19 F	GAAGATCAGTTGGGTGCACG	10XARS1	Speck lab
1568	Amp pUC19 R	Biotin-GCATCTTTTACTTTCACCAGCG	10XARS1	Speck lab
1567	Amp pUC19 F	Biotin-GAAGATCAGTTGGGTGCACG	1XARS1	Speck lab
1569	Amp pUC19 R	GCATCTTTTACTTTCACCAGCG	1XARS1	Speck lab
1574	pUC57_fw	AACAGCTATGACCATGATTACG	10Xshort ARS1	This study
2322	pUC57_fw	biotin-ACGGTTCCTGGCCTTTTGCT	10Xshort ARS1	This study
2323	pUC57_rev	GGGCGACACGGAAATGTTGA	10Xshort ARS1	This study
2324	pUC57_rev	biotin-GATTGTACTGAGAGTGCACC	10Xshort ARS1	This study
2325	GC rich_FW	biotin-AGTGGACCGAGCCCAAGGAC	10XAB1	This study
2326	GC rich_rev1	CCAGGAACAGGGTGAGGTGG	10XAB1	This study
2327	GC rich_rev2	TCAAGCCCTTCCTCCTCAAGAAG	10XAB1	This study
2328	GC rich_rev3	CCCCACCACGATCACGCTC	10XAB1	This study

2.1.8. Yeast media

Table 2.7. **List of yeast media and their components used in this study**

	SC agar	SC broth	SC dropout for Gal induction	Rich medium
Yeast nitrogen base without amino acids	0.69%	0.69%	0.69%	---
Yeast extract	---	---	---	10g/l
Peptone	---	---	---	20g/l
Supplement mix (-His,-Ura,-Leu,-Trp)	0.06%	0.06%	0.06%	--
Histidine	20mg/l	20mg/l	20mg/l	---
Adenine	20mg/l	20mg/l	20mg/l	---
Glucose	20g/l	20g/l	5g/l	0.1g/l
Agar	20g/l	---	---	---
Glycerol	---	---	3%	3% (w/v)
Lactic acid	---	---	2%	2%(w/v)
pH	6.7/7	6.7/7	6.7/7	5.5/6

2.1.9. Bacterial competent cells

DHα cells (Invitrogen) were used for routine transformation, BL21 Codon Plus – RIL cells (Stratagene) were used for protein overexpression.

2.2. Molecular biology

2.2.1. Cloning

Many of the plasmids used in this study were pre-existing in the Speck lab. A number of novel plasmids were designed by myself during this work and produced by commercial supplier (Genscript), which facilitated the cloning and subcloning procedures. All the plasmids used in this study are listed in Table 2.2.

2.2.2. Mutagenesis

All mutagenised constructs were commercially generated (Genscript) in the plasmid pUC57.

2.2.3. DNA precipitation

Ethanol precipitation was performed by adding 1/10 volume of sodium acetate 3M pH 5.2 into the DNA solution, 1 µl of glycogen and 2.5 volumes of ice cold 100% ethanol and incubated at -80°C for at least 20 minutes. The DNA was centrifuged at 13000 rpm at 4°C for 30 minutes and the supernatant discarded. The pellet was washed with 70% ethanol and centrifuged at 13000 rpm at 4°C for 5 minutes. The supernatant was removed and the pellet dried at room temperature and resupended in the desired volume of TE buffer (Qiagen).

2.2.4. Phenol-chloroform DNA extraction

An equal volume of phenol is added to the DNA solution and the mixture is vortexed for 3 minutes and centrifuged for 5 minutes at 13000 rpm. The aqueous phase (top) is removed to a new tube and one volume of chloroform is added, mixed and centrifuged for 5 minutes at 13000 rpm. 1/10 volume of 3M sodium acetate pH 5.2 is added to the aqueous phase, mixed by vortexing. 2.5 volumes of ice-cold 100% ethanol is added and incubated at -80°C for at least 20 minutes. The pellet was washed with 70% ethanol and centrifuged for 10 minutes at 13000 rpm. The supernatant was removed and the pellet air-dried and resuspeded in the desired volume of EB buffer (Qiagen).

2.2.5. Plasmid DNA preparation

All the plasmid constructs used in the experimental results discussed in the text are listed in Table 2.2. Plasmids were transformed (see paragraph 2.3.2), individual colonies were picked and grown overnight into 5ml, 25ml or 500ml LB selective culture using Qiagen Miniprep, MidiPrep and MaxiPreps respectively, according to manufacturer's guidelines.

2.2.6. Agarose gel electrophoresis

DNA samples were analysed in a homemade casted agarose gel, using an agarose concentration appropriate for the size of the DNA to analyse (0.8% to 2%). The samples were mixed with Orange G loading buffer (0.1% (w/V) Orange G dye, 50% (v/v) glycerol), loaded on a gel and analysed by electrophoresis at 100V for 30 minutes. As a reference 1kb DNA ladder was used. The running buffer (TBE) is the same used to prepare the gel. The gel was stained adding SYBR Safe (Invitrogen) in agarose gel buffer and visualised by blue-light using Fujifilm FUJI FLA 5100 imaging system.

2.3. Bacterial manipulations

2.3.1. Competent cells

The competent cells were inoculated in an overnight culture with the appropriate antibiotics in LB at 37°C. The preculture was diluted into a 500 ml LB culture while shaking at 37°C until the OD_{600}=0.6. The flasks were then cooled down on ice for 30 minutes and harvested by centrifugation for 10 minutes at 4000 rpm at 4°C. The pellet was resuspened into ice-cold 0.1M $CaCl_2$ and incubated on ice for one hour. The pellet was spun down for 10 minutes at 4000 rpm at 4°C and resuspended in 0.1 volume of the initial culture in 0.1M $CaCl_2$ and 15% (v/v) glycerol. The aliquots were frozen in liquid nitrogen and stored at -80°C.

2.3.2. Transformation

For each transformation 50 µl of competent cells were thawed on ice, mixed with 10 ng of DNA, incubated on ice for 30 minutes and heat-shocked at 42°C for 90 seconds. The cells were diluted with 950 µl of SOC medium (2% tryptone, 0.5% yeast extract, 10 mM NaCl, 2.5 mM KCl, 10 mM $MgCl_2$, 20 mM glucose) and incubated for 60 minutes at 37°C with shaking (250 rpm). 50-100 µl of cells were spread onto appropriate selection plate and incubated overnight at 37°C.

2.3.3. Cultures

One single colony from a transformation was isolated and grown into the appropriate liquid media with antibiotic selection until culture saturation (OD_{600}: 1-2 x 10^9 cells/ml).

2.3.4. Protein expression

For protein expression in *E.coli* BL21 codonPlus RIL (Stratagene, cat.: 230240) competent cells were used and supplemented with 34 µg/ml chloramphenicol and 75 µg/ml ampicillin. The protein expression was induced by adding 0.5 mM IPTG to the cultures for 5 hours at 16°C.

2.4. Yeast manipulations

2.4.1. Competent cells

Yeast competent cells containing the wild type strain (AS499) were available in the laboratory as a common stock.

2.4.2. Strain construction

The background strain used to generate all the yeast constructs during this study was AS499 (MATa bar1Δ leu2-3,112 ura3-52 his3-Δ200 trp1-Δ 63 ade2-1lys2-801 pep4) wild type, and was a gift by Luis Aragon (MRC LMS, London, UK).

2.4.3. Transformation

50 ul of competent cells containing the wild type strain (AS499) were thawed on ice, mixed with 300-500 ng of each plasmid DNA and 6 volumes of polyethylene

glycol (PEG) solution (100 mM LiAc, 10 mM Tris–HCl pH 8, 1 mM EDTA/NaOH pH 8, 40% (w/v) PEG3350), and incubated for 30 minutes at room temperature. 1/9 volume of DMSO was added, mixed and the cells were heat-shocked at 42°C for 15 minutes. Cells were spun down at 2000 rpm for 3 minutes, the supernatand discared and the pellet resuspended in 100 ul of minimal medium and plated onto SC medium (free of tryptophane, leucin and uracil) Petri plates (see Table 2.7). The plates were incubated at 30°C for 72 hours.

2.4.4. Cultures and yeast growth

A single colony obtained from the transformation was isolated and re-streaked onto fresh selective plate. After 48 hours at 30°C a single colony was picked and inoculated in SC liquid media (see table 2.7 for media composition) until saturation (OD_{600} >1.5). The culture was spun down and the pellet resuspended in 50% (w/v) glycerol and stored at -80°C as a glycerol stock.

2.4.5. Dominant lethality assay (spotting assay)

A yeast strain was plated on a SC agar dropout plate (4% glucose) and incubated at 30°C for 48 hours. Cells from the plate were transferred onto 20 ml of SC dropout medium containing lactic acid and glycerol and grown overnight at 30°C with agitation. OD_{600} of each culture was measured and adjusted to OD_{600} = 0.6. A five-fold dilution series was performed and 3 ul of each dilution were spotted onto the plates containing glucose (non-inducing condition) or galactose (inducing condition) and incubated at 30°C for the appropriate time (24-72 hours). Pictures of the plates were taken using a scanner.

2.4.6. Protein expression

Frozen cells from a glycerol stock were streaked on an agar plate in SC and dropout medium to select for the appropriate auxotrophies for three days at 30°C. The cells were removed from the plate and grown overnight in 250 ml of

liquid media SC dropout with 2% glucose. The culture was then diluted to OD_{600}=0.5 in 1.25 litres of Minimal Growth Medium for Gal Induction (Glucose 0.5% (w/v), glycerol 3% (w/v)) media and grown for 10 hours. Then 100 ml of the culture were diluted in 500 ml of the same medium overnight. At an OD_{600} in between 1.4-1.9 one volume (600 ml) of rich medium (Glucose 0.01% (w/v), glycerol 3% (w/v)) was added. After 3 hours, MCM2-7 over-expression was induced by supplementing with 20 g/L of galactose. For the G1 arrest, 5 mg/ml of α-factor was added for 2 hours before harvesting. The pellet was resuspended in a half of the pellet volume (w/v) of purification buffer, drop frozen in a beaker containing liquid nitrogen to generate frozen beads of cell suspension and stored at -80°C.

2.4.7. Cell lysis

Frozen yeast cells were lysed with mechanical lysis in the presence of liquid nitrogen in a SPEX Sample Prep 6780 freezer mill (15 cycles of 4 minutes pre-cooling, 3 minutes grinding at 15 pulses/second and 3 minutes cooling interval each) in the presence of EDTA-Free Protease Inhibitor Cocktail (Roche). After thawing the powder at 4°C with one volume (w/v) of purification buffer, the yeast extract was incubated for 2 hours with mixing and centrifuged at 28000 g for one hour. The supernatant was collected, frozen in liquid nitrogen and stored at -80°C.

2.5. Protein purifications

MCM2-7 wild type and all the variants mutants were purified by myself, unless indicated. I was involved in the purifications of Cdc6 (Speck et al., 2005) and Cdt1 (Evrin et al., 2009) proteins, whereas ORC protein was available in the laboratory (Speck et al., 2005).

Cdc6 was expressed in *E.coli* as a GST-fusion protein and purified by glutathione-agarose beads, followed by cleavage with PreScission protease and by hydroxyapatite resin. The protocol of Cdt1 expression and purification is

similar to Cdc6, with the exception that the SP sepharose was used instead of the hydroxyapatite resin (Evrin et al., 2009).

MCM2-7 was purified as previously described (Evrin et al., 2009). The Mcm3 subunit contains a HA-tag at its N-terminus. The lysed cells were resuspended in buffer (25 mM HEPES KOH pH 7.5, 10 mM magnesium acetate, 50 µM zinc acetate, 10% glycerol (w/v), 0.1% triton (w/v), 50 µM EDTA, 300 mM potassium glutamate, 3 mM ATP) with a EDTA-Free Protease Inhibitor Cocktail and extracted for 2 hours while mixing at 4°C. The cells were then centrifuged for one hour at 13000 rpm at 4°C and the extract (supernatant) incubated with anti-HA affinity beads resin (EZviewTM Red Anti-HA Affinity Gel, Sigma) for 2 hours in a rotating wheel at 4°C. The beads were rinsed with 8 column volumes of buffer supplemented with protease inhibitor and then washed with 20 column volumes of the same buffer. To elute the protein, the beads were incubated with HA peptide (0.5 mg/ml) for 3 hours at 16°C and the eluted material was concentrated using a 15 ml Amicon Ultra 100K centrifugal filter (Millipore). The concentrated eluate was injected to a gel filtration column (Increase Superose 6 10/300 GE) to remove the contaminating Mcm3/Mcm5 dimer. A sample of each fraction was analysed using Coomassie Blue-stained SDS-PAGE gel and the protein concentration was measured by Bradford. Relevant fractions containing the full MCM2-7 complex were pooled and concentrated as above. The final protein was snap-frozen in aliquots of 5 µl.

2.6. Protein analysis

2.6.1. SDS-PAGE

SDS-PAGE was carried out using either home-made or commercial pre-cast gels. For the home-made gels, 7.5% polyacrylamide gel was used and run in Tris-Glycine buffer (3% (w/v) Tris, 14% (w/v) glycine, 1% (w/v) SDS) at 250V for 35 minutes at 4°C. Alternatively, a NuPage Novex 4-12% Bis-Tris gels were used and run in either 0.5% MOPS (50 mM MOPS, 50 mM Tris Base, 0.1% SDS, 1 mM EDTA, pH 7.7) or MES buffer (50 mM MES, 50 mM Tris Base, 0.1% SDS, 1 mM EDTA, pH 7.3) at 200V for the appropriate time. As a reference a

broad range molecular weight marker (Biorad) was added. A 2X SDS-PAGE loading buffer was prepared (Laemmli buffer).

2.6.2. Protein staining

Protein samples were resolved by SDS-PAGE gel and stained with Coomassie Instant Blue (Expedeon) for one hour. Alternatively, for samples containing a lower protein amount (0.5-5 ng) silver staining was performed. The gel was initially fixed in 40% (v/v) Methanol, and 13.5% (v/v) Formaldehyde for 15 minutes and then washed twice with ultrapure water for 20 minutes. A solution containing 0.02% (w/v) sodium thiosulphate was used to sensitise the gel for 1 minute, and then washed twice with ultrapure water for 20 seconds. The gel was incubated in 0.1% (w/v) silver nitrate for 15 minutes, washed for 20 seconds and then developed with 3% (w/v) Sodium Carbonate, 0.05% (v/v) Formaldehyde, 0.0004% (w/v) Sodium Thiosulphate. The staining was stopped with 48% (w/v) citric acid for ten minutes.

2.6.3. Western blotting

Following protein resolution by SDS-PAGE, proteins were transferred to nitrocellulose membrane (GE Healthcare) in transfer buffer (6 mM sodium bicarbonate, 4 mM sodium carbonate, 20% (v/v) ethanol pH 12) at 250 mA for 3.5h at 4°C. Membranes were blocked in TBST and 5% milk for 30 minutes before being probed with primary antibodies overnight at 4°C. After 3 washes of 15 minutes each in TBST, the membranes were incubated with HRP-secondary antibody for one hour. Membranes were washed again and detection was carried out using enhanced chemiluminescence and exposed onto X-ray films (Thermo Scientific). After immunodetection, whenever re-blotting was required, the membranes were washed with TBST and incubated with Restore Western Blot Stripping Buffer for 15 min. Membranes were then washed three times for 10 min and re-probed.

2.6.4. ^{32}P visualisation

Samples containing ^{32}P radiolabel were analysed by thin layer chromatography (TCL), the plate was dried and exposed to a phosphor imaging screen for the appropriate time. After the exposure, the screen was scanned using the Phosphoimager (Fujifilm FUJI FLA 5100).

2.7. Bead-based helicase loading assay

2.7.1. Origin DNA amplification

Different DNA containing one or ten yeast origins were used during this study, either already pre-existing in the Speck lab (1XARS1, 10XARS1, 10XARS1short) or generated during this study (10XAB1). Each of these DNA constructs is generated in a pUC19 plasmid and the relevant fragment was amplified by PCR using one biotinylated and one non-biotinylated primer. The resulting linear DNA was purified with the QIA quick spin column purification kit, following manufacturer's instructions.

2.7.2. Conjugation of origin DNA to magnetic beads

MyOne Streptavidin T1 dynabeads (Invitrogen) were washed in 10 mM TRIS-HCl pH7.5, 1mM EDTA, 2M sodium chloride and incubated overnight at 24°C at 1400 rpm with the purified DNA from 2.7.1. The beads-DNA were then washed twice, resuspended and stored at 4°C in 10 mM TRIS-HCl pH7.5, 1mM EDTA, 2M NaCl.

2.7.3. *In vitro* reconstitution of MCM loading (pre-RC assay)

The in vitro pre-RC assay was performed as previously described (Evrin et al., 2009; Fernandez-Cid et al., 2013; Sun et al., 2013; Yuan et al., 2017). 40 nM ORC, 80 nM Cdc6, 40 nM Cdt1 and 40 nM MCM2-7 were incubated on ice for 20 minutes in pre-RC buffer (50 nM HEPES KOH pH 7.5, 10 mM magnesium acetate, 10% glycerol, 100 uM zinc acetate, 100 mM potassium glutamate, 50 uM EDTA, 0.1% triton X-100, 5 mM DTT, 3 mM ATP or ATPγS) followed by another incubation for 20 minutes at 24°C. 6 nM of origin containing DNA coupled to magnetic beads were added to the proteins and incubated for 20 minutes at 24°C. Beads were washed 3 times with either pre-RC buffer or high salt buffer (pre-RC buffer plus 300 mM NaCl) before the complexes were eluted from the beads with DNaseI. Final products were analysed by SDS-PAGE and silver staining (Figure 2.1).

Each experiment performed using the pre-RC assay, showed in this thesis was repeated at least twice.

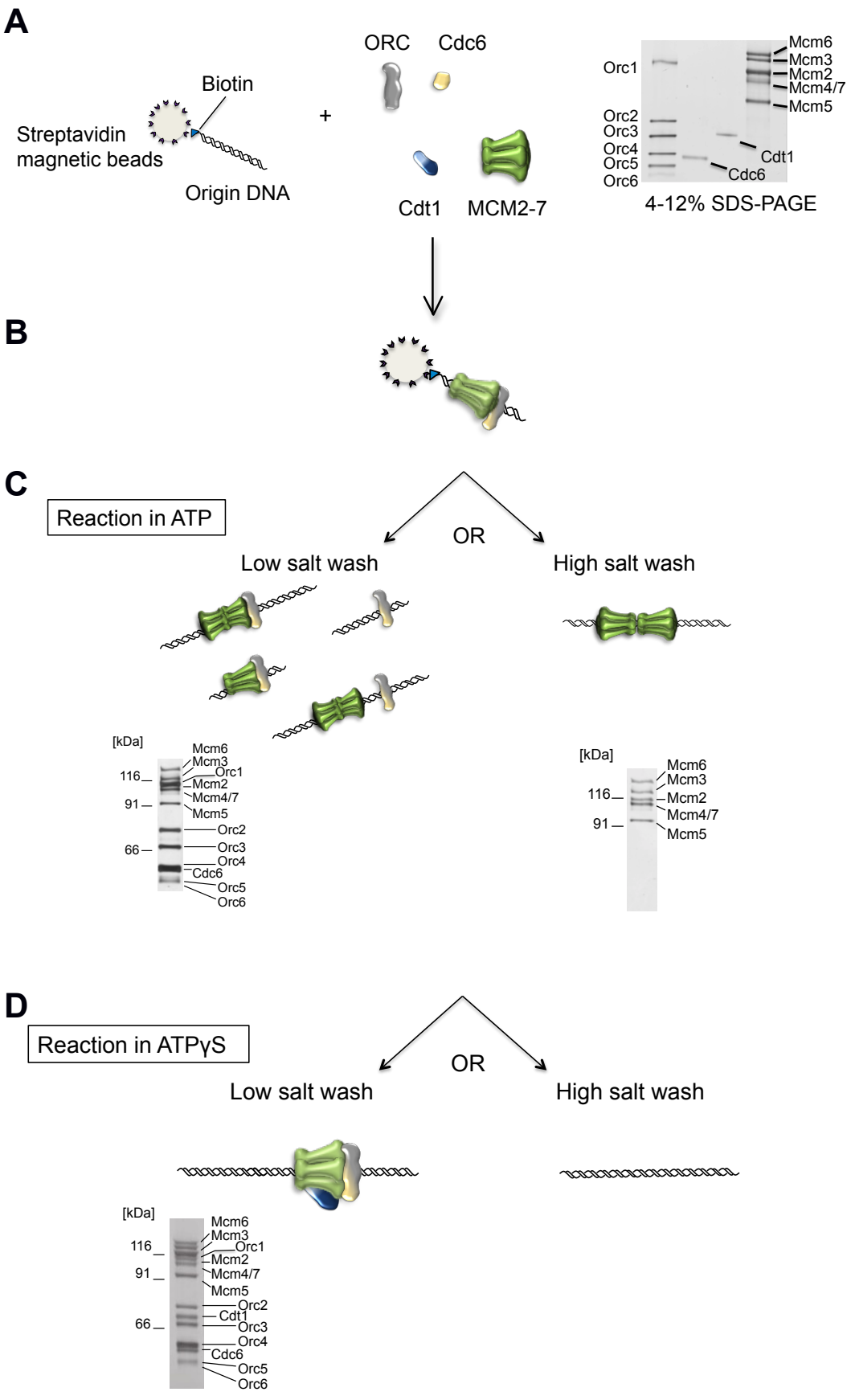

A
Biotin
Streptavidin
magnetic beads
Origin DNA
+
ORC
Cdc6
Cdt1
MCM2-7
Orc1
Orc2
Orc3
Orc4
Orc5
Orc6
Mcm6
Mcm3
Mcm2
Mcm4/7
Mcm5
Cdt1
Cdc6
4-12% SDS-PAGE
B
C
Reaction in ATP
OR
Low salt wash
High salt wash
[kDa]
116
91
66
Mcm6
Mcm3
Orc1
Mcm2
Mcm4/7
Mcm5
Orc2
Orc3
Orc4
Cdc6
Orc5
Orc6
D
Reaction in ATPγS
OR
Low salt wash
High salt wash
Cdt1

Figure 2.1. Schematic representation of *in vitro* reconstitution of pre-RC

A) Biotinylated DNA containing origin of replication is immobilised on streptavidin-coated magnetic beads. Purified ORC, Cdc6, Cdt1 and MCM2-7 are incubated with the DNA in buffer containing either ATP or ATPγS. The silver stained SDS-PAGE on the right hand side shows the purified proteins. **B**) The proteins are associated in a complex on DNA bound to beads. **C**) For the reactions set up in ATP, after low salt washes the reaction contains a mixture of complexes with the retention of ORC, Cdc6 and MCM2-7, as Cdt1 is released upon ATP hydrolysis. The silver stained gel on the left hand side shows a typical result. High salt wash (300 mM sodium chloride) washes away all the proteins but retains on DNA the loaded double hexamer. The gel shows the absence of ORC, Cdc6 and Cdt1. **D**) For the reaction assembled in the presence of ATPγS, low salt wash shows that all the proteins are recruited on origin DNA. Note on the silver stained gel the presence of Cdt1, which is still bound since ATP hydrolysis is blocked. Under high salt wash, all proteins are washed away. (Evrin et al., 2009; Remus et al., 2009)

2.8. Immuno-precipitations

To generate anti-GST, anti-HA, anti-MBP antibody beads, 50 µl of Dynabeads Protein G (Invitrogen) were washed with PBS-T. 10 µg of each appropriate antibody was added to the beads and incubated for 15 minutes at 24°C while mixing. The beads were then washed 3 times with PBS-T to remove unbound antibody and resuspended in 2 volumes of PBS-T.

2.9. MCM2-7 immuno-precipitation assay

A double size pre-RC reaction was assembled as described above (2.7.3) using either MBP-tagged MCM2-7 (80 nM) or untagged MCM2-7 (80 nM) or MBP-tagged MCM2-7 (40 nM) and tagged-MCM2-7 (40 nM) together. After elution of the complex from the beads using DNaseI, anti-MBP dynabeads were added to the elution and incubated for 7.5 minutes at 24°C with mixing. After immunoprecipitation of the reaction, the beads were washed 3 times with pre-RC buffer and analysed by western blot.

2.10. ATPase assay

The ATPase assay was performed as previously described (Fernandez-Cid et al., 2013; Speck and Stillman, 2007) . A 150 bp fragment containing the ARS1 sequence was amplified with forward primer (CAAAATAGCAAATTTCGTCAAAAATGC) and reverse primer (TTTACATCTTGTTATTTTACAGATTTTATGTTTAGATC) from the template plasmid pUC19 ARS1 (pCS372). 2.5 pmol of DNA was incubated with 2.5 pmol of MCM2-7 (or mutants), ORC, Cdc6 (or Cdc6 E224Q, Cdc6 E224G) and Cdt1 in 12 µl of buffer (25 mM Hepes, pH 7.6, 100 mM KGlu, 5 mM MgAc, 1 mM DTT, 1 mM EDTA, 1 mM EGTA, 0.1% (v/v) Triton X-100, 10% (w/v) glycerol) for 30 minutes on ice. 5 µCi of [α-32P] ATP (3000 Ci/mmol) were added to each reactions and incubated at 24°C. After 15, 30, 45, 60 minutes 2 µl were taken from each sample and incubated with 0.5 µl of stopping solution (2% SDS, 50 mM EDTA, 20 mM ATP, 20 mM ADP). 1 µl sample was spotted on TLC cellulose plate and developed in 1 M formic acid and 0.5 M lithium chloride for 20 minutes. The plates were washed in ultra pure water for 10 minutes, dried and exposed on an imaging plate. The ^{32}P was visualised using the Phosphoimager as described in 2.6.4 (Figure 2.2).

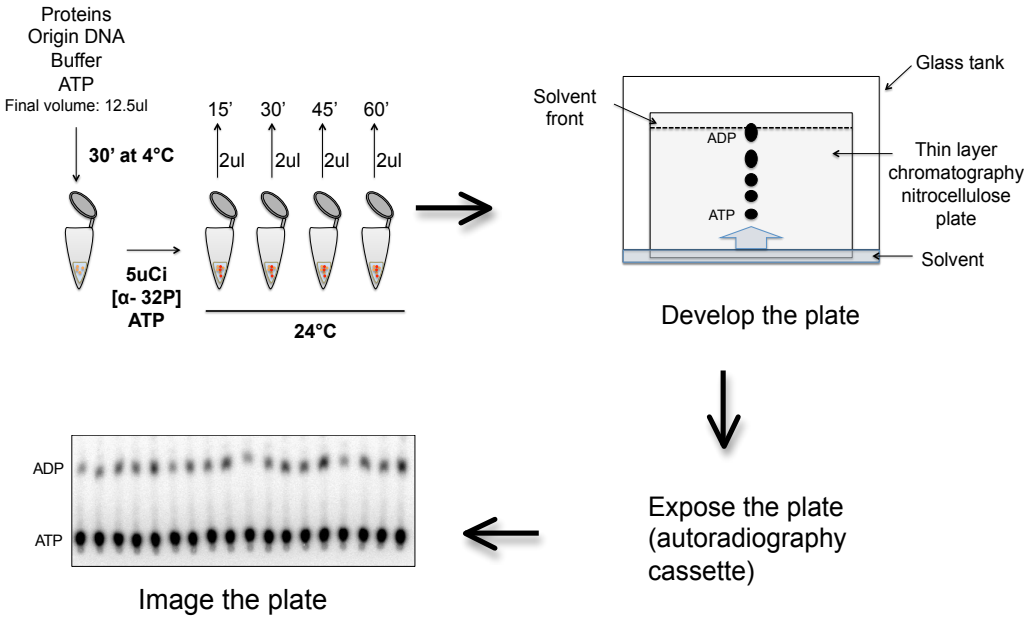


Figure 2.2. ATPase assay

The proteins of interest are incubated with origin DNA in buffer containing ATP for 30 minutes at 4°C. Then, [α-32P]-ATP is added and the reactions incubated at 24°C. 2 µl are collected every 15 minutes and stopped with SDS and spotted on a thin layer chromatography (TLC) plate. The plate is developed in a TLC tank, exposed using an autoradiography cassette and imaged.

2.11. Single particle Electron Microscopy

2.11.1. Samples preparation

In vitro pre-RC reactions on linear ARS1 containing DNA were prepared following the standard protocol described in 2.7.3. The proteins were incubated in pre-RC buffer (50 nM HEPES KOH pH 7.5, 10 mM magnesium acetate, 10% glycerol, 100 µM zinc acetate, 100 mM potassium glutamate, 50 µM EDTA, 0.1% triton X-100, 5 mM DTT, 3 mM ATP or ATPγS). The beads were washed with pre-RC buffer before digestion with DNaseI in EM buffer (50 mM HEPES KOH pH 7.5, 100 mM potassium acetate, 5 mM magnesium acetate) with the addition of 5% pre-RC buffer for 6 minutes at 24°C.

2.11.2. Grids preparation (negative staining)

3 µl of the pre-RC sample was applied to a glow-discharged (PELCO easiGlow) grid for 30 seconds. The grid was blotted with filter paper, washed with a 3 µl drop of EM buffer and blotted, before a 3 µl drop of an 2% uranyl acetate aqueous solution was deposited. After 30 seconds, it was blotted and air-dried.

2.12. Statistical analysis

Where appropriate, comparison of data between multiple groups was performed by using Anova followed by Turkey's post hoc test or Bonferroni correction. *P* values equal or less than 0.05 were considered statistically significant.

Chapter 3

Function of the Mcm5 carboxyl-terminus during pre-RC

3.1. Introduction

The carboxyl-terminal domain of the Mcm5 subunit (Mcm5C) contains a WHD. Preliminary data obtained by the Speck lab (Winkler and Speck, unpublished) have suggested that Mcm5C plays an essential role in the formation of the pre-RC, however no published studies have reported to date on the function of the Mcm5 C-terminal region. At the time when this study was started, no high-resolution structures of the pre-RC intermediates were available. In the existing low-resolution structures, the WHDs of the MCM subunits were not revealed, possibly due to the flexible nature of the C-terminal domains and the limited resolution. Recently the Speck group in collaboration with the Li group, obtained a high resolution structure of the OCCM intermediate in which the C-terminal regions of the MCM subunit were revealed (Yuan et al., 2017). In contrast to the corresponding regions of the other Mcm subunits, the position of the C-terminal WHD of Mcm5 in the context of the OCCM complex was not resolved. This perhaps suggests that this domain exhibits a greater degree of flexibility in this complex than is seen in the other Mcm subunits. We therefore hypothesised that the Mcm5C may have a divergent role in complex formation, and may regulate the transition from OCCM to OCM during the pre-RC formation pathway. This hypothesis is examined through the experimental work described in this thesis chapter, investigating the function of the Mcm5C through combined use of structural, biochemical and *in vivo* techniques.

To examine the role of the Mcm5C, the Speck lab had generated a full-length MCM2-7 construct exhibiting deletion of the entire C-terminal region of Mcm5 (Winkler and Speck, unpublished). This construct was first expressed and purified from *S. cerevisiae* (Figure 3.1). As previously described in the introductory chapter, the model for formation of the pre-RC progresses through several defined stages. Therefore, in this chapter the effect of the C-terminal deletion of Mcm5 on pre-RC formation at different stages we examined using

assays reconstituting these different processes to identify specific defects in pre-RC formation. This included an assessment of salt stability in pre-RC formation (Figure 3.2), ability to engage Cdt1 (Figure 3.3) and the effect of the C-terminal region on ATP-hydrolysis of the multiple ATPases present in the wider complex (Figure 3.9). The effect of the C-terminal deletion on cell viability was also assessed *in vivo* in yeast (Figure 3.2). The purified helicase loading intermediate complex was also subjected to structural analysis by Cryo-EM, preliminary data for which is presented in Figure 3.6. Taken together, this functional analysis presented here strongly suggests an essential role of the Mcm5C in the MCM2-7 complex.

3.2. The Mcm5 C-terminus is essential for double hexamer formation and for cell viability

To investigate the role of the *S. cerevisiae* Mcm5C in pre-RC formation, a MCM2-7 construct harbouring deletion of amino acids 693-775 in Mcm5 was generated (MCM2-7ΔC5) (Winkler and Speck, unpublished) and expressed in *S. cerevisiae* as described previously (Material and Methods paragraph 2.4.6). The purified MCM2-7 complex was obtained after HA affinity tag purification and size exclusion chromatography, following the protocol described in Materials and Methods (paragraph 2.5). A Coomassie stained gel of the fractions obtained during the MCM2-7ΔC5 purification is shown in Figure 3.1 A and the final product of the purification is shown in Figure 3.1 B, together with a WT for comparison.

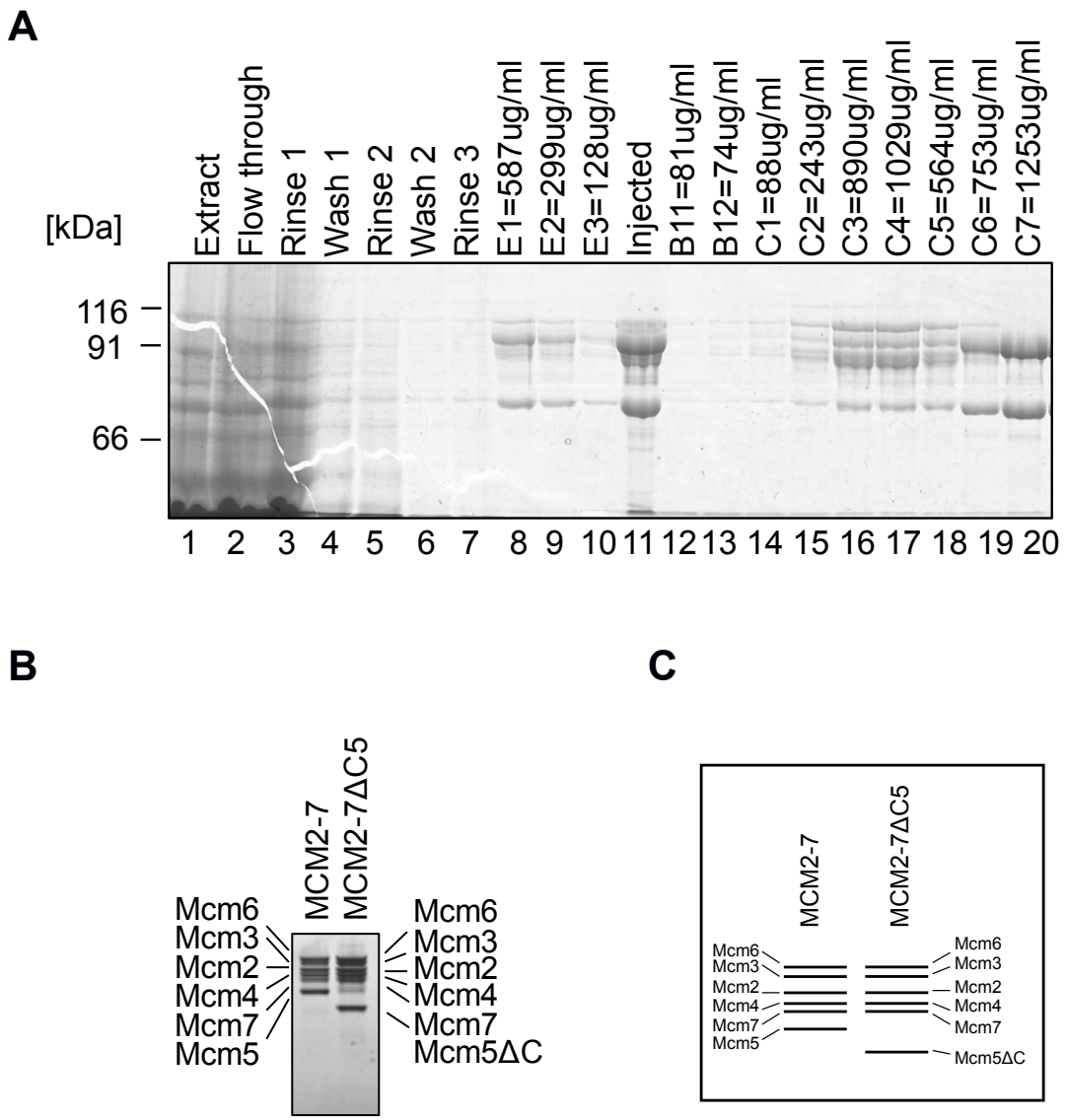


Figure 3.1. Purification MCM2-7ΔC5 from *S.cerevisiae*

A) Comassie-blue stained gel of the two-step MCM2-7ΔC5 purification. Yeast extract produced via freezer milling was incubated with anti-HA beads, rinsed and washed twice (lanes 3-7) before bound MCM2-7ΔC5 (via HA-Mcm3) was eluted three times with HA peptide (lanes 8-10). The eluate was concentrated and injected into a size-exclusion chromatography column (lane 11). The fractions were collected and analysed in a 7.5% SDS-PAGE (lanes 12-20). Fractions from lanes 15 to 18 were collected, concentrated and aliquoted. Bradford concentrations are indicated on top of each lane. **B)** Silver stained SDS-PAGE showing the purified MCM2-7 and MCM2-7ΔC5. The band corresponding to each Mcm subunits are labelled. **C**) Schematic diagram of figure B, showing the six different bands representing the Mcm subunits.

The purified protein was tested for its function to form a pre-RC *in vitro*. The ability of the protein to form the double hexamer was assessed relative to the wild-type complex employing the pre-RC assay, following the protocol previously described (Materials and methods section 2.7.3). The assay employs biotinylated origin DNA that is immobilised on streptavidin beads. The helicase loading complexes were assembled in the presence of origin DNA, ORC/Cdc6, Cdt1 and ATP, and consequently washed with low salt buffer (300 mM potassium glutamate) in order to remove loosely associated and unbound proteins or high salt buffer (300 mM sodium chloride) to retain the DNA-loaded double hexamer. The pre-RC proteins assembled with DNA in the presence of ATPγS, a slowly hydrolysable ATP-analogue, allows association of MCM2-7/Cdt1 to origin-bound ORC/Cdc6, but inhibits salt-stable double hexamer formation (Randell et al., 2006). Following complex assembly, the DNA is finally eluted from the beads using DNaseI, which degrades the DNA. The eluted fraction was run on the gel, visualising proteins that have formed a stable association with the DNA (Figure 3.2 A). In both, WT and mutant, a similar level of complex assembly was observed in the presence of ATPγS (Figure 3.2 A, lanes 6 and 9). In contrast, in the presence of hydrolysable ATP, the wild-type MCM2-7 remains bound to DNA, but association of the mutant MCM2-7ΔC5 complex was reduced in low salt conditions (compare Figure 3.2 A, lanes 7 and 10). Under high salt conditions, the association of the MCM2-7ΔC5 complex was completely abolished, whereas the wild-type complex was observed to remain bound to the DNA (Figure 3.2 A, lanes 8 and 11). This result shows that the MCM2-7 mutant lacking the Mcm5C does not support DNA-loaded double hexamer formation. Together this suggests that MCM2-7ΔC5 is less stably bound to the DNA in the presence of ATP hydrolysis and high salt conditions compared to the wild type.

To determine if overexpression of MCM2-7 containing the deletion of Mcm5C affects the cell viability, an *in vivo* dominant lethality assay was performed (Figure 3.2 B). The wild type MCM2-7 and the deletion mutant overexpression strains were spotted in a 5-fold serial dilution on dropout media containing either 2% glucose (no protein expression induced) or 2% galactose (inducing condition) and grown at 30°C. Dominant lethality of the deletion

mutant was observed in the presence of galactose, suggesting that the mutant protein is not fully functional.

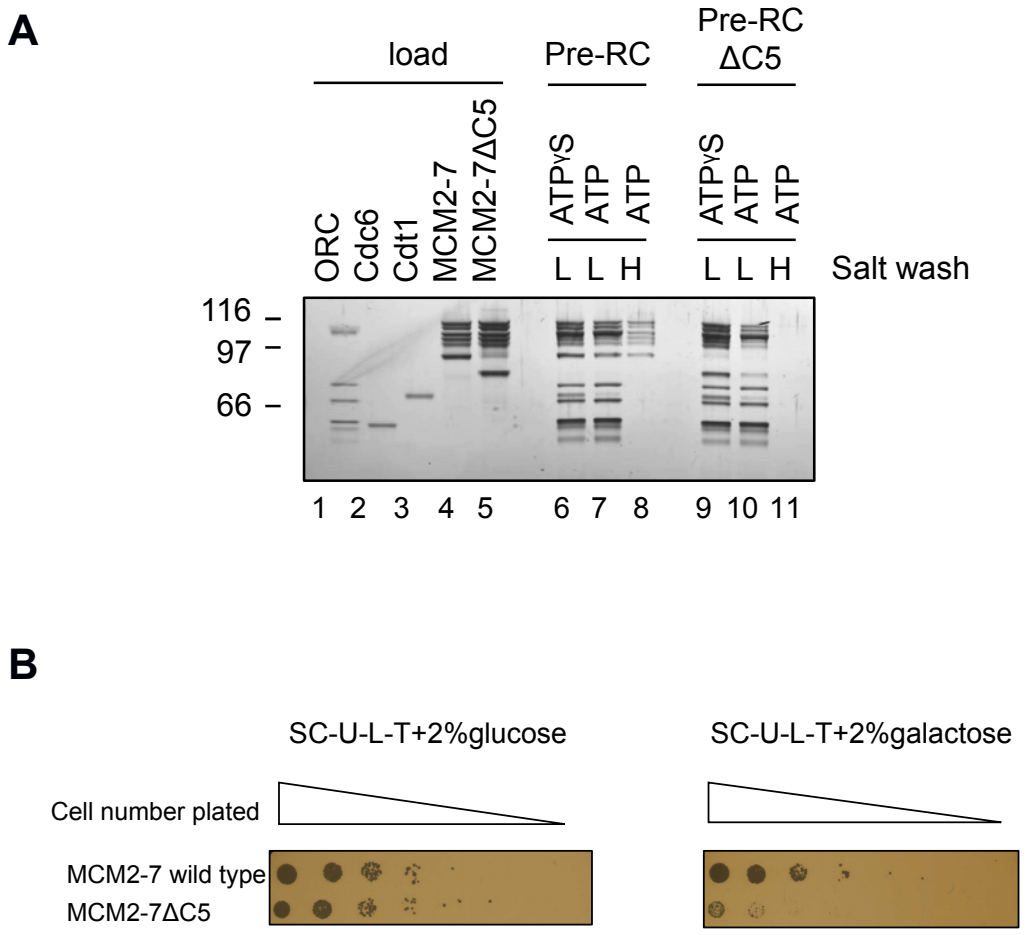


Figure 3.2. In *vitro* and *in vivo* test of MCM2-7ΔC5 activity

A) Silver stained gel showing the in vitro reconstitution of the pre-RC to test the ability of Mcm2-7ΔC5 to associate with origin DNA in the presence of ORC, Cdc6, Cdt1 and to load in a salt stable way onto DNA. The assay was performed as previously described (Evrin et al., 2009). Lanes 1-5: 20% load of each protein used in the reaction. Pre-RC reactions were formed in the presence of ATPγS (lanes 6 and 9) or ATP and washed with low salt buffer (lane 7 and 10) or with buffer containing 300 mM sodium chloride (lanes 8 and 11) and released from DNA with DNaseI. The experiment was performed three times. **B)** Yeast growth assay showing the effect of overexpression of the wild type MCM2-7 and the MCM2-7ΔC5 strains. A 5-fold serial dilution of cells at the starting density of 10^7 was spotted onto selective dropout plates with either 2% glucose or 2% galactose. The plates were incubated at 30°C for two and four days respectively. The experiment was performed in duplicate.

3.3. Cdt1 is required for OCM complex assembly with MCM2-7ΔC5

An interaction between Cdt1 and the Mcm6C has previously been reported (Fernandez-Cid et al., 2013; Zhang et al., 2010). Here it was observed that the Mcm6C contains an auto-inhibitory domain that is alleviated by the binding of Cdt1.

The cryo-EM structure of the OCCM complex (Yuan et al., 2017) provided no evidence for a direct interaction between Mcm5C and Cdt1. However, if Mcm5C bypasses the requirement for Cdt1 dependent OCCM formation is not known. In order to test this idea, a pre-RC assay in the presence and absence of Cdt1 was performed (Figure 3.3). Consistent with previous data (Fernandez-Cid et al., 2013), WT MCM2-7 was not recruited by ORC/Cdc6 (Figure 3.3, lane 9). Whilst MCM2-7ΔC5 was able to associate with ORC/Cdc6 in the presence of Cdt1, no Cdt1 independent interaction of MCM2-7ΔC5 with ORC/Cdc6 was observed (Figure 3.3, lanes 12 and 15). Although the deletion of Mcm5C and removal of Cdt1 both block MCM2-7 double-hexamer formation, the mechanisms are likely very different (Figure 3.3, lanes 11 and 14).

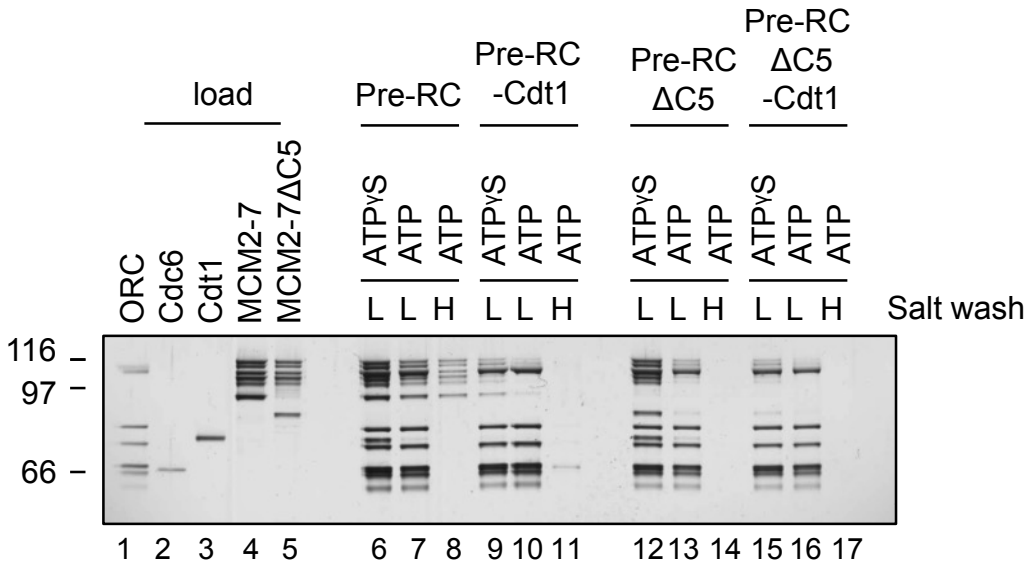


Figure 3.3. Analysis of the effect of Cdt1 on pre-RC formation in the presence of MCM2-7ΔC5

In vitro pre-RC assay was performed as previously described (Evrin, 2009). The reactions were assembled on DNA, using ORC, Cdc6 and in the presence or absence of Cdt1. The MCM2-7 wild type was used as a control (lanes 6-11) to compare the activity of MCM2-7ΔC5 (lanes 12-17). The experiment was performed twice.

3.4. Both hexamers require a functional Mcm5 C-terminus

Figure 3.2 showed that the MCM2-7ΔC5 is not functional in double hexamer formation. If the second hexamer is recruited in a Mcm5C independent way, then the MCM2-7ΔC5 should be recruited as the second hexamer in the presence of WT MCM2-7. In order to assess whether stable double hexamer formation requires both hexamers to possess the full-length MCM5 protein, the pre-RC assay was performed with a 1:1 mixture of WT and mutant protein. Addition of MCM2-7 wild type to MCM2-7ΔC5 did not help the loading of the mutant complex, as only the WT, but not the lower-running ΔC5 construct was retained on the DNA (Figure 3.4 A, lane 10). This indicates that both MCM2-7 hexamers require a functional Mcm5C to form a double hexamer.

To determine whether the C-terminal region alone could restore the function of double hexamer formation in the context of the truncated protein, the Mcm5C was purified from *E. coli* and added to MCM2-7ΔC5 in a pre-RC assay. Consistent with the previous data, double hexamer formation was essentially abolished in the mutant protein following high salt wash, and was not enhanced in the presence of the added C-terminal construct (Figure 3.4 B).

Taken together these results indicate that the Mcm5C is not required for the initial recruitment of MCM2-7 to ORC/Cdc6, but that this domain is essential for double hexamer formation.

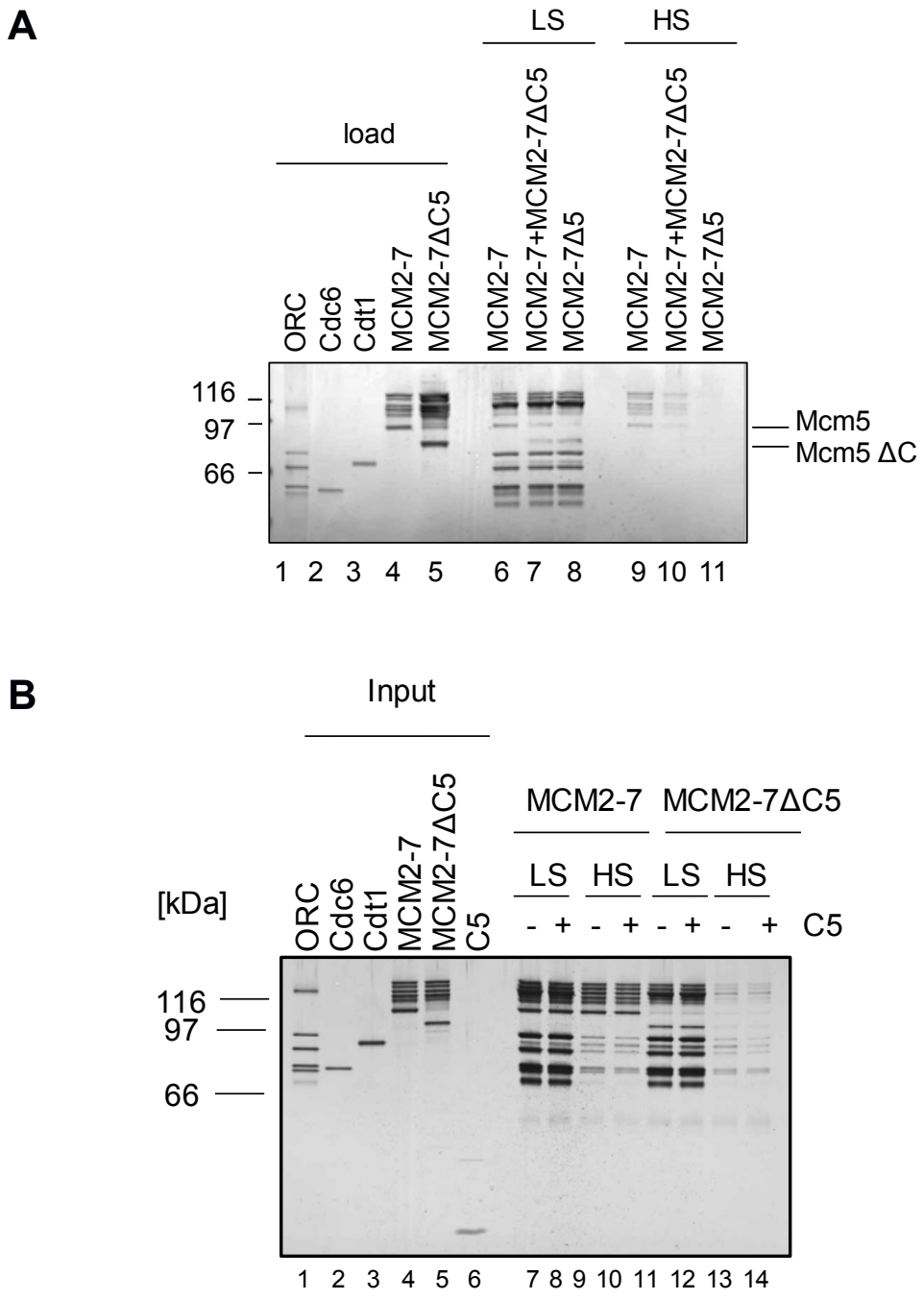


Figure 3.4. Analysis of pre-RC assembly in the presence of MCM2-7 WT and soluble Mcm5 C-terminus

A) Silver stained gel showing the reconstituted pre-RC in the presence of MCM2-7 wild type alone (40 mM), MCM2-7ΔC5 alone (40 mM) or together in a ratio 1:1 (20 mM of each protein) (lanes 7 and 10). The reactions were washed with low or high salt buffer. A 20% load of the proteins used is shown in lanes 1-5. **B)** Pre-RC assay using the wild type protein and MCM2-7ΔC5 mutant in the presence or absence of the soluble C-terminus of Mcm5 purified from *E. coli*. The reactions were assembled in pre-RC buffer in the presence of ATP and washed with low salt (LS) or high salt (HS) (300 mM NaCl). The experiments were performed twice.

3.5. The MCM5 C-terminus is not required for insertion of DNA into the MCM2-7 ring

It has been shown previously that DNA loading of MCM2-7 occurs at the stage of OCCM formation (Samel et al., 2014). Recent structural data supported this analysis by directly visualising the DNA inside the OCCM (Yuan et al., 2017).

Consistent with the previous data, the MCM2-7ΔC5 complex assembled in the presence of ORC, Cdc6, Cdt1 and ATPγS remained bound to the DNA beads, even following a higher salt (300mM NaCl) wash, while ORC, Cdc6, Cdt1 become destabilised (Figure 3.5, lane 9). This suggests that MCM2-7ΔC5 is loaded on DNA at the stage of OCCM, similarly to the WT (Figure 3.5 lane 8).

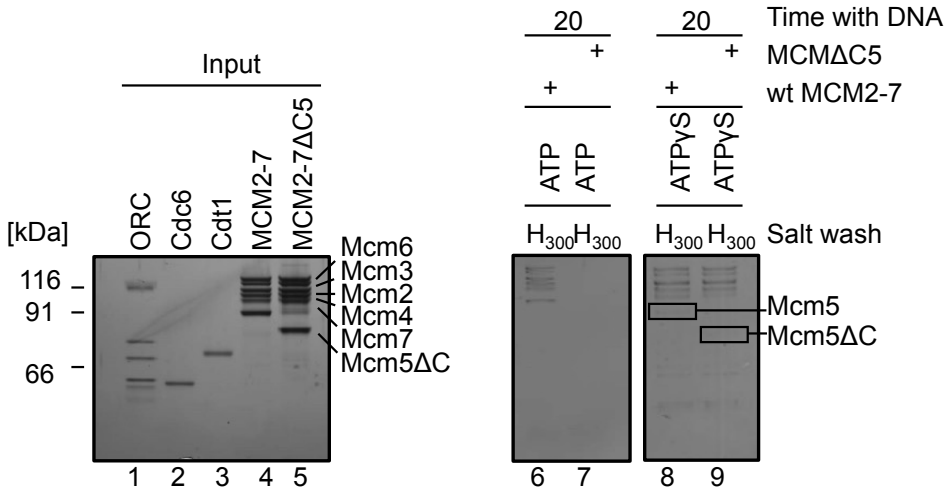


Figure 3.5. DNA is inserted into the MCM2-7ΔC5 ring

Pre-RC reactions with MCM2-7 or MCM2-7ΔC5 were assembled in the presence of ATP (lanes 6 and 7) or ATPγS (lanes 8 and 9), washed with high salt (H300= 300 mM NaCl) and analysed by silver staining. The MCM2-7ΔC5 mutant did not support salt stable double hexamer (lane 7) but showed helicase loading around DNA in the presence of ATPγS (lane 9). The wild type MCM2-7 is shown as a control. The experiment was repeated three times.

As shown in Figure 3.2, MCM2-7ΔC5 supports the stable assembly of an OCCM in the presence of ATPγS. We reasoned that the identification of this

stable intermediate presented an opportunity to obtain structural information of MCM2-7ΔC5, specifically, to determine whether full DNA insertion and OCCM formation could be achieved in the absence of the C-terminal domain of Mcm5 or if the mutant OCCM displays any other significant structural change.

ORC, Cdc6, Cdt1 and MCM2-7ΔC5 were assembled on DNA in the presence of ATPγS to form a stable DNA-bound OCCMΔC5. The sample was released from the beads using DNaseI, applied to a cryo-grid and visualised by cryo-EM, in collaboration with the group of Huilin Li (USA). The 2D classification of this intermediate showed the correct insertion of DNA inside the MCM2-7ΔC5 ring. The 2D averages show no evident differences to the wild type OCCM (Figure 3.6 A), suggesting that no major conformational changes are happening in this intermediate complex. The three-dimensional classification of the particles confirms that the general conformation of the OCCM is not affected by the absence of the Mcm5C (Figure 3.6 C, D).

Together, these experiments show that deletion of the Mcm5C does not compromise the initial helicase recruitment to ORC/Cdc6 and that MCM2-7ΔC5 is competent for DNA insertion OCCM formation. Given the inability of the mutant complex to form a stable double hexamer in the presence of hydrolysable ATP, this suggests that the C-terminal region of Mcm5 is likely to be involved in a later stage of the loading process.

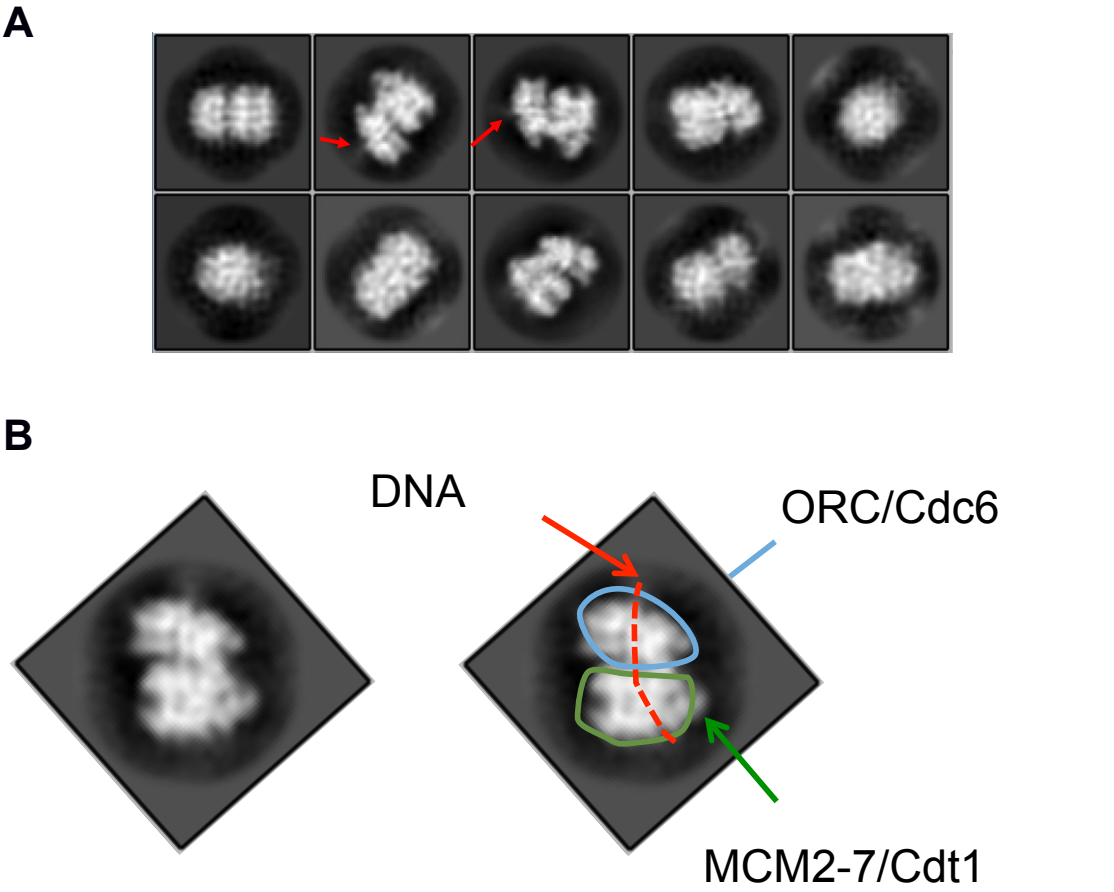

A
B
DNA
ORC/Cdc6
MCM2-7/Cdt1
C
DNA
ORC/Cdc6
MCM2-7/Cdt1
D
DNA
Cdt1
Cdt1
OCCMΔC5
OCCM wt

Figure 3.6. MCM2-7ΔC5 mutant does not affect helicase loading

A) Representative 2D classification showing various projections of the OCCMΔC5 complex assembled on DNA in the presence of ATPγS and release with DNaseI. The red arrow indicates the DNA. **B)** Enlarged view of one of the 2D classes, with the path of DNA highlighted in red. **C)** Surface view of the cryo-EM 3D classification of the different particles. **D)** Comparison between OCCMΔC5 (left) and OCCM WT (right). Red path highlights the DNA in the first 3D class, while in green Cdt1 density in indicated.

3.6. The MCM5 C-terminus role in the transition from OCCM to OCM

One possible explanation for the inability of MCM2-7ΔC5 to form a double hexamer is that the mutant complex exhibits a reduced stability, and therefore the complex disassembles and cannot maintain interaction with DNA. In order to test this possibility, the temporal stability of the wild type and MCM2-7ΔC5 complexes bound on the bead-associated DNA was tested under low salt conditions. MCM2-7ΔC5 was assembled with pre-RC proteins on DNA in buffer containing ATP for 2.5 minutes and then the unbound proteins were washed away with low salt buffer, which blocks further complex assembly. Under these conditions the OCM complex can form, but double-hexamer formation is largely suppressed (Fernandez-Cid et al., 2013). Consequently, the reactions were incubated for further 5,10,15,20 minutes in the presence of buffer only (Figure 3.7 A). Whilst some dissociation of the MCM2-7ΔC5 is observed over 20 minutes, a similar dissociation is observed with the wild type (Figure 3.7 B). Most dissociation occurs within the first 5 minutes, with no significant increase afterwards. The lack of dissociation over a long period, once an initial dissociation has occurred, strongly suggested that the stability of the mutant complex is not greatly reduced. Therefore other potential mechanisms for the defect of MCM2-7ΔC5 in MCM2-7 double hexamer formation were investigated.

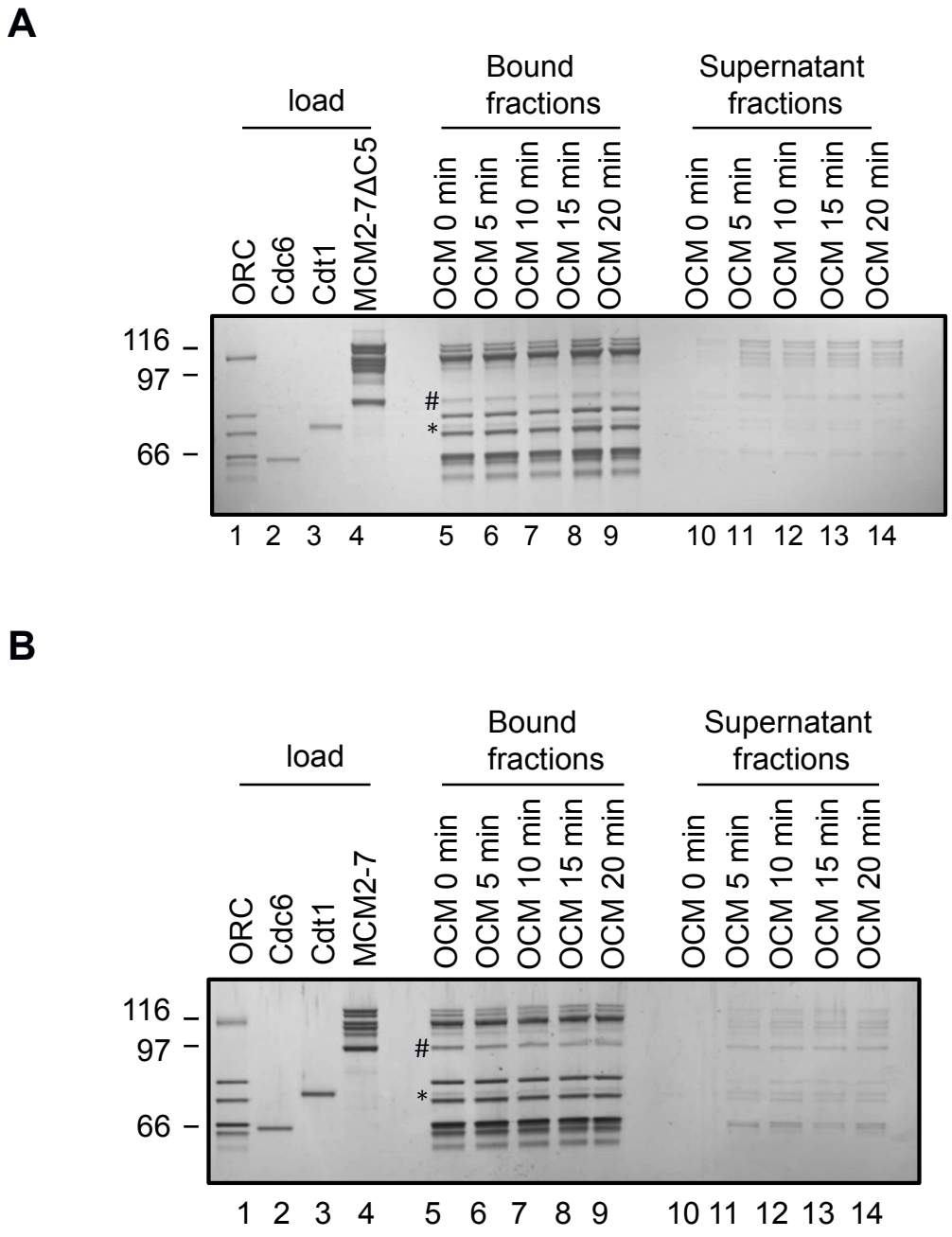
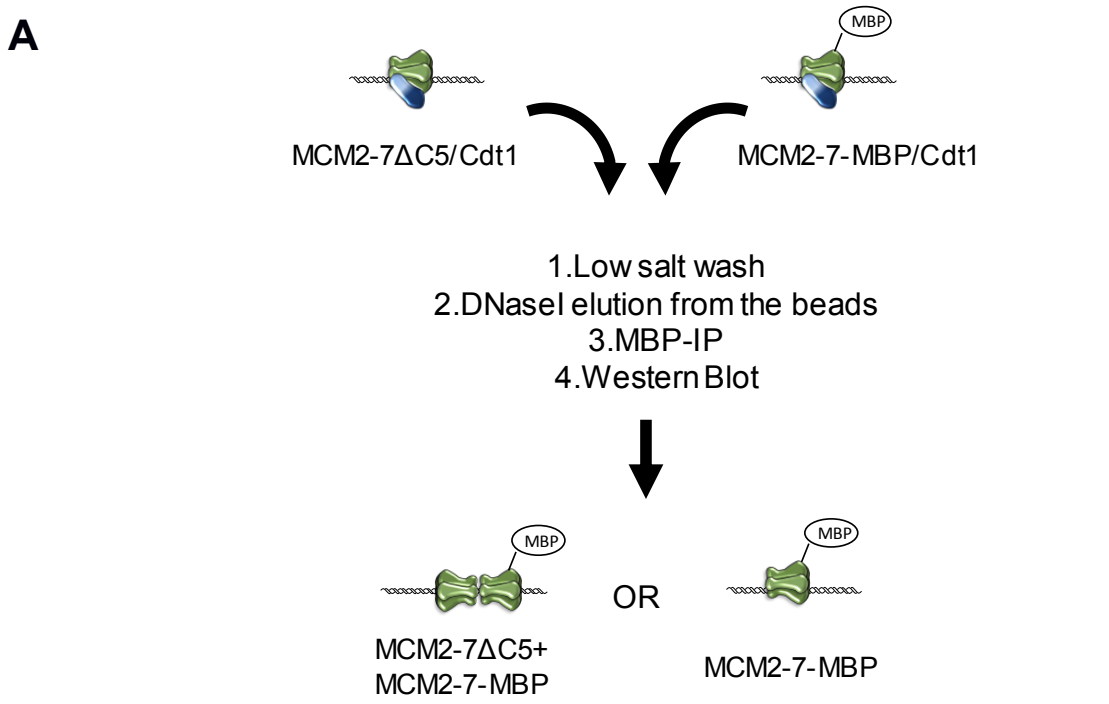


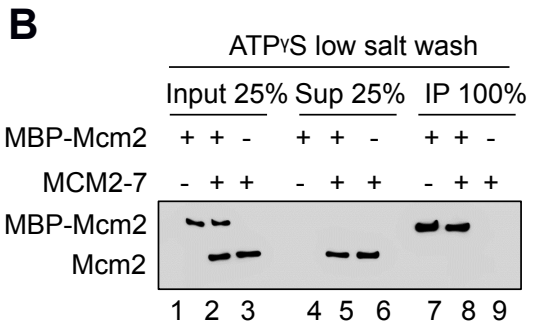
Figure 3.7. MCM2-7ΔC5 forms a stable OCM complex

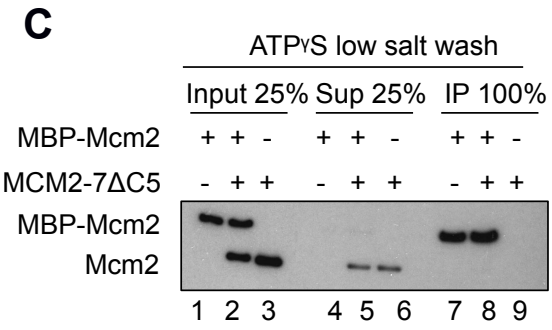
Pre-RC reactions with MCM2-7ΔC5 **(A)** or MCM2-7 **(B)** were assembled for 2.5 minutes on beads-bound DNA, washed with low salt and incubated for further 5,10,15,20 minutes. The "bound fractions" represents the DNA bound complex and the "supernatant fractions" is the proteins that were released from DNA after the second incubation. The experiment was repeated three times and reproducible. The Mcm5ΔC band is marked with # and the Cdt1 band is marked with the asterisk.

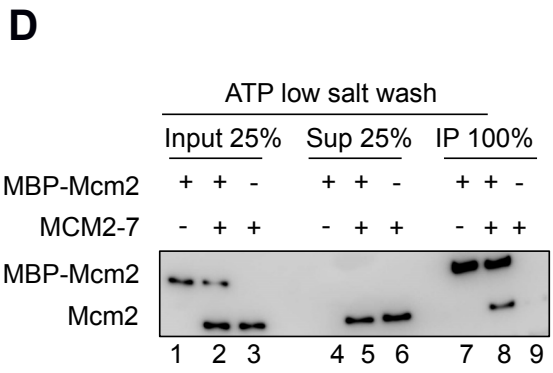
3.7. The MCM5 C-terminus in the transition from OCM to double hexamer

Previous data by the group showed that the OCM complex acts as a platform for the recruitment of a second MCM2-7 during double hexamer formation, while the OCCM complex, which forms in the presence of ATPγS, only supports recruitment of a single MCM2-7 hexamer (Fernandez-Cid et al., 2013). Here it was shown that MCM2-7ΔC5 supports the formation of the OCM complex at a reduced efficiency, but the complexes appear to be stable over time. One possibility is that these OCM complexes do not support the transition to double hexamer. In order to test this hypothesis, the ability of the OCMΔC5 to recruit a second hexamer was investigated. The experiment was performed as described in Figure 3.8 A. A pre-RC reaction was assembled with a mixed population of MBP-tagged MCM2-7 and untagged wild type or mutant MCM2-7 in the presence of ATPγS or ATP. The resulting complexes were released from DNA with DNaseI, immunoprecipitated with anti-MBP conjugated beads for 7.5 minutes and analysed by western blot for the presence of tagged or untagged MCM2-7. In the presence of ATPγS and WT MCM2-7, only the MBP-tagged MCM2-7 is detected (Figure 3.8 B, lane 8), consistent with previous results, which demonstrated that only a single hexamer becomes recruited to DNA under these conditions (Samel et al., 2014). The mutant MCM2-7ΔC5 behaved in the same way as the wild type protein (Figure 3.8 C, lane 8), consistent with previous results showing that the mutant forms an OCCM complex. In the case of ATP, untagged wild type MCM2-7 was immonoprecipitated together with the MBP-tagged MCM2-7, indicating that the second hexamer is recruited (Figure 3.8 D, lane 8). This result confirmed previously published data, showing that the MCM2-7 WT hexamers dimerise in ATP, resulting in double hexamers (Fernandez-Cid et al., 2013). When the same experiment was performed using untagged MCM2-7ΔC5, only the MBP-tagged WT MCM5-containing complexes were observed (Figure 3.8 E lane 8). These results strongly suggest that MCM2-7ΔC5 produces unproductive OCM complexes, which are unable to dimerise to form the stable double hexamer.


A
MBP
MCM2-7ΔC5/Cdt1
MCM2-7-MBP/Cdt1
1.Low salt wash
2.DNaseI elution from the beads
3.MBP-IP
4.Western Blot
MBP
MBP
OR
MCM2-7ΔC5+
MCM2-7-MBP
MCM2-7-MBP


B
ATPγS low salt wash
Input 25%
Sup 25%
IP 100%
MBP-Mcm2
MCM2-7
MBP-Mcm2
Mcm2
1 2 3 4 5 6 7 8 9


C
ATPγS low salt wash
Input 25%
Sup 25%
IP 100%
MBP-Mcm2
MCM2-7ΔC5
MBP-Mcm2
Mcm2
1 2 3 4 5 6 7 8 9


D
ATP low salt wash
Input 25%
Sup 25%
IP 100%
MBP-Mcm2
MCM2-7
MBP-Mcm2
Mcm2
1 2 3 4 5 6 7 8 9

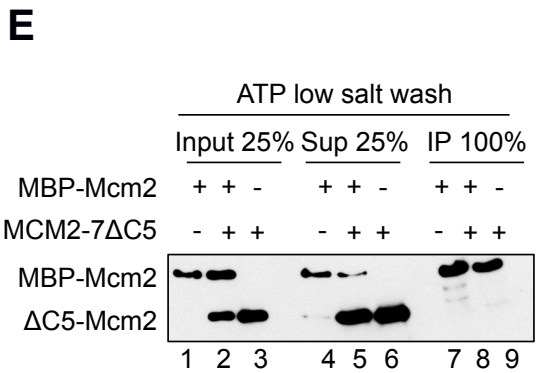

E
ATP low salt wash
Input 25%
Sup 25%
IP 100%
MBP-Mcm2
MCM2-7ΔC5
MBP-Mcm2
ΔC5-Mcm2
1 2 3 4 5 6 7 8 9

Figure 3.8. MCM7ΔC5 is not able to recruit a second hexamer.

A) Experimental outline for B-E. A mixture of MBP-tagged MCM2-7 and untagged MCM2-7/MCM2-7ΔC5 was assembled for pre-RC formation in the presence of ATP or ATPγS. The resulting complexes were released from DNA using DnaseI, MBP immunoprecipitated for 7.5 minutes and analysed by western blot for the presence of tagged or untagged MCM2-7. **B-E)** A 25% load of purified protein is shown, along with 25% IP flowthrough (sup) and 100% of the IP. (The experiments were repeated three times) **B)** MCM2-7 wild type in the presence of ATPγS was used as a control as it forms an OCCM and does not recruit a second hexamer (lane 8). **C)** MCM2-7ΔC5 in the presence of ATPγS behaves as the WT, it forms OCCM and does not recruit a second hexamer (lane 8). **D)** MCM2-7 wild type can form a mixed tagged/untagged MCM2-7 double hexamer in the presence of ATP (lane 8). **E)** MCM2-7ΔC5 in the presence of ATP and upon low salt wash does not recruit a second hexamer and only the untagged MCM2-7 is immunoprecipitated.

3.8. WT and MCM2-7ΔC5 complexes exhibit similar pre-RC induced ATPase activity

In a wild type situation, Cdt1 is released from the OCCM complex after ATP hydrolysis, forming the OCM. Furthermore, a functional Mcm6C interaction with the C-terminus of Cdt1 was described to be absolutely essential to induce ATP hydrolysis during OCM formation (Fernandez-Cid et al., 2013). We observed that the MCM2-7ΔC5 allowed the inefficient formation of OCM complexes that are completely unable to mature into the double hexamer (Figure 3.9 A, compare lane 10 vs lane 7). The rate of ATP hydrolysis of MCM2-7ΔC5 was measured using the ATPase assay previously described in the methods section (chapter 2.10). In accordance with previously published data (Fernandez-Cid et al., 2013), it was found that the rate of ORC/Cdc6 ATP-hydrolysis is very low, and that wild type MCM2-7 has a high ATPase activity which is significantly reduced by the binding of Cdt1 (Figure 3.9 B). Similarly, when the ATPase activity of the mutant MCM2-7ΔC5 was measured, alone or in complex with Cdt1, it was found that this was similar to the wild type protein. The ATPase activity of the full pre-RC reaction minus the activity of the individual components (MCM2-7/Cdt1 + ORC/Cdc6) was defined as the “pre-RC induced activity” (Fernandez-Cid et al., 2013) and is shown in red (Figure 3.9 C). These results suggest that the MCM2-7ΔC5 complex has near normal ATP hydrolysis, consistent with the observation that the complex facilitates near normal Cdt1 release during the OCCM-OCM transition (Figure 3.9 A lane 10).

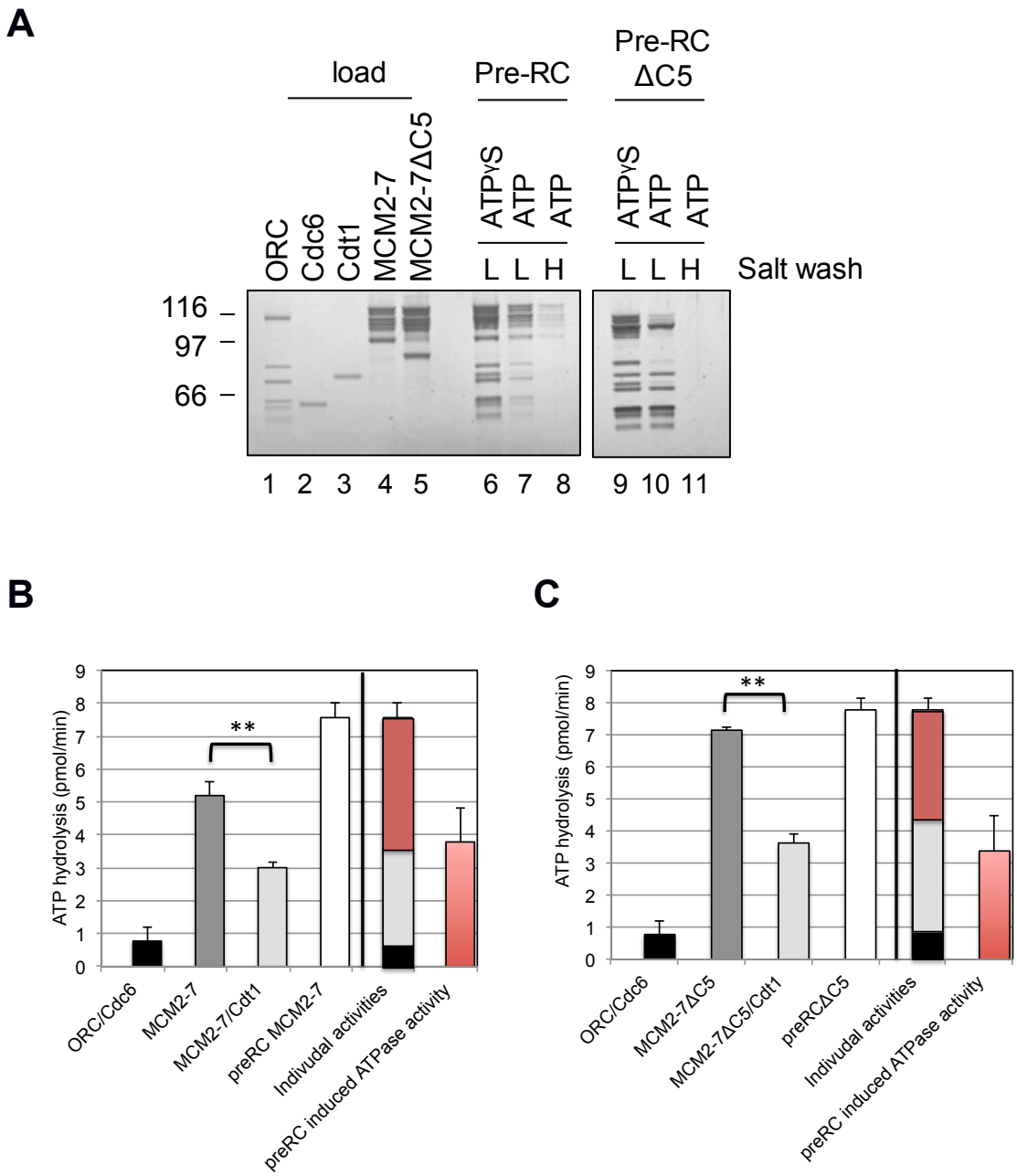


Figure 3.9. The ATP-hydrolysis produced by MCM2-7ΔC5 is similar to the MCM2-7 wild type

A) *In vitro* pre-RC in the presence of MCM2-7 WT and vs MCM2-7ΔC5. The reactions were washed with low (L) or high (H) salt buffer. **B-C)** Analysis of ATPase activities during pre-RC formation in the presence of MCM2-7 wild type or MCM2-7ΔC5. The experiment was performed as previously described (Fernandez-Cid et al., 2013; Speck and Stillman, 2007). The red bars represent the ATPase activity of MCM proteins in the presence of ORC/Cdc6. Results are plotted as average of three independent experiments. Error bars represent the standard deviation. Statistically significant results determined by one tailed t-test are indicated: ** P<0.01.

Initially, Cdc6 was thought to function mainly for Cdt1 release (Fernandez-Cid et al., 2013; Randell et al., 2006), but consequently it was shown that Cdc6 ATP-hydrolysis has a major role in the pre-RC quality control pathway, which leads to Cdc6 ATP-hydrolysis dependent complex disassembly at the OCCM stage (Coster et al., 2014). This quality control pathway becomes induced in the context of mutant ORC complexes, e.g. for Orc1-5, which does not support pre-RC formation. In order to investigate whether Cdc6 ATP hydrolysis is induced during OCCMΔC5 complex formation and if it could be responsible for the reduced efficiency of OCCMΔC5 complex formation, we measured pre-RC complex stability in the presence of a Cdc6 ATP mutant and the Cdc6 ATPase activity during pre-RC formation. Here a Cdc6 ATPase mutant (E224Q) was employed, which has previously been shown to abolish the ATPase activity of Cdc6 (Chang et al., 2015). ORC, Cdc6 E224Q, Cdt1 and MCM2-7 wild type/MCMΔC5 were assembled in the pre-RC reaction, in the presence of either ATP or ATPγS. The association of MCM2-7ΔC5 to ORC/Cdc6 in ATPγS is similar in the presence of Cdc6 wild type or Cdc6 E224Q (Figure 3.10 A, lanes 13 and 16). Remarkably, the MCM2-7ΔC5 complex formed in the presence of ATP is stabilised by the Cdc6 mutant, and exhibits reduced Cdt1 release (Figure 3.10 A, compare lane 17 vs 14). These data suggest that OCCMΔC5 induces the Cdc6 ATP-hydrolysis dependent quality control pathway significantly stronger than the wt OCCM. In order to test the hypothesis the ATP-hydrolysis rates was measured directly.

Cdc6 E224Q led to a significant reduction on pre-RC ATP hydrolysis ($p>0.05$) in the context of the WT and MCM2-7ΔC5 (Figure 3.10 B). Even though there is a trend for a decrease in the pre-RC induced ATPase activity in the context of MCM2-7ΔC5 and Cdc6Q compared to the WT, this difference is not significant (Figure 3.10 C). A stabilisation of the complex formed in the presence of MCM2-7ΔC5 and Cdc6 E224Q over time was observed in Figure 3.10 D (“bound fractions”) in comparison to the complex formed in the presence of WT Cdc6 (asterisk indicate the band of Cdt1). Taken together, these experiments showed that MCM2-7ΔC5 induces a Cdc6 ATP hydrolysis dependent quality control pathway, which leads to OCCMΔC5 complex disassembly. This can be supressed by a Cdc6 ATPase mutant, but the mutant does not support bypass of the MCM2-7ΔC5 defect, as MCM2-7 double-

hexamer formation was still blocked. Moreover, consistent with previous findings Cdc6 ATP-hydrolysis has a role in Cdt1 release (Figure 3.10 A lane 17) (Fernandez-Cid et al., 2013).

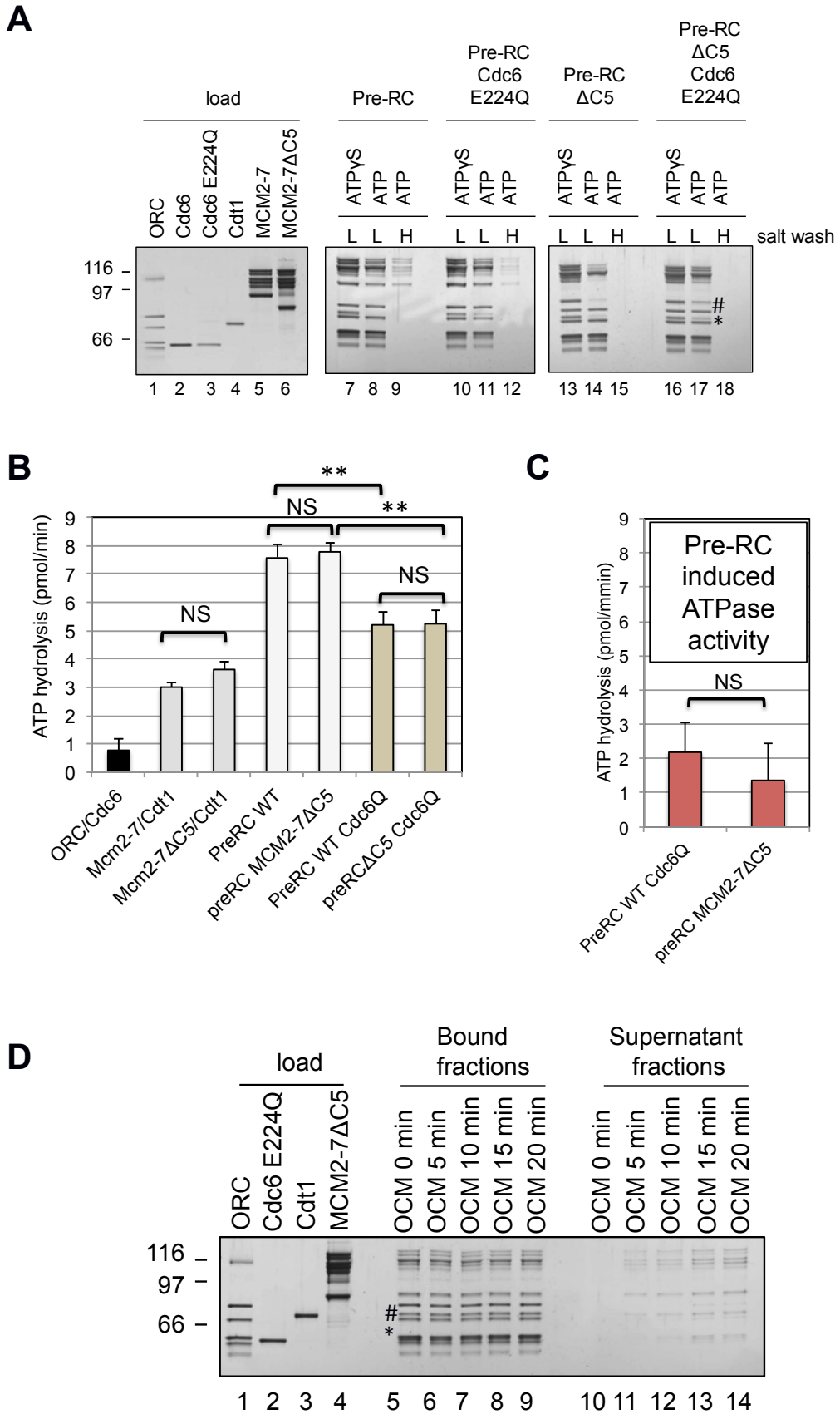


Figure 3.10. Down-regulation of Cdc6-induced ATP hydrolysis is required for OCM stability in MCM2-7ΔC5

A) Analysis of *in vitro* pre-RC assembly in the presence of Cdc6 or Cdc6 E224Q with MCM2-7 wild type (lane 7-12) or MCM2-7ΔC5 (lane 13-18). The reactions are assembled in pre-RC buffer with ATPγS or ATP, washed with low (L) or high (H) salt buffer and eluted with DNaseI. **B)** Analysis of ATPase activities during pre-RC formation using the ATPase assay previously described. The pre-RC activities of the MCM2-7 and MCM2-7ΔC5 are shown in light grey. Results are for three independent experiments, and are plotted as average and error bars represent the standard deviation. Statistically significant results, determined by one-way ANOVA followed by post hoc test using Bonferroni correction, are indicated (** $P<0.05$). No statistical difference is indicated as NS. **C)** Analysis of pre-RC induced ATPase activities in the presence of Cdc6 E224Q with MCM2-7 wild type or MCM2-7ΔC5. There was no statistical difference (NS) between the WT and MCM2-7ΔC5. **D)** Pre-RC reactions using ORC/Cdc6 E224Q and MCM2-7ΔC5/Cdt1 were assembled for 2.5 minutes, washed and incubated for further 0 to 20 minutes. The "bound fractions" represent the DNA-bound proteins and the "supernatant fractions" are the unbound proteins. The Mcm5ΔC band is marked with # and the Cdt1 band is marked with the asterisk. Refer to Figure 3.7 A for comparison with MCM2-7ΔC5 in the presence of Cdc6 WT.

3.9. Generation of an MCM2-7 construct with protease-inducible C-terminus cleavage

The experiments described in this chapter have shown that deleting the Mcm5C prevents the loading of the helicase into a double hexamer. The data further suggest that the Mcm5C is involved in down-regulating Cdc6 ATPase activity during OCCM formation and it is required during the transition from OCM to the double hexamer. In order to disentangle these two reactions further we hypothesised that a construct that allows proteolytic removal of the Mcm5C could allow conditionally assays e.g. WT C5 during OCM formation, and MCM2-7ΔC5 during double-hexamer formation. We envisaged a system by which the Mcm5C could be cleaved through addition of a site-specific protease, by engineering a cleavage site in the flexible C-terminal linker region. A protease-specific cleavage site was introduced in the linker region between the ATPase domain of Mcm5 and the WHD5 in the full-length MCM2-7 protein (Figure 3.11). With all constructs generated, care was being taken to alter the sequence as little as possible, preserving the natural linker sequence if possible. The template plasmid pCS232 (pESC-URA_Mcm5-Mcm3) was modified to generate the plasmids pCS782, pCS783, pCS816 and pCS817 (See Table 2.2 in

Materials and Methods) in the following way: a synthetic DNA fragment encoding part of the Mcm5 sequence was generated, in which the 14 amino acid long sequence SQDPIGGLNQASGT (amino acid 693 to 706) was replaced by modified sequences containing cleavage sites for TEV (Tobacco Etch Virus) or PreScission proteases. The TEV cleavage site (ENLYQ/G) was inserted generating the sequence SQDPIGENLYFQGT, which did not affect the length of the total protein. A second construct was generated by inserting a PreScission protease cleavage site (LEVLFQ/GP) producing a longer linker with the following sequence: SGALEVLFQGPIGGLQASGTS. Following the same logic, we also generated constructs containing a tandem Prescission-cleavage site, resulting in an even longer linker (Figure 3.11).

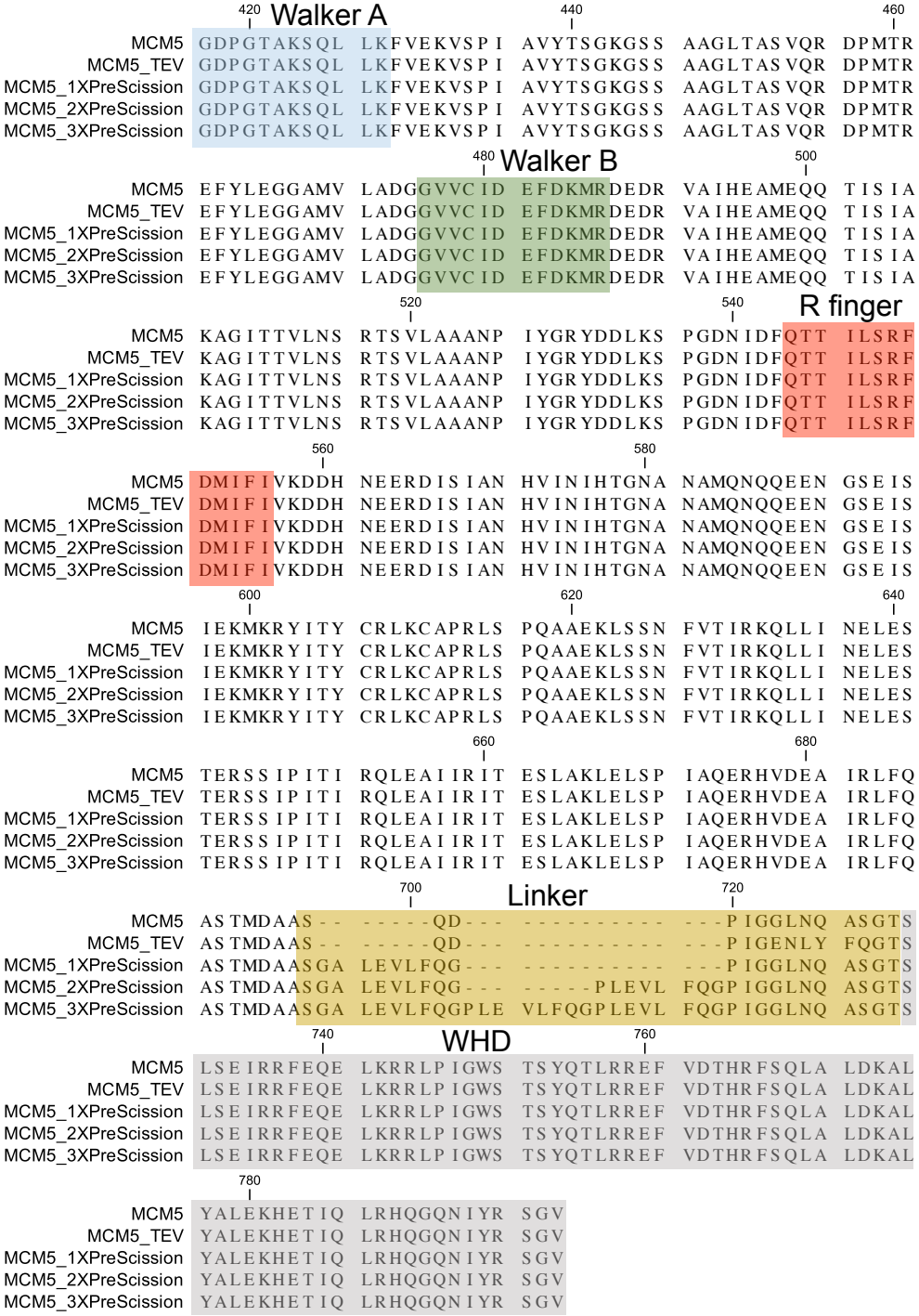


Figure 3.11. Design of cleavable MCM2-7 constructs

Multiple sequence alignment showing the ScMcm5 from amino acid 416 to 775 and the four alternative Mcm5 constructs containing cleavage sites for TEV or PreScission proteases. In the sequence, the AAA+ motifs are highlighted: the Walker A domain in blue, the Walker B in green, the arginine finger in red. The linker region between the AAA+ domain and the WHD (grey) is highlighted in yellow.

In order to generate the final yeast strains containing all six MCM subunits, the plasmids were transformed into the wild type yeast strain W303 together with the plasmids containing the other MCMs subunits (pCS14 and pCS15, also see Table 2.2 in Materials and Methods). The strains did not show growth defects *in vivo* (Figure 3.12 A). Consequently, the mutant proteins were purified (data not shown), and they proved fully functional in pre-RC formation (Figure 3.12 B, C).

Because PreScission protease is maximally active at 5°C (Cordingley et al., 1990; Ullah et al., 2016; Waugh, 2011; Young et al., 2012) and common protocols (GE Healthcare) recommend overnight incubation with the substrate, MCM2-7 containing the PreScission cleavage site was incubated in pre-RC buffer (ATP) with an 8 fold excess Prescission protease at 5°C overnight. Alternatively, the reaction was incubated at 12°C for one hour, in order to address if the cleavage could occur in shorter time frames. The cleavage appeared to be more effective when the longer incubation at lower temperature was performed (Figure 3.13, compare lane 6 and 8).

In order to assess the accessibility of the cleavage site in Mcm5 in the context of helicase loading, the most stable helicase loading intermediate was used, the OCCM, which allows long incubation times. Surprisingly, in this complex the cleavage site in the linker of Mcm5 appeared not accessible to the protease, as no cleaved product was detected in any of the tested conditions (Figure 3.13, lanes 5 and 7). TEV protease is maximally active at 34°C (Waugh, 2011) but this temperature would cause denaturation of MCM2-7, therefore we tested the cleavage at lower temperatures (12°C and 20°C) for a long period (overnight), however no improved cleavage was observed. For whatever reason, the TEV protease appears unable to cleave this construct under conditions that support cleavage of the MCM complex. Because PreScission protease showed better cleavage of the Mcm5C in the MCM2-7, it was decided to focus on using the PreScission rather than the TEV protease.

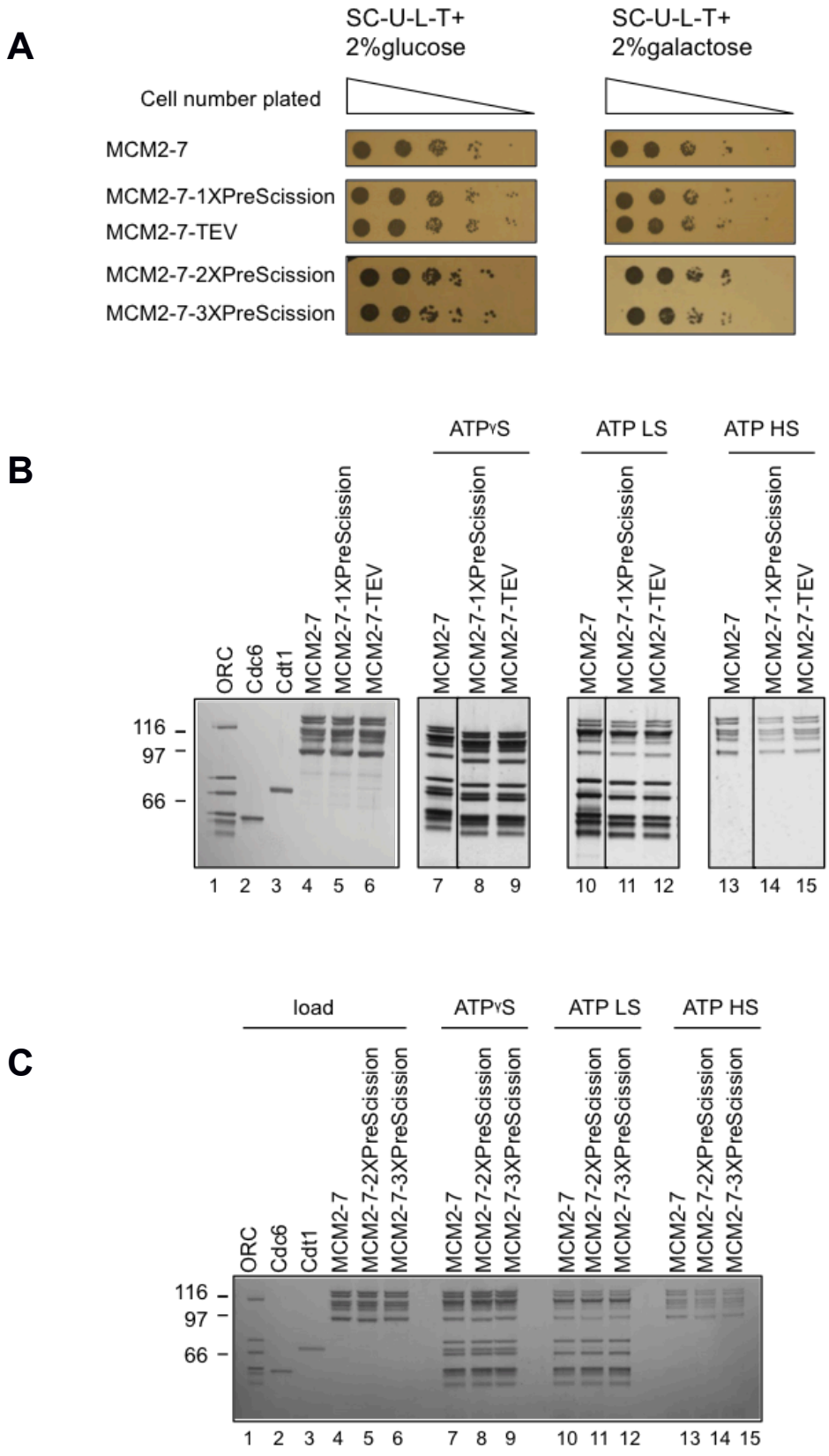

A
SC-U-L-T+
2%glucose
SC-U-L-T+
2%galactose
Cell number plated
MCM2-7
MCM2-7-1XPreScission
MCM2-7-TEV
MCM2-7-2XPreScission
MCM2-7-3XPreScission
B
ATPγS
ATP LS
ATP HS
ORC
Cdc6
Cdt1
MCM2-7
MCM2-7-1XPreScission
MCM2-7-TEV
116
97
66
1 2 3 4 5 6 7 8 9 10 11 12 13 14 15
C
load
ATPγS
ATP LS
ATP HS
ORC
Cdc6
Cdt1
MCM2-7
MCM2-7-2XPreScission
MCM2-7-3XPreScission
116
97
66
1 2 3 4 5 6 7 8 9 10 11 12 13 14 15

Figure 3.12. *In vivo* and *in vitro* activity of the cleavable MCM2-7 proteins

A) Yeast growth assay showing the effect of overexpression of the wild type and the four cleavable MCM2-7 constructs. A 5-fold serial dilution of cells at the starting density of 10^7 was spotted onto selective dropout plates with either 2% glucose or 2% galactose. The plates were incubated at 30°C for two and four days respectively. (The experiment was performed as two independent duplicates) **B-C)** Silver-stained gels showing the *in vitro* reconstitution of the pre-RC to test the ability of the purified cleavable MCM2-7 proteins to associate with DNA in the presence of Cdt1, ORC/Cdc6 (low salt, LS) and to form a salt stable complex in high salt (HS). The experiments were repeated twice.

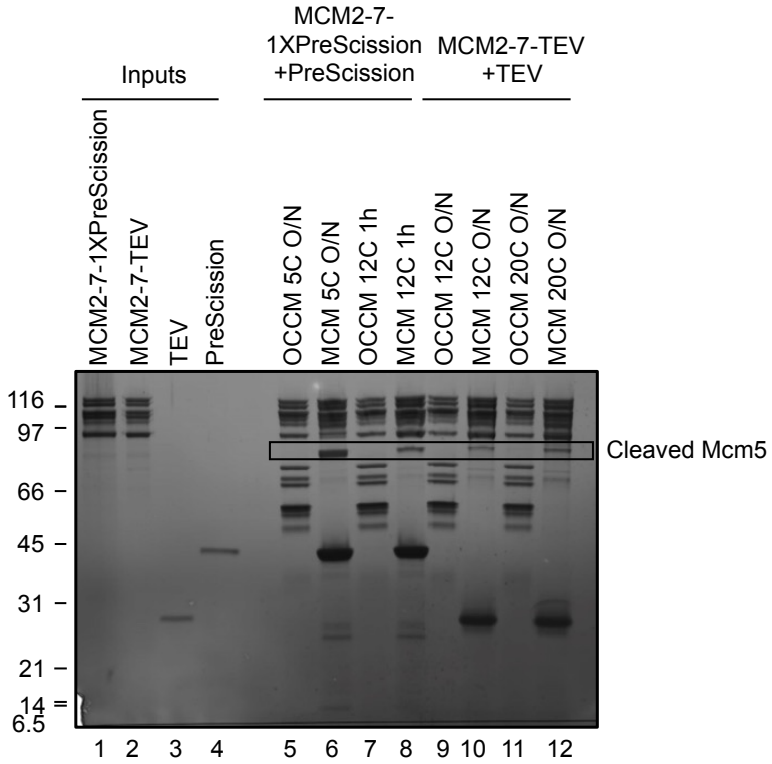


Figure 3.13. Test the accessibility of the cleavage sites

Silver stained gel showing the effect of the PreScission protease in the contest of MCM2-7-1XPreScission alone or in the OCCM, at different temperatures and time (lanes 5-8). The construct MCM2-7-TEV was incubated with TEV protease in solution or in the OCCM complex formed on beads-bound DNA for at 12°C and 20°C overnight. The experiment was repeated twice.

First, the MCM2-7 construct containing three PreScission protease cleavage sites in the linker of Mcm5 was tested. The efficiency of cleavage was tested by incubating MCM2-7 in the presence of an 8-fold protease excess for 5 hours at different temperatures (10, 15, 25°C). In the context of MCM2-7, the

Mcm5 WHD was efficiently cleaved in all tested conditions (Figure 3.14 A, lanes 5-7). The cleavage was also observed in the context of the OCCM and OCM, when the incubation was carried out for 5 hours with PreScission protease (Figure 3.14 A, lanes 8-13). To identify if a shorter incubation time would support a similar efficient cleavage, a time-course from one to four hours was performed at 15°C. Interestingly, MCM2-7 in solution was cleaved rapidly, as well as when it was in complex with OCM (Figure 3.14 B, lanes 13-16). However, with the OCCM complex a longer incubation was necessary (Figure 3.14 B, lanes 9-12). These observations suggest that the WHD5 might adopt a different conformation in the different pre-RC intermediates, in particular the Mcm5 linker region might be more buried in the OCCM than in the OCM or might adopt a more structured conformation making it a less good substrate for the protease.

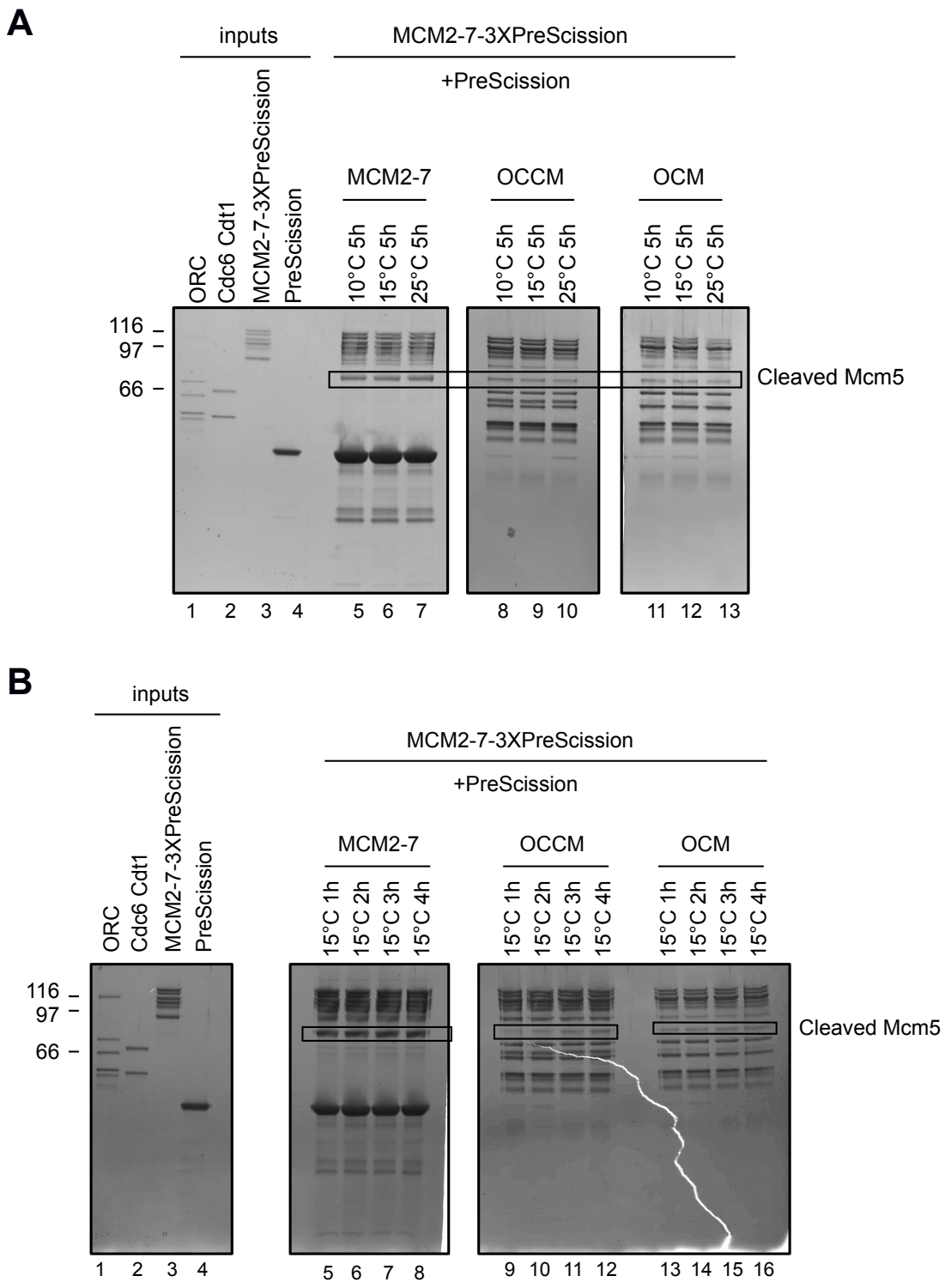


Figure 3.14. Test the accessibility of the cleavage sites in the contest of MCM2-7, OCCM and OCM using the cleavable MCM2-7-3XPreScission construct.

A) The construct MCM2-7-3XPreScission was incubated with the protease in ratio 1:4 for 5 hours at different temperatures at the stage of OCCM (lanes 8-10) and OCM (lanes 11-13). The cleaved C5 is highlighted. **B)** The construct MCM2-7-3XPreScission was incubated with the protease in ratio 1:4 at 15°C for up to 4 hours, and tested for cleavage site accessibility at the stage of OCCM (lanes 9-12) and OCM (lanes 13-16). The cleaved C5 is labelled on the right hand side of the gel. The experiments were performed twice.

Having successfully generated mutants that support conditional proteolytic removal of the Mcm5 C-terminus, we sought to test if the Mcm5 WHD is required for double hexamer stability. This was analysed by assembling high salt resistant double-hexamer using the MCM2-7 3xPreScission construct, followed by incubation in pre-RC buffer (ATP) with PreScission protease at 15°C up to 5 hours (Figure 3.15 A). It was surprising to observe that no double hexamers were retained on the DNA. It was hypothesised that this effect could reflect the instability of the complex due to the missing C5 or, alternatively, the double hexamers could be sliding off the linear DNA (Evrin et al., 2009; Remus et al., 2009). To test these ideas, DNA containing a biotin molecule at each end was used, generating in the context of streptavidin coated beads a looped DNA, which stops the double hexamers sliding off from DNA. Indeed, now using looped DNA the double hexamers were retained on DNA even after cleavage of the WHD5 by PreScission (Figure 3.13 B, lanes 5-8). As a control, un-cleaved MCM2-7 double hexamer were used (Figure 3.13 B, lanes 9-12), demonstrating that the double biotin prevents the helicase complex from sliding off the DNA. Remarkably, the Mcm5C in the double hexamer state was cleaved very rapidly, suggesting that in this complex the cleavage site is more accessible. This observation is perhaps consistent with the structural information for the double hexamer, in which the Mcm5C is not visible, suggesting a high degree of flexibility (Abid Ali et al., 2017; Li et al., 2015; Noguchi et al., 2017).

Taken together, these experiments show that the Mcm5C can be cleaved in the context of the MCM2-7 hexamer or when in complex with other pre-RC proteins if a protease cleavage site is inserted in the linker region before the WHD5. The stability of the pre-RC intermediates does not seem to be affected by the removal of the Mcm5C, suggesting that this domain is not essential for the maintenance of these intermediates. The stability of the double hexamer on closed-looped DNA with the Mcm5C cleaved following double hexamer assembly further suggests that the Mcm5C is critical to the loading of the second hexamer.

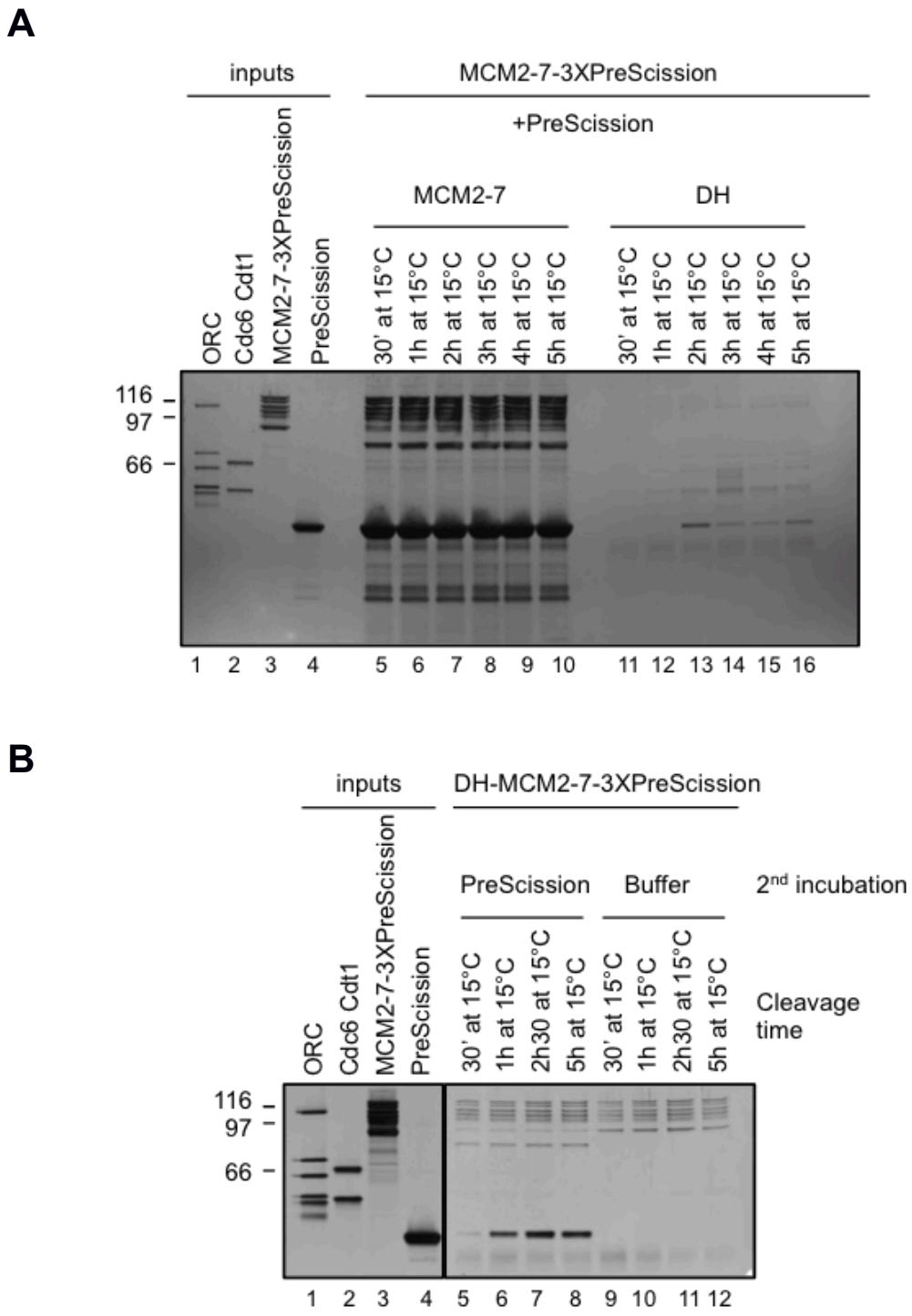


Figure 3.15. Test the accessibility of the cleavage site in the double hexamer complex.

A)The construct MCM2-7-3XPreScission was incubated with PreScission protease in a ratio 1:4 at 15°C for up to 5 hours, in solution and in the beads-bound double hexamer. Linear ARS1 DNA was used. **B)** Time-dependent MCM2-7-3XPreScission double hexamer retention on circular ARS1 DNA in the presence (lanes 5-8) or absence (lanes 9-12) of PreScission protease. (Both experiments were repeated twice)

3.10. Discussion

ORC, Cdc6, MCM2-7 and Cdt1 are recruited to origin DNA initiating a multi-step helicase loading reaction (Fernandez-Cid et al., 2013; Remus et al., 2009; Sun et al., 2013; Ticau et al., 2015). The OCCM complex forms rapidly in an ATP-hydrolysis independent manner, but is a very short-lived intermediate. Upon ATP hydrolysis the OCCM complex rapidly disassociates with the release of Cdc6 and then Cdt1, followed by rebinding of Cdc6, resulting in the formation of the OCM intermediate (Fernandez-Cid et al., 2013; Ticau et al., 2015). The OCCM complex has been isolated *in vitro* by the Speck lab, by employing the slowly hydrolysable ATP analogue, ATPγS. In collaboration with the Li lab, a 3.9 Å cryo-EM structure of this intermediate has been solved, revealing several important features (Yuan et al., 2017). In particular, the structure showed the location and nature of the interactions between the C-terminal WHDs of each MCM2-7 subunit with the ORC/Cdc6 complex. Importantly, in the OCCM EM map the WHD5 was the only C-terminus domain that was not visible, indicating increased flexibility of this region.

As discussed in the Introduction (Chapter 1), the role of the C-terminus of Mcm3 and Mcm6 has already been described (Fernandez-Cid et al., 2013; Frigola et al., 2013). However, the function of the Mcm5C has not been investigated in before. Through the experimental work described in this thesis chapter, it was found that this domain is not required for the initial recruitment of MCM2-7 to ORC/Cdc6, in which the WHD of Mcm3 is the main player (Frigola et al., 2013). Structural information originating from the recent cryo-EM structures of several pre-RC intermediates obtained by different groups has helped in the understanding of the localisation of the WHD5 during the different stages of helicase loading. In the MCM2-7-Cdt1 (Zhai et al., 2017a) and the CMG (Yuan et al., 2016) structures, the WHD5 is located inside the MCM2-7 pore occluding the central channel, with the WHD of Mcm6 on top of it. In both structures, DNA is not present. The position of the WHD5 in these structures suggests that this may prevent dsDNA from entering the central channel. In the CMG structure, obtained in the presence of ssDNA, the WHD5 is no longer observed in the central channel, but moves out and adopts a different, more flexible, conformation (Georgescu et al., 2017).

The DNA loading of MCM2-7 occurs at the stage of OCCM formation prior to ATP hydrolysis (Sun et al., 2013). Upon ATP hydrolysis only MCM2-7 complexes successfully loaded onto DNA lead to productive OCM (Samel et al., 2014). Our biochemical and structural data showed that MCM2-7 lacking the Mcm5C is competent for DNA loading even though in a reduced way. However, in this thesis it has been shown that OCMΔC5 is not a productive complex, because is not able to recruit a second hexamer. It has been shown that Cdt1 release is temporally linked with the MCM2-7 gate closure (Ticau et al., 2017). However, in the OCCM structure, which contains Cdt1, it was found that the gate is still partially open (Yuan et al., 2017). Moreover, it has been shown that ATP hydrolysis is required for Cdt1 and Cdc6 release and for the optimal transition from an initial MCM2-7 recruitment to the later stages complexes OCM and DH (Bell, 2014). Multiple ATPases have been implicated in that, Orc1 and Cdc6 (Fernandez-Cid et al., 2013; Randell et al., 2006) and MCM2-7 (Coster et al., 2014; Kang et al., 2014). Consequently, it was found that Cdc6 ATPase has a major role to activate the quality control pathway of ATPase activated pre-RC disassembly, which occurs in the context of an ORC complex missing Orc6, but could be also important in the context of other scenarios (Coster et al., 2014). The idea is that a failed helicase loading could inhibit replication at a given origin and the quality control induced disassembly clears the site to allow another helicase loading attempt (Coster et al., 2014; Fernandez-Cid et al., 2013). Here, it has been shown that when Cdc6 ATP hydrolysis is blocked by a Walker B ATPase mutant (Cdc6 E224Q), a higher Cdt1 retention in MCM2-7ΔC5 containing pre-RC intermediates was observed. It has been suggested that MCM2-7ΔC5 induces quality control, which leads to frequent pre-RC reassembly. The early pre-RC intermediates contain Cdt1 and therefore Cdt1 appears enriched with MCM2-7ΔC5 pre-RC complexes. This is consistent with observations made by other group (Kang et al., 2014). Therefore, it has been proposed that the WHD of Mcm5 may function for quality control in preventing the licensing of inappropriate protein complexes though the regulation of Cdc6-induced ATP hydrolysis.

It has been suggested that in the context of MCM2-7ΔC5, after initial Mcm3 mediated recruitment of MCM2-7ΔC5/Cdt1 to ORC/Cdc6, two scenarios are possible (Figure 3.16). On the one hand, the lack of Mcm5C leads to OCCM

formation, but this complex is not functional to mature into an OCM resulting in induction of a quality control pathway and Cdc6 ATPase dependent complex disassembly. On the other hand, a proportion of MCM2-7ΔC5/Cdt1 is able to escape the quality control or form a functional OCCM, resulting in an OCM complex that stays bound to DNA. However, such a complex is not functional for double hexamer formation.

It is conceivable that Mcm5C has multiple different roles during helicase loading and DNA synthesis. Thus, the complete deletion of the Mcm5C limits the analysis to some degree, since such a construct only allows the discovery of the first defect in double hexamer assembly pathway, while later defect cannot be easily observed. The generation of the protease-inducible cleavage mutant produces a system that enable analysis of the role of the C-terminal region in a more controlled manner. Thus, the removal of the Mcm5C was induced following either stable OCCM formation in ATPγS, or after full pre-RC formation when the double hexamer is formed around DNA. This system allowed us to determine that the C-terminal region does not have an apparent role in maintaining the double hexamer complex stability.

In conclusion, the data in this chapter are consistent with the idea that (1) Mcm5C is required to suppress the quality control pathway during pre-RC formation, and that (2) the WHD5 is essential for the OCM to double-hexamer transition, in particular for the successful stable recruitment of the second MCM2-7 hexamer. These are exciting observations, but what is the molecular mechanism for the observed defects in pre-RC formation? The ATP hydrolysis data suggest that the Mcm5C might exhibit a role in regulating ATP hydrolysis as part of the pre-RC quality control reaction. In the next chapter, an investigation into the effect of the Mcm5C on complex loading and ATPase activity is presented using a mutational strategy, which involves a domain swap approach and point mutations in the WHD5.

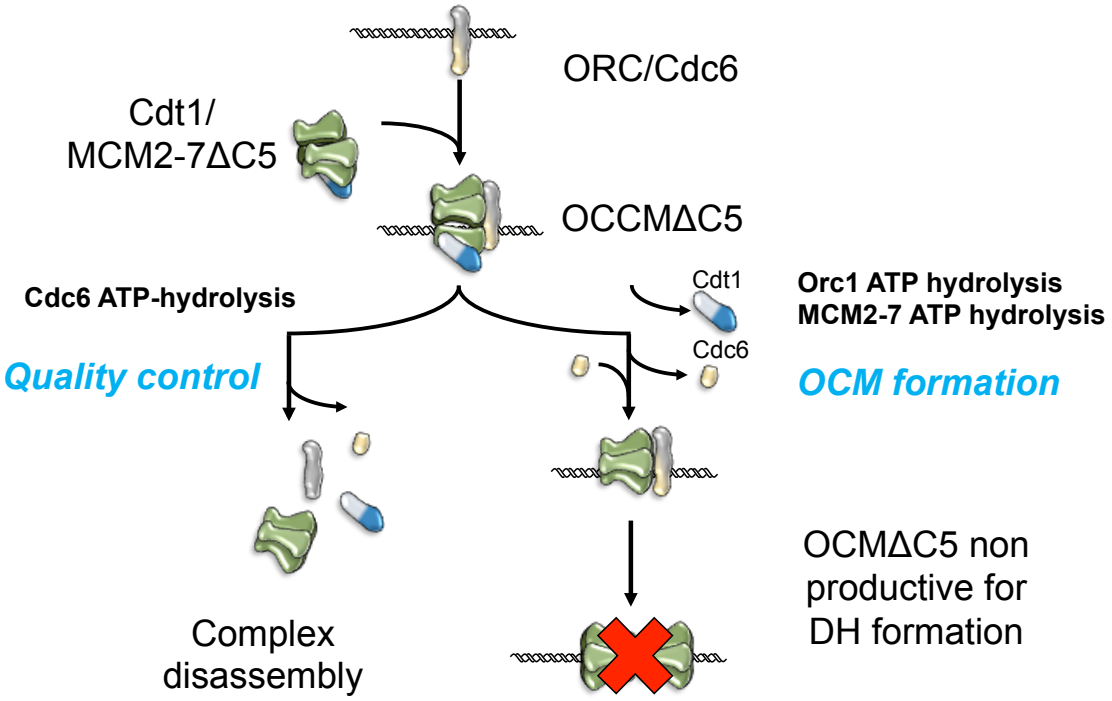


Figure 3.16. Model for the Mcm5C-induced quality control mechanism during pre-RC formation

MCM2-7ΔC5/Cdt1 is recruited to DNA-bound ORC/Cdc6 forming an incomplete OCCMΔC5, a situation that induce a quality control pathway and Cdc6 ATP hydrolysis-dependent complex disassembly. A proportion of MCM2-7ΔC5/Cdt1 is able to escape the quality control or form a functional OCCM, and consequent OCM complex that stays bound to DNA. However, such a complex is not functional for double hexamer formation and ATP hydrolysis leads to its disassembly.

Chapter 4

Understanding the mechanism of the Mcm5 carboxyl terminal domain

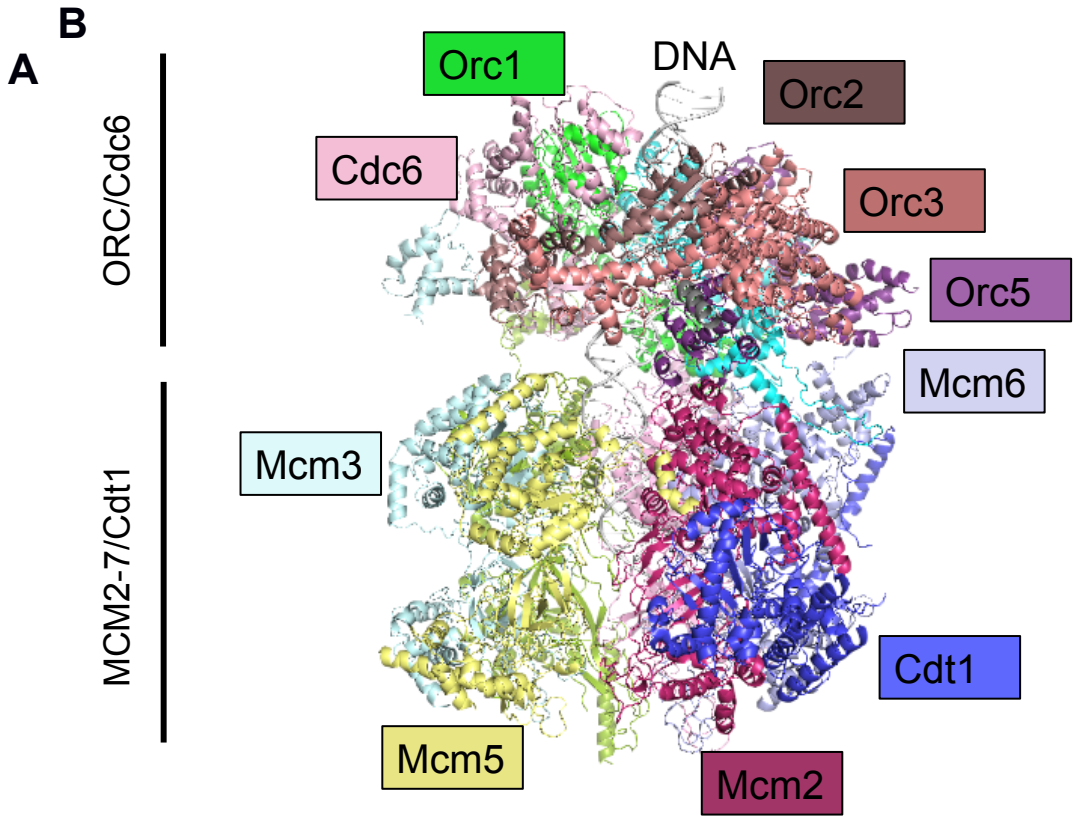
4.1. Introduction

The availability of the high-resolution OCCM structure was essential to understand the structural framework of the Mcm WHDs (Yuan et al., 2017), which was described in Chapter 1. Chapter 3 investigated the role of the WHD5, which was not observed in the OCCM structure, and it was discovered that this domain is necessary during pre-RC formation. In particular, it is required for the assembly of the double hexamer. Based on our data, we hypothesised that this region could play a role in quality control functioning as a sensor of pre-RC assembly, signalling that correct DNA insertion into the helicase has occurred.

In the OCCM structure, the so called “gate” between the Mcm5 and Mcm2 subunits is partially open (Figure 4.1 A, Mcm5 in yellow and Mcm2 in magenta). Recent reanalysis of the OCCM cryo-EM data by our cryo-EM collaborator (Huilin Li, USA), involving sub-classification, revealed one OCCM subpopulation in which the Mcm2-5 gate is fully closed (Figure 4.1 B and 4.2) (Yuan et al; unpublished). Interestingly, in this conformation, in which the general location of the proteins did not change, the WHD5 became visible, even though at low resolution. Because of the limited resolution, the WHD5 was initially modelled as a poly-alanine chain.

In the published structures of MCM2-7 (Zhai et al., 2017a) and CMG (Georgescu et al., 2017) the WHD5 is located inside the central channel, suggesting that it could prevent dsDNA insertion into the MCM2-7 ring. In the new structural data from the Li lab, WHD5 is located outside the central channel, at the interface between the Mcm5 AAA+ domain and the Orc3 and Orc2 subunits (Figure 4.1 B, WHD5 shown as surface view in red).

Cross linking mass spectrometry (CLMS) data acquired in collaboration with Juri Rappsilber (Edinburgh, UK), suggested an interaction between WHD5 and the N-terminus of Orc2 ((Yuan et al., 2017) and chapter 1).


B
A
ORC/Cdc6
MCM2-7/Cdt1
Orc1
DNA
Orc2
Cdc6
Orc3
Orc5
Mcm6
Mcm3
Cdt1
Mcm5
Mcm2

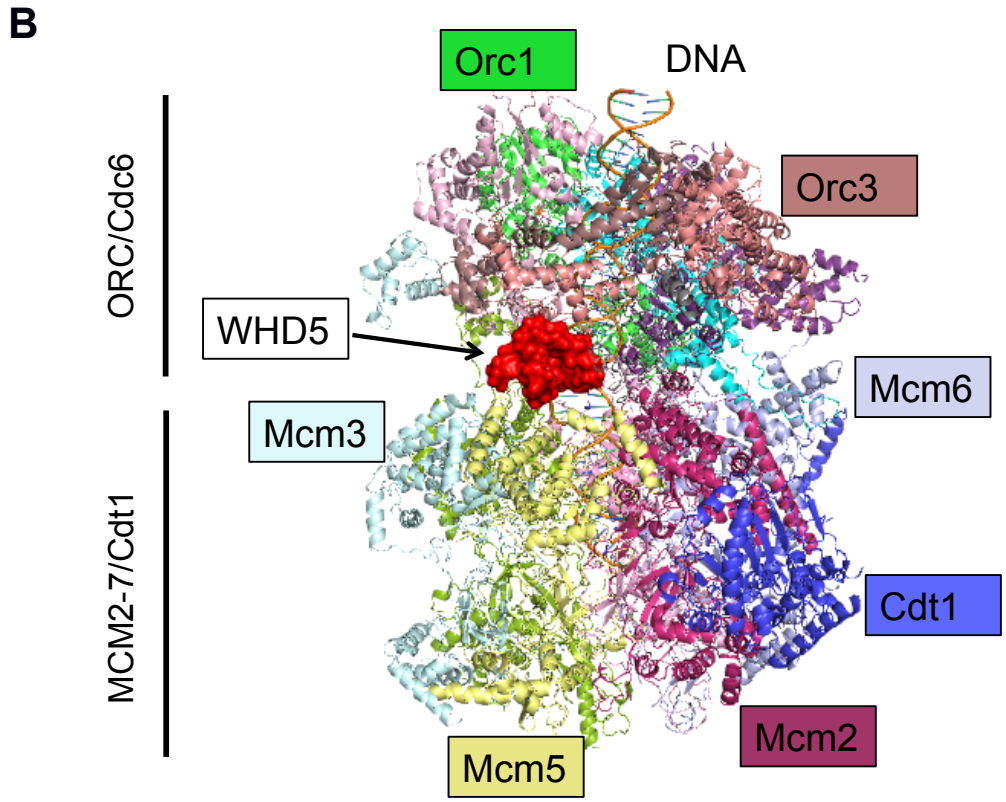

B
ORC/Cdc6
MCM2-7/Cdt1
Orc1
DNA
Orc3
WHD5
Mcm6
Mcm3
Cdt1
Mcm2
Mcm5

Figure 4.1. The C-terminus of Mcm5 contains a winged helix domain

A) Structure of OCCM complex in a partially open (Yuan et al., 2017), shown in a cartoon view. In the top part, the following subunits of ORC/Cdc6 are labelled: Orc1 in green, Orc2 in brown, Orc3 in salmon, Orc5 in violet and Cdc6 in pink. In the lower side of the complex, Cdt1 is coloured in blue, Mcm5 in yellow, Mcm2 in red, Mcm3 in light blue, and Mcm2 in magenta. DNA can be seen inside the OCCM. **B)** Structure of OCCM complex in a closed conformation (unpublished data). The WHD5 is shown in red as surface view.

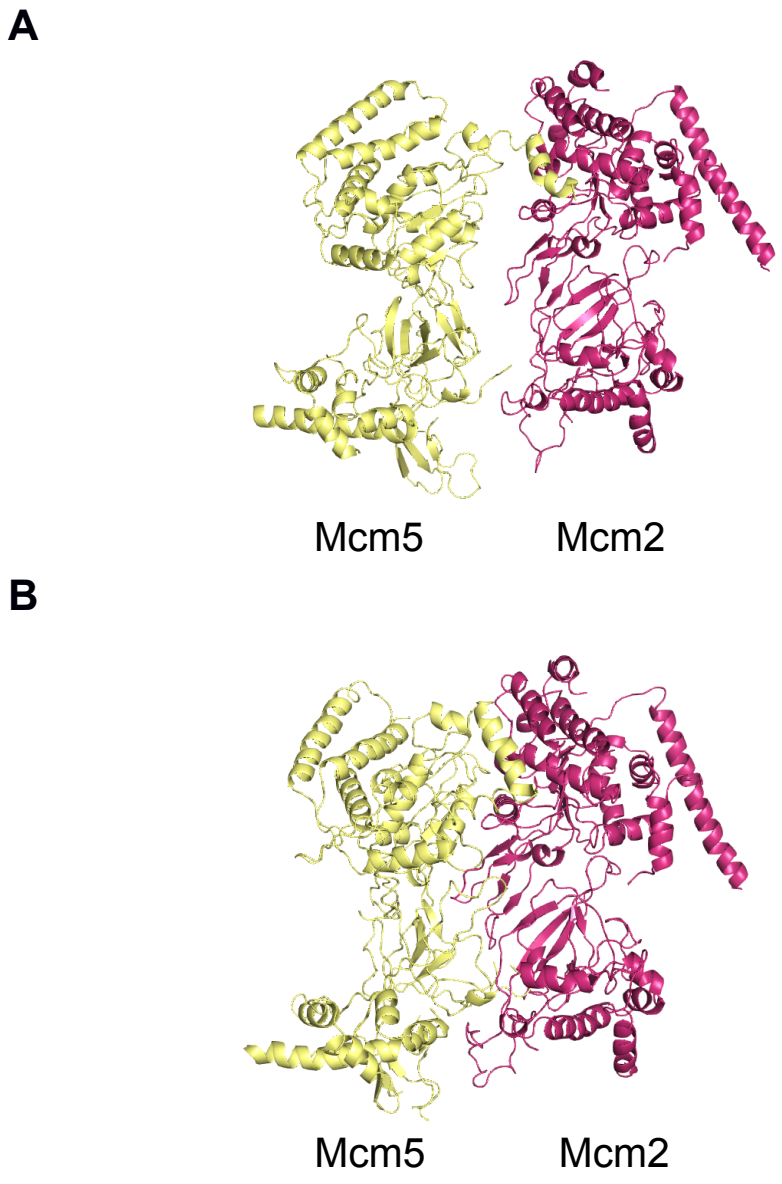


Figure 4.2. The Mcm5-Mcm2 gate

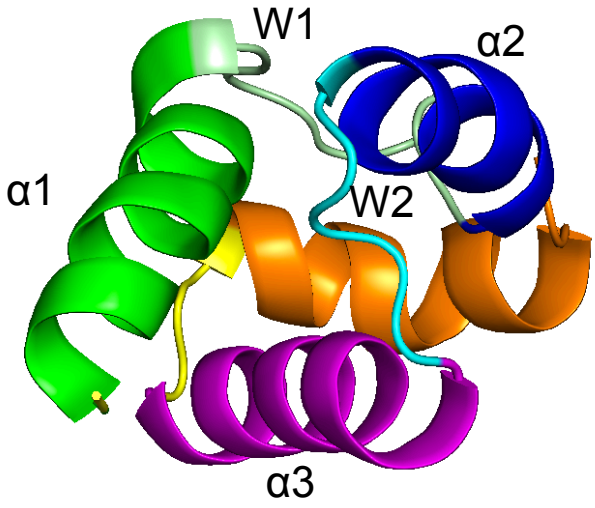
A) In yellow the Mcm5 subunit and in red the Mcm2 extracted from the OCCM complex in a partially open configuration (Yuan et al., 2017), shown in a cartoon view. B) The two subunits (Mcm5 and Mcm2) as they appear in the OCCM closed conformation (Yuan et al, unpublished).

Initially, to analyse the role of the flexible linker region that precedes the WHD5, the length and the degree of flexibility of this region was altered (Figure 4.11). Additionally, domain swap experiments were performed, where the WHD5 was replaced with the human version and assessed all mutants for their viability and ability to form the pre-RC (Figure 4.5). Given that the Mcm5C is observed in proximity to other pre-RC proteins, we reasoned that disruption of potential WHD5 protein-protein by site-directed mutagenesis may result in specific defects. Furthermore, these mutants can be assessed through our panel of functional assays, which could lead to important mechanistic insights into pre-RC formation. The point mutants in the WHD5 (Figures 4.14, 4.15) were assessed regarding their effect on pre-RC assembly (Figures 4.19, 4.20). This work led to a novel functional description of the WHD5 in pre-RC formation, identifying a key role in quality control.

4.2. Mcm5C contains a winged helix domain

The general structural organisation of the Mcm subunits was already described in the introduction (Chapter 1.8.6). Mcm5 contains a C-terminal extension formed by a 13 amino acid-long flexible linker and a WHD. This domain consists of three alpha-helices (α1, α2, α3) and two wings (W1, W2), arranged in the order α1-W1-α2-W2-α3 (Figure 4.3 A). The WHD is a structural element found in core proteins of all kingdom of life and participates in establishing protein-DNA or protein-protein interactions (Gajiwala and Burley, 2000). The linker that connects the WHD to the main body of Mcm5 is not visible in the cryo-EM structures available. A sequence alignment of Mcm5C from *S. cerevisiae* (amino acids 692-775) and other eukaryotes was performed using Clustal (Goujon et al., 2010; Larkin et al., 2007) and shown in Figure 4.3 B. The structural components are marked on top of the *S. cerevisiae* Mcm5C sequence. Conserved amino acids are indicated with a symbol below the alignment based on the degree of conservation.

A



B

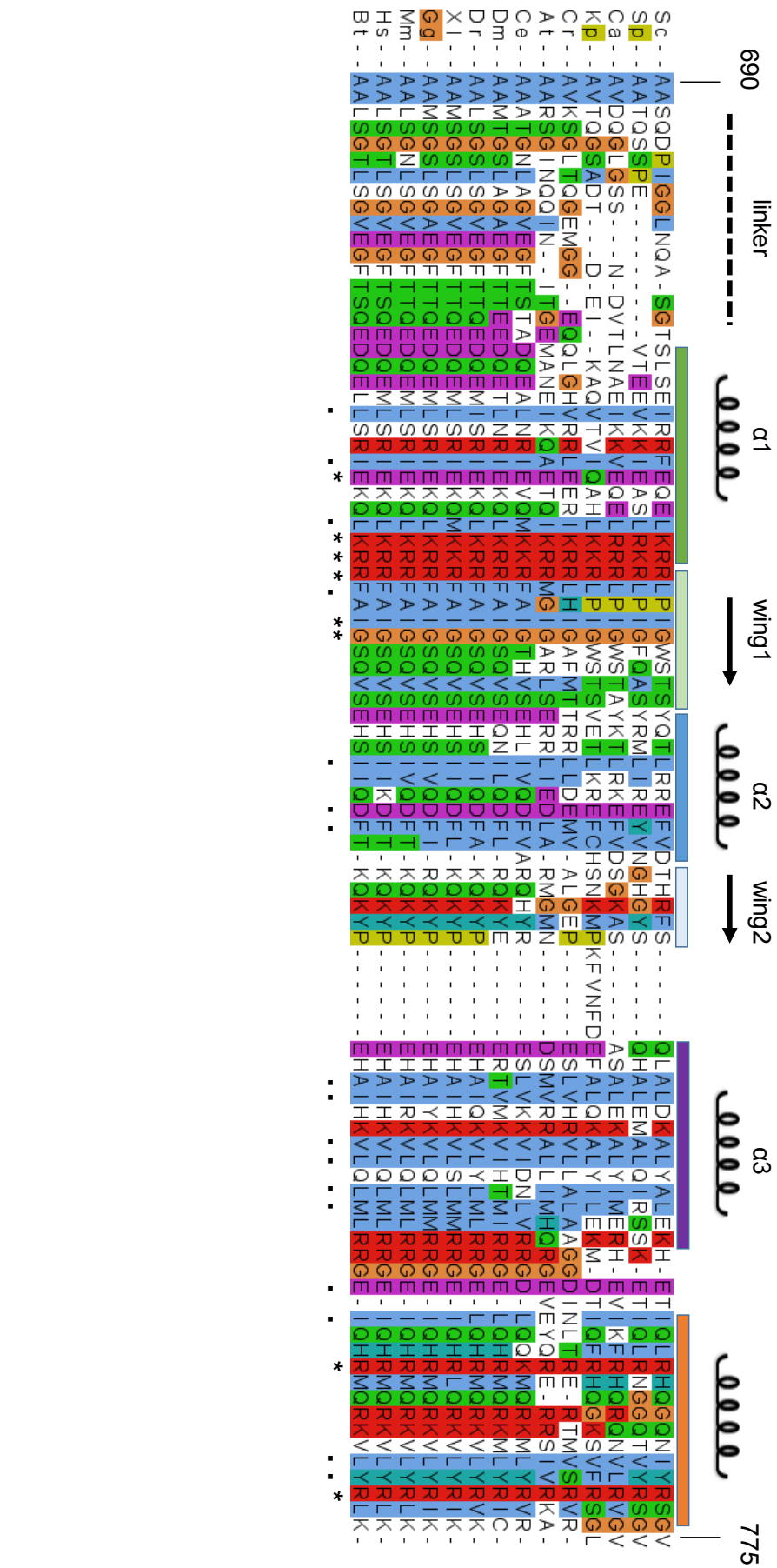


Figure 4.3. The C-terminus of Mcm5 contains a winged helix domain

A) Structure of the WHD5. The three alpha-helices (α1 in green, α2 in blue, α3 in purple) and two wings (W1 in pale green, W2 in cyan), arranged in the order α1-W1-α2-W2-α3. **B)** Multiple sequence alignment of the Mcm5C from *S.cerevisiae* and other eukaryotes (from Uniprot database). The coloured bars match the colouring domains in A. Degree of amino acids conservation among species is indicated below the sequences by a star (identical) or a dot (strong conservation). Sc, *Saccaromyces cerevisiae*; Sp, *Saccaromyces pombe; Ca, Candida albicans; Kr, Komatomagella pastoris; Cr, chlamydomonas reinhardtii; At, Arabidopsis thaliana; Ce, Caenorhabditis elegans; Dm, Drosophila melanogaster; Xl, Xenopus laevis; Gg, Gallus gallus; Mm, Mus musculus; Hs, Homo sapiens; Bt, Bos tauris.*

4.3. Domain swap mutants

The data so far indicate that the WHD5 has an essential role in pre-RC formation. We wondered whether a different Mcm WHD, that conserves the general structure but altered its sequence, was sufficient to functionally replace the WHD5. In order to test this hypothesis, this domain was swapped by engineering chimeric MCM2-7 constructs. One approach was to replace the WHD5 with the WHD4 of the yeast MCM2-7. This sequence was generated to test whether the general structural conformation (WHD) is sufficient to allow the correct function of Mcm5. A sequence and structural alignment of the two domains is shown in Figure 4.4 A. A second mutant was engineered by replacing the yWHD5 with the FRB (FKBP12-Rapamycin Binding) domain of mTOR. This construct was generated in order to minimise sequence conservation with the WHD5, but maintain some structural similarity, as the FRB contains also a helix-wing-helix domain (Figure 4.4 B). A third protein construct was constructed by swapping the WHD5 with the homologous human WHD5, which contains several amino acids that are also conserved in the yWHD5. This constructs allows to ask the question, whether the conserved amino-acids are sufficient to function for productive pre-RC formation. Even though the structure of the human WHD5 is not available, a structural prediction generated by PSIPRED software (Buchan et al., 2013) indicates a conserved WHD organisation (Figure 4.4 C)..

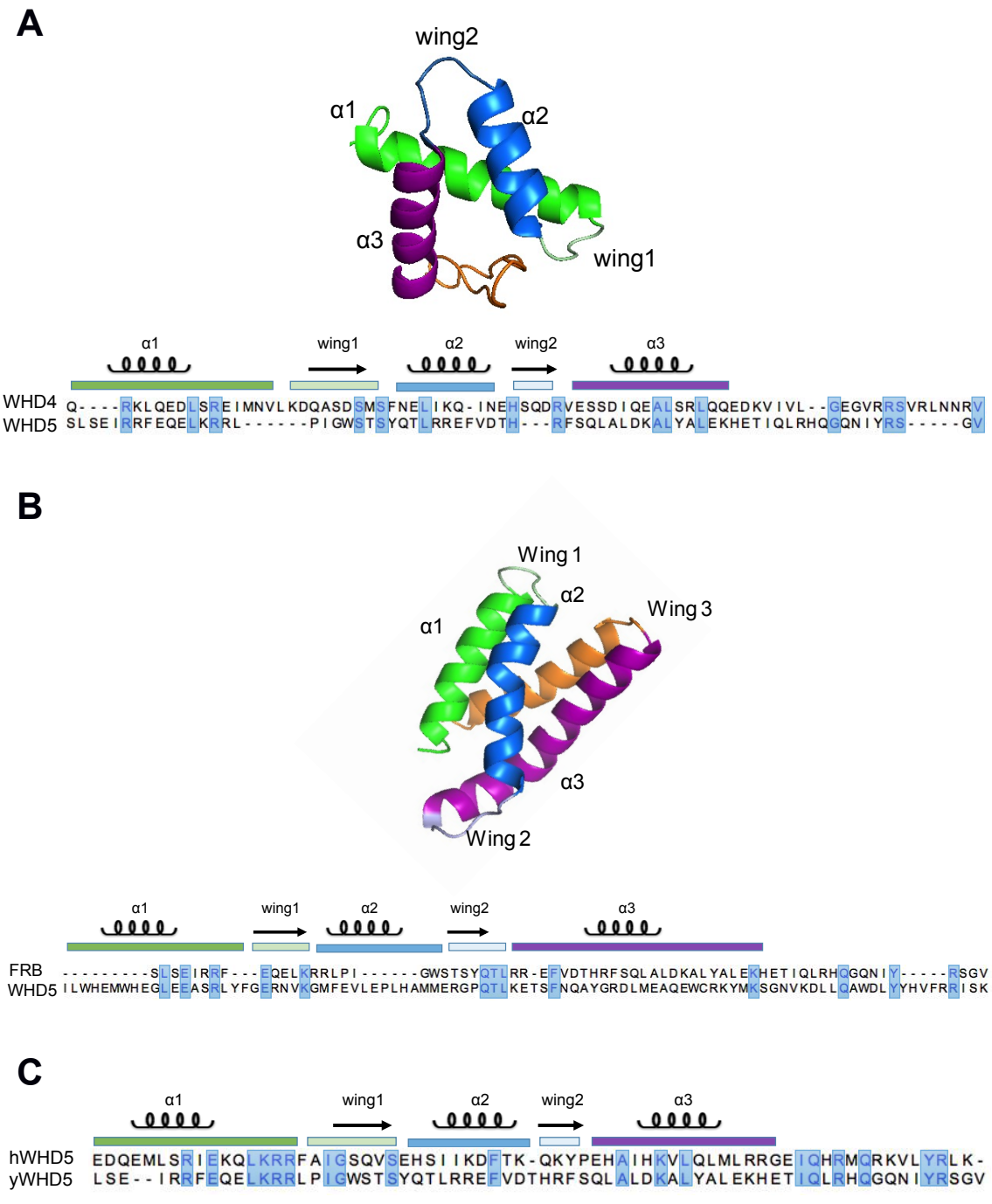


Figure 4.4. Sequence alignment and structural representation of the Mcm5 domain swap mutants

A) The winged helix domain of *S. cerevisiae* Mcm4 isolated from the OCCM structure (Yuan et al., 2017) and sequences alignment with the WHD5. Coloured bars matches the colour of the helices and wings in the structure. Conserved amino acids are highlighted. **B)** Structural prediction of the hWHD5 obtained by PSIPRED server. Amino acid sequences alignment between the human WHD5 and yWHD5. **C)** Structural representation of the FRB domain of mTOR and sequence alignment with WHD5. Coloured bars match the coloured domain in the structure.

The mutant constructs were generated (Genscript), expressed in *S. cerevisiae* and purified as described in the Materials and Methods chapter (2.5) (data not shown). The various complexes were overexpressed in budding yeast to identify if they cause dominant lethality, as described (Materials and Methods 2.4.5). All the domain-swap MCM2-7 mutants resulted in a dominant lethal phenotype (Figure 4.5 A), highlighting that replacing the WHD5 with a different WHD affects essential cell functions. The purified proteins were tested for their ability to form a pre-RC *in vitro*. When ATP hydrolysis is blocked, with ATPγS, the recruitment of all the domain-swap MCM2-7 mutants by ORC/Cdc6 was equivalent to WT MCM2-7 (Figure 4.5 B lanes 7-10). When ATP hydrolysis is permitted and pre-RC formation can occur, only the Mcm5-hWHD5 mutant showed a level of association similar to WT MCM2-7, suggesting that a stable OCM is formed (Figure 4.5 B, lane 13). Mcm5-yWHD4 and Mcm5-FRB showed reduced MCM2-7 association (Figure 4.5 B, lanes 11 and 12), indicating that some complex disassembly occurred following ATP hydrolysis. All three domain-swap mutants were defective in MCM2-7 double-hexamer formation, with Mcm5-yWHD4 displaying the strongest defect (Figure 4.5 B lanes 15-17). This result confirms previous data shown in this chapter and in the previous one, that the WHD5 is not required for the initial binding to the helicase loader. Moreover, this domain can be replaced with a completely different one without affecting the initial MCM2-7 recruitment. In the presence of ATP, Mcm5-hWHD5 supports formation of a stable complex. Nevertheless, this mutant and the two others did not support double-hexamer formation. This demonstrates that the correct WHD is essential for fully functional OCM and double hexamer formation.

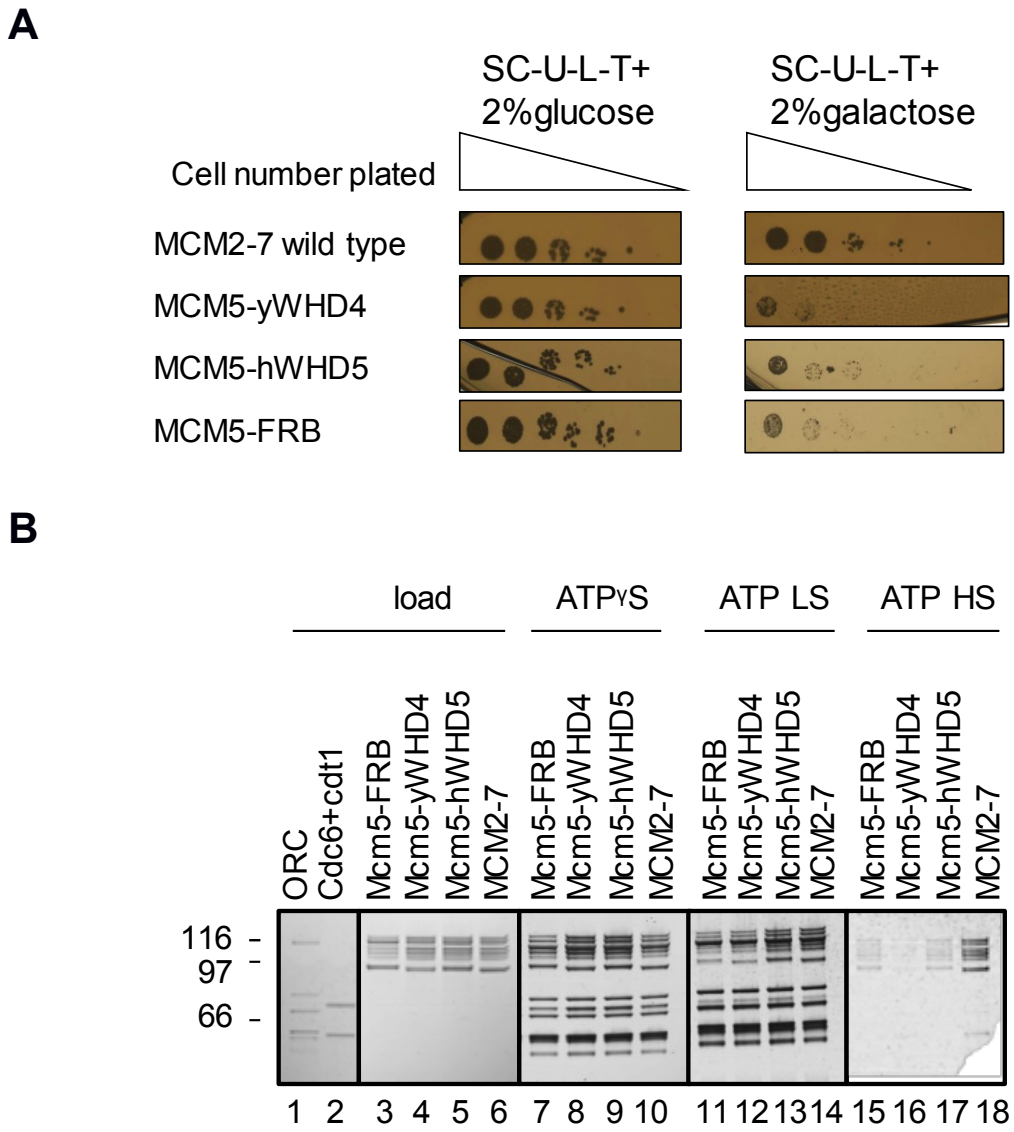


Figure 4.5. Test for *in vivo* dominant lethality and *in vitro* pre-RC activity of the Mcm5-domain swap

A) In vivo test for dominant lethality in overexpression of the yeast strains WT MCM2-7, Mcm5-yWHD4, Mcm5-hWHD5, Mcm5-FRB. A 5 fold dilution series of the yeast strains was spotted on dropout plates containing either 2% glucose (non-inducing condition) or 2% galactose (inducing condition) and grown at 30°C for the appropriate time. (The experiment was performed as independent duplicate) **B)** In vitro pre-RC reconstituted assay testing the ability of the three domain swapped Mcm5 mutants to bind to ORC/Cdc6 in ATPγS compared with the WT MCM2-7 (lanes 7-10). Pre-RC reactions were assembled in ATP followed by low salt washes (LS) (lanes 11-14) or high salt washes (HS) (lanes 15-18). The experiment was repeated twice.

4.4. ATPase activity of domain swapped complexes

The ATPase activity of each of the domain-swap MCM2-7 complexes was analysed in the ATPase assay, as previously described (Chapter 2.10). It was found that the individual ATP hydrolysis activity of the mutants was significantly ($p<0.05$) higher than that of WT MCM2-7 with the exception of Mcm5-FRB, which displayed no significant difference from the WT. In all of the cases but Mcm5-hWHD5, Cdt1 significantly decreased MCM2-7 ATP hydrolysis to a level similar to WT MCM2-7 (Figure 4.6 A). This suggests that Cdt1 reorganises the complexes, so that they adopt a conformation more similar to the WT. The pre-RC induced ATPase activities of Mcm5-FRB appeared to be slightly increased compared to WT MCM2-7, while the other two proteins showed levels similar to WT. However, there is no significant difference among these proteins. This might suggest surprisingly that a different and unrelated domain is possibly capable of providing a certain degree of stabilisation in complex formation.

We wondered if Cdc6-mediated ATP hydrolysis is affected by these mutants and we found that Cdc6 E224Q did not lead to a significant reduction in the pre-RC induced ATPase activity in all the mutants. A trend for a decrease was observed with Mcm5-FRB, suggesting that this mutant in particular activates the Cdc6 dependent quality control pathway, similar as with MCM2-7ΔC5, which in consequence leads to complex disassembly (Figure 4.6 B).

In the following, the influence of Cdc6 E224Q on the domain swap mutants was analysed in the context of the pre-RC assay (Figure 4.6 C). It was found that Cdc6 E224Q reduced Cdt1 and MCM2-7 release, as seen in WT MCM2-7 (Figure 4.6 C, compare lane 4, 7, 10).

These data show that replacing the WHD5 with a similar domain, such as FRB, yields in activation of Cdc6 ATP hydrolysis mediated quality control, inefficient formation of the OCM and a loss in MCM2-7 double-hexamer formation, similar as with MCM2-7ΔC5. Likewise, the similarity in structure and sequence of the yWHD4 and the yWHD5 was not sufficient to allow fully functional OCM formation. The human WHD5 is most similar to the yWHD5 and it might retain some functionality. Indeed, Mcm5-hWHD5 forms a very stable

complex in the presence of ATP, but still fails to form MCM2-7 double-hexamers in an efficient way. This suggests that the WHD5 has a role after ATP hydrolysis, potentially in the OCM to MCM2-7 double hexamer transition.

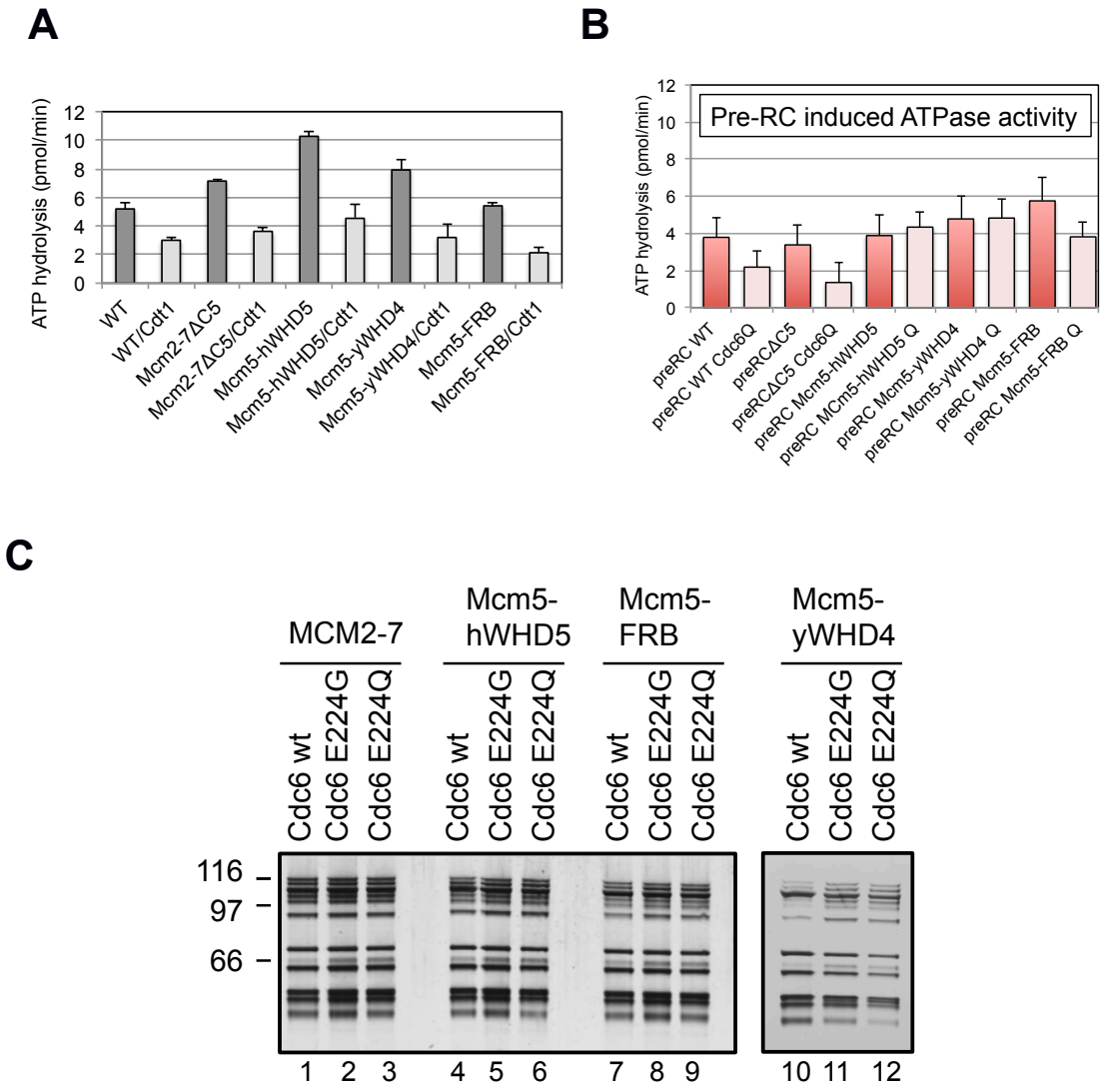


Figure 4.6. Analysis of the ATPase activity of the Mcm2-7 domain swapped.

A) Analysis of the ATP hydrolysis rate of WT MCM2-7, MCM2-7ΔC5, Mcm5-yWHD4, Mcm5-hWHD5, Mcm5-FRB individually (dark grey bar) and in the presence of Cdt1 (light grey bar). **B)** Analysis of pre-RC induced ATPase activity of the WT MCM2-7, MCM2-7ΔC5, Mcm5-yWHD4, Mcm5-hWHD5, Mcm5-FRB in the presence of Cdc6 (red bar) and Cdc6E224Q (pink bar). Results are for at least three independent experiments, and are plotted as average and error bars represent the standard deviation. Statistical analysis was determined by one-way ANOVA followed by post hoc test using Bonferroni correction. Refer to text for description of the results. **C)** Pre-RC assay showing the effect of Cdc6 ATPase mutants (E224G and E224Q) on Mcm5-yWHD4, Mcm5-hWHD5, Mcm5-FRB in ATP low salt buffer.

4.5. Double deletion mutants

In order to test whether multiple C-termini of MCM2-7 act in a cooperative way in establishing interactions with ORC/Cdc6, it was decided to combine the deletion of two of the McmC together. Since the removal of Mcm3C was shown to prevent the initial recruitment to ORC/Cdc6, none of the following mutants contain MCM2-7ΔC3 (Frigola et al., 2013). With this in mind, MCM2-7ΔC5 was combined with 1) MCM2-7ΔC4, 2) MCM2-7ΔC6, 3) MCM2-7ΔC7. The yeast strains containing double deletion mutants were tested for dominant lethality upon overexpression, following the protocol described in materials and methods (2.4.5). They all showed dominant lethality in galactose (Figure 4.7), suggesting that they affect essential functions vital for the cell. The proteins were expressed in *S. cerevisiae* and purified following the standard protocol for MCM2-7 purification (Materials and Methods 2.5).

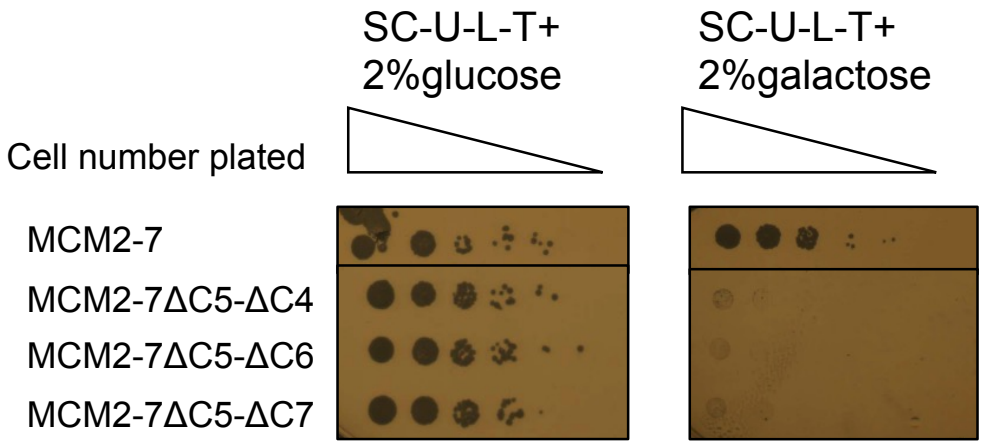
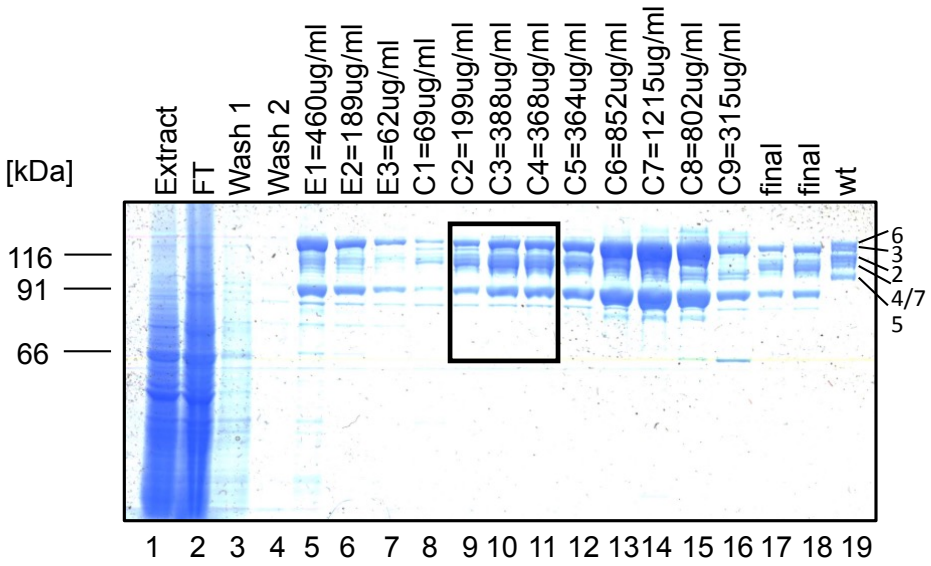


Figure 4.7. *In vivo* assay of the double deletion mutants

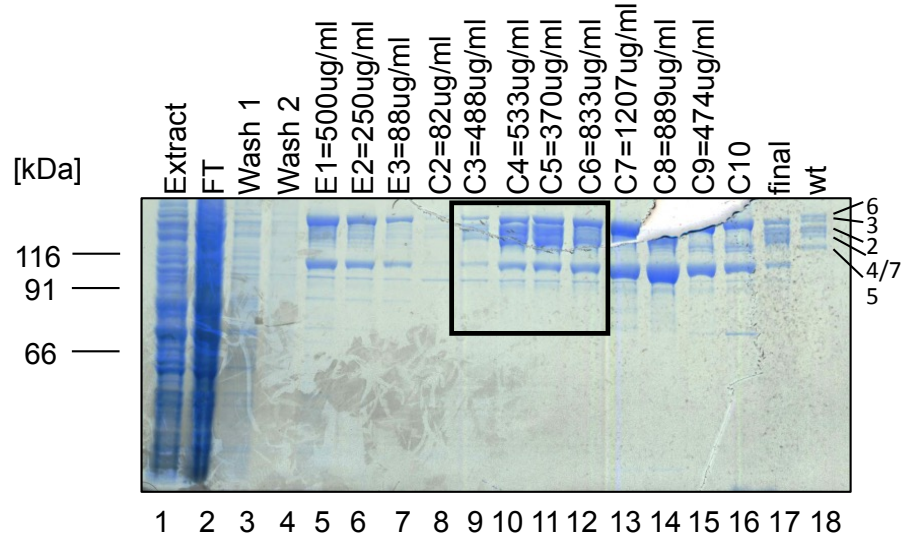
In vivo assay showing the effect of the overexpression of WT MCM2-7, MCM2-7ΔC5ΔC4, MCM2-7ΔC5ΔC6, MCM2-7ΔC5ΔC7 in generated yeast strains. A 5-fold dilution series of the yeast strains grown at the density of 10^7 was spotted on a selective plate, without uracil (U), leucine (L) and tryptophan (T) in the presence of 2% glucose (non-inducing condition) or 2% galactose (inducing condition). The plates were incubated at 30°C for two and four days respectively. The experiment was repeated twice.

The Coomassie stained gels of the purifications are showed in Figure 4.8 and the fractions containing the relevant proteins are highlighted. The final product of each purification was loaded in lane 17 of each gel, next to the WT MCM for stoichiometry comparison. It appeared evident that the MCM2-7ΔC4-ΔC5 (Figure 4.8 A) was lacking of the subunits Mcm6 (upper band), Mcm2 and Mcm4, leaving a trimer formed by Mcm3, Mcm7 and Mcm5ΔC5. This result suggests that Mcm5C and Mcm4C might be involved in MCM2-7 complex assembly or stability. MCM2-7ΔC5-ΔC6 and MCM2-7ΔC5-ΔC7 successfully purified with a yield comparable to WT purifications (Figure 4.8 B, C). The three proteins were assessed *in vitro* for their ability to form pre-RC. For a better comparison, reactions with MCM2-7 carrying the individual C-terminus deletions were also performed. Due to the large number of reactions, the results are shown in two separate panels (Figure 4.9 A-B). The mutants were assembled on origin DNA in the presence of ORC/Cdc6 and Cdt1 in buffer containing ATPγS showing that all (excluded MCM2-7ΔC4-ΔC5) bind ORC/Cdc6 in a similar way than WT (Figure 4.9 A lanes 12-19). When the double mutants were subjected to low salt washes, only the MCM2-7ΔC5-ΔC7 showed a stably bound protein complex, with no Cdt1 release, reflecting the effect of the individual MCM2-7ΔC7 (Figure 4.9 B compare lane 8 with 5). None of the three double deletion mutants supported a salt-stable complex formation (Figure 4.9 B lanes 14-16). Interestingly, while the effect produced by MCM2-7ΔC7 seems to be dominant in MCM2-7ΔC5-ΔC7 under low salt washes, this is not reflected under high salt washes, suggesting that a functional Mcm5C is required for double hexamer formation. This fits with the idea that the Mcm C-termini act in a temporal order during pre-RC formation and some C-termini act in addition for initial complex formation or stability.

A


[kDa]
Extract
FT
Wash 1
Wash 2
E1=460ug/ml
E2=189ug/ml
E3=62ug/ml
C1=69ug/ml
C2=199ug/ml
C3=388ug/ml
C4=368ug/ml
C5=364ug/ml
C6=852ug/ml
C7=1215ug/ml
C8=802ug/ml
C9=315ug/ml
final
final
wt
116
91
66
6
3
2
4/7
5
1 2 3 4 5 6 7 8 9 10 11 12 13 14 15 16 17 18 19

B


[kDa]
Extract
FT
Wash 1
Wash 2
E1=500ug/ml
E2=250ug/ml
E3=88ug/ml
C2=82ug/ml
C3=488ug/ml
C4=533ug/ml
C5=370ug/ml
C6=833ug/ml
C7=1207ug/ml
C8=889ug/ml
C9=474ug/ml
C10
final
wt
116
91
66
6
3
2
4/7
5
1 2 3 4 5 6 7 8 9 10 11 12 13 14 15 16 17 18

C

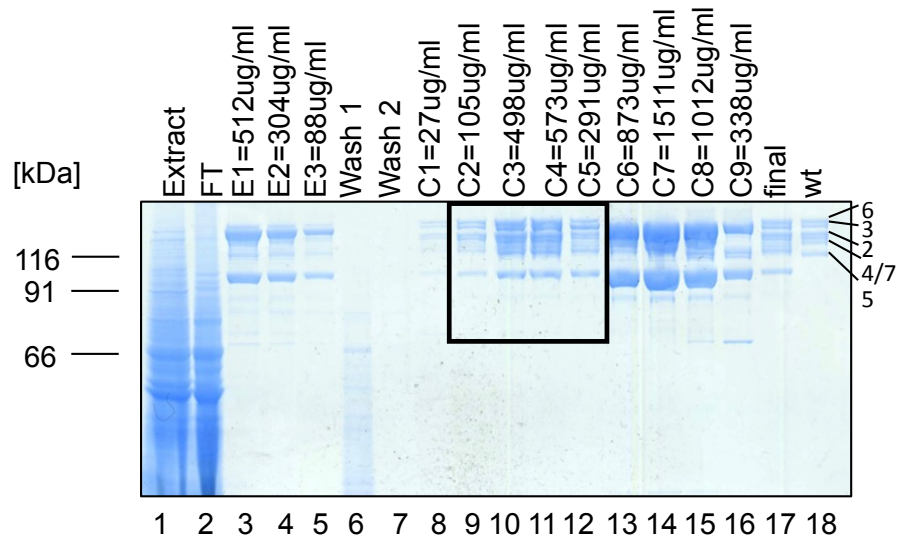

[kDa]
Extract
FT
E1=512ug/ml
E2=304ug/ml
E3=88ug/ml
Wash 1
Wash 2
C1=27ug/ml
C2=105ug/ml
C3=498ug/ml
C4=573ug/ml
C5=291ug/ml
C6=873ug/ml
C7=1511ug/ml
C8=1012ug/ml
C9=338ug/ml
final
wt
116
91
66
6
3
2
4/7
5
1 2 3 4 5 6 7 8 9 10 11 12 13 14 15 16 17 18

Figure 4.8. Purifications of MCM2-7ΔC5-ΔC4, MCM2-7ΔC5-ΔC6, MCM2-7ΔC5-ΔC7

A-C) Coomassie-stained SDS-PAGE showing the two-step purifications of MCM2-7ΔC5-ΔC4, MCM2-7ΔC5-ΔC6, MCM2-7ΔC5-ΔC7. The protocol was performed as described in Evrin et al, 2009. The relevant fractions containing the pure protein of interest are marked in black in each gel. Lane 17 of each gel shows the final product of the purifications and in the last lane a sample of WT MCM2-7 was loaded for stoichiometry comparison.

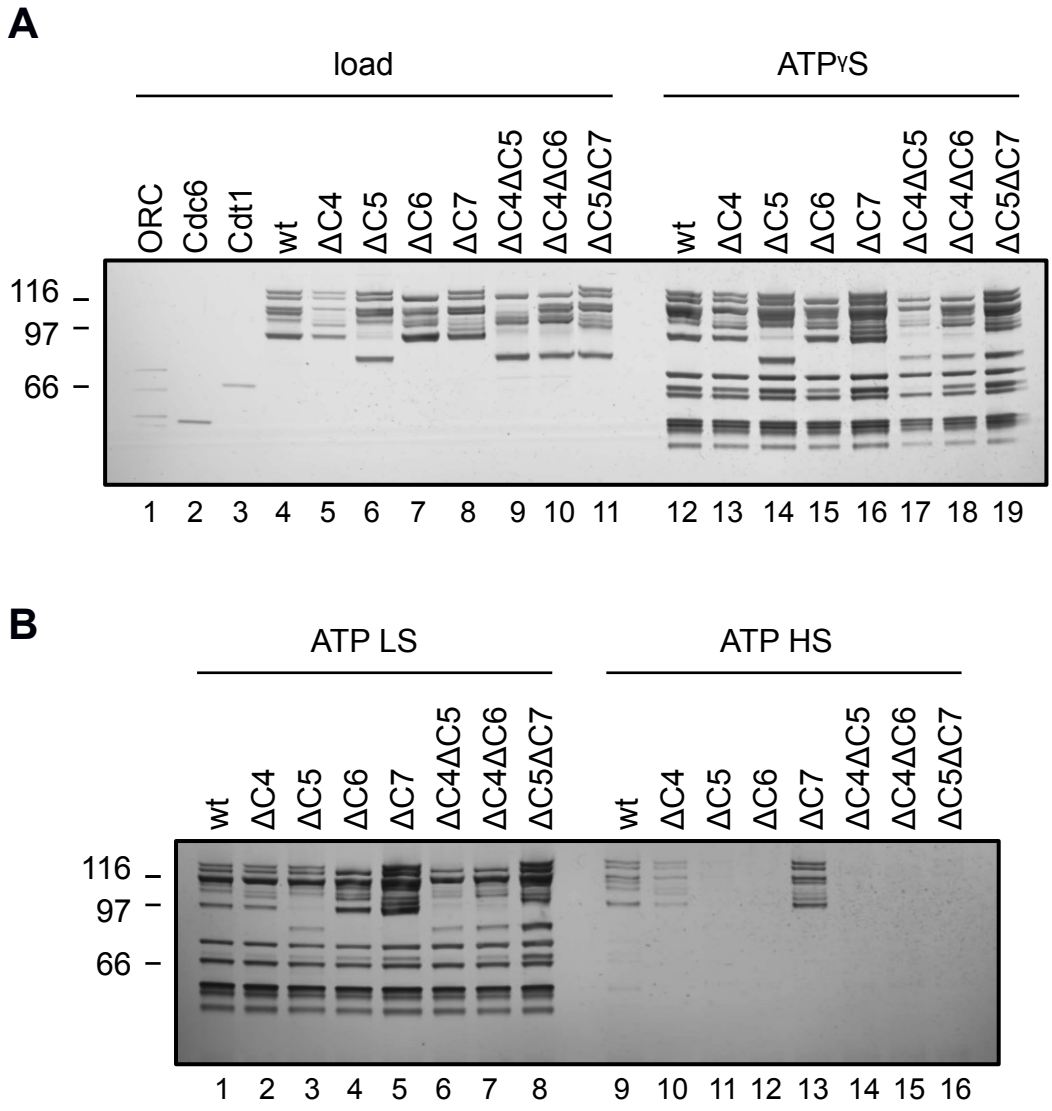


Figure 4.9. *In vitro* activity of the double deletion mutants of MCM2-7

A) Silver stained SDS-PAG gel with lanes 1-11 showing the purified proteins used in the assay. Pre-RC reactions in the presence of ATPγS were assembled on bead-bound DNA, washed and eluted. **B)** Silver stained gel showing the pre-RC reactions assembled in the presence of the single or double deletion MCM2-7 mutants in the presence of ATP. Reactions were washed with low salt (LS) or high salt (HS) washes prior elution from the beads. The experiment was performed twice.

4.6. Mutation of the linker region in the Mcm5C

The detailed structural organisation of Mcm5C was described at the beginning of this chapter. The focus in the following is the linker, which connects the main body of Mcm5 to the WHD. This 13 amino acid-long linker region (693-707) was not visible in the published structures of pre-RC intermediates, or in the unpublished structure of the "OCCM-closed" conformation presented at the beginning of this chapter, suggesting that it is highly flexible.

In the MCM2-7ΔC5 mutant this linker along with the WHD was completely removed. The functional role of this linker region, if any, is not known. Interestingly, the linker is well conserved in sequence and length in several higher eukaryotes (*C. elegans, D. melanogaster, X. laevis, G. gallus, M. musculus, H. sapiens*), whereas in yeast *(S. cerevisiae, S.pombe, C. albicans, K. pastoris*), a certain degree of variability can be observed (Figure 4.10 A). Here we undertook a mutational approach to investigate the contribution of the linker on pre-RC formation.

To address the role of the linker region, four mutants were created. The first mutant consisted only of the linker by itself and was lacking the entire WHD5 (amino acids 708-775) and is termed "Mcm5-linker only". The three other constructs kept the WHD5 intact, but altered the sequence and length of the linker region. In order to address the role of the linker in providing spatial separation between the Mcm5 base and the WHD, the original linker sequence (QDPIGGLNQASGT) was replaced with a shorter one (7 amino acids, QDPASGT). To ask whether the linker sequence was important, a new flexible linker with an entire new sequence, but conserving the original length (QDPGGSGGGGSGG), was introduced. Small, non-polar (Gly) and polar (Ser) amino acids provides flexibility, and allows for mobility of the connecting functional domains. The incorporation of Ser allows formation of hydrogen bonds with the water molecules stabilizing the linker in aqueous solutions and therefore reducing the unfavorable interactions (Argos, 1990). Finally, to address the role of flexibility, a more rigid sequence was tested (QPDEAAAKEAAAK), which displays alpha helical conformation and was used as a rigid spacer between domain in other studies (Chen et al., 2013) (Figure

4.10 B). The attempt to purify MCM2-7 with a rigid linker failed, for unknown reasons. The other protein constructs were successfully purified following the standard MCM2-7 purification protocol (Materials and Methods 2.5) (data not shown).

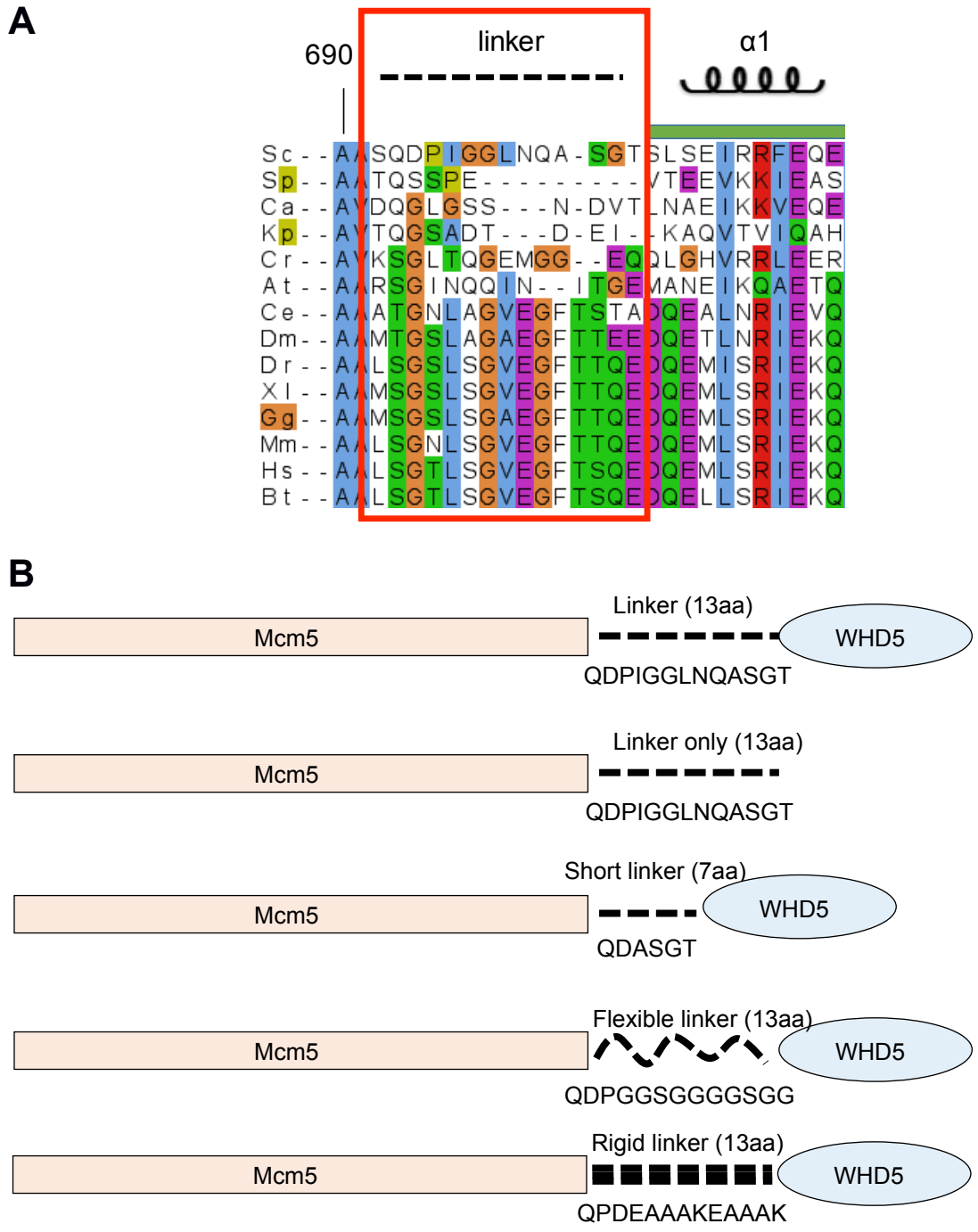


Figure 4.10. Design of the Mcm5C linker mutants

A) Sequence alignment of the linker of Mcm5C from *S.cerevisiae* compared to other eukaryotic species (amino acids 693-706 in *S.cerevisiae*). **B)** Schematic representation of the linker mutants generated in Mcm5C in the context of the full length MCM2-7.

Initially, it was tested if overexpression of the constructs results in dominant lethality (Materials and Methods 2.4.5). The MCM2-7 strains were grown on solid media containing 2% glucose, which does not induce overexpression or 2% galactose which induces overexpression. The WT MCM2-7 strain was used as a positive control (no dominant lethality) and MCM2-7ΔC5 as negative control (dominant lethality). The strain “Mcm5-linker only” displayed dominant lethality, suggesting that a functional WHD5 plays an essential function. The other strains were viable in galactose, indicating that reducing the length or changing the amino acids sequence of the linker did not affect vital functions in cells (Figure 4.11 A). It is to note that in this experiment the chromosomal wild type copy has not been deleted therefore it may be possible that these mutants may exhibit a phenotype in the absence of the WT copy.

In order to assess the ability of the linker mutants to associate with the origin and form double-hexamer around DNA, the purified MCM2-7 linker mutants were tested in the pre-RC assay, as described (Materials and Methods 2.7.3). “Mcm5-linker only” behaved similar as MCM2-7ΔC5, with normal recruitment in the presence of ATPγS (OCCM), a reduction in the association with DNA when incubated with ATP (OCM), but increased levels of Cdt1 and complete defect in double hexamer formation (Figure 4.11 B). This result suggests that the linker does not alleviate any of the defects observed with MCM2-7ΔC5.

The other two linker mutants showed recruitment (OCCM), OCM formation and double-hexamer formation at a level similar to WT MCM2-7. These data suggest that changes affecting the sequence or length of the linker, but not the WHD5, do not appear to affect pre-RC formation *in vitro*. Mcm5C can function with a modified linker region in pre-RC formation, which fits with the observation that in lower eukaryotes the sequence and length of the linker various widely. It has not been tested here the effect of a longer linker sequence, but indirectly tested this in the context of cleavable MCM2-7 mutants discussed in the Chapter 3. Briefly, the insertion of multiple PreScission cleavage sites in the linker region generated a 28 amino acids sequence, which also involved a change of the original amino acid sequence. It was found that the pre-RC activity of this construct was not affected. Therefore, taken together,

these experiments demonstrate that the linker connecting the WHD5 to the Mcm5 base, does not have an obvious function in pre-RC formation. The observed *in vivo* effects correlate very well with the pre-RC assembly results, further strengthening the conclusion.

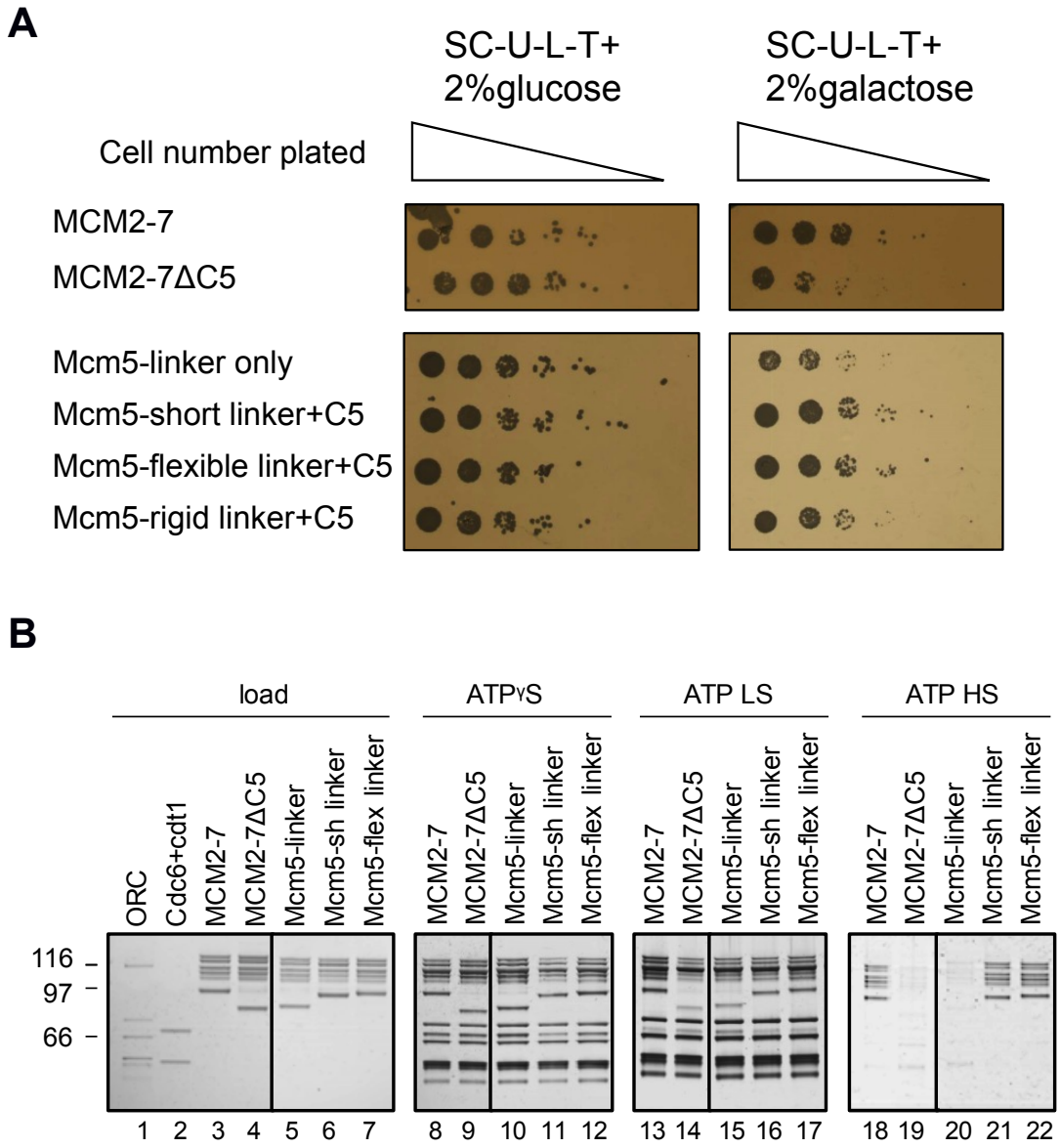


Figure 4.11. Analysis of the linker mutants *in vivo* and *in vitro*

A) Test for *in vivo* dominant lethality in overexpression. A dilution series of the yeast strains was spotted on 2% glucose and 2% galactose plates. The WT MCM2-7 is used as a positive control (viable) and MCM2-7ΔC5 as a negative control (dominant lethal). (The experiement was performed twice) **B)** The Mcm5 linker mutants proteins were assembled in pre-RC reactions and tested for their ability to recruit MCM2-7 complex to ORC/Cdc6 in ATPγS (lanes 10-12), to associate with pre-RC proteins in ATP low salt washes (LS) and to form salt stable double hexamer (HS, high salt washes, 300 mM sodium chloride). The experiment was repeated twice.

In order to investigate if the linker has a role in the pre-RC induced ATPase activity, the ATP hydrolysis rate of these mutants was measured in the ATPase assay, as previously described. The intrinsic ATP hydrolysis rate of the "Mcm5 linker only" was similar to MCM2-7ΔC5, and in both cases it was significantly ($p<0.01$) decreased by the presence of Cdt1 (Figure 4.12 A). The "Mcm5-short linker+C5" had a very low basal ATPase activity by itself (1.5 pmol/min), which was further suppressed by the binding of Cdt1. The ATPase activity of "Mcm5-flexbile linker+C5" was significantly ($p<0.01$) lower than WT MCM2-7 (3.8 pmol/min) and supressed by Cdt1.

These results suggest that a short linker+C5 can drastically suppress the MCM2-7/Cdt1 ATP-hydrolysis rate. The mechanism is not entirely clear, but could have significance in the context of the CMG helicase. The pre-RC induced ATPase activity (total pre-RC activity minus the contribution of ORC/Cdc6 and MCM2-7/Cdt1) for these mutants is shown in Figure 4.12 B. The "Mcm5-linker only" complex had low pre-RC induced ATPase activity. This result with the observation that the mutant shows reduced Cdt1 release, suggests a slow or defective transition to the OCM complex. Even though the other two Mcm5 linker mutants form a fully functional double hexamer in pre-RC assay, the pre-RC induced ATPase activity is lower than WT. Cdc6 E224Q had no major effect on the ATPase rate, suggesting that most ATP hydrolysis is channelled into productive Cdt1 release ATP-hydrolysis cycle and pre-RC formation. It is surprising that the flexible linker+C5 mutant was fully functional in pre-RC formation, while it was displaying much reduced ATP-hydrolysis. Even though there is a trend for a decrease in all of the three linker mutants, this difference is not statistically significant ($n=2$).

Taken together, these results indicate that, within reason, changing the length or sequence of the linker region in Mcm5 does not affect the ability of Mcm2-7 to form a stable double hexamer. The ATPase assay data suggest that the total pre-RC ATPase activity is affected by modification of the linker, but not the Cdc6 contribution to it. Whereas the effect of the linker mutations on pre-RC assay appeared to correlate with the observed effects *in vivo,* the effect on ATPase hydrolysis is not consistent with changes in this measure. Thus, the linker region might indirectly regulate the overall MCM2-7 ATP hydrolysis rate.

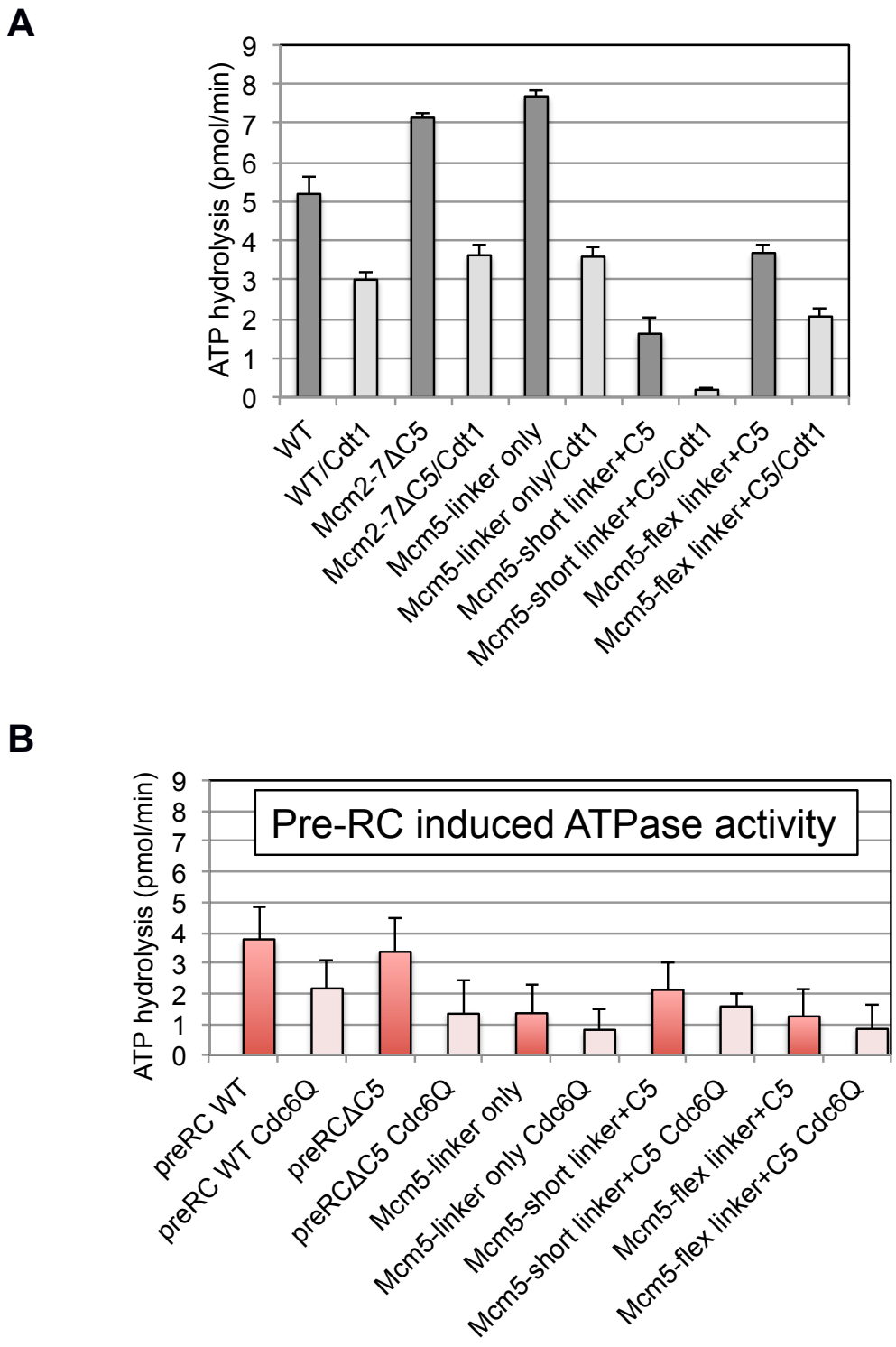


Figure 4.12. Analysis of ATPase activity of the linker mutants in Mcm5C

The ATP hydrolysis rate was measured using a ATPase assay, described previously. **A)** Analysis of the ATPase activity of WT MCM2-7, MCM2-7ΔC5, Mcm5-linker only, Mcm5-short linker+C5, Mcm5-flexible linker+C5 individually (dark grey) and in the presence of Cdt1 (light grey). **B)** Analysis of the pre-RC induced activity of the Mcm5C linker mutants in the presence of Cdc6 (red) and Cdc6E224Q (pink bar). Results for B and C are for two independent experiments, and are plotted as average. Error bars represent the standard deviation. Statistical analysis was determined by one-way ANOVA followed by post hoc test using Bonferroni correction.

4.7. Rationale for the design of point mutant constructs

In the previous chapter, the data showed that Mcm5C is not required for the initial recruitment of the OCCM, but it is essential for a functional OCM and double hexamer formation. We hypothesise that one or multiple important interactions of WHD5 with ORC subunits are required for WHD5 function during pre-RC formation. In particular, removing Mcm5C could lead to loss of interaction with Orc2, based on the interactions revealed by CLMS (Yuan et al., 2017). Furthermore, the newly available cryo-EM structure (Yuan et al, unpublished), suggests WHD5 interactions with Orc3 (Figure 4.13).

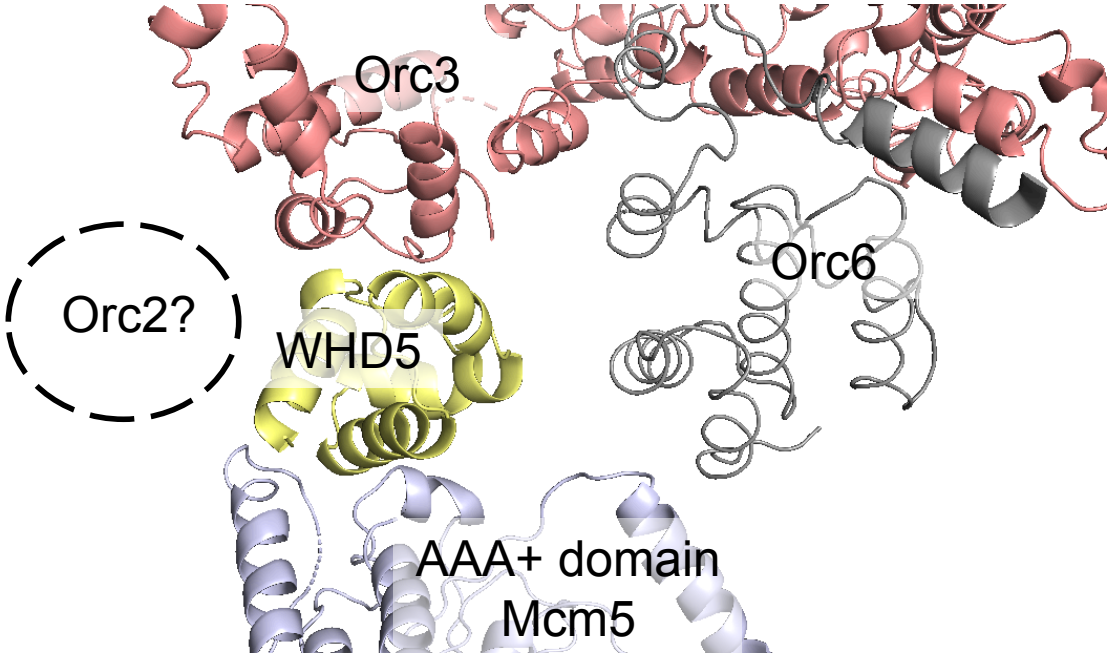


Figure 4.13. Position of WHD5 and Orc3 in the context of the OCCM

In the OCCM structure (closed conformation), the WHD5 (yellow) is located in close proximity to Orc3 (coloured in salmon). Orc2 was not visible in the cryo-EM (presented as dashed circle). Orc6 (in grey) was visible at low threshold but its N-terminus was not resolved.

In order to test our hypotheses, a series of Mcm5C point mutants were created in the context of the full-length MCM2-7 complex. Since the resolution of the new cryo-EM structure was limited in the region of WHD5, a low risk

approach was adopted, involving combinations of two/three point mutations, with reduced impact on the local secondary structure, but maximised chances to obtain a phenotype. The mutants were targeting charge-based interactions of WHD5 with surrounding pre-RC proteins. Positively charged amino acids were changed to negative ones and vice versa (Figure 4.14 A). Groups of amino acids were mutated in the helices that are in the structure either (1) facing “up” towards ORC, (2) “down” towards the AAA+ domain of Mcm5, and (3) on the “side” facing either Orc2 or Orc6. The location of the individual amino acids is shown in the panels A-F.

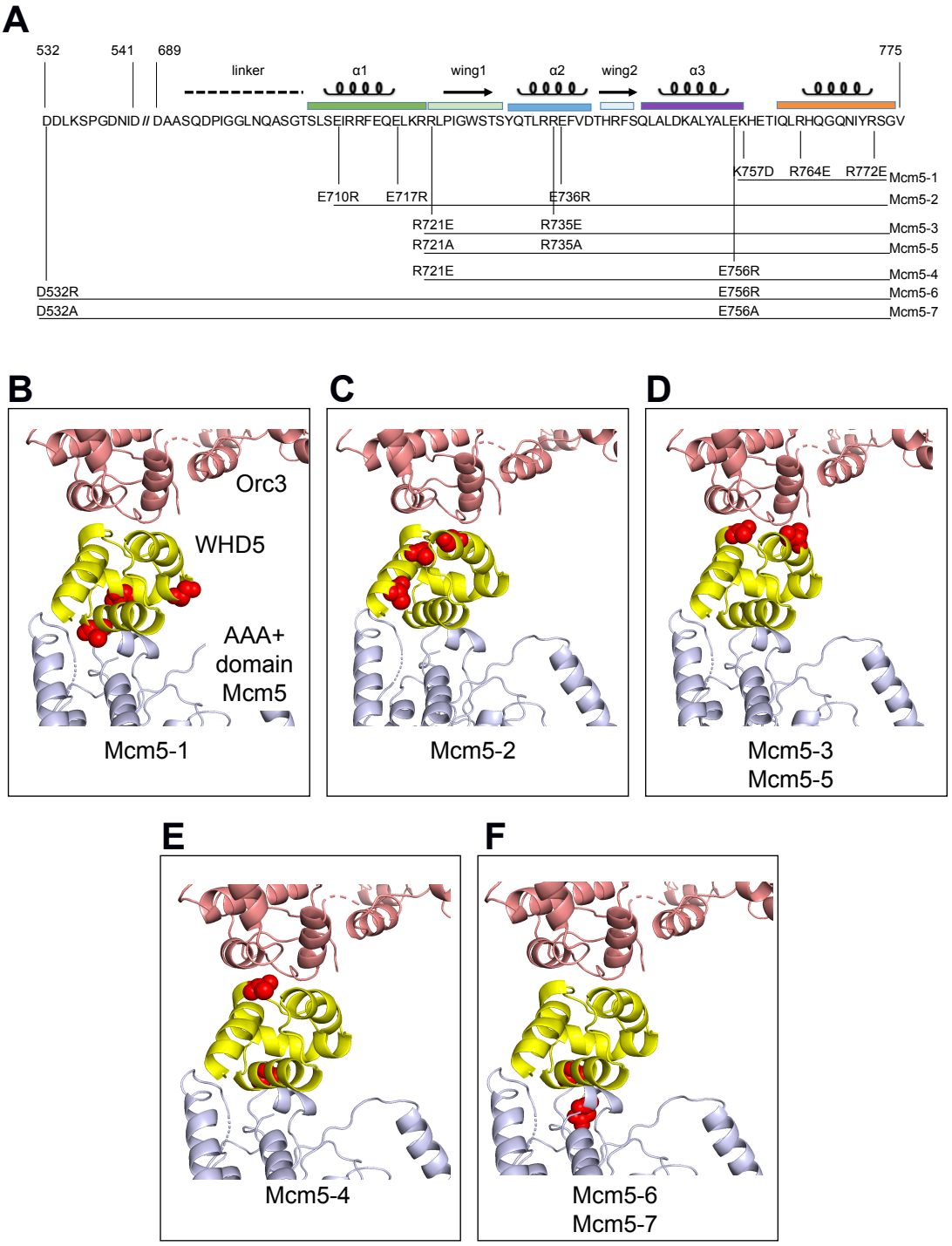


Figure 4.14. Double and triple point mutations in Mcm5 C-terminus

A) Sequence of the *S. cerevisiae* Mcm5C. The position of various mutants generated during this study is shown by vertical lines and the mutant amino acid is shown at the bottom of the line. Name of the mutants on the right. Double and triple amino acids mutants are shown. **B-F)** The mutated amino acids are indicated as red spheres in the structure of the OCCM-closed conformation, zoomed on the WHD5 (yellow) and the neighboring Orc3 (salmon).

In order to obtain even larger effects on pre-RC formation various mutants were combined resulting in versions containing a larger number of amino acid changes, specifically combining the “side + down” and “side + up” mutants (Figure 4.15 A, B). I refer to MCM2-7 complexes harbouring point mutations in Mcm5C as “Mcm5-” followed by a number.

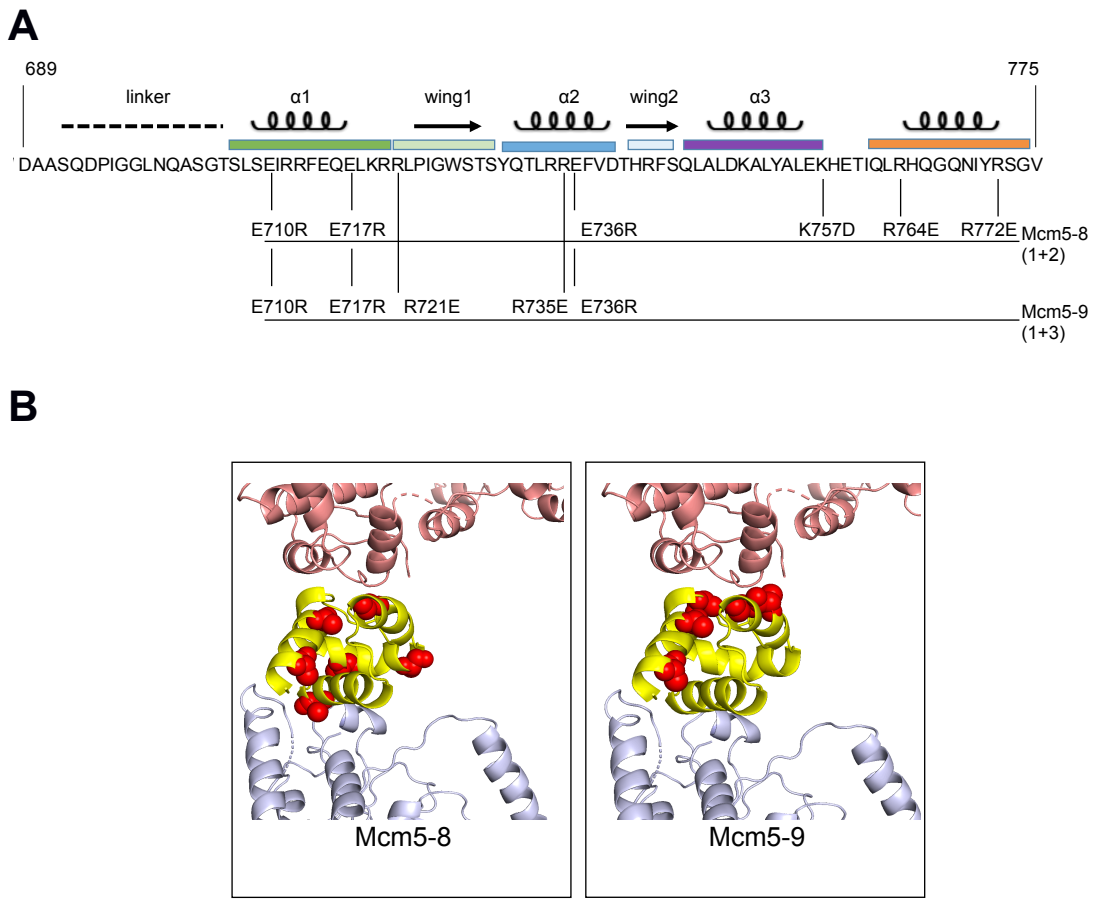


Figure 4.15. Combination of point mutations in Mcm5 C-terminus

A) Sequence of the *S. cerevisiae* Mcm5C. The position of the mutants Mcm5-8 and Mcm5-9 by vertical lines and the mutant amino acid is shown at the bottom of the line. The name of the mutants is on the right. **B)** The mutated amino acids are indicated as red spheres in the structure of the OCCM-closed conformation, zoomed on the WHD5 (yellow) and the neighboring Orc3 (salmon).

4.8. Point mutations in Mcm5C affects helicase loading

Each plasmid containing specific point mutations in Mcm5C was designed, synthesised by Genscript, and consequently transformed into yeast cells. Initially, the yeast strains were tested *in vivo* for dominant lethality upon overexpression (Figure 4.16), as described in the Materials and Methods chapter (2.4.5). A strain overexpressing WT MCM2-7 served as an example of a viable strain, while the strain overexpressing MCM2-7ΔC5 strain served as a negative control, as it causes dominant lethality. In the case of the strains Mcm5-2 ("up+side"), Mcm5-3 ("up"), Mcm5-4 ("up+down") and Mcm5-5 ("up") dominant lethality was observed in 2% galactose. These results suggests that these mutations abolished an essential function *in vivo*.

In order to determine whether the point mutations had a specific effect on double hexamer assembly, all of the mutants were expressed in *S. cerevisiae* and purified following the protocol described in Materials and Methods for MCM2-7 purification (paragraph 2.5). All of the mutant MCM2-7 complexes eluted during the gel filtration at the same position as the WT and three representative Coomassie stained gels of the purifications are shown in Figure 4.17. Figure 4.18 shows a silver stained gel of the purified proteins showing the equivalent subunit stoichiometry of the mutants complexes in comparison to the WT.

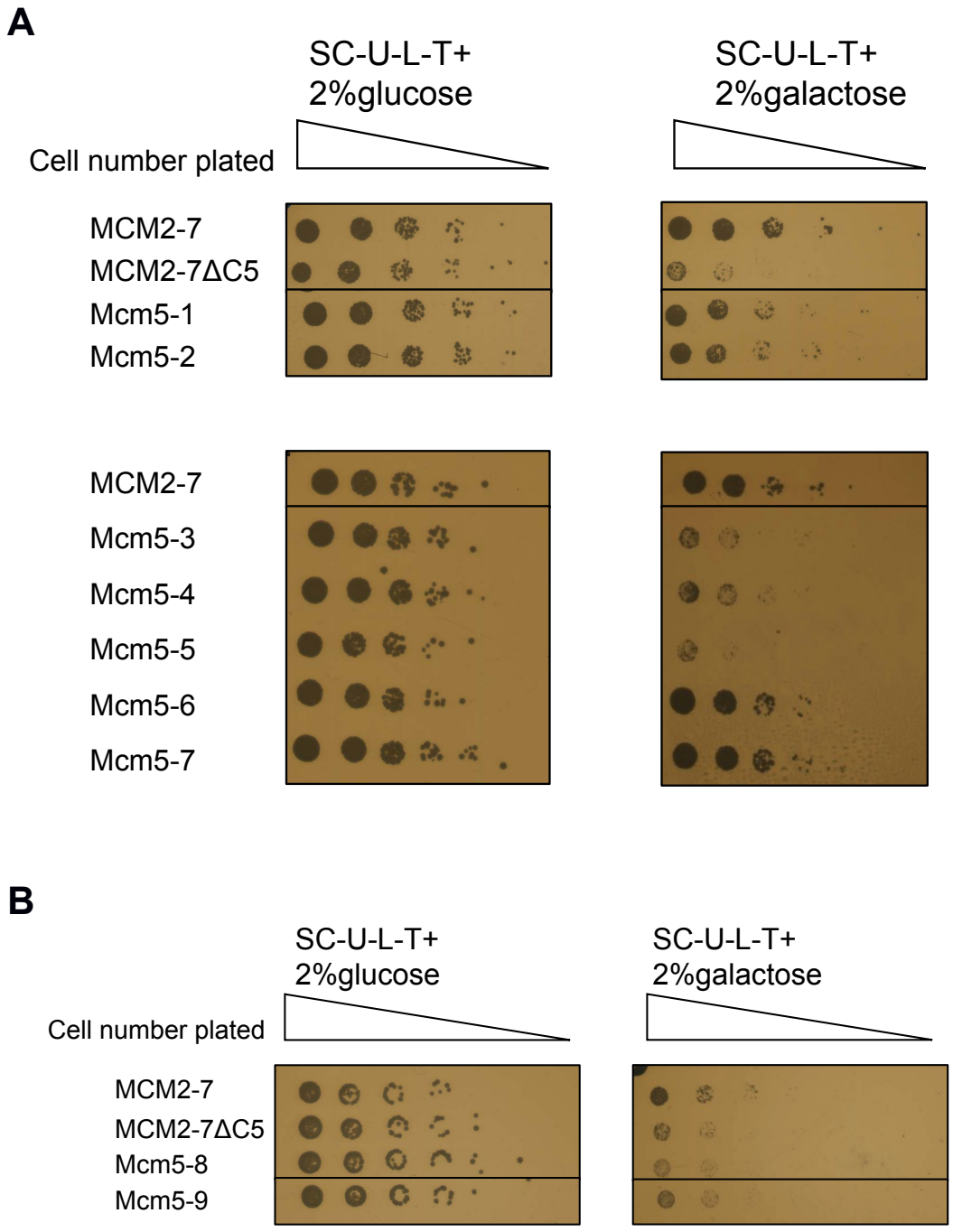


Figure 4.16. *In vivo* dominant lethality test of the point mutants

A-B) Yeast dominant lethality assay showing the effect of overexpression of the wild type MCM2-7 and the Mcm5C point mutants strains. A 5-fold dilution of the cells at the starting density of 107 was spotted onto selective dropout plates with either 2% glucose or galactose. The plates were incubated for two and four days respectively. The experiment was performed three times.

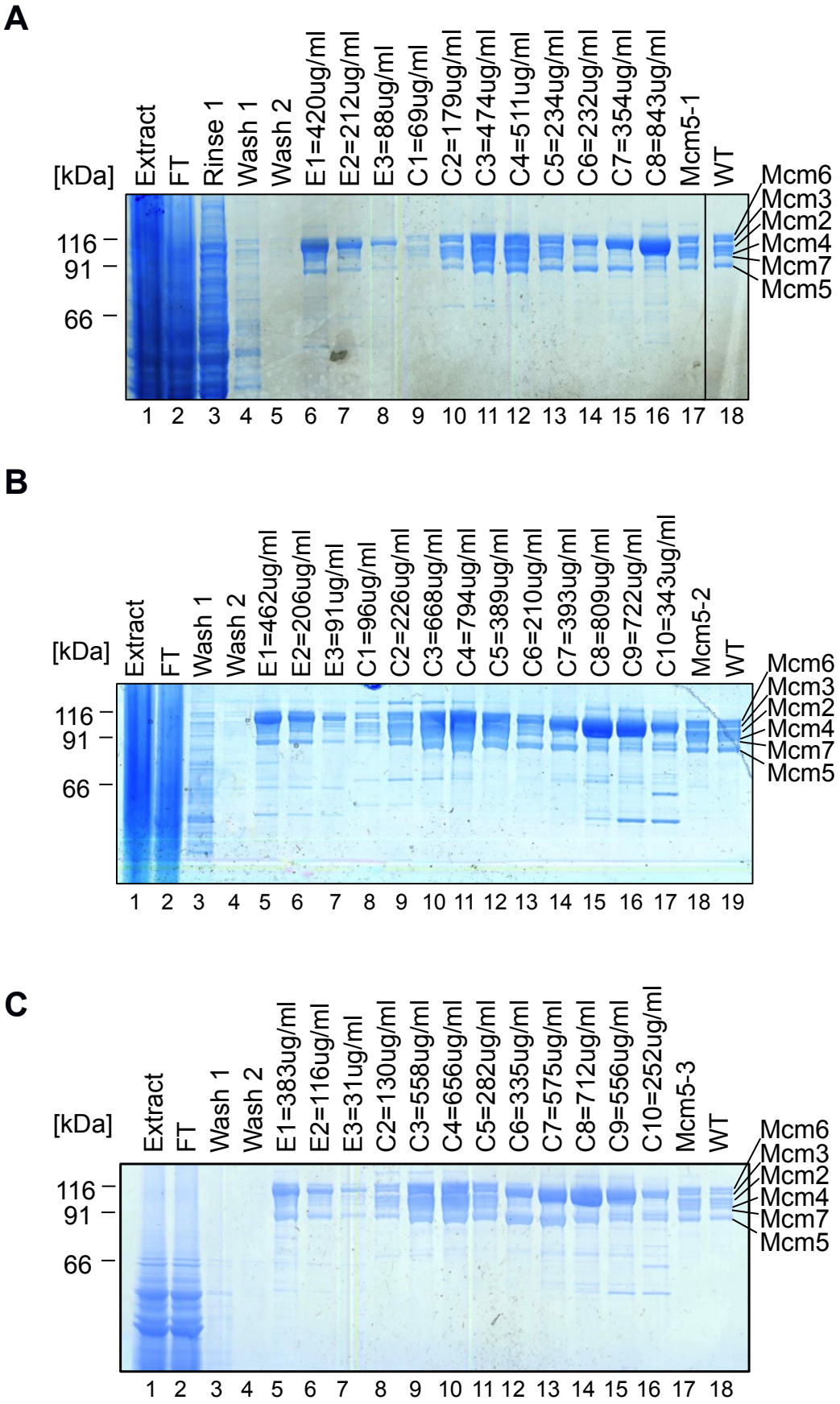

A
[kDa]
Extract
FT
Rinse 1
Wash 1
Wash 2
E1=420ug/ml
E2=212ug/ml
E3=88ug/ml
C1=69ug/ml
C2=179ug/ml
C3=474ug/ml
C4=511ug/ml
C5=234ug/ml
C6=232ug/ml
C7=354ug/ml
C8=843ug/ml
Mcm5-1
WT
116
91
66
Mcm6
Mcm3
Mcm2
Mcm4
Mcm7
Mcm5
1 2 3 4 5 6 7 8 9 10 11 12 13 14 15 16 17 18
B
[kDa]
Extract
FT
Wash 1
Wash 2
E1=462ug/ml
E2=206ug/ml
E3=91ug/ml
C1=96ug/ml
C2=226ug/ml
C3=668ug/ml
C4=794ug/ml
C5=389ug/ml
C6=210ug/ml
C7=393ug/ml
C8=809ug/ml
C9=722ug/ml
C10=343ug/ml
Mcm5-2
WT
116
91
66
Mcm6
Mcm3
Mcm2
Mcm4
Mcm7
Mcm5
1 2 3 4 5 6 7 8 9 10 11 12 13 14 15 16 17 18 19
C
[kDa]
Extract
FT
Wash 1
Wash 2
E1=383ug/ml
E2=116ug/ml
E3=31ug/ml
C2=130ug/ml
C3=558ug/ml
C4=656ug/ml
C5=282ug/ml
C6=335ug/ml
C7=575ug/ml
C8=712ug/ml
C9=556ug/ml
C10=252ug/ml
Mcm5-3
WT
116
91
66
Mcm6
Mcm3
Mcm2
Mcm4
Mcm7
Mcm5
1 2 3 4 5 6 7 8 9 10 11 12 13 14 15 16 17 18

Figure 4.17. Purification of Mcm5C point mutants

Comassie-blue stained gels of the two-step purification of the point mutants Mcm5-1 **(A)**, Mcm5-2 **(B)** and Mcm5-3 **(C)**, performed following the WT MCM2-7 protocol (Evrin et al, 2009). Yeast extract produced via freezer milling was incubated with anti-HA beads, rinsed and washed twice before bound MCM2-7 (via HA-Mcm3) was eluted three times with HA peptide (E1, E2, E3). The eluate was concentrated and injected into a size-exclusion chromatography column and fractions collected and analysed in a 4-12% SDS-PAGE (labeled "C" followed by a number on top of the gel). Fractions C2-C5 contain the pure hexameric protein and were collected, concentrated and aliquoted. The final protein is loaded at the end together with the WT for comparison. Bradford concentrations of the elution and gel filtration fractions are indicated on top of each lane.

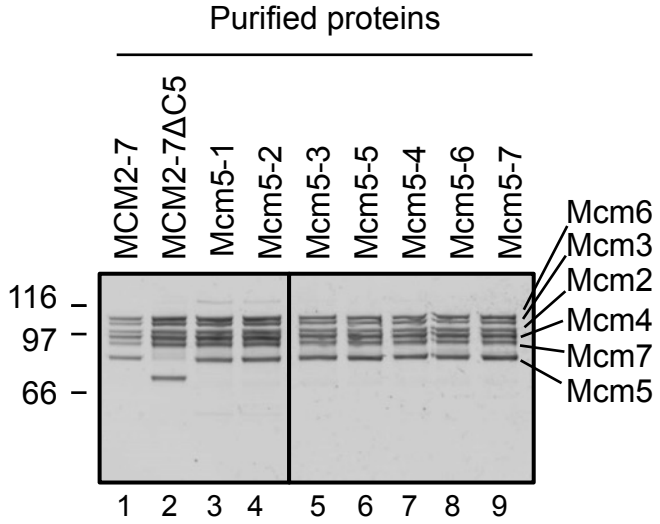


Figure 4.18. Purified Mcm5C point mutants

Silver stained gel showing the purified Mcm5C point mutants proteins (lanes 3-9), compared with WT MCM2-7 (lane 1) and MCM2-7ΔC5 (lane 2) for comparison.

The purified mutant MCM2-7 complexes were tested for their ability to be recruited to and loaded onto origin DNA using an *in vitro* reconstituted pre-RC assay (Figure 4.19). Due to the number of mutants, and to enable easy comparison, the results are presented as panels, each representing different assembly conditions. To investigate whether the Mcm5C point mutants altered the initial recruitment of MCM2-7/Cdt1 to ORC/Cdc6, pre-RC assays were performed in the presence of ATPγS. A silver stained gel displaying the results is shown in Figure 4.19 A. Under these conditions, helicase loading is arrested prior to Cdt1 release and MCM2-7/Cdt1 are associated with DNA via ORC and

Cdc6 (Randell et al., 2006). All of the Mcm5C mutant complexes were recruited to origin DNA at levels similar to WT MCM2-7. To assess whether the Mcm5C point mutants were defective in OCM formation and/or salt stable MCM2-7 double-hexamer formation, pre-RC reactions followed by a low or high salt wash were performed. A silver stained gel of the mutant complexes assembled in ATP following low salt washes is shown (Figure 4.19 B). Under low salt wash conditions, stable association of ORC, Cdc6 and MCM2-7 was observed in all of the mutants, except for Mcm5-1 ("down") and Mcm5-4 ("up+down"). These two exhibited in comparison to the WT slightly reduced association with ORC/Cdc6.

Under high salt wash conditions only MCM2-7 complexes that have successfully formed double-hexamers on DNA are retained. A silver stained gel of the high salt washed pre-RC reactions with WT and mutant MCM2-7 is shown in Figure 4.19 C. Among the seven mutants, one of them was fully functional in double hexamer formation (Mcm5-7 – "down") (Figure 4.19 C, lane 7), suggesting that the respective mutations do not affect successful pre-RC formation. The other six mutants were all defective in helicase loading but with various degrees of defect. The highest deficiency was observed in Mcm5-1 ("down"), Mcm5-2 ("up+side") and Mcm5-3 ("up"), which displayed a strong reduction in double-hexamer formation (Figure 9C, lanes 3, 4, 6). Mcm5-4 ("up+down"), Mcm5-5 ("up") and Mcm5-6 ("down") were less defective (Figure 4.19 C, lanes 5, 8, 9). Thus, although the mutants supported under low salt conditions mostly efficient complex formation, some displayed drastically reduced salt stable double-hexamer formation. This suggests that Mcm5-1,-2 and-3 affect the OCM to double-hexamer transition. The small amount of high salt resistant MCM2-7, as observed with Mcm5-1,-2 and-3, could reflect a small amount of WT protein being co-purified with the mutants, as they are purified from yeast, which contains a chromosomal not overexpressed WT *Mcm5*.

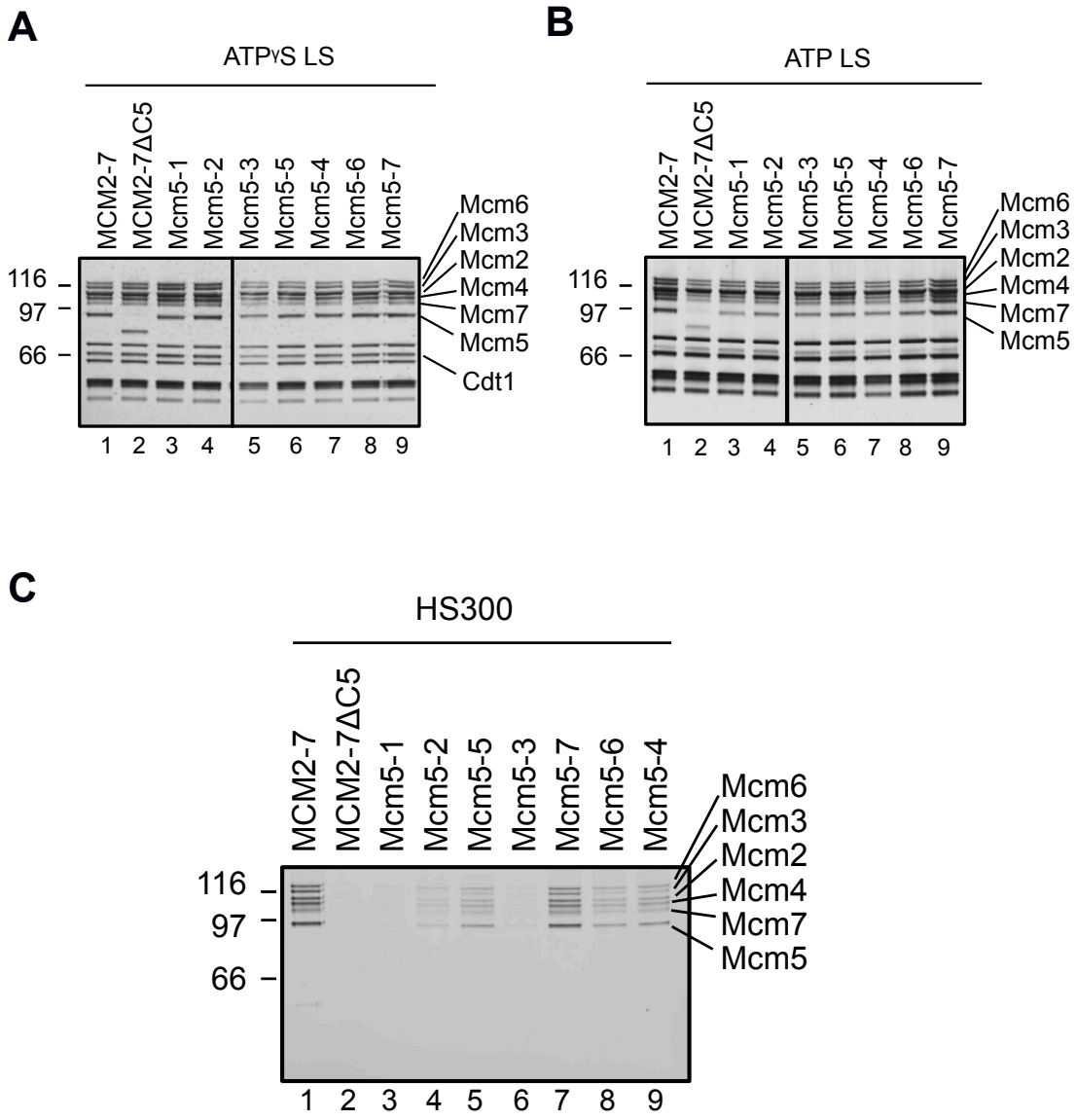

A
ATPγS LS
MCM2-7
MCM2-7ΔC5
Mcm5-1
Mcm5-2
Mcm5-3
Mcm5-5
Mcm5-4
Mcm5-6
Mcm5-7
116
97
66
Mcm6
Mcm3
Mcm2
Mcm4
Mcm7
Mcm5
Cdt1
1 2 3 4 5 6 7 8 9
B
ATP LS
MCM2-7
MCM2-7ΔC5
Mcm5-1
Mcm5-2
Mcm5-3
Mcm5-5
Mcm5-4
Mcm5-6
Mcm5-7
116
97
66
Mcm6
Mcm3
Mcm2
Mcm4
Mcm7
Mcm5
1 2 3 4 5 6 7 8 9
C
HS300
MCM2-7
MCM2-7ΔC5
Mcm5-1
Mcm5-2
Mcm5-5
Mcm5-3
Mcm5-7
Mcm5-6
Mcm5-4
116
97
66
Mcm6
Mcm3
Mcm2
Mcm4
Mcm7
Mcm5
1 2 3 4 5 6 7 8 9
D
Relative band intensity
1.4
1.2
1
0.8
0.6
0.4
0.2
0
WT
ΔC5
Mcm5-1
Mcm5-2
Mcm5-3
Mcm5-4
Mcm5-5
Mcm5-6
Mcm5-7

Figure 4.19. *In vitro* assay to test the activity of the mutants

Silver stained gels showing the *in vitro* reconstitution of pre-RC formation to test the ability of the point mutants in Mcm5 to associate with origin DNA in the presence of ORC, Cdc6, Cdt1 and to form a salt stable complex. Reactions containing the wild type MCM2-7 are used as a positive control and MCM2-7ΔC5 is used as a negative control **A)** Reactions were assembled in pre-RC buffer in the presence of ATPγS to test the ability of the mutant proteins to be recruited by ORC/Cdc6. **B)** Reactions were assembled on DNA and washed with buffer containing 300 mM potassium glutamate (LS, low salt). **C)** Reactions were assembled on DNA bound to beads and washed with buffer containing 500 mM NaCl (HS, high salt). **D**) Quantification of gel in panel C using Multi Gauge software. Plots of the relative band intensity of each mutant compared to the WT (lane 1) based on two independent experiments. Error bars indicate standard deviation.

Combining multiple mutations in Mcm5-8 (Mcm5-1+Mcm5-2) and Mcm5-9 (Mcm5-2+Mcm5-3) did not cause a more prominent defect than the individual mutants (Figure 4.20). This suggests that the mutants do not act in an additive way and probably act in the same way. Similar as Mcm5-1, both mutants showed in the presence of ATP and low salt conditions reduced MCM2-7/Cdt1 association levels when compared to the WT (Figure 4.20, compare lane 7 with 10 and 13) and both failed in double hexamer formation (Figure 4.20, lanes 11 and 14).

Taken together these results indicate that Mcm5-1/-2/-3 do not affect the initial OCCM formation, but steps beyond that. Then again, Mcm5-1/-4 displayed reduced OCM formation, while Mcm5-1/-2/-3 affected strongly MCM2-7 double-hexamer formation. For simplicity, Table 4.1 contains a summary of the tested point mutants with their effect in the pre-RC assay, relative to WT.

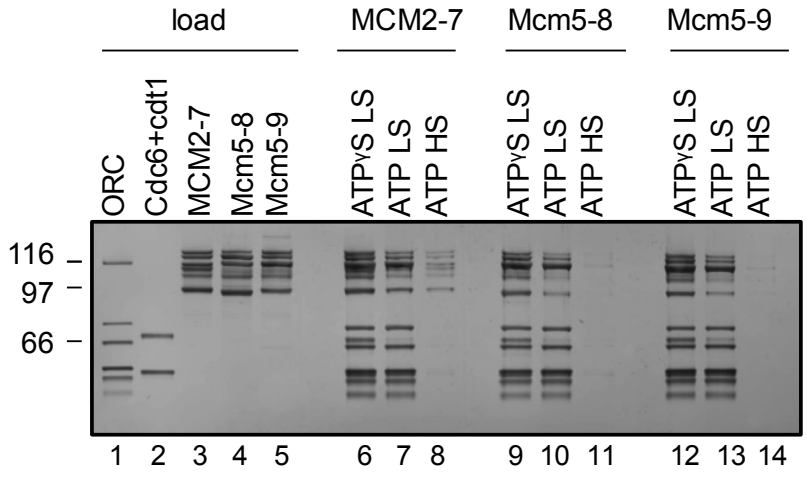


Figure 4.20. *In vitro* assay to test the activity of the mutants Mcm5-8 and Mcm5-9

Silver stained gel showing the pre-RC assay to test the activity of the combination mutants Mcm5-8 (Mcm5-1+Mcm5+2) and Mcm5-9 (Mcm5-2+Mcm5-3) in ATPγS and ATP low salt (LS) and high salt (HS), compared with WT Mcm2-7 (lanes 6-8). The experiment was performed twice.

Table 4.1. Summary of the Mcm5C point mutants

List of point mutants generated during this study, with the amino acids mutated and their location in the context of the OCCM structure (see text). Their effect on double hexamer (DH) formation is summarised with a "0" in case of severe defects, "-" in the case of reduced DH when compared to WT.

Name of mutant	Amino acids mutated	Location	Dominant lethal	DH formation
Mcm5-1	K757D, R764E, R772E	Bottom	Yes	0
Mcm5-2	E710R, E717R, E736R	Up+Side	Yes	0
Mcm5-3	R721E, R735E	Up	Yes	0
Mcm5-4	R721E, E756R	Up+Bottom	Yes	-
Mcm5-5	R721A, R735A	Up	Yes	-
Mcm5-6	D532R, E756R	Bottom	No	-
Mcm5-7	D532A, E756A	Bottom	No	As WT
Mcm5-8	K757D, R764E, R772E, E710R, E717R, E736R	Bottom+Up+Side	Yes	0
Mcm5-9	E710R, E717R, E736R, R721E, R735E	Bottom+Up	Yes	0

4.9. ATPase activity of the point mutants

The results in Chapter 3 suggest that Mcm5C regulates Cdc6 induced ATP-hydrolysis and in this sense provides quality control during pre-RC formation. We hypothesised that specific protein-protein interactions between Mcm5C and ORC subunits are involved in this process. In order to better understand how Cdc6 ATP hydrolysis is induced and quality control is instigated, we investigated here the role of the point mutants in Cdc6 ATP hydrolysis.

To address this question, the ATPase activities of all mutants were measured using a previously described ATPase assay (Materials and methods 2.10). Each bar represents the mean from three independent measurements and error bars show the standard deviation between independent experiments (Figure 4.21).

Initially the rate of the intrinsic MCM2-7 ATPase activity for each point mutant was measured to determine if the point mutations affect the basal level of ATPase activity (Davey et al., 2003; Schwacha and Bell, 2001) (Figure 4.21 A, grey bars). Interestingly, Mcm5-1 and Mcm5-2 showed appreciable ATPase activity by themselves (14 and 8 pmol/min, respectively), significantly higher than observed with the WT MCM2-7 (6 pmol/min). There was no significant difference between the intrinsic ATPase activity of Mcm5-3 and WT. In all the cases, the addition of Cdt1 to MCM2-7 complex resulted in a significant (P<0.01) decrease in their ATPase activities, consistent with previous findings (Fernandez-Cid et al., 2013) (Figure 4.21 A, dark grey bars).

MCM2-7, Orc1 and Cdc6 represent the active ATPases (Masai et al., 2010) and Cdc6 and Orc1 induced ATP hydrolysis was shown to be important for Cdt1 release from MCM2-7 during helicase loading (Evrin et al., 2013; Fernandez-Cid et al., 2013; Perkins and Diffley, 1998; Randell et al., 2006). We were interested in asking if the point mutants in Mcm5C affect the total pre-RC induced activity. The “pre-RC induced ATPase activity” is defined as the ATPase activity of the full pre-RC reaction minus the sum of the ATPase activities of the individual components (ORC/Cdc6/DNA + Cdt1/MCM2-7) (Fernandez-Cid et al., 2013). The three mutants shown in Figure 4.21 B exhibited a trend for higher rate of pre-RC induced activity when compared to

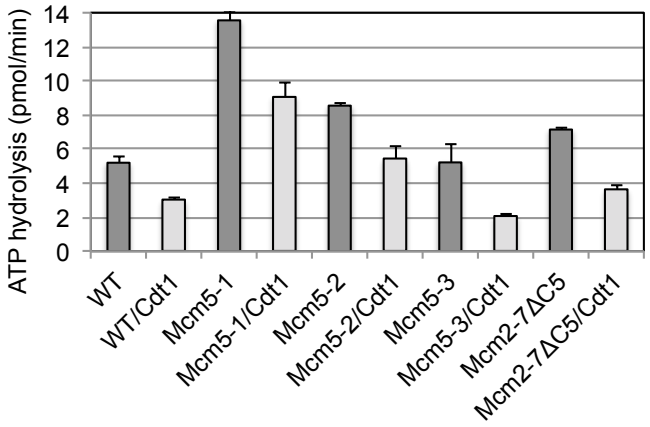
the WT (Figure 4.21 B, red bars), however this is statistically significant only in the case of Mcm5-2 and Mcm5-3. A very significant increase is shown in Mcm5-3, suggesting that the charge inversion mutations (R721E + R735E) facing “up” (towards ORC) in Mcm5-3 have no effect on MCM2-7 ATP hydrolysis, but specifically stimulate pre-RC induced ATP hydrolysis.

Previously pre-RC ATP-hydrolysis measurements have implicated Orc1 and Cdc6 ATP-hydrolysis in this process (Fernandez-Cid et al., 2013). In order to measure the contribution of Cdc6 ATP hydrolysis towards the full pre-RC ATP hydrolysis rate, a Cdc6 Walker B ATP-hydrolysis mutant (Cdc6 E224Q) was employed, which was previously described (Chang et al., 2015). Cdc6 E224Q, when added into the pre-RC ATP hydrolysis reaction containing WT MCM2-7, caused a non significant reduction in the ATP hydrolysis rate of the pre-RC, similar to what was previously observed (Chang et al., 2015). Here it is shown that the addition of Cdc6 E224Q to pre-RC ATP-hydrolysis measurement with Mcm5-1, Mcm5-2 and Mcm5-3 almost completely blocked pre-RC induced ATP hydrolysis (Figure 4.21 B, pink bars). The decrease in pre-RC induced ATP hydrolysis was significant ($p<0.01$) in all of the three mutants, with the strongest effect observed with Mcm5-3. Here, the rate of the pre-RC induced ATP hydrolysis decreased dramatically, from 11 pmol/min in the context of Cdc6 to 1 pmol/min when Cdc6 E224Q was added.

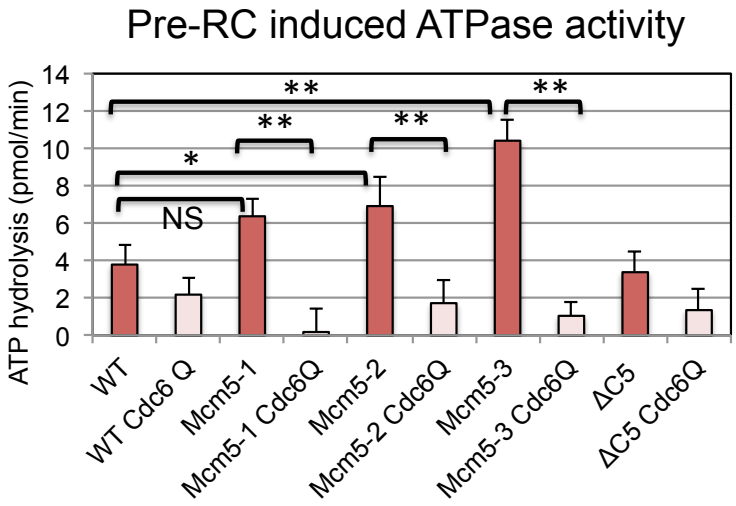
In order to understand if the point mutant induced Cdc6 ATP-hydrolysis leads to complex disassembly, a Cdc6 ATPase mutants was employed in the context of the reconstituted pre-RC assay and monitored complex stability in low salt conditions using ATP (Figure 4.21 C). Three conditions were compared: 1) WT Cdc6, 2) Cdc6 E224G, which reduces Cdc6 induced ATP-hydrolysis to an intermediate level and 3) Cdc6 E224Q, which has the strongest effect on ATP hydrolysis. The effect of the Cdc6 ATPase mutants can be observed in the pre-RC assay in a twofold way: 1) increased MCM2-7 levels and 2) increased Cdt1 levels, as OCCM complexes destined for complex disassembly become stabilised on DNA. Remarkably, with Mcm5-1, Mcm5-2 and Mcm5-3 a robust stabilisation of MCM2-7 and reduction in Cdt1 release was observed, although to different degrees.

Taken together, these results show that point mutations in Mcm5C, particular Mcm5-3 (facing “up”), increased the total rate of pre-RC induced ATP hydrolysis. As a Cdc6 ATPase mutant almost completely suppressed it, this shows that most pre-RC ATP hydrolysis is channelled through Cdc6. Moreover, the Cdc6 ATP-hydrolysis mutant stabilised Mcm5-1/2/3. This suggests that the mutants hyper-activate Cdc6 ATP-hydrolysis, which leads to increased complex disassembly. Moreover, the OCM formed appears not functional, as MCM2-7 double-hexamer formation is largely blocked. It is possible that an interaction between these amino acids in Mcm5C and specific amino acids in the adjacent Orc2 or Orc3 subunits might be involved. Surprisingly, Mcm5-1 and Mcm5-2 displayed higher MCM2-7 ATPase activity. These mutations are localised in the WHD5 surface facing ORC (“up”) and facing the AAA+ domain (“down”), respectively. How this results in increased MCM2-7 ATP-hydrolysis is not immediately clear.

A


ATP hydrolysis (pmol/min)
14
12
10
8
6
4
2
0
WT
WT/Cdt1
Mcm5-1
Mcm5-1/Cdt1
Mcm5-2
Mcm5-2/Cdt1
Mcm5-3
Mcm5-3/Cdt1
Mcm2-7ΔC5
Mcm2-7ΔC5/Cdt1

B


Pre-RC induced ATPase activity
ATP hydrolysis (pmol/min)
14
12
10
8
6
4
2
0
**
**
**
**
*
NS
WT
WT Cdc6 Q
Mcm5-1
Mcm5-1 Cdc6Q
Mcm5-2
Mcm5-2 Cdc6Q
Mcm5-3
Mcm5-3 Cdc6Q
ΔC5
ΔC5 Cdc6Q

C

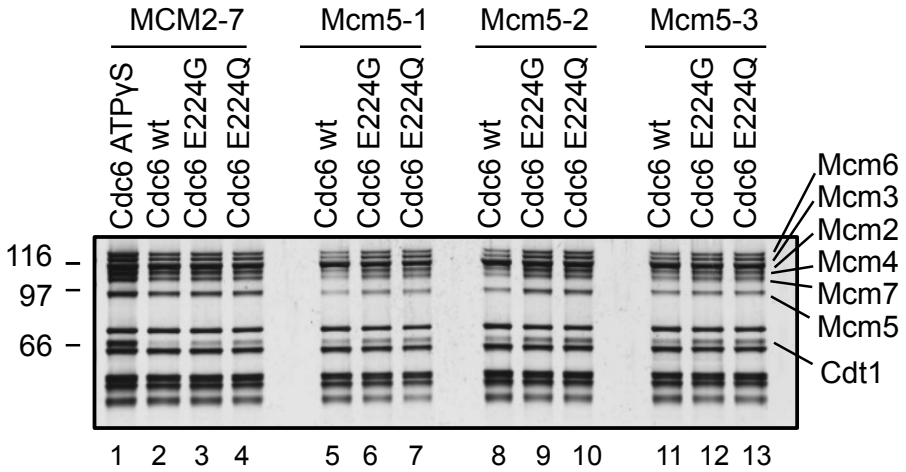

MCM2-7
Mcm5-1
Mcm5-2
Mcm5-3
Cdc6 ATPγS
Cdc6 wt
Cdc6 E224G
Cdc6 E224Q
Cdc6 wt
Cdc6 E224G
Cdc6 E224Q
Cdc6 wt
Cdc6 E224G
Cdc6 E224Q
Cdc6 wt
Cdc6 E224G
Cdc6 E224Q
116
97
66
Mcm6
Mcm3
Mcm2
Mcm4
Mcm7
Mcm5
Cdt1
1 2 3 4 5 6 7 8 9 10 11 12 13

Figure 4.21. ATPase activity of Mcm5-1, Mcm5-2, Mcm5-3

A) Analysis of the ATPase activity rate of WT Mcm2-7, Mcm5-1, Mcm5-2, Mcm5-3 individually and in the presence of Cdt1. **B)** Analysis of pre-RC induced ATPase activity of WT Mcm2-7, Mcm5-1, Mcm5-2, Mcm5-3 with Cdc6 (red) and Cdc6E224Q (orange). Results for A and B are plotted as average of at least three independent experiments. Error bars represent the standard deviation. Statistical analysis was determined by one-way ANOVA followed by post hoc test using Bonferroni correction. Statistically significant results determined by one tailed t-test are indicated: *P<0.05; ** P<0.01. **C)** Analysis of pre-RC assembly using Cdc6E224G and Cdc6E224Q with MCM2-7, Mcm5-1, Mcm5-2 and Mcm5-3. The reactions were washed with low salt buffer before releasing them from the beads using DNaseI.

The combination mutants, Mcm5-8 (Mcm5-1+Mcm5-3) and Mcm5-9 (Mcm5-2+Mcm5-3), showed significant ($p<0.01$) higher constitutive ATPase activity when compared to WT MCM2-7 (7.9 pmol/min and 8.8 pmol/min, respectively) (Figure 4.22 A). However, only the presence of Mcm5-9 significantly increased the pre-RC induced ATPase activity, compared to WT (Figure 4.22 B). The addition of Cdc6E224Q showed a trend for suppression of the pre-RC induced ATPase activity compared with the WT MCM2-7, however this difference was significant ($p<0.01$) only in the Mcm5-9 (Mcm5-2+Mcm5-3) (Figure 4.22 B). Interestingly, pre-RC assembly experiments showed a reduced stability for Mcm5-8, which was stabilised by a Cdc6 ATPase mutant, while Mcm5-9 displayed stronger binding to origins, which was only slightly stabilised by the Cdc6 ATPase mutant (Figure 4.22 C, lanes 4-5 and 7-8).

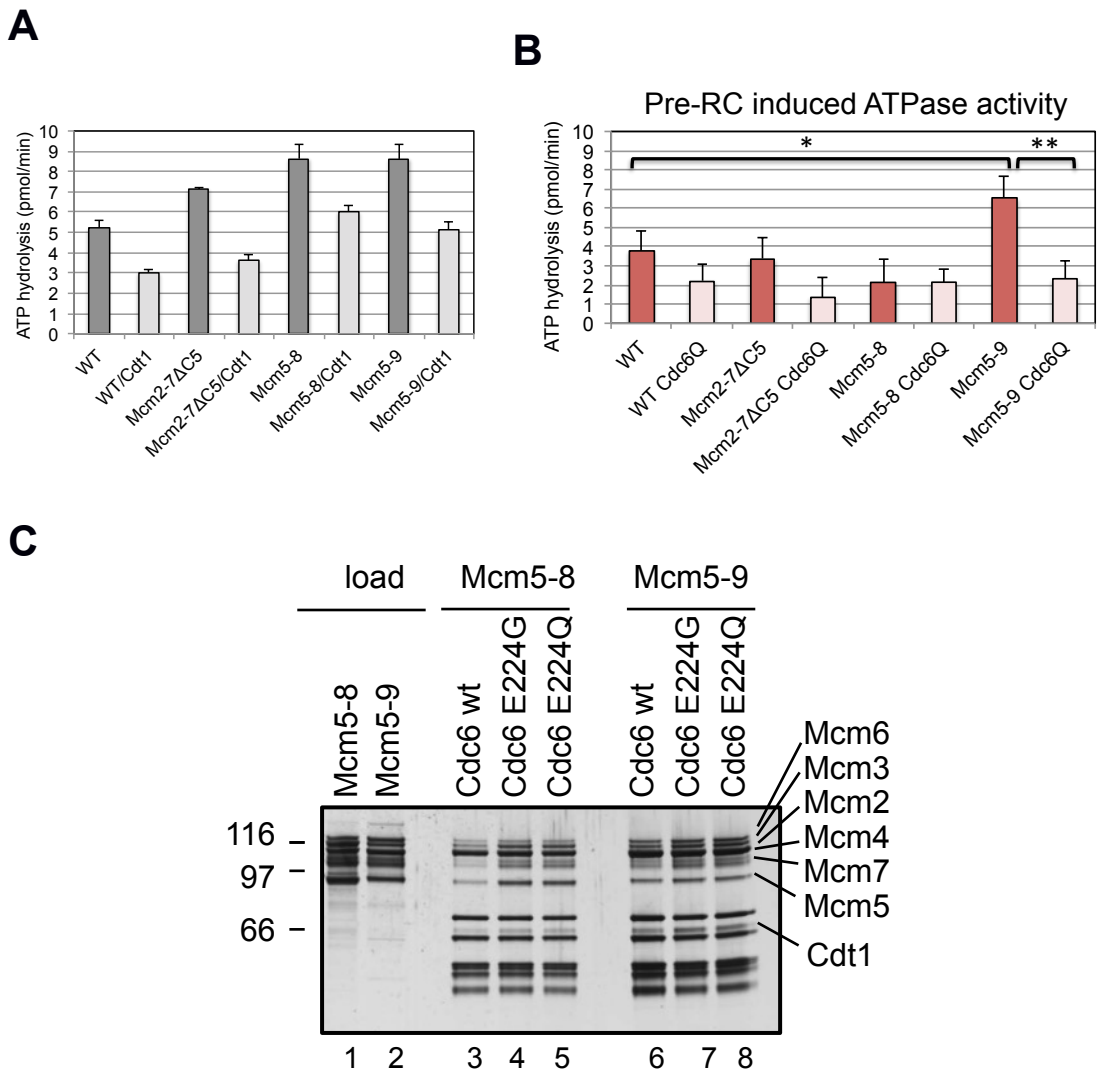


Figure 4.22. Analysis of ATPase activity of the mutants Mcm5-8 and Mcm5-9

The ATP hydrolysis rate of pre-RC was measured as described (Speck and Stilman, 1992). **A)** ATP hydrolysis rate of MCM2-7, Mcm5-8 and Mcm5-9 individually (dark grey) and in the presence of Cdt1 (light grey). **B)** pre-RC induced ATPase activity of MCM2-7, Mcm5-8 and Mcm5-9 in the presence of Cdc6 (red bars) and Cdc6E224Q (pink bars). Results for A and B are plotted as average of at least three independent experiments. Error bars represent the standard deviation. Statistical analysis was determined by one-way ANOVA followed by post hoc test using Bonferroni correction. *P<0.05, **P<0.01 **C)** Analysis of pre-RC assembly of the mutants Mcm5-8 and Mcm5-9 in the presence of WT Cdc6, Cdc6E224G and Cdc6E224Q after low salt washes (300 mM potassium glutamate). The experiment was repeated twice.

These experiments suggest that introducing multiple mutations in Mcm5C generated stronger effects compared to what observed with MCM2-7ΔC5. Indeed, changing several residues could affect multiple functions of Mcm5C, preventing simultaneously interactions that affect OCM complex

stability and Cdc6 ATP-hydrolysis. The Mcm5-8 and Mcm5-9 mutants contained a larger number of mutations. This did not impact on the overall stability of the complex, as judged from the purification. However, it cannot be excluded that the mutations resulted in some local structural changes in Mcm5C, which impact on its function. As Mcm5-8 very closely resembled MCM2-7ΔC5 it appears possible that this mutant has a larger degree of structural changes in its Mcm5C.

4.10. CDK regulation of the helicase loading

CDK is the main negative regulator of pre-RC formation in budding yeast. During G1 phase, CDK activity is very low, which allows pre-RC formation. During the G1 to S-phase transition CDK activity picks up, which leads to phosphorylation of ORC and block of the helicase loading until the next cell cycle, which guarantees that only a single round of DNA synthesis can occur during each cell cycle (Tanaka and Araki, 2010). CDK specifically phosphorylates Orc2 and Orc6, which inhibits ORCs ability to load MCM2-7 onto origin DNA (Chen and Bell, 2011; Nguyen et al., 2001). Consequently, it was shown in a reconstituted system that CDK phosphorylated ORC does not affect OCCM formation, but specifically blocks OCM formation, suggesting that this pre-RC intermediate is a target for quality control (Fernandez-Cid et al., 2013; Frigola et al., 2013).

CDK is known to phosphorylate Orc6 and several residues in the N-terminal domain of Orc2 (Nguyen et al., 2001). This region was not visible in the OCCM structure, likely due to its flexibility. However, cross linking mass spectrometry analysis revealed that the Mcm5 WHD and the Orc2 N-terminus are located in close proximity (Yuan et al., 2017). Since the data link WHD5 to quality control, and WHD5 and a CDK target – Orc2 N-terminus – are in proximity, we asked whether the Mcm5C is also involved in CDK mediated quality control.

Initially we wanted to analyse if the ORC phosphorylation by CDK would affect the recruitment of the mutants MCM2-7 to ORC/Cdc6. In this experiment,

ORC was loaded on ARS1 DNA and treated with 40 nM of purified CDK in the presence of pre-RC buffer (50 mM HEPES, pH 7.6, 100 mM KGlu, 10 mM MgAc, 50uM ZnAc, 3mM ATP, 5 mM DTT, 0.1% Triton X-100, 5% glycerol). After phosphorylation, CDK was washed away to prevent the phosphorylation of other pre-RC proteins. Cdc6, Cdt1 and WT MCM2-7 were then added in the presence of ATPγS (Figure 4.23 A lane 7). The reaction was compared with the non phosphorylated ORC (Figure 4.23 A lane 6). With ATPγS, CDK phosphorylation of ORC (P-ORC) reduced the initial association of MCM2-7 with ORC/Cdc6 onto origin DNA (Figure 4.23 A, compare lane 5 and 6). The experiment was then performed using MCM2-7ΔC5, Mcm5-hWHD5, Mcm5-yWHD4, Mcm5-FRB (Figure 4.23 A). As expected, MCM2-7ΔC5 and the domain swap mutants supported initial association of ORC/Cdc6 with MCM2-7/Cdt1 to a very similar degree. While P-ORC affected OCCM formation, the mutants were binding in the presence of ATPγS very efficiently to P-ORC (Figure 4.23 A lanes 10-15). This indicates that the removal or replacement of the WHD5 can bypass the initial MCM/Cdt1 recruitment inhibition caused by P-ORC.

In the presence of ATP and P-ORC, pre-RC formation is heavily compromised. Only much reduced amounts of MCM2-7 can be detected after a low salt wash and double hexamer formation is completely blocked (Figure 4.23 B). In the case of MCM2-7ΔC5 and the domain swap mutants pre-RC formation was similarly compromised (Figure 4.23 B).

Taken together these data show that the removal of the WHD5 or its replacement with a different domain alleviated the CDK mediated inhibition of Mcm2-7/Cdt1 recruitment, suggesting that Mcm5C plays a role in sensing the P-ORC. The position of the phosphate of P-ORC, relative to the WHD5 is not known, but it seems possible that the winged helix could directly sense the presence of the negatively charged phosphate through the many positively charged residues in the WHD. However, the phosphorylation of Orc2 could also result in changes in its structure or positioning that do not require a direct interaction with the phosphate. Following this observation, we sought to determine if any of the point mutants analysed during this study - which include mutations in charged residues in the WHD5, would produce the same effect as the domain swap or deletion mutants.

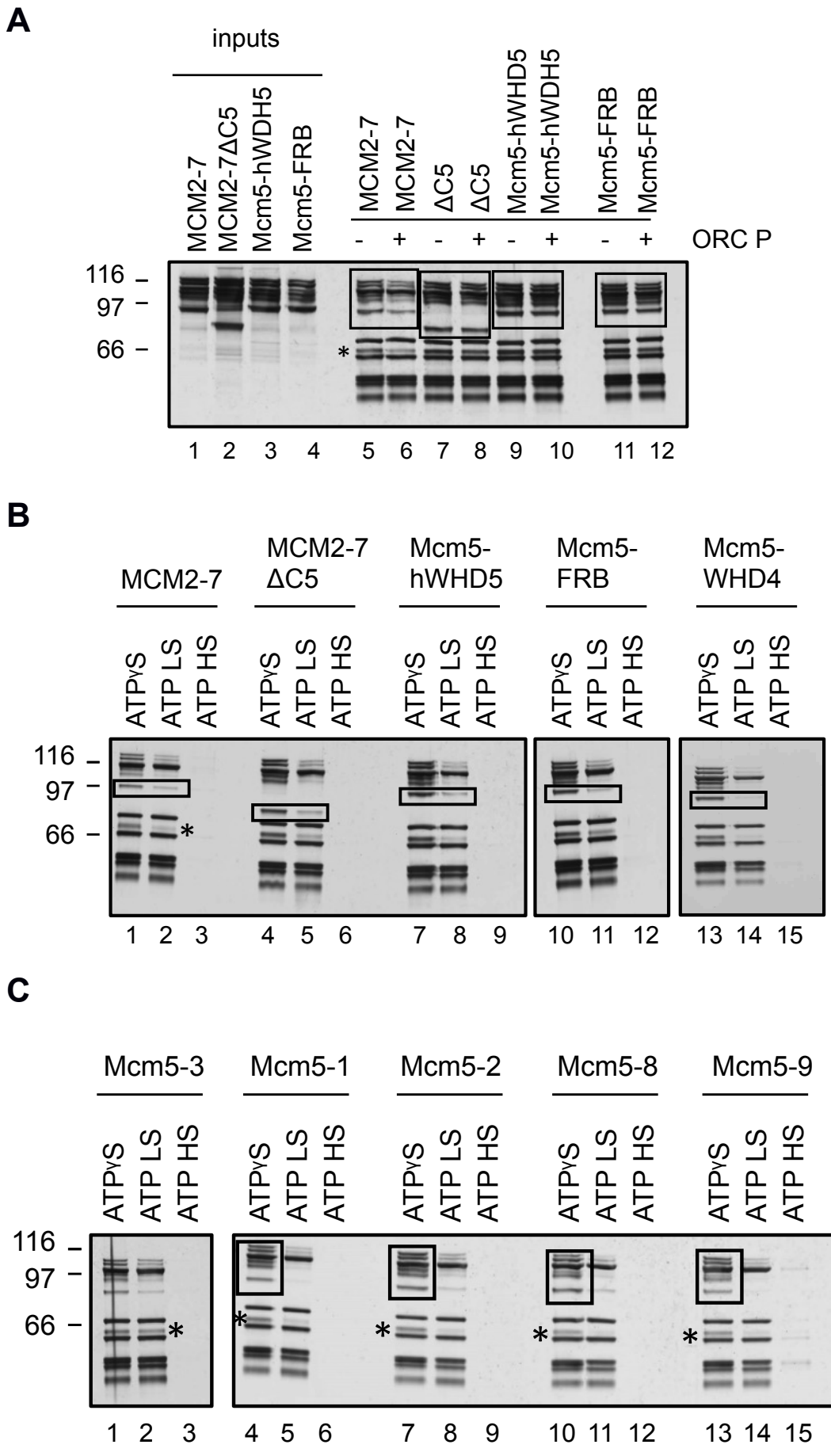

A
inputs
MCM2-7
MCM2-7ΔC5
Mcm5-hWDH5
Mcm5-FRB
MCM2-7
MCM2-7
ΔC5
ΔC5
Mcm5-hWHD5
Mcm5-hWDH5
Mcm5-FRB
Mcm5-FRB
- + - + - + - +
ORC P
116
97
66
*
1 2 3 4 5 6 7 8 9 10 11 12
B
MCM2-7
MCM2-7 ΔC5
Mcm5-hWHD5
Mcm5-FRB
Mcm5-WHD4
ATPγS
ATP LS
ATP HS
116
97
66
*
1 2 3 4 5 6 7 8 9 10 11 12 13 14 15
C
Mcm5-3
Mcm5-1
Mcm5-2
Mcm5-8
Mcm5-9
ATPγS
ATP LS
ATP HS
116
97
66
*
1 2 3 4 5 6 7 8 9 10 11 12 13 14 15

Figure 4.23. CDK regulation of helicase loading.

A) *In vitro* pre-RC assay to test the ability of WT MCM2-7, MCM2-7ΔC5, Mcm5-hWHD5, Mcm5-FRB and Mcm5-yWHD4 to be recruited by unphosphorylated and CDK-phosphorylated ORC in the presence of ATPγS. Squares highlight the MCM proteins. Asterisk refers to the Cdt1 band. **B)** Analysis of pre-RC assembly in the presence of CDK-phosphorylated ORC and WT MCM2-7, MCM2-7ΔC5, Mcm5-hWHD5, Mcm5-FRB and Mcm5-yWHD4. The reactions were assembled in ATPγS or ATP followed by low salt (LS) or high salt (HS) washes. Squares highlight the Mcm5 band and asterisks indicate the Cdt1 band. **C**) Analysis of pre-RC assembly in the presence of CDK-phosphorylated ORC and point mutants Mcm5-1, Mcm5-2, Mcm5-3, Mcm8-9 and Mcm5-9. The reactions were assembled in ATPγS or ATP followed by low salt (LS) or high salt (HS) washes. Squares highlight the MCM protein. Asterisk refers to the Cdt1 band. The experiments were repeated at least two times and reproducible.

ORC was phosphorylated and its ability to recruit a selection of the Mcm5C point mutants was examined, which did not support double hexamer formation (Mcm5-1, Mcm5-2, Mcm5-3, Mcm5-8, Mcm5-9). The results of the mutants are shown in Figure 4.23C. In ATPγS none of the point mutants replicated the same effect seen with the deletion and domain swap mutants, which were binding very efficiently to P-ORC. In the presence of ATP hydrolysis, OCM formation was blocked in the point mutants (Figure 4.23 C) similarly to what observed in the WT (Figure 4.23 B lane 2). This result suggests that the Mcm5C point mutants did not bypass the initial inhibition of MCM2-7/Cdt1 recruitment by P-ORC. These data suggest that either the complete removal of WHD5 is required to bypass the P-ORC/Cdc6 recruitment block, or that mutations in a different area of WHD5 are needed. Further investigation is required in order to identify which amino acids in the Mcm5C are directly involved to act as sensor for phosphorylated ORC.

4.11. Discussion

In the previous chapter it was described the effect of the Mcm5C deletion on pre-RC formation. Whilst it has been shown that deletion of Mcm3C prevents the initial recruitment of Mcm2-7 to ORC/Cdc6 in ATPγS (Frigola et al., 2013), here it was demonstrated that removing Mcm5C did not affect this initial stage. It has also been shown previously that Mcm3C is necessary for binding of

Mcm2-7 to ORC/Cdc6, activating the ATPase (Cdc6) (Coster et al., 2014; Frigola et al., 2013).

It was showed that MCM2-7 lacking Mcm5C has a specific role in regulating quality control. It illicitly activates a Cdc6 ATP hydrolysis dependent quality control mechanism, which leads to partial complex disassembly. Consistent with that we showed that in the absence of Cdc6 ATPase activity the pre-RC induced ATPase activity was reduced and MCM2-7ΔC5 was stabilised on DNA together with ORC/Cdc6 (Figure 3.10). Thus it was concluded that Mcm5C functions normally to engage with ORC/Cdc6 and in turn to down-regulate the quality control pathway. It was suggested that Mcm5C acts as a signal for correct complex formation and that in its absence Cdc6 induced ATP hydrolysis is responsible for complex disassembly.

Besides regulating ATP-hydrolysis dependent quality control, the WHD5 has an additional role in double hexamer formation. Removal of Mcm5C does not stop the loading of the first hexamer of MCM2-7 onto origin DNA during OCCM formation, but impacts the OCCM to double hexamer transition. Here, the release of Cdt1 is slightly reduced and double hexamer formation is completely blocked. The reason for this could be that OCCM complexes destined for disassembly become stabilised on DNA. It was therefore hypothesised that Mcm5C establishes protein-protein interactions with ORC subunits in order to down-regulate the quality control pathway and these interactions could also be required for formation of a functional OCM complex that is able to successfully load the double hexamer on DNA. This hypothesis led to an extensive mutational analysis of MCM2-7 in the Mcm5C, which is presented in this chapter. The experiments were performed in order to identify evidence to support the idea that the WHD5 functions as a quality control sensor during pre-RC formation and the OCCM to double hexamer transition. The hope was to identify separation of functions mutants, which generate a more specific phenotype than MCM2-7ΔC5.

Domain swap MCM2-7 mutants were generated in order to test whether a different domain showing similarity in either the sequence or the structure to the WHD5 would be sufficient to replace it in a functional way. It was found that the structural component of the Mcm5C (helix-wing-helix) is

important to ensure its function in quality control for correct protein complex formation. Indeed, when this domain was replaced with a different but similar overall structure in the form of the FRB, this still induced Cdc6 ATP hydrolysis even though no productive protein complexes were formed. It is surprising that a small amount of Mcm5-FRB was loaded. Further to this observation with structural similarity, it was found that a certain degree of amino acid conservation is sufficient to establish high affinity interactions with ORC/Cdc6 for OCM formation, as observed in the swap of the yeast WHD5 with the homologous human WHD5. These similarities are however not sufficient, and ATP hydrolysis is coupled to irreversible disassembly of non productive protein complexes. The Mcm5-hWHD5 is an exception since it is bypassing the Cdc6 induction of ATPase and results in a more stable OCM complex, suggesting that it may form tighter interactions with Orc3.

These data showed that the deletion of Mcm5C combined with Mcm4C lead to failure in hexamer formation, hence the two domains may be involved in the initial hexamer assembly.
It was found that changing the characteristics of the linker that precedes WHD5 in Mcm5C did not affect the pre-RC formation *in vitro* but reduced the rate of pre-RC induced ATP hydrolysis. One possible explanation could be that initial steps in pre-RC formation might be slowed down producing a lower ATP hydrolysis rate, without affecting the final double hexamer formation.

The effect of double, triple or multiple amino acid substitution mutations in Mcm5C on helicase loading *in vitro* was analysed. The amino acids in the Mcm5C that are oriented either towards ORC or the AAA+ domain of Mcm5, relative to the OCCM conformation were mutated. After a high salt wash the effect of the mutations is generally more easy to judge, since the salt removes all intermediates but the MCM2-7 double hexamer and as such reduces complexity. In contrast, an ATP based *in vitro* pre-RC reaction retains after a low salt wash all helicase-loading intermediates. In six out of nine mutants, a medium to very strong reduction of high salt-stable MCM2-7 was observed, suggesting that double hexamer formation is blocked prior to helicase loading. This means in turn that after a low salt wash a collection of incompletely loaded

MCM2-7 complexes are retained on DNA, similar as seen in the Mcm5C deletion mutant. Non-functional helicase loading intermediates represent a problem for the cell, as they hinder the efficient loading of the replicative helicase. However, at least some intermediates can be disassembled in Cdc6-dependent ATP hydrolysis process (Kang et al., 2014). Indeed, in the double (Mcm5-3, “up” towards ORC) and triple mutants Mcm5-1 (“down” towards the AAA+ domain of Mcm5) and Mcm5-2 (“up+side”), which displayed double hexamer formation defects and therefore accumulated non-functional helicase loading intermediates, pre-RC induced ATP hydrolysis was increased. This would suggest that the quality control mechanism could work via specific amino acids in Mcm5C, potentially affecting interactions with ORC and thus generating complexes that assembled on the DNA but are not functional. Because of the close proximity of the Mcm5C to Orc3 and Orc2, it is possible that specific amino acids in the Mcm5 might interact with certain amino acids in the two ORC subunits. Thus, it is suggested that when these interactions fail, structural rearrangements in ORC/Cdc6 would trigger Cdc6 ATP hydrolysis and disassembly of unproductive complexes. The described mutations in Mcm5C combined with a Cdc6 ATPase mutant supressed pre-RC induced ATPase activity very strongly. This striking result suggests that Mcm5C is a highly significant player in inducing Cdc6 ATP hydrolysis for complex disassembly. In the presence of the Mcm5 mutants the largest part of ATPase activity is channelled through Cdc6, while the other ATPases (Orc1 and Mcm2-7) remain inactive. This could possibly mean that “concerted” ATP hydrolysis by Orc1 and Mcm2-7, which is present in wild type complexes, may be involved in progression of correctly assembled complexes. In the presence of the mutants, this ATPase activity is inactive, and the energy from ATP-hydrolysis is not linked to complex assembly, but diverted to drive the disassembly process.

The combination of Mcm5-2 (E710R, E717R, E736R) with Mcm5-1 (K757D, R764E, R772E) or Mcm5-3 (R721E, R735E), Mcm5-8 and Mcm5-9 respectively, generated an effect very similar to the deletion of the Mcm5C, with an inefficient formation of low salt stable complexes and no high salt-stable double hexamer. Because the mutations in Mcm5-2 (“side”) are present in both Mcm5-8 and Mcm5-9, this could suggest that these amino acids are the main

players in establishing interactions with ORC during the formation of a productive pre-RC complex.

Mcm5C double and triple mutant complexes are initially able to start the MCM2-7/Cdt1 interaction with DNA bound ORC/Cdc6, but are not able to generate productive OCM and stable double hexamers. These results suggest that the Mcm5C is responsible for assessing the quality of the protein complex and, via interactions with ORC, inducing Cdc6 ATP hydrolysis for disassembly of unsuccessfully loaded complexes. This disassembly process involves the simultaneous release of MCM2-7/Cdt1. Obviously, in these assembled-based reactions complex assembly and disassembly is occurring simultaneously. Some complexes appear to satisfy the quality control checkpoint and successfully release Cdt1, but retain MCM2-7. In context of MCM2-7ΔC5 we observed that these complexes were successfully loaded onto DNA, so likely the same is true here. That leaves the question why these mutants fail to produce MCM2-7 double-hexamers.

Based on these results, together with the data from the newly obtained OCCM cryo-EM structure, which capture the complex in a fully closed conformation, we propose the following model (Figure 4.24). Once the OCCM is formed and DNA is inserted in the Mcm2-7 ring, the gate between Mcm5 and Mcm2 must close. The closing of the ring positions WHD5 at the interface between the AAA+ domain of Mcm5, Orc2 and Orc3. We propose that specific amino acids in Mcm5C are essential for the establishment of the WHD5 interactions with the AAA+ domain of Mcm5, Orc2 and Orc3. We suggest that these interactions 1) generate a conformational change in ORC/Cdc6, which downregulates the quality control pathway and inhibits Cdc6-induced ATP hydrolysis 2) promote ATP hydrolysis by Orc1 and Mcm2-7, which contributes to the pre-RC ATPase activity, leading to Cdt1 release and formation of the OCM. Mcm5C interactions with ORC subunits could also be needed at a later step during OCM formation. If this interaction cannot take place, for example as in Mcm5-3, the pathway is altered. In this way, the network of interactions between the WHD5 and the main body of Mcm5, Orc2 and Orc3 is disturbed. This reconfigures the ATP-hydrolysis pathway. Now, Orc1/MCM2-7 ATP hydrolysis is blocked and instead all ATP-hydrolysis is channelled through

Cdc6. In this configuration, the complete Cdt1/MCM2-7 complex becomes released, resulting in complex disassembly.

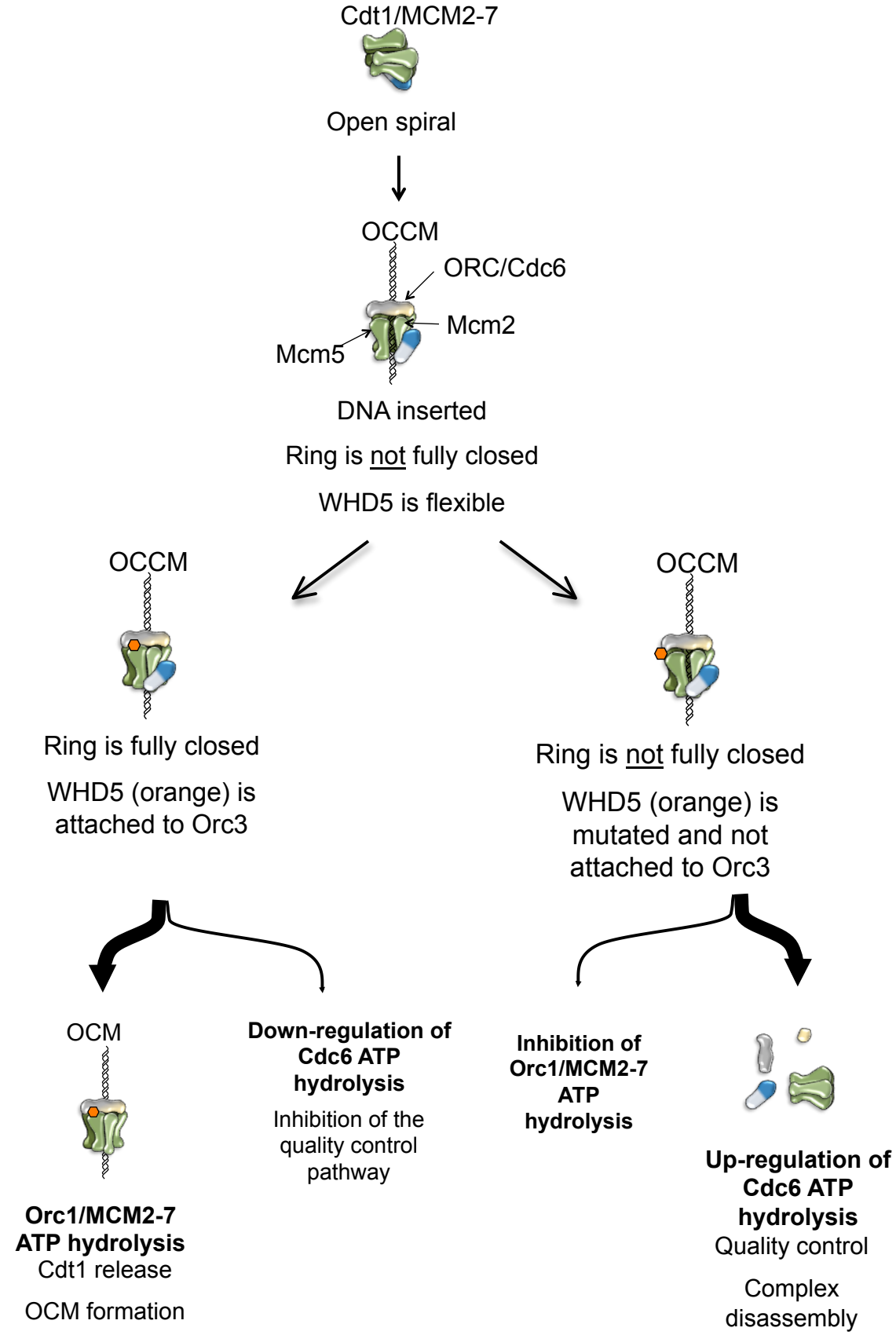

Cdt1/MCM2-7
Open spiral
OCCM
ORC/Cdc6
Mcm2
Mcm5
DNA inserted
Ring is not fully closed
WHD5 is flexible
OCCM
Ring is fully closed
WHD5 (orange) is attached to Orc3
OCCM
Ring is not fully closed
WHD5 (orange) is mutated and not attached to Orc3
OCM
Orc1/MCM2-7 ATP hydrolysis
Cdt1 release
OCM formation
Down-regulation of Cdc6 ATP hydrolysis
Inhibition of the quality control pathway
Inhibition of Orc1/MCM2-7 ATP hydrolysis
Up-regulation of Cdc6 ATP hydrolysis
Quality control
Complex disassembly

Figure 4.24. Model for Mcm5C-induced quality control pathway.

MCM2-7/Cdt1 is present in solution as an open ring, which is loaded on origin DNA by ORC/Cdc6. In the resulting complex (OCCM), dsDNA is inserted into the MCM2-7 ring which is partially closed. The closure of the ring induces a repositioning of the WHD5. Left hand side of the figure: When the WHD5 interacts with Orc3, this interaction induces a conformation change in ORC/Cdc6, which downregulates the quality control pathway and inhibits Cdc6-induced ATP hydrolysis. At the same time, it promotes ATP hydrolysis by Orc1 and Mcm2-7, which contributes to the pre-RC ATPase activity, leading to Cdt1 release and formation of the OCM. Right hand side of the figure: If the interaction WHD5-Orc3 cannot take place, for example as in Mcm5-3, the pathway is altered. As a consequence, the ATP-hydrolysis pathway is reconfigured towards the activation of the quality control. Orc1/MCM2-7 ATP hydrolysis is inhibited and Cdc6-induced ATP-hydrolysis is up-regulated with the release of Cdt1/MCM2-7 and complex disassembly.

It was shown that successful OCM formation was inhibited by CDK phosphorylation of the ORC complex (Fernandez-Cid et al., 2013). In the present study, none of the analysed point mutants showed ability to be recruited and loaded by the P-ORC in the presence of ATP. However, we found that removing the Mcm5C or replacing it with a different domain bypassed the P-ORC dependent inhibition in MCM2-7 recruitment. These results suggest that Mcm5C also has a role in discriminating phosphorylated from non-phosphorylated ORC and ensuring that only non-phosphorylated ORC is licensed during G1 phase. We identified three ways in which CDK regualates pre-RC formation (Figure 4.25). One level of control is at the stage of the OCCM, since we observed that P-ORC was not able to recruit the helicase. The second mechanism of control occurs during the OCCM to OCM transition, when incomplete loaded MCM2-7 to P-ORC disassemble upon activation of the Cdc6 dependent ATP hydrolysis quality control pathway. A third level of control occurs at the OCM stage, since this complex formed with P-ORC is not able to support double hexamer formation.

The observation of another novel Mcm5C mechanism, which regulates complex assembly, warrants further investigation. In the future, one could ask how Mcm5C is sensing ORC phosphorylation. Orc2 is a main target of CDK and is located in proximity to Mcm5C. Thus, by mutating CDK target sites in Orc2, which could abolish an interaction with Mcm5C, one could alleviate the initial

inhibition in recruitment. For instance, one candidate phosphor-sensing residue in Mcm5 is R742, which was not mutated during the present study. The positive charge, the location of this residue in a flexible region - the W2 (loop), and the high degree of conservation among species seems to make it a good candidate for monitoring the presence of a bulky charged phosphate group.

In summary, the mutational analysis indicates that integrity and species-specific elements of the entire Mcm5 C-terminal domain (WH domain plus linker) are essential for assessing the quality of the protein complex during the pre-RC formation.

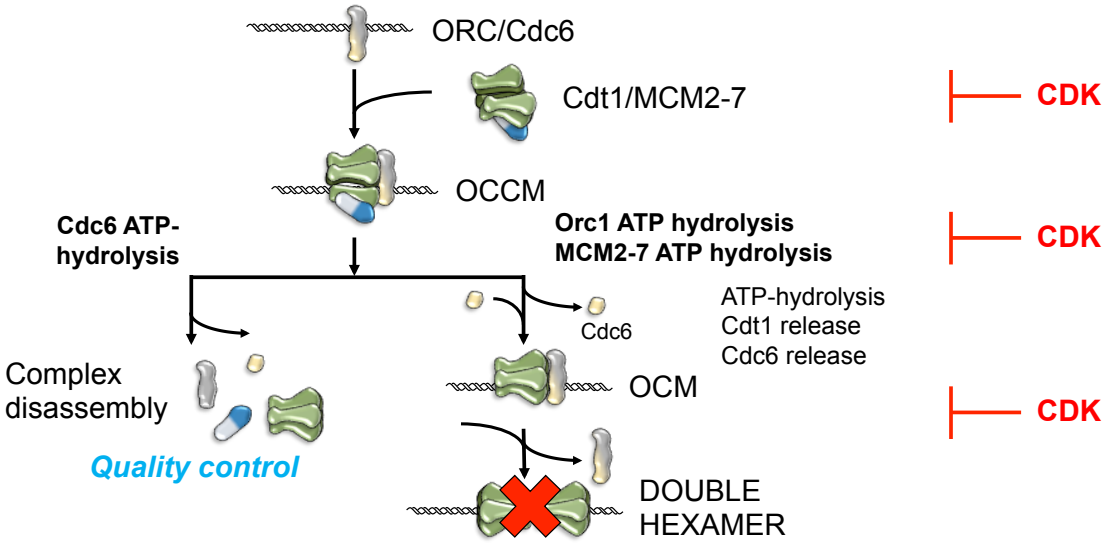


Figure 4.25. Model for the mechanisms of CDK-phosphorylated ORC during pre-RC formation

The kinase CDK acts at different levels of regulation of pre-RC formation. The first level of control occurs at the OCCM stage, since phosphorylated ORC recruits MCM2-7/Cdt1 with low efficiency than the unphosphorylated ORC. The second level of control is during the OCCM-OCM transition inhibiting the Orc1/MCM2-7 ATP hydrolysis and activating the Cdc6 ATP hydrolysis disassembly pathway. A final level of control is at the OCM stage, producing a complex that is not functional for the recruitment of the second hexamer preventing double hexamer formation.

Chapter 5

Understanding the role of the C-termini of Mcm2, Mcm4 and Mcm7

5.1. Introduction

The Mcm2-7 proteins are composed of three domains, a central conserved ATPase domain and two divergent N- and C-terminal domains. The AAA+ core that defines each of these structural domains is highly conserved in eukaryotic and archaeal Mcm proteins (Figure 5.1). The N-termini are important for helicase activation during S-phase acting as a target for DDK phosphorylation (Bruck and Kaplan, 2015; Deegan et al., 2016; Fang et al., 2016; Herrera et al., 2015; Randell et al., 2010; Sheu and Stillman, 2006). The C-termini of Mcm2-7, except for Mcm2, contain each a winged helix domain (WHD). Mcm3C is essential for ORC/Cdc6 dependent recruitment of Cdt1/MCM2-7 to origins and induces ORC/Cdc6 ATP hydrolysis (Frigola et al., 2013; Sun et al., 2013). Biochemical studies showed that the Mcm6C adopts an auto-inhibited conformation that blocks in the absence of Cdt1 the binding of MCM2-7 to ORC/Cdc6 (Fernandez-Cid et al., 2013). However, the function of the other MCM C-termini have not been described and remains to be investigated. When this work started, high-resolution structures of key DNA replication initiation intermediates had not been obtained yet and no structural information were available. In this chapter the function of the C-terminal domains of Mcm2 (Mcm2C), Mcm4 (Mcm4C) and Mcm7 (Mcm7C) during pre-RC formation were investigated using structural, biochemical and *in vivo* techniques. An in-depth study aimed at understanding the function of Mcm5C was undertaken and was described in Chapters 3 and 4.

Initially, six MCM2-7 mutants missing individual C-termini were generated and were tested for their lethality *in vivo* (Figure 5.2). The six protein complexes were then purified (Figure 5.3). It was observed that all of the deletion mutants with the exception of MCM2-7ΔC3 were competent for binding

to ORC/Cdc6 but not all of them allowed high salt resistant MCM2-7 double hexamer (Figure 5.4). Based on a low resolution electron microscopy structure, it was hypothesised that the helicase loader ORC/Cdc6 interacts specifically with the C-terminal portion of MCM subunits promoting structural changes in MCM2-7 itself (Sun et al., 2013). In order to gain insight into the specific protein-protein interactions between the helicase and the helicase loader at high resolution, two independent approaches were used: cryo-EM in collaboration with Prof. Hulin Li (USA) and cross-linking mass spectrometry (CLMS) in collaboration with Prof. Juri Rappilsber (Edinburgh).

5.2. *In vivo* characterisation of the Mcm C-termini

In order to investigate the role of the MCM2-7 C-termini six mutants had been generated - each one containing a deletion of this domain (Winkler and Speck; unpublished). The residues that were deleted from the full length MCM2-7 are highlighted in red in Figure 5.1. These mutants will be referred as "MCM2-7ΔC" followed by the number of the corresponding MCM subunit.

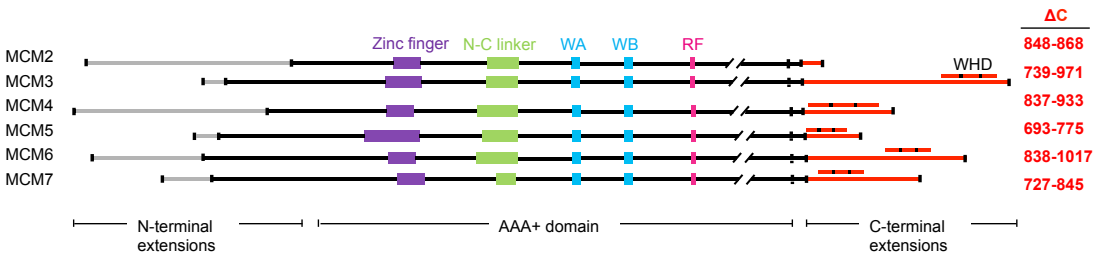


Figure 5.1. Design of the MCM2-7 deletion mutants

The MCM2-7 proteins each contain a conserved AAA+ domain, comprising a zinc finger domain (purple), a linker (green), a Walker A motif (WA, blue), a Walker B motif (WB, blue) and an arginine finger (RG, pink). The C-terminal extensions contain a structurally conserved winged helix domain (WHD, red). Six MCM2-7 truncation mutants were generated each containing a deletion of one individual C-terminal extension. The deleted amino acids are indicated in red and each mutant is defined as MCM2-7ΔC followed by the number of each subunit (e.g. MCM2-7ΔC2 refers to the full length MCM2-7 without the amino-acids 828-868 in the subunit Mcm2).

Each of the six constructs was used in an overexpression assay to detect dominant lethality *in vivo*, which was performed as described in Materials and

Methods (2.4.5). Briefly, a dilution series of yeast cultures was spotted on dropout plates containing either 2% glucose (non-inducing condition) or 2% galactose (inducing condition). The overexpression of the WT MCM2-7 strain was used as a positive control. All of the mutants, but not MCM2-7ΔC4, showed lethality when overexpressed, indicating that these Mcm C-termini are essential for cell proliferation (Figure 5.2 A, B). The Mcm4 C-terminus caused no dominant lethality, with the chromosomal WT copy being present on the genome. It is possible that a complete chromosomal replacement could result in a phenotype, but this was not addressed here.

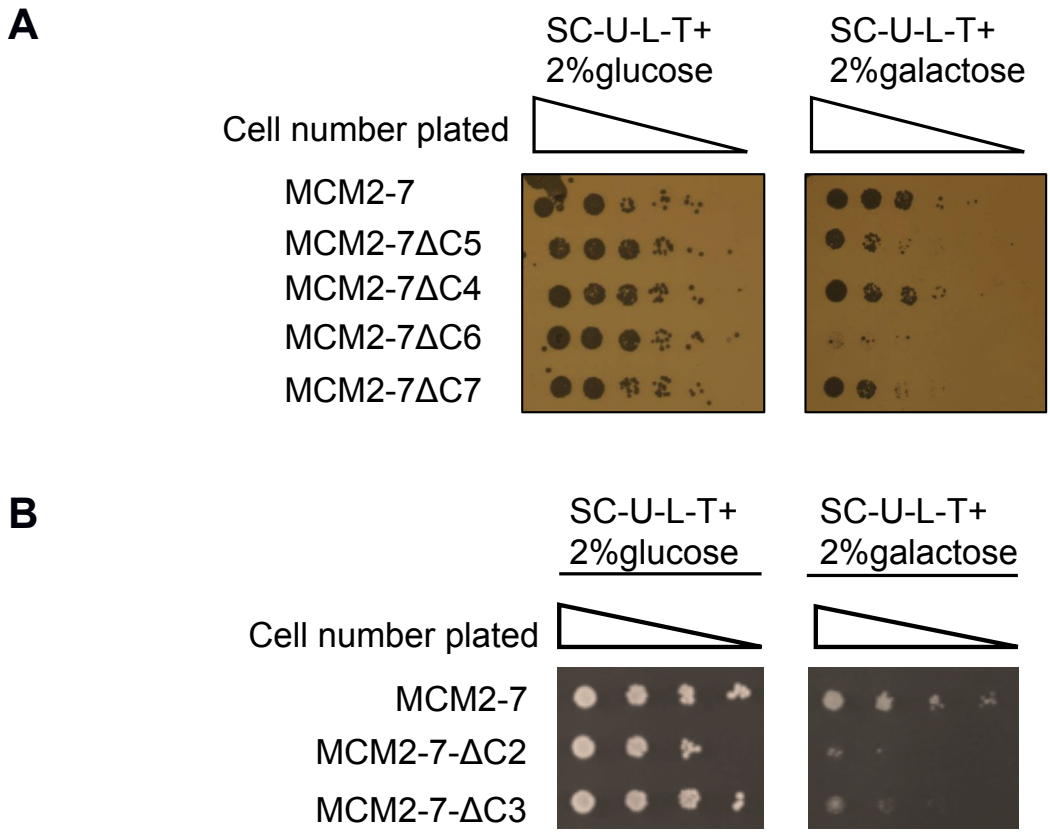


Figure 5.2. In vivo analysis of the MCM2-7 deletion mutants

In vivo dominant lethality assay to test the effect of overexpression of the yeast strains containing the ΔC mutations. A 5-fold dilution of cells at the starting density of 10^7 was spotted onto selective plates (dropout for uracil, leucine and tryptophan) with either 2% glucose (non-inducing condition) or 2% galactose (inducing condition). The plates were incubated at 30°C for two and four days respectively. (The experiments were performed twice). **A**) Plates containing the WT MCM2-7, MCM2-7ΔC5, MCM2-7ΔC4, MCM2-7ΔC6 and MCM2-7ΔC7. **B**) Plates containing the WT MCM2-7, MCM2-7ΔC2 and MCM2-7ΔC3.

5.3. *In vitro* functional analysis of the deletion mutants

To test the effect of the deletion mutants on pre-RC formation, the mutant complexes were expressed in *S. cerevisiae* and purified following the protocol described in Materials and Methods (2.5). The Coomassie stained gels of the purifications performed during this study (MCM2-7ΔC2 and MCM2-7ΔC7) are shown in Figure 5.3 (A and B). MCM2-7ΔC4 and MCM2-7ΔC6 were purified by other members of the group (Christian Winkler and Alberto Riera) and are not shown. The fractions obtained during the purifications were analysed by SDS-PAGE and the concentrations measured by Bradford. The gel-filtration fractions containing the full MCM2-7 complex (highlighted by a black square in the gels in Figure 5.3) were pooled, concentrated and aliquoted. All the mutants yielded a protein amount similar or even higher than the wild type protein (around 1 mg).

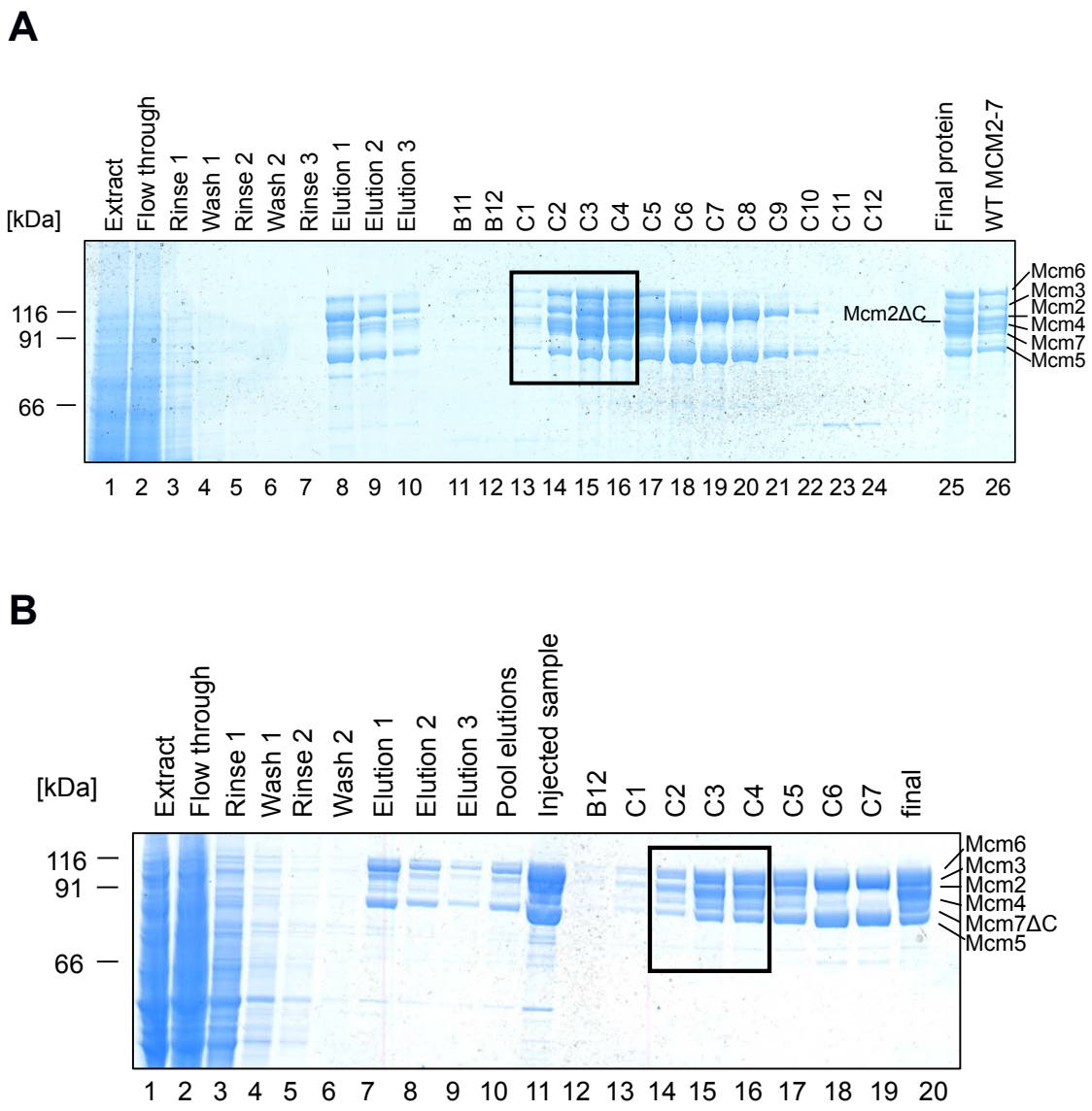


Figure 5.3. Purification of MCM2-7ΔC2 and MCM2-7ΔC7 from *S. cerevisiae*

Coomassie-blue stained SDS-PAGE gels of the two-step MCM2-7ΔC2 and MCM2-7ΔC7 purifications. The protocol was carried out as previously described (Evrin et al, 2009). Yeast extracts were incubated with anti-HA beads, rinsed and washed twice before MCM2-7ΔC-bound to the beads was eluted with HA peptide. The bead eluates were concentrated and subjected to size-exclusion chromatography. The fractions containing the protein of interest were collected, concentrated and aliquoted prior to flash-freezing. **A)** SDS-PAGE from the MCM2-7ΔC2 purification. The fractions containing MCM2-7ΔC2 are marked by a black square (lanes 13-16) and the final protein is loaded in lane 25 next to a WT for comparison of stoichiometry. **B)** SDS-PAGE from the MCM2-7ΔC7 purification. Lanes 14-16 contain the protein of interest, and the final product was loaded in lane 20.

The purified mutants were used in the fully reconstituted *in vitro* pre-RC assay, as described in Materials and Methods (2.7.3). The complexes were assembled in buffer containing ATPγS, origin DNA, ORC, Cdc6 and Cdt1 (Figure 5.4 A). In these conditions an OCCM complex is formed on DNA, since ATP hydrolysis is not required for the assembly of this intermediate. Employing ATPγS prevents ATP hydrolysis and therefore allows the isolation of the OCCM. All of the mutants (except for MCM2-7ΔC3) showed a similar level of DNA binding to WT MCM2-7, indicating that they are not required for OCCM formation. Upon ATP-hydrolysis various pre-RC intermediates are formed, which remain associated with DNA prior to formation of the MCM2-7 double-hexamer. To test for the mutants ability to associate with DNA and form high salt stable MCM2-7 double hexamers, pre-RC reactions were performed in the presence of ATP followed by low salt and high salt washes respectively (Figure 5.4 B, C). MCM2-7ΔC2, MCM2-7ΔC5 and MCM2-7ΔC6 support helicase association with ORC/Cdc6 (Figure 5.4 B, lanes 2, 5 and 6), but MCM2-7ΔC5 and MCM2-7ΔC6 failed salt stable double hexamer formation, while MCM2-7ΔC2 had reduced activity (Figure 5.4 C, lanes 2, 5 and 6). MCM2-7ΔC4 was not defective in forming a salt stable complex (Figure 5.4 C, lane 4). It is intriguing that Mcm7C is not required for double hexamer formation (Figure 5.4 C lane 7), but affects the release of Cdt1 (Figure 5.4 B lane 7), as Mcm7 has not been known to affect Cdt1 release until now.

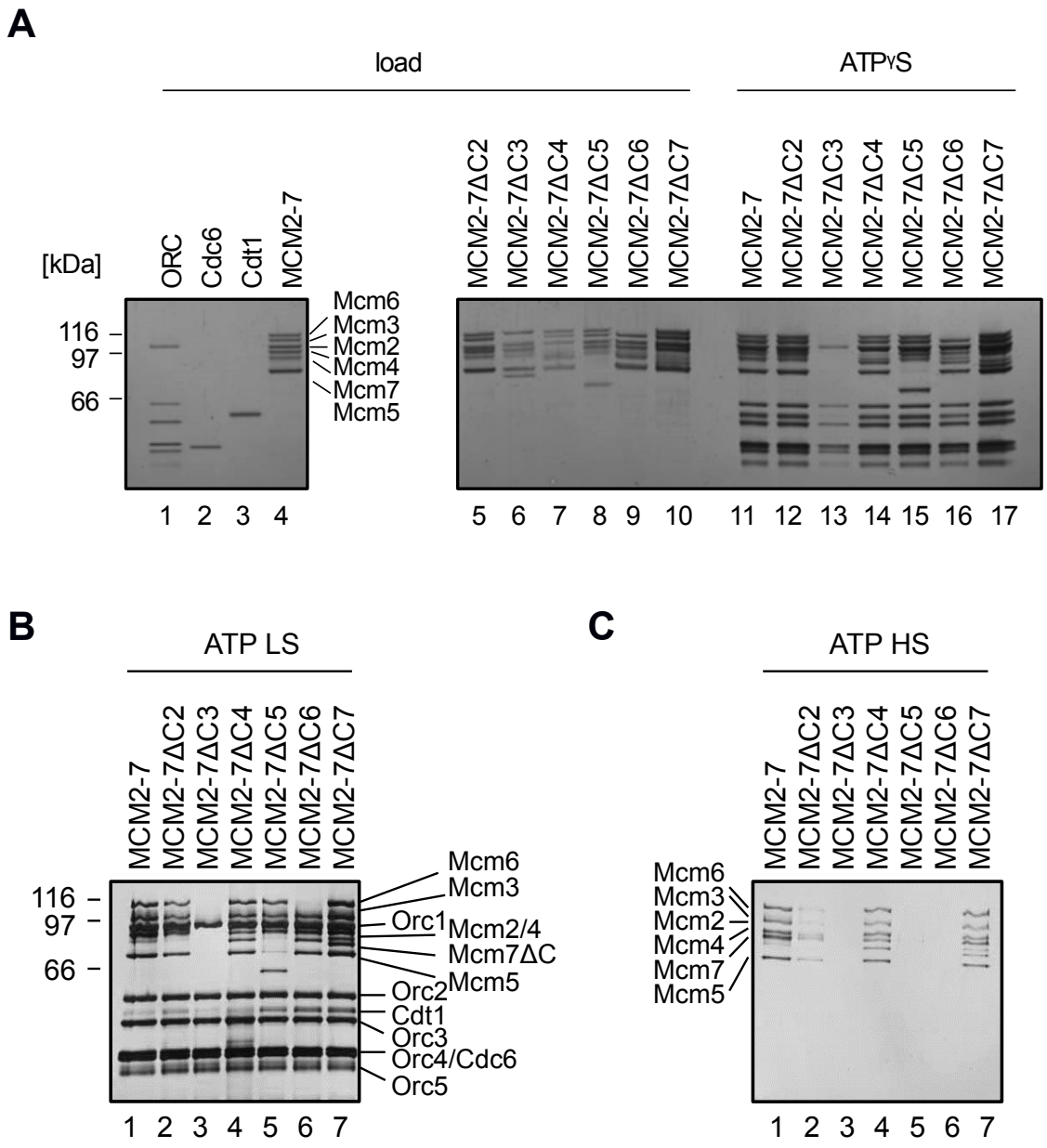


Figure 5.4. *In vitro* test of MCM2-7ΔC activity

A) Silver stained gel showing the *in vitro* reconstitution assay of the pre-RC reactions, performed as previously described (Evrin et al., 2009). Lanes 1-10: purified proteins used in the assay. Pre-RC reactions were assembled in the presence of ATPγS, washed and eluted with DNaseI (lanes 11-17). **B**) Pre-RC reactions were assembled in the presence of ATP and washed with low salt buffer (LS) before elution from the beads. **C**) Pre-RC reactions were assembled in the presence of ATP and washed with 300 mM sodium chloride (high salt, HS). The experiments were performed twice.

Previous studies showed that in ATPγS and in the absence of Cdt1, WT MCM2-7 binds very weakly to ORC/Cdc6, but MCM2-7ΔC6 bypasses this Cdt1 requirement and can bind to ORC/Cdc6 independent of Cdt1 (Evrin et al., 2009; Fernandez-Cid et al., 2013). It was described that Mcm6C contains an auto-inhibitory domain that is alleviated by the interaction with Cdt1 (Fernandez-Cid et al., 2013). We wondered whether any of the deletion mutants were equally able to bypass the initial Cdt1 requirement for complex formation, therefore we tested them in the pre-RC assay. Reactions containing ORC, Cdc6, MCM2-7ΔC without Cdt1 were assembled on DNA in the presence of ATPγS. We found that MCM2-7ΔC7 was able to bind ORC/Cdc6 without Cdt1, similarly or better than MCM2-7ΔC6 (Figure 5.5, compare lane 18 and lane 17).

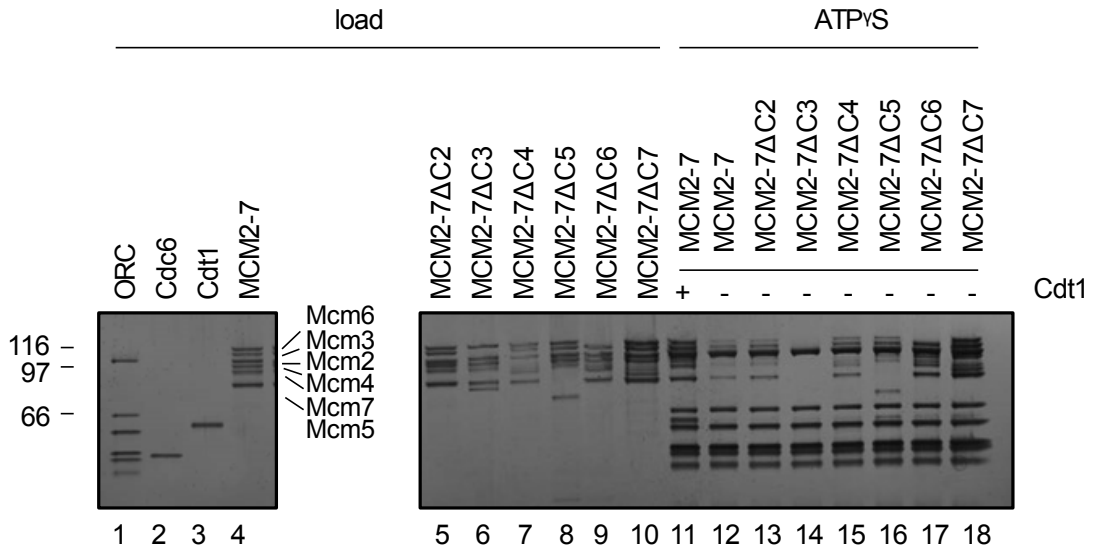


Figure 5.5. *In vitro* activity of the deletion mutants in the absence of Cdt1

Silver stained SDS-PAGE showing the *in vitro* pre-RC reactions assembled in the absence of Cdt1 in buffer containing ATPγS (lanes 12-18). Purified proteins used in the assay are shown in lanes 1-10. A pre-RC reaction assembled in the presence of Cdt1 is shown in lane 11. The experiment was performed three times and reproducible.

5.4. MCM2-7ΔC2

In *S.cerevisiae* Mcm2C is only 20 amino acids long and does not contain a WHD that is present in the other subunits. Interestingly, a C-terminal Mcm2 WHD is found in all higher eukaryotes (Figure 5.6 A). The Mcm2 deletion mutant missing amino acids 848-868 was tested in the pre-RC assay for functionality. MCM2-7ΔC2 did not affect the assembly with ORC, Cdc6, Cdt1 onto origin DNA under low salt conditions with ATP when compared to the WT (Figure 5.6 B, compare lanes 6 and 7). However, the Mcm2C deletion severely impaired the formation of the high salt stable double-hexamer (Figure 5.6 B, lane 9). CLMS data showed that Mcm2C is involved in dynamic interactions with flexible sections of Orc6, Orc2 and Mcm5 (Yuan et al., 2017). Moreover, CLMS analysis of the OCCM performed by the collaborator (Juri Rappsilber) using a new method (Mendes et al., 2018 bioRxiv) revealed additional interactions. Together with the already reported interaction between Cdt1 and Mcm2, an interaction between Mcm2 and Orc5 (Mcm2-850, Orc5-369) is reported. These results suggest that even though Mcm2C is a short domain, it is required for double hexamer formation. It is possible that this domain is involved in stabilising important interactions with ORC/Cdc6 during the OCCM to OCM transition. The intrinsic ATPase activity of this protein was strongly reduced, compared with the WT. However, the ATP hydrolysis induced by the presence of ORC/Cdc6 and Cdt1 did not appear to be altered (Alberto Riera, personal communication). These data suggest that Mcm2C does not affect the overall ATP hydrolysis of the pre-RC complex.

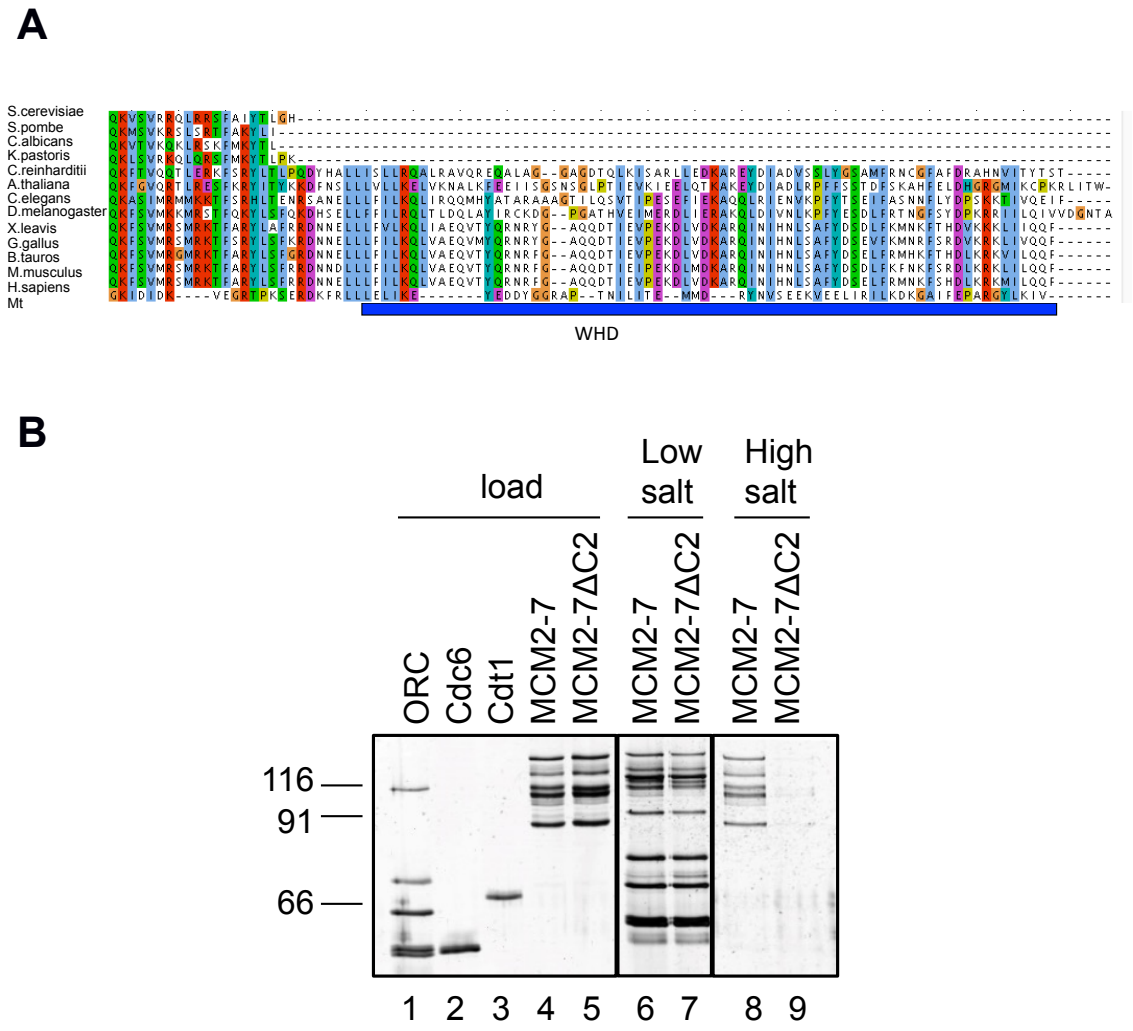


Figure 5.6. MCM2-7ΔC2

A) Sequence alignment among eukaryotic species of the C-terminus of the *S.cerevisiae* Mcm2 realised with Clustal. The winged helix domain (WHD) is highlighted with the blue bar. Note that this domain is missing in yeast. **B)** Silver stained SDS-PAGE showing the *in vitro* pre-RC reconstituted assay in the presence of WT MCM2-7 and MCM2-7ΔC2. The reactions were assembled in ATP and washed with low (300 mM potassium glutamate, lanes 6 and 7) or high (300 mM sodium chloride, lanes 8 and 9) salt buffer. The experiment was repeated three times.

5.5. MCM2-7ΔC7

To better characterise the effect of Mcm7C on pre-RC formation, MCM2-7ΔC7 activity in the pre-RC assay was tested separately, in the presence and absence of Cdt1 and compared it with WT MCM2-7 (Figure 5.7). The results confirmed that the deletion of Mcm7C retained Cdt1 efficiently on DNA after low salt treatment (Figure 5.7 lane 13). However, it did not affect double hexamer formation, suggesting that this domain is not essential for the formation of a salt stable complex (Figure 5.7 lane 14). Although MCM2-7ΔC7 is recruited to ORC/Cdc6 without Cdt1, Cdt1 is still required for salt-stable double hexamer formation (Figure 5.7 lane 15-17). This means that Mcm7C acts also in an auto-inhibitory way, similar as Mcm6C, since it blocks Cdt1-independent MCM2-7 recruitment.

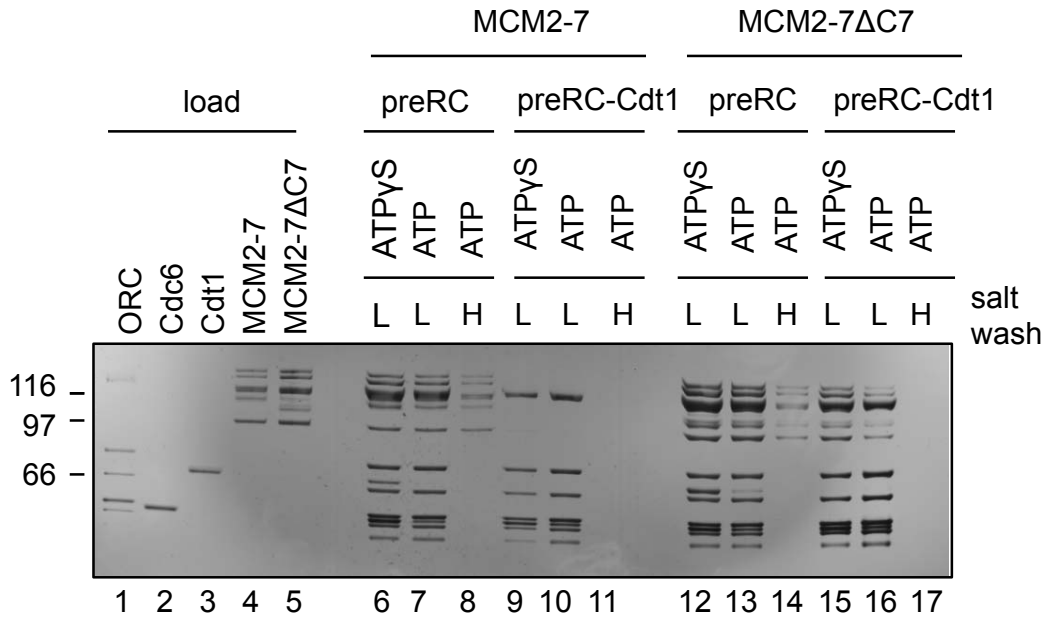


Figure 5.7. *In vitro* activity of MCM2-7ΔC7

Silver stained SDS-PAGE showing the *in vitro* reconstituted pre-RC in the presence of WT MCM2-7 or MCM2-7ΔC7. The reactions were assembled in ATPγS or ATP followed by low (L) or high (H) salt washes. Pre-RC reaction in the absence of Cdt1 are shown with the WT MCM2-7 (lanes 9-11) and with the MCM2-7ΔC7 (lanes 15-17). The experiment was repeated three times.

It was previously shown that Cdt1 release is required to form a double hexamer (Ticau et al., 2015) and its release requires ATP hydrolysis by Mcm subunits (Coster et al., 2014; Kang et al., 2014). It was also described that while the OCCM is rapidly formed, double hexamer formation is a slow process, as it is a multi-step reaction (Fernandez-Cid et al., 2013). In order to test the stability of the OCM over time, WT MCM2-7 was incubated with ORC/Cdc6, Cdt1 and DNA in ATP for 2.5 minutes. During this time an OCM but not a double hexamer can form. The reaction was washed with low salt to remove the unbound proteins and the DNA-bound proteins were further incubated in buffer for 0, 5, 10, 15 and 20 minutes. The “supernatant fractions” contain the proteins that dissociate from DNA during the second incubation and the “bound fractions” are the proteins that remain bound to DNA. In accordance with previous results, the OCM is formed and is a stable complex (Figure 5.8 A). The experiment was repeated in the presence of MCM2-7ΔC7 and it was found that Cdt1 was not released during the time analysed (Figure 5.8 B, asterisk indicates the band of Cdt1, also see Figure 5.8 A for comparison). A stable OCCM rather than an OCM is retained on DNA in the presence of ATP. This result suggests that Mcm7C might be involved in stimulating ATP hydrolysis required for Cdt1 release. One possibility is that Mcm7C could affect pre-RC ATP-hydrolysis, and in this way affects Cdt1 release.

In order to investigate whether this mutant had an effect on ATP hydrolysis during pre-RC formation, the ATPase activity was measured (Alberto Riera; personal communication). Interestingly, the intrinsic ATP hydrolysis rate of MCM2-7ΔC7 was very low compared to WT. However, the ATP hydrolysis induced by the presence of ORC/Cdc6 and Cdt1 was similar to WT MCM2-7. These data demonstrate that Mcm7C does not affect the overall ATP hydrolysis of the pre-RC complex. This result is very interesting, as it shows that the deletion of WHD7 genuinely blocks Cdt1 release and that ATP-hydrolysis and Cdt1 release can be uncoupled. This raises the question what is ATP-hydrolysis actually doing, as it was thought that the main role of ATP-hydrolysis is the release of Cdt1.

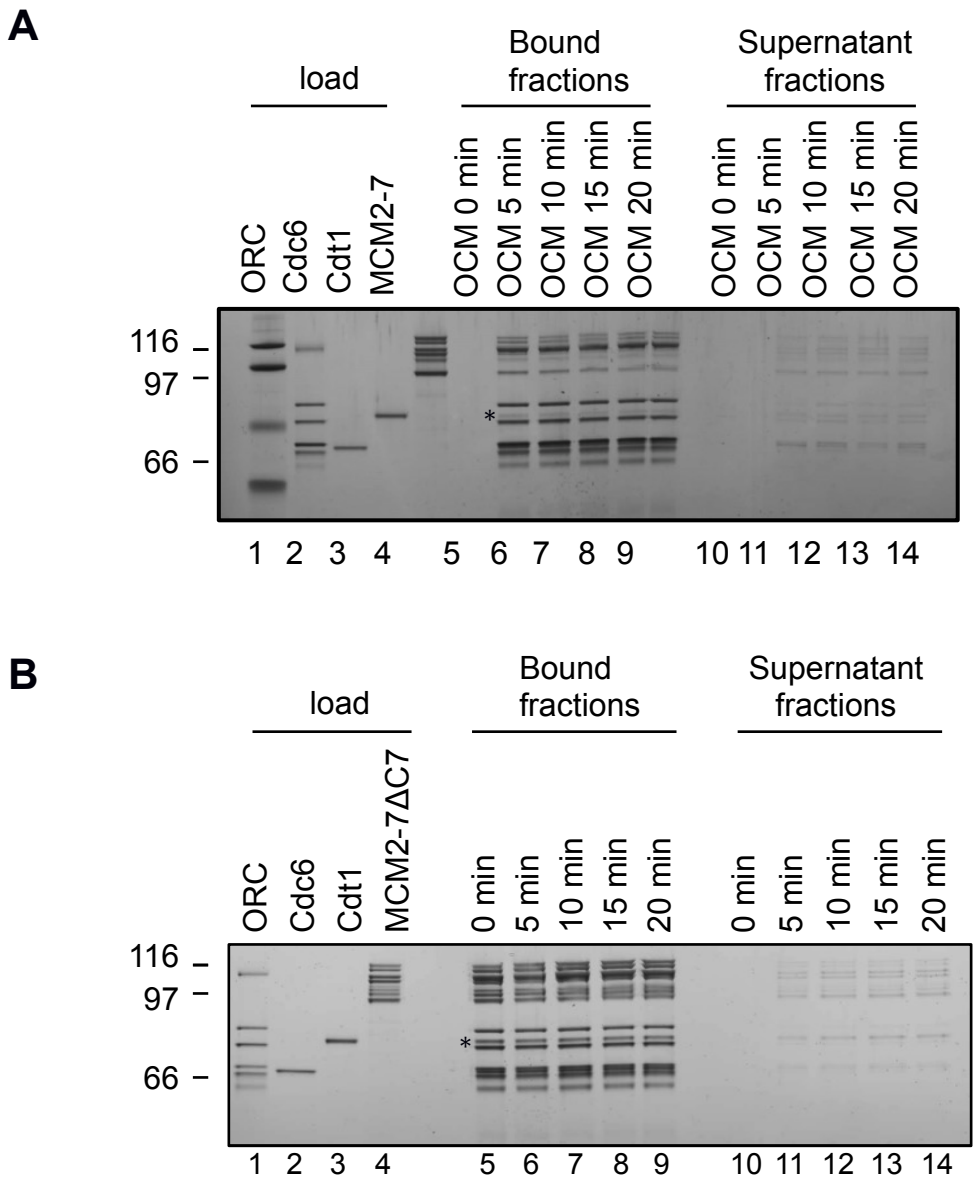


Figure 5.8. MCM2-7ΔC7 form a stable complex in the presence of ORC, Cdc6 and Cdt1.

ORC, Cdc6, Cdt1 were incubated with WT MCM2-7 (**A**) or MCM2-7ΔC7 (**B**) with beads-bound DNA for 2.5 minutes, washed with low salt and incubated for up to 20 minutes, before elution from the beads. The "bound fractions" represent the proteins bound to the DNA; the "supernatant fractions" contains the proteins that are released from the beads after the second incubation. The asterisk indicates the band of Cdt1, which is not released on B (lanes 5-9).

MCM2-7ΔC7 was able to bind to ORC/Cdc6 in the presence of ATP and form a stable complex. We wondered if Cdt1 could bind to such an ORC/Cdc6/MCM2-7 complex and if this Cdt1 could promote MCM2-7 double-hexamer formation. A reaction containing ORC, Cdc6 and MCM2-7ΔC7 was

assembled on bead-bound DNA in the presence of ATPγS, washed with low salt buffer and further incubated in the presence of Cdt1 (Figure 5.9 A lane 7). The presence of the Cdt1 band suggests that this protein is able to bind to the ORC-Cdc6-MCM2-7ΔC7 complex. The same reaction was assembled in ATP and washed with low or high salt buffer and the protein complex was eluted from the beads (Figure 5.9 B). Decreased band intensity for Cdt1 in lane 4 compared to lane 2 suggests that Cdt1 seems to bind inefficiently to the preformed ORC/Cdc6/MCM2-7ΔC7. The addition of Cdt1 at this point is however not able to aid the recruitment of the second hexamer for the formation of a salt-stable double hexamer (Figure 5.9 B lane 7). In the WT situation, the helicase does not bind to ORC/Cdc6 in the absence of Cdt1. This suggests that Cdt1 is needed at an earlier time point in complex formation, when MCM2-7/Cdt1 makes contact with ORC/Cdc6.

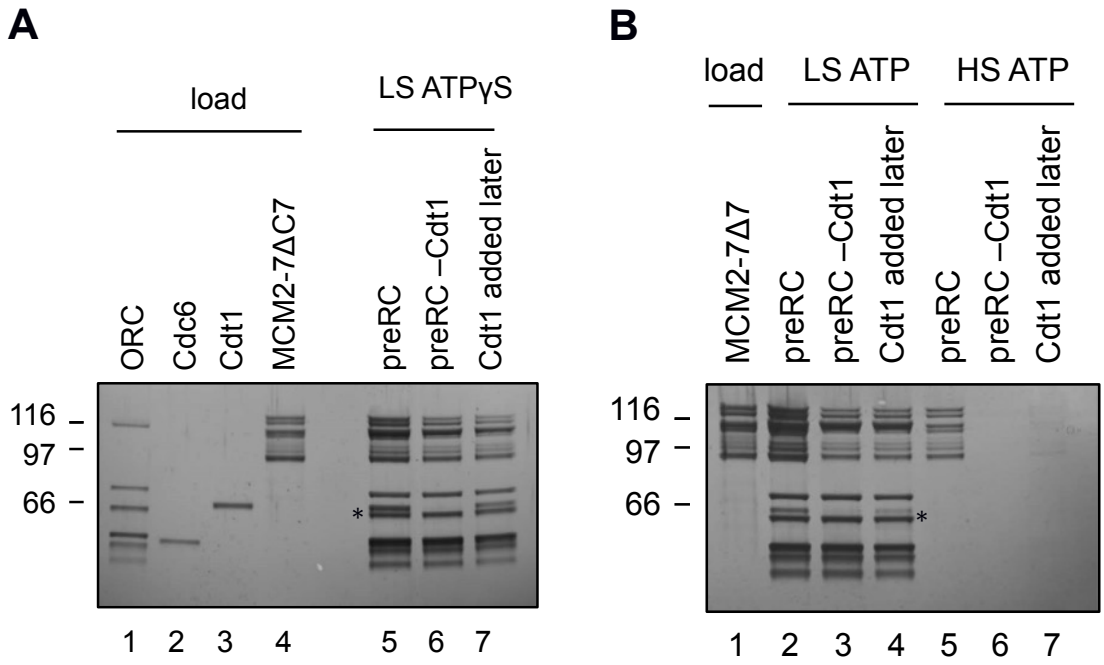


Figure 5.9. Cdt1 binds to the ORC-Cdc6-MCM2-7ΔC7 complex

A) Silver stained SDS-PAGE showing the pre-RC reconstituted assay in the presence of MCM2-7ΔC7 and ATPγS, with Cdt1 (lane 5), without Cdt1 (lane 6) or with addition of Cdt1 after initial complex formation (lane 7). The asterisk indicates the band of Cdt1. **B)** pre-RC reactions with MCM2-7ΔC7 assembled in ATP and analysed on silver stained SDS-PAGE after low salt washes (lanes 2) or high salt washes (lane 5). Reactions in the presence of ORC, Cdc6 and MCM2-7ΔC7 but not Cdt1 were assembled and washed with low (lane 3) or high (lane 6) salt washes prior elution. Reactions assembled in the same way were further incubated in the presence of Cdt1 and washed with low (lane 4) or high (lane 7) salt washes. (The experiments were repeated twice.)

Taken together these experiments show that MCM2-7 lacking the Mcm7C does not require Cdt1 for the binding to ORC/Cdc6, but Cdt1 is essential for double hexamer formation. While pre-RC ATP hydrolysis is normal and salt resistant double hexamer loading is supported, Cdt1 is not released upon ATP hydrolysis, demonstrating that ATP hydrolysis is required for a different function than Cdt1 release.. Moreover, it was discovered here that Cdt1 has an essential function early in OCCM formation, while efficient Cdt1 release is not essential for MCM2-7 double-hexamer formation.

5.6. OCCM WT and OCCMΔC7

5.6.1. WT OCCM

ORC/Cdc6 is responsible for MCM2-7/Cdt1 recruitment. The resulting complex, the so-called OCCM, contains 14 proteins (Yuan et al., 2017). It was hypothesised that ORC/Cdc6 interacts specifically with the C-terminal extensions of MCM2-7 promoting structural changes in the helicase. OCCM formation is an ATP-hydrolysis independent process, but ATP hydrolysis induced by the interactions between ORC/Cdc6 and MCM2-7/Cdt1 is thought to be responsible for Cdt1 release. Therefore, the OCCM can be isolated *in vitro* in the presence of ATPγS, which slows down ATP hydrolysis, preventing Cdt1 release. Using this approach, a structure of this intermediate was obtained (Sun et al., 2013) but the resolution at the time was too low (around 14 Å) to allow atomic details to be revealed.

Recently, with the advent of the “resolution revolution” of cryo-EM, it has been possible to obtain a 3.9 Å resolution of the OCCM (Yuan et al., 2017) (Figure 5.10). The samples were prepared by a colleague (Alberto Riera) in the following way. The purified proteins (ORC, Cdc6, MCM2-7, Cdt1) were assembled on biotinylated DNA containing origins of replication and bound to streptavidin-coated magnetic beads, in the presence of ATPγS. Upon release with DNaseI, the sample was applied on a cryo-grid and imaged by the group of the collaborator (Huilin Li, USA). Important protein-protein interactions were revealed. In particular, for the relevance of this study, the WHDs of four MCM subunits (Mcm3, Mcm4, Mcm6 and Mcm7) were resolved (Figure 5.10). These

WHDs are establishing interactions with ORC/Cdc6, indicating their importance in the binding of MCM2-7 to the helicase loader. Mcm5C was not visible in the EM map. Importantly, the MCM2-7 ring was loaded on dsDNA, with DNA traversing through ORC/Cdc6 into the MCM2-7 complex, as suggested by the previous structure. Furthermore, the open spiral MCM2-7 (Zhai et al., 2017a) has now changed to a planar ring which remains partially open.

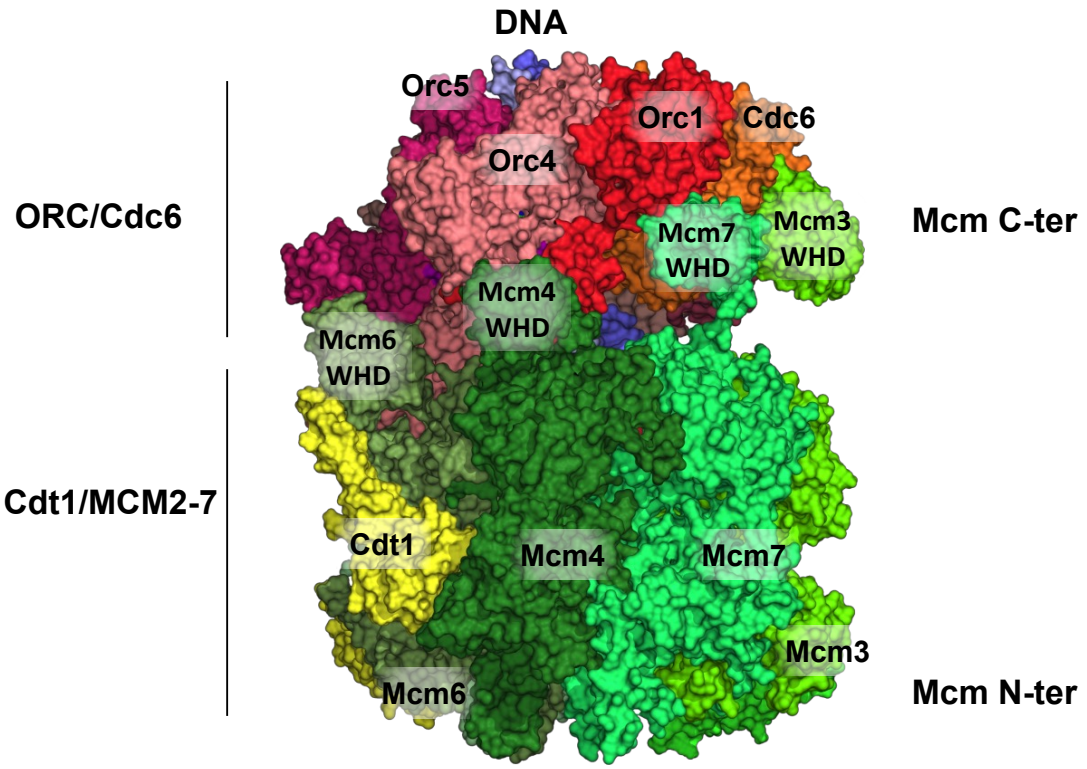


Figure 5.10. Structure of the ORC/Cdc6/MCM2-7/Cdt1 complex.

Side view of the cryo-EM density map with surface representation (Yuan et al, 2017). The location of the individual proteins and DNA are labelled. Note the localisation of the winged helix domains (WHDs) of Mcm2-7. The figure was generated with pyMOL.

In order to better understand the overall architecture of this complex, specifically in the flexible regions that are not resolved by cryo-EM, an independent approach was employed. Cross-linking mass spectrometry provides proximity data on intra and inter-protein interactions identifying spatially proximal lysine residues that have been covalently linked by a cross-linking reagent. The protocol established by the collaborator Juri Rappsilber

employs bis(sulfosuccinimidyl)suberate (BS3), which contains a carbon chain spacer arm with a total length of 11.4 Å. The MCM2-7 purification protocol and the pre-RC assay use potassium glutamate as the main salt. However, the presence of amine groups interferes with the cross-linking reaction, as the BS3 reacts with the NH_2 group. Consequently, we had to identify an alternative salt that allowed crosslinking, but also support full pre-RC activity. Figure 5.11 illustrates the different salts tested as part of this thesis. Among them, potassium formate and potassium acetate supported stable MCM2-7 association with ORC, Ccd6, Cdt1 and DNA, comparable to the standard condition using potassium glutamate (Figure 5.11 compare lanes 5, 6 and 12). However, when the reactions were washed with high salt (300 mM sodium chloride) in order to detect successful MCM2-7 double hexamer formation, only potassium acetate proofed to function as efficient as the positive control, potassium glutamate (Figure 5.11 compare lane 20 with 13).

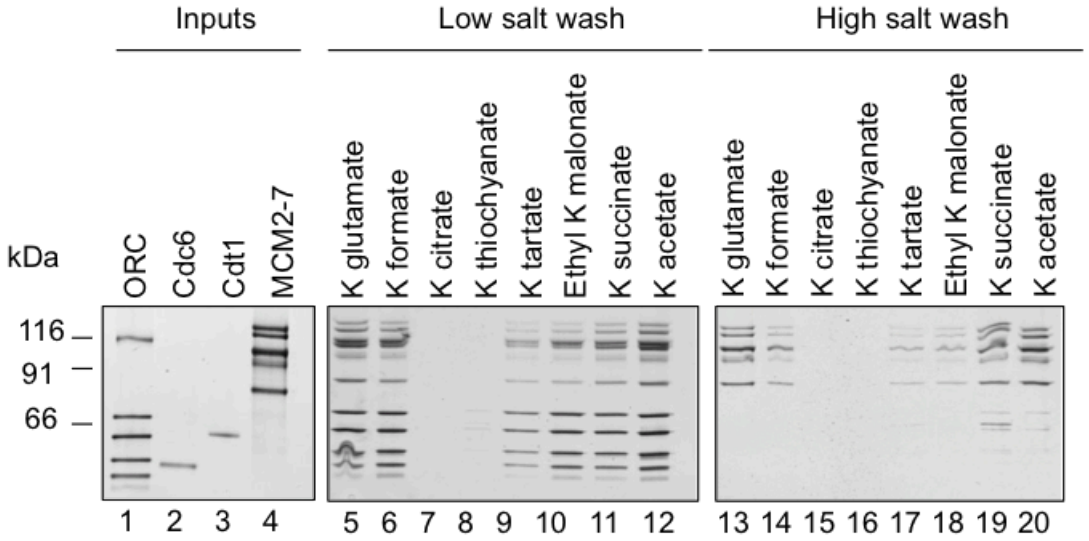


Figure 5.11. Effect of different salts on pre-RC formation

Silver stained gel showing the effect of a range of salts on pre-RC formation. Complete pre-RC reactions assembled in the presence of 300 mM of the following salts: potassium glutamate, potassium formate, potassium citrate, potassium thiochyanate, potassium tartate, ethyl potassium malonate, potassium succinate, potassium acetate. Reactions were washed with low (lanes 5-12) or high (lanes 13-20) salt washes prior to elution. Lanes 1-4: 20% of the proteins used on the assay. The experiment was performed three times.

This result may suggest that the salts cause destabilisation of the protein complex. In order to minimise any risk and stick to the established conditions it was decided to assemble the OCCM in standard pre-RC buffer (100 mM potassium glutamate) and then replace the buffer afterwards with 100 mM potassium acetate. Consequently, BS3 at 1:8100 (molar protein:cross-linker ratio) was added for 2 hours at 4°C. The products were then processed and analysed by mass-spectrometry by Juri Rappsilber (Yuan et al., 2017). The analysed cross-linked reactions showed that the C-terminal regions of MCM2-7 cross-linked with some subunits of ORC complex and Cdc6 (Figure 5.12). In particular, two areas of interactions were identified: (1) the MCM WHDs and (2) a region just before or after this domain. Specifically, the WHD of Mcm7 cross-links with Cdc6, whereas its nearby ATPase domain cross-links with Cdc6, Orc1 and Orc2. The WHD of Mcm3 did not show any cross-links with ORC/Cdc6, but it did react with it in the region before and after the WHD (Figure 5.12 B). The long and floppy Mcm5C exhibited a cross-link with the N-terminus of Orc2 (750 Mcm5, 362 Orc2, Figure 5.12 D). Interestingly, these domains were not visible in the cryo-EM map of the OCCM. A more detailed CLMS analysis performed using the same sample (Riera et al., unpublished) also showed interactions between Mcm6C (693) and Orc4 (2) and between Mcm4C (860) and Orc1 (902) (Figure 5.12 C, E). In summary, these results show that a network of interactions between the C-terminal regions of MCM2-7 and ORC subunits is established during the OCCM formation. The specific functions of these protein-protein interactions remain to be described.

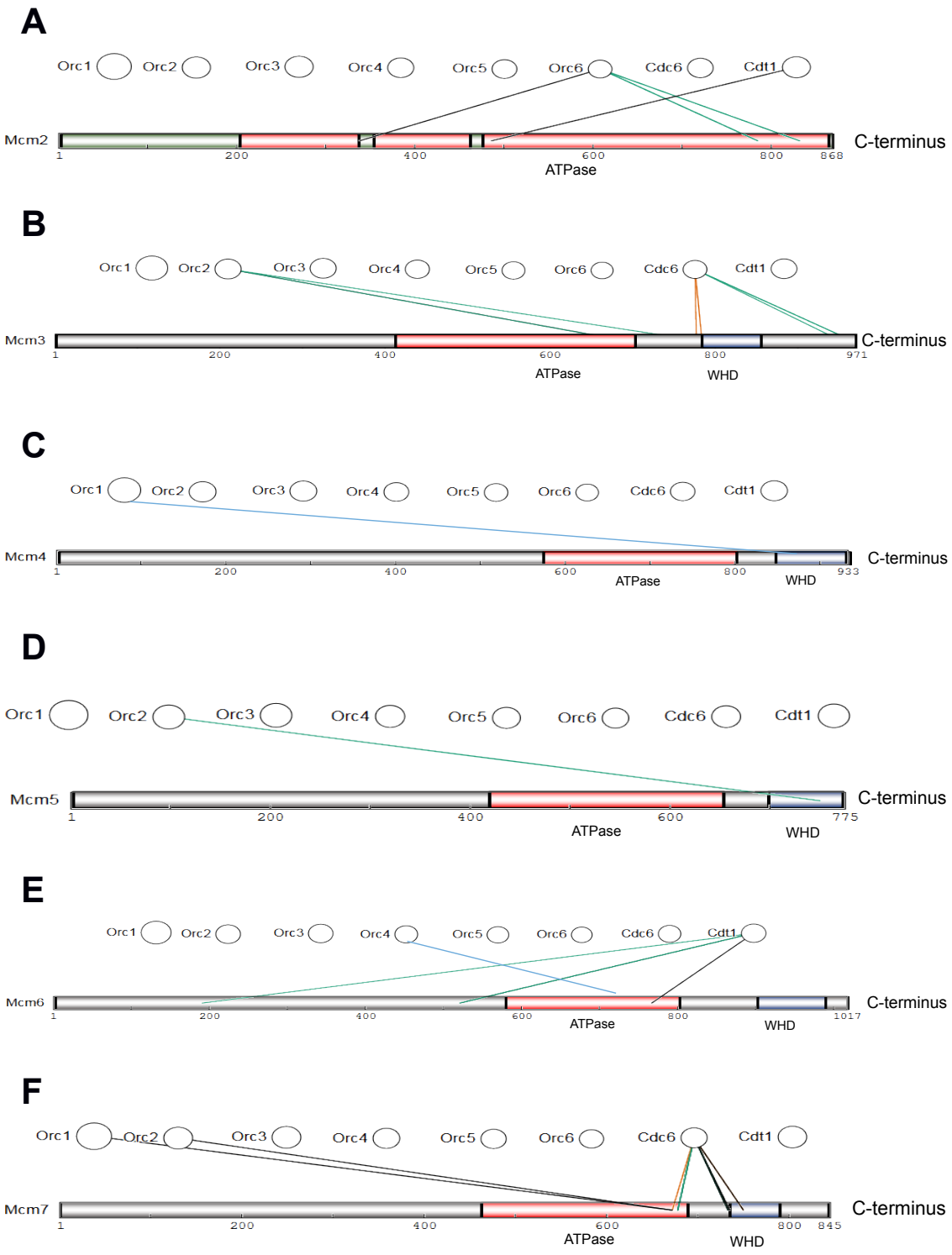


Figure 5.12. Cross-linking mass spectrometry

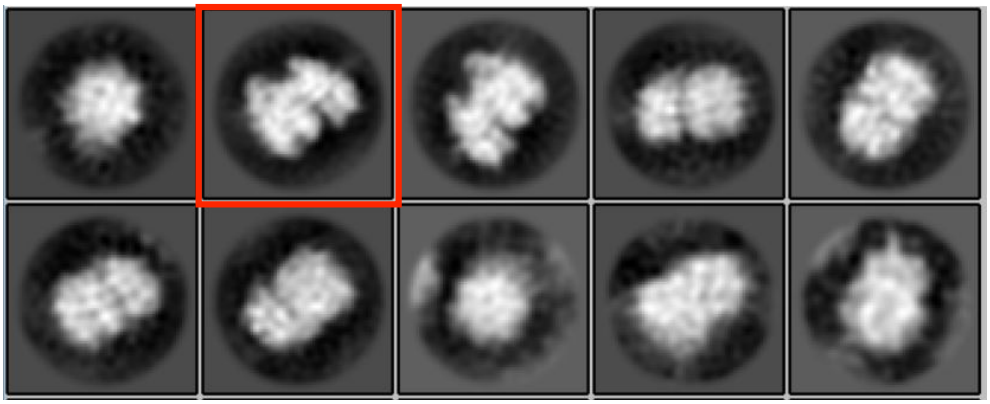
A-F) Summary of the interactions between the C-termini of MCM2-7 and ORC identified by cross-linking mass spectrometry, in the contest of OCCM. Each bar represents a MCM subunit, in which the ATPase domain (red) and the WHD (light blue) are highlighted. The circles refer to Orc1-6, Cdc6 and Cdt1. The lines connecting the MCM subunit to the ORC, Cdc6 or Cdt1 indicate the detected interactions within the proteins.

5.6.2. OCCMΔC7

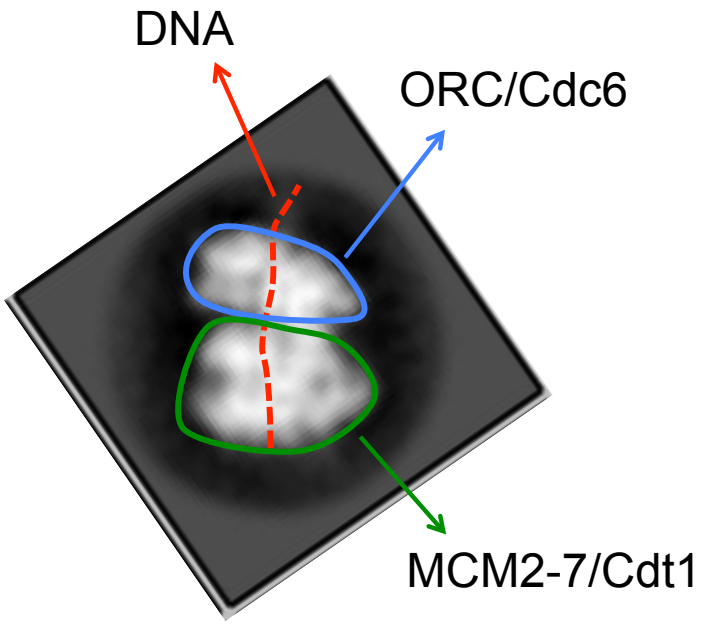
The recent cryo-EM structure of the *S. cerevisiae* OCCM complex showed that in the absence of ATP hydrolysis, the first Mcm2-7 hexamer is recruited by ORC-Cdc6 and encircles the origin DNA. However, it has been unclear how the Mcm2-7 hexamer latches onto the ORC-Cdc6 and how the DNA enters the central channel of the MCM ring. Here, a mutant Mcm2-7 hexamer in which the WHD of Mcm7 was deleted (MCM2-7ΔC7) has enabled us to capture structural information for several initial intermediates between ORC-Cdc6 and Cdt1/Mcm2-7 using cryo-EM.

Following the established protocol by Alberto Riera, OCCM samples with MCM2-7ΔC7 were prepared by myself. MCM2-7ΔC7 was assembled on DNA in the presence of ORC/Cdc6 and Cdt1 in buffer containing ATPγS. After complex formation, low salt washes were performed followed by DNaseI elution of the proteins bound to DNA. The complex was then applied to a cryo-grid and imaged with a Talos Arctica TEM (Thermo Scientific) by the Li group (USA) (Figure 5.13 A). In Figure 5.13 A a 2D classification analysis is shown which sorts all the different particles present in the sample into classes. In Figure 5.13 B, highlighted in red is the pathway of DNA, which can be seen traversing the ORC/Cdc6 and MCM2-7/Cdt1 rings. Preliminary cryo-EM data of OCCMΔC7 showed that in this complex and at the current resolution, no obvious conformational changes are observed if compared to WT. While the resolution is very low, dsDNA can be seen correctly inserted in the MCM ring (Figure 5.13 C). From these results, it was concluded that the deletion of Mcm7C does not affect DNA insertion.

A



B



C

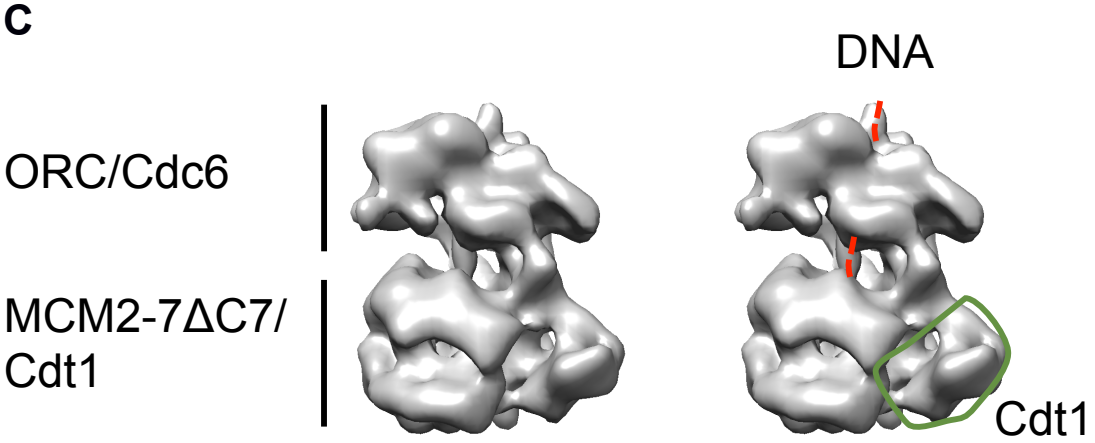
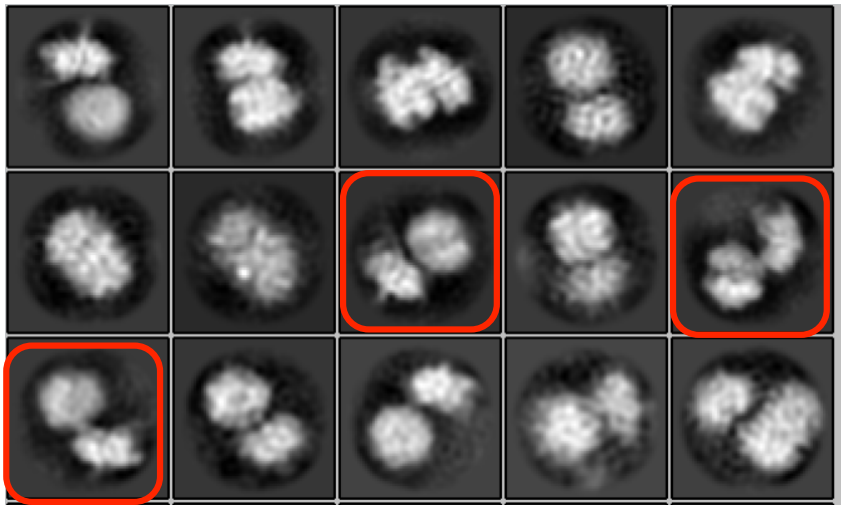


Figure 5.13. OCCMΔC7

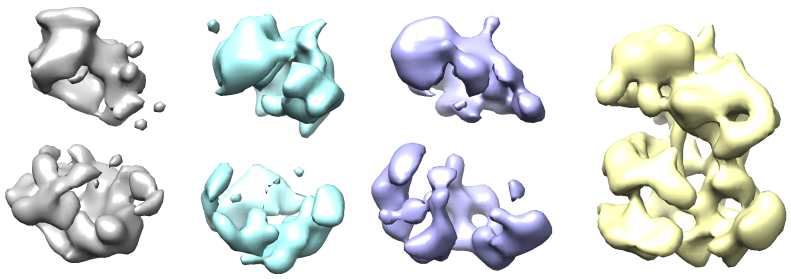
ORC, Cdc6, Cdt1 and MCM2-7ΔC7 were assembled on DNA-containing replication origin in the presence of ATPγS. The sample was applied to a cryo grid, frozen and imaged (Huilin Li, USA). **A)** 2D average classification of the particles present on the grid. **B)** Zoom on one representative 2D class, in which ORC/Cdc6 were circled in blue and MCM2-7ΔC7/Cdt1 in green; the DNA path is highlighted in red. **C)** 3D reconstruction of the OCCMΔC7 (resolution around 20 Å). In red the DNA path is highlighted and in green the Cdt1 density.

The biochemical analysis of MCM2-7ΔC7 in the pre-RC assay showed that in contrast to the WT this mutant is able to bind ORC/Cdc6 in the absence of Cdt1 (Figure 5.7). We wanted to determine if a structural rationale could be determined, which could explain this difference. Therefore, a protein complex formed by ORC/Cdc6/MCM2-7ΔC7 in ATPγS was assembled onto origin DNA, and applied to a cryo-grid. The 2D classification analysis showed the presence of particles that are loaded on DNA, and others in which DNA can be seen bending along the ORC/Cdc6 ring, but are clearly not inserted into the MCM ring (Figure 5.14 A circled in red). An initial three dimensional model of these particles showed that 35% of the particles analysed contained a complex in which Cdt1 is visible ("loaded conformation", Figure 5.14 B, on the right hand side). It is possible that endogenous Cdt1 from yeast could be co-purifying with the overexpressed MCM2-7ΔC7, explaining the presence of Cdt1 in a small proportion of the complexes. The remaining particles showed a novel conformation that could be identified as "pre-loading" since DNA is not inserted into the MCM2-7 ring (Figure 5.14 B, C). These results demonstrate that Cdt1 is essential to allow tight engagement of ORC/Cdc6 with MCM2-7, for DNA insertion into the MCM2-7 ring and for the spiral to ring transition. Furthermore, these results confirm previous data showing that Cdt1 is essential for pre-RC formation, since its removal blocks MCM2-7 association (Fernandez-Cid et al., 2013). It also reveals that Mcm7C plays an essential role in the helicase interactions with ORC/Cdc6 and DNA insertion.

A



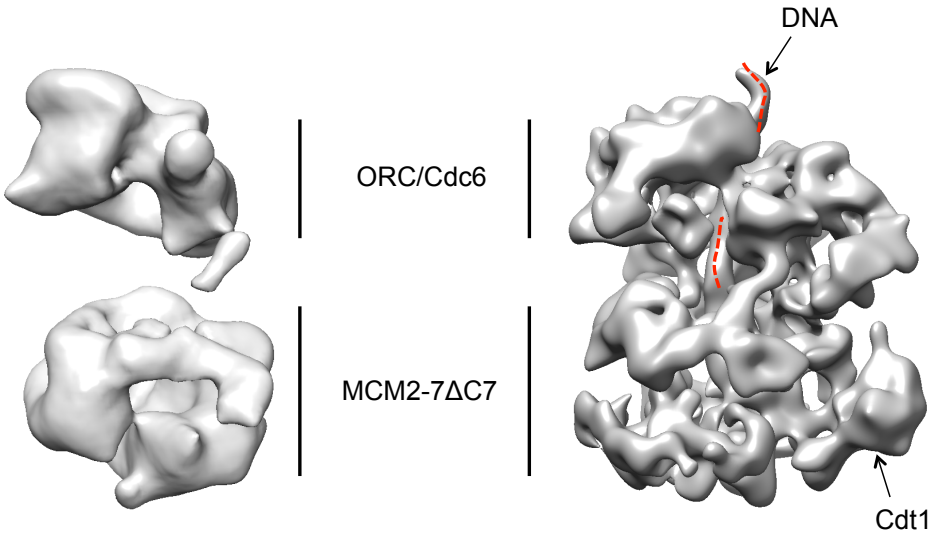
B



25 % 23 % 17 % 35 %

"pre-loaded" conformation "loaded" conformation

C



"pre-loaded" conformation
23Å
4585 particles

"loaded" conformation
15Å
6250 particles

Figure 5.14. ORC/Cdc6/MCM2-7ΔC7 in ATPγS.

ORC, Cdc6 and MCM2-7ΔC7 were assembled on DNA-containing origin in the presence of ATPγS, washed and eluted from the beads. The sample was applied to a cryo-grid and analysed by cryo-EM. **A)** 2D average classification of the particles present in the sample, from top left the population with the most abundant particles. The classes that show a different configuration from the others ("pre-loaded" conformation) are highlighted in red. **B)** 3D classification with percentage showing the abundance of each particle. **C)** 3D reconstruction of the "pre-loaded" conformation at around 23 Å and the "loaded" conformation at a resolution of about 15 Å.

5.7. MCM2-7ΔC6-ΔC7

The effect of MCM2-7ΔC6 and MCM2-7ΔC7 in pre-RC formation has previously been analysed and it was observed that both mutants were able to allow an initial binding to ORC/Cdc6 in the presence of ATPγS. However, in the presence of ATP, Cdt1 release was blocked. Mcm6C was described to be essential for inducing ORC/Cdc6 ATP hydrolysis (Fernandez-Cid et al., 2013). The role of Mcm7C had not been described previously, however in the work presented in this chapter, we showed that this domain is involved in Cdt1 release, but the removal of this domain does not affect double hexamer formation. We wondered whether combining the deletion of the two Mcm C-termini in one single MCM2-7 would generate a similar effect or if this could affect Cdt1 recruitment.

To test this hypothesis, a MCM2-7 without the Mcm6C and Mcm7C (MCM2-7ΔC6-ΔC7) was generated and purified following the standard protocol for WT MCM (Materials and Methods 2.5). A Coomassie stained gel of the purification is shown in Figure 5.15 A. Fractions containing MCM2-7ΔC6-ΔC7 (Figure 5.15 A, lanes 15-18) were collected, concentrated and aliquoted. The final product of the purification is shown in a silver stained gel, together with WT, MCM2-7ΔC6 and MCM2-7ΔC7 (Figure 5.15 B). The subunits stoichiometry of the double mutant is consistent with that of the WT, indicating that a hexameric complex is assembled.

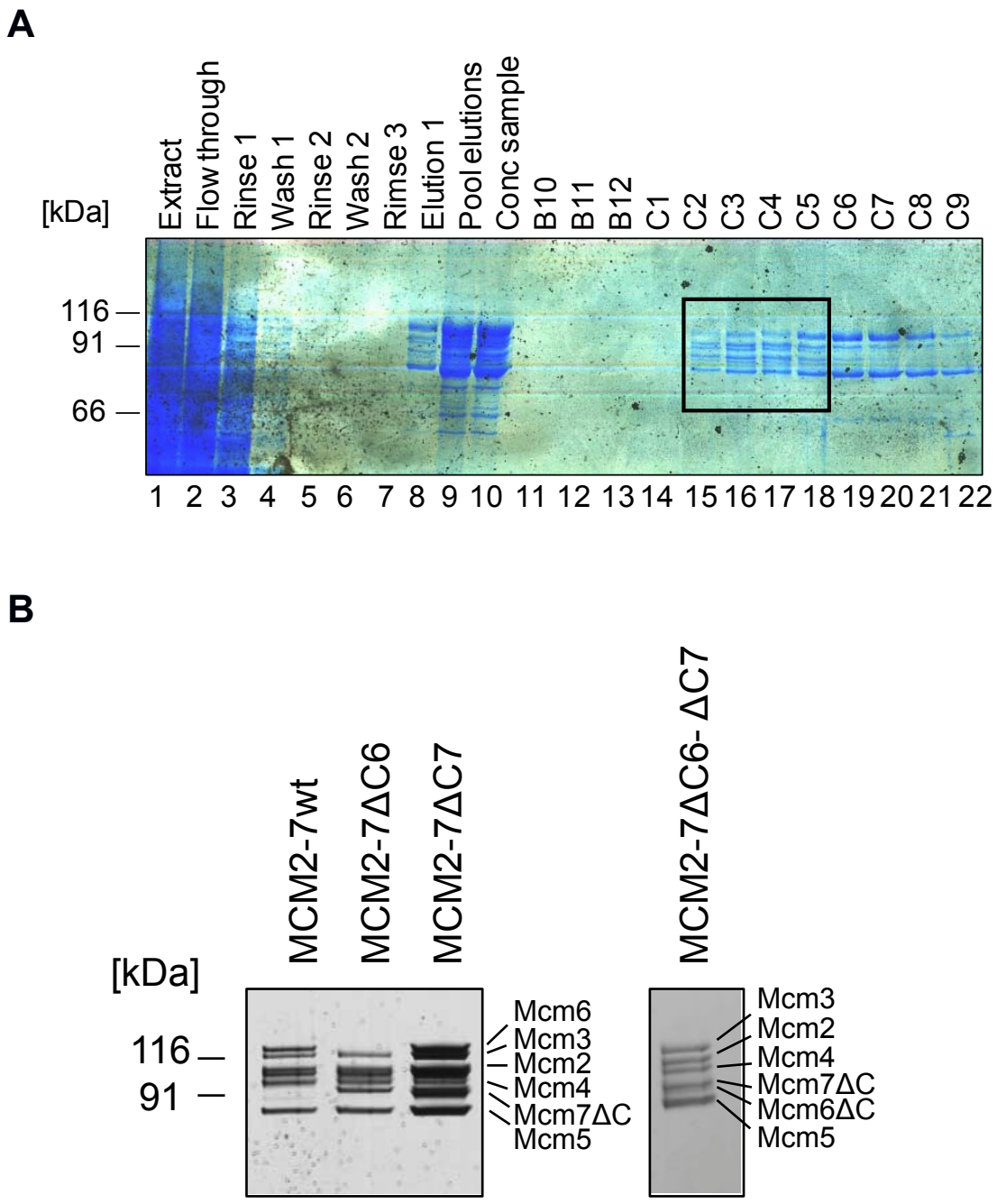


Figure 5.15. MCM2-7ΔC6ΔC7

A) Coomassie blue stained SDS-PAGE showing the purification of MCM2-7ΔC6ΔC7. The protocol of the two-step purification was performed as described in Evrin et al, 2009. The yeast extract was incubated with HA-bound agarose beads, washed and rinsed (lanes 3-7) before elution of the MCM2-7ΔC6ΔC7 bound to the beads. Size-exclusion chromatography was performed to separate the hexamer from the contaminant dimer Mcm3-Mcm5. The relevant fractions are highlighted by a black square (lanes 15-18), concentrated and aliquoted. **B)** Silver stained gel of the MCM2-7ΔC6ΔC7 purified protein compared to WT MCM2-7, MCM2-7ΔC6, MCM2-7ΔC7 to assess the stoichiometry. Bands on the gel are labelled with the relative Mcm subunit.

The purified protein was tested in a functional pre-RC assay (Figure 5.16) along with the WT, MCM2-7ΔC6 and MCM2-7ΔC7. The double deletion MCM mutant is recruited to ORC/Cdc6 in the presence of ATPγS and associated with the pre-RC proteins in ATP (Figure 5.16 A, lanes 17 and 18). Remarkably, Cdt1 is still being recruited, not released and behaved similar as MCM2-7ΔC7 (Figure 5.16 compare lane 18 with 15). Under high salt conditions, no double hexamer formation was detected. This is not surprising, since the mutant carries also an Mcm6C deletion, which does not support salt stable helicase loading (Figure 5.16 compare lane 19 with 13) (Fernandez-Cid et al., 2013). Interestingly, the MCM2-7ΔC6-ΔC7 was able to bind ORC/Cdc6 in the absence of Cdt1 (Figure 5.16 B), suggesting that these two domains are not required for the initial binding of MCM to the helicase loader.

In conclusion, these data showed that combining the deletion of the two Mcm C-termini (Mcm6C and Mcm7C) does not affect Cdt1 recruitment but its release during the OCCM to OCM transition. This suggests that Mcm7C might adopt an auto-inhibitory conformation, that alleviated the requirement of Cdt1 for ORC/Cdc6 interaction with MCM2-7. Direct binding of Cdt1 to Mcm6C has already been described to relieve the auto-inhibitory conformation of Mcm6C (Fernandez-Cid et al., 2013).

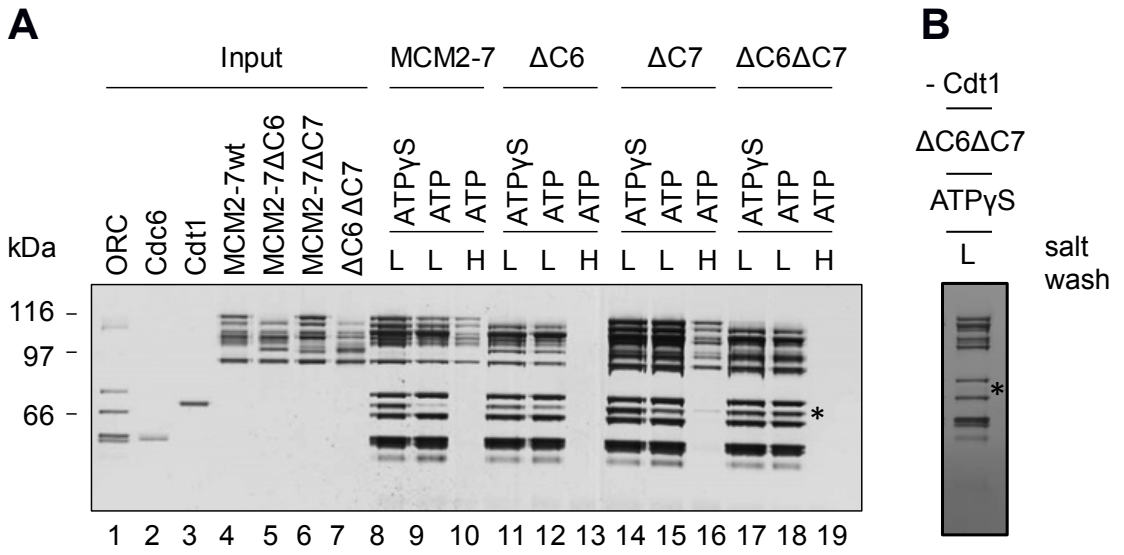


Figure 5.16. *In vitro* activity of the MCM2-7ΔC6ΔC7

A) Silver stained gel showing the *in vitro* reconstruction of pre-RC reactions in ATPγS or ATP followed by low (L) or high (H) salt washes, in the presence of WT MCM2-7, MCM2-7ΔC6, MCM2-7ΔC7 and MCM2-7ΔC6ΔC7. The experiment was performed twice. **B)** Silver stained gel showing reactions assembled in the presence of ORC, Cdc6, MCM2-7 or MCM2-7ΔC6ΔC7 in ATPγS in the absence of Cdt1. The asterisk indicates the band representing Cdt1.

5.8. Discussion

The C-terminal extensions of eukaryotic MCM2-7 contain defined WHDs that are conserved among species. In recent years the combined biochemistry and structural biology approach has led to outstanding biological insights into DNA replication. Cryo-EM structures of the OCCM (Sun et al., 2013; Yuan et al., 2017) and biochemical experiments (Fernandez-Cid et al., 2013; Frigola et al., 2013) have shown the important roles of the Mcm C-termini during pre-RC formation. In this chapter we have obtained new biochemical data that detail mechanism and function of Mcm2C, Mcm4C, Mcm7C.

Mcm2-7 mutants lacking individual C-termini were generated and tested for lethality in overexpression *in vivo,* and for pre-RC formation *in vitro*. Surprisingly, removing the short 20 amino-acid Mcm2C from the full length MCM2-7 exhibited lethality *in vivo* and failure in double hexamer production.

Mcm2 in yeast does not contain a WHD, but in higher eukaryotes a WHD is found. Interestingly, these eukaryotes also contain the protein geminin, an inhibitor of pre-RC formation (Wohlschlegel et al., 2000). The N-terminal domain of human Cdt1 interacts with geminin (Lee et al., 2004). Due to this vicinity, geminin is well placed to interact with the Mcm2C. One hypothesis is that the Mcm2 WHD might have coevolved as an additional geminin-anchoring surface and in this way could inhibit pre-RC formation by interfering with direct MCM2-7/Cdt1 interactions (Riera et al., 2017). In the context of the OCCM, CLMS data suggest the presence of interactions between Mcm2C and Orc6 (Yuan et al., 2017). Mcm2 C-terminal extension affects the OCM to double hexamer transition, and we propose that Mcm2C functions to stabilise the OCM or to facilitate the fusion of the two hexamers and the consequential ORC release. In the context of the active helicase (CMG), the polymerase ε was found to be localised in the C-terminal face of MCM2-7, contacting Mcm2C, placed in a suitable location to carry out the synthesis of the leading strand (Sun et al., 2015).

Mcm4C and Mcm7C do not seem to have an essential role in pre-RC formation, since the removal of these domains does not affect salt-stable double hexamer formation. Interestingly, Mcm4C is observed in the cryo-EM structures of MCM2-7/Cdt1 (PDB 5H7I, (Zhai et al., 2017a)) and CMG (PDB 3JC5, (Sun et al., 2015) and 5U8S, (Georgescu et al., 2017)) while Mcm7C is not visible in either of these structures. In the MCM2-7/Cdt1, in which DNA is not inserted in the ring, Mcm4C is located next to Mcm6C, whilst Mcm5C is occluding the central channel. Two CMG cryo-EM structures have shown that the C-terminal extensions of MCM2-7 adopt different conformations in the presence or absence of DNA. Interestingly, without DNA (PDB 3JC5), Mcm5C and Mcm6C partially occlude the central channel; but in the presence of ssDNA (PDB 5U8S) these domains are rearranged vacating the helicase channel. Mcm4C partially occludes the central channel, touching the DNA itself. Therefore it is possible that Mcm4 does not function in pre-RC formation; instead it might be involved in a complex mechanism of DNA sensing during DNA unwinding. In the OCCM, all Mcm C-termini (except Mcm5C) are connected with the WHD of Orc subunits,

as seen in cryo-EM and CLMS analysis (Yuan et al., 2017). In particular, Mcm4C interacts with Orc1 and is in proximity to Orc4.

Mcm7C was not resolved in either the MCM2-7 or CMG structures. Additionally, it has not been implicated in interactions during the CLMS analysis, but in the OCCM structure it is in close vicinity to Cdc6 and Orc1, which are the only two active ATPase proteins in ORC/Cdc6. We showed that deletion of Mcm7C did not affect the formation of a salt stable complex in the pre-RC assay, but blocked Cdt1 release. This was surprising, since Cdt1 release has been shown to occur during OCM formation, providing a platform for the recruitment of the second hexamer (Fernandez-Cid et al., 2013). Whilst ATP hydrolysis was described to drive Cdt1 release, and to be blocked by the lack of Mcm6C, because of missing interactions between the two proteins, a different mechanism appears to be involved in the case of the MCM2-7ΔC7. Indeed, a direct interactions between Mcm7C and Cdt1 was not described and appeared not to be possible due to the distance between the two proteins in the OCCM. It was shown that MCM2-7 carrying mutations in the ATP hydrolysis sites did not eject Cdt1 efficiently preventing the transition from initial MCM2-7 recruitment to double hexamer (Kang et al., 2014). Moreover, single molecule experiments demonstrated that Cdt1 release occurs prior to ring closure (Ticau et al., 2017). One hypothesis could be that ATP hydrolysis induced by Orc1/Cdc6 leads to a structural change in MCM2-7 via Mcm7. This structural rearrangement induces Cdt1 release. In the case of the mutant MCM2-7ΔC7, the network of interactions between Orc1, Cdc6 and Mcm7C is altered. As a consequence, Orc1 and Cdc6 induced ATP hydrolysis is not associated with a structural rearrangement in MCM2-7, preventing Cdt1 release but not double hexamer formation. Obtaining high resolution structures of the OCCMΔC7 formed in the presence of ATP could shed light and show the location of Cdt1. Similarly, high resolution of the ORC/Cdc6/MCM2-7ΔC7, which is formed in ATPγS (Figure 5.14) could reveal details about the protein-protein interactions involved between ORC/Cdc6 and MCM2-7. Indeed the preliminary cryo-EM structure identified a novel conformation, with an MCM2-7 spiral attached to ORC/Cdc6, but DNA not being inserted into the MCM2-7 complex. Currently, the resolution of the complex is limited to explain more details.

In contrast to the OCCM, the Mcm C-termini appear mostly flexible in the MCM2-7 double hexamer, since they are not visible in these cryo-EM structures (Abid Ali et al., 2017; Li et al., 2015; Noguchi et al., 2017).

These results are consistent with the idea that the C-termini of MCM2-7 play an important role during pre-RC formation. In this study, we showed that Mcm2C is required for double hexamer formation, possibly establishing essential interactions with Orc6 at the stage of the OCCM, as suggested by the CLMS analysis (Yuan et al., 2017). On the other hand, the removal of Mcm4C and Mcm7C does not affect double hexamer formation. We propose that Mcm7C might be directly affected by Orc1/Cdc6 ATP hydrolysis and thus inducing Cdt1 release. The deletion of Mcm7C in MCM2-7 showed that an efficient Cdt1 release is not essential for double hexamer formation. This result is very interesting, since it was thought that ATP hydrolysis dependent Cdt1 release would occur during the OCM to double hexamer transition.

More investigation will be required for understanding the function of Mcm7C during pre-RC formation and its implication in Cdt1 release and ATP hydrolysis after OCCM formation.

Chapter 6

Progresses towards the high resolution structure of OCM

6.1. Electron microscopy

Modern cryo-electron microscopy (cryo-EM) started in the 1980s with the work from Dubochet and colleagues (Dubochet et al., 1988), but it is only in the last decade that this technique has seen major developments with the achievements of near-atomic resolution (<4 Å). Together with X-ray crystallography and NMR spectroscopy, cryo-EM is used to solve the structure of biomolecules. Unlike the first two techniques, cryo-EM has several advantages: (1) the sample does not need to be crystallised, (2) a small amount of sample is required, (3) large range of molecules are accepted (from intact eukaryotic cells to individual proteins). However, it is a young technique compared to crystallography with unique challenges and opportunities. Here, a brief introduction on the workflow of cryo-EM, from sample preparation to 3D model building will be provided (Figure 6.1).

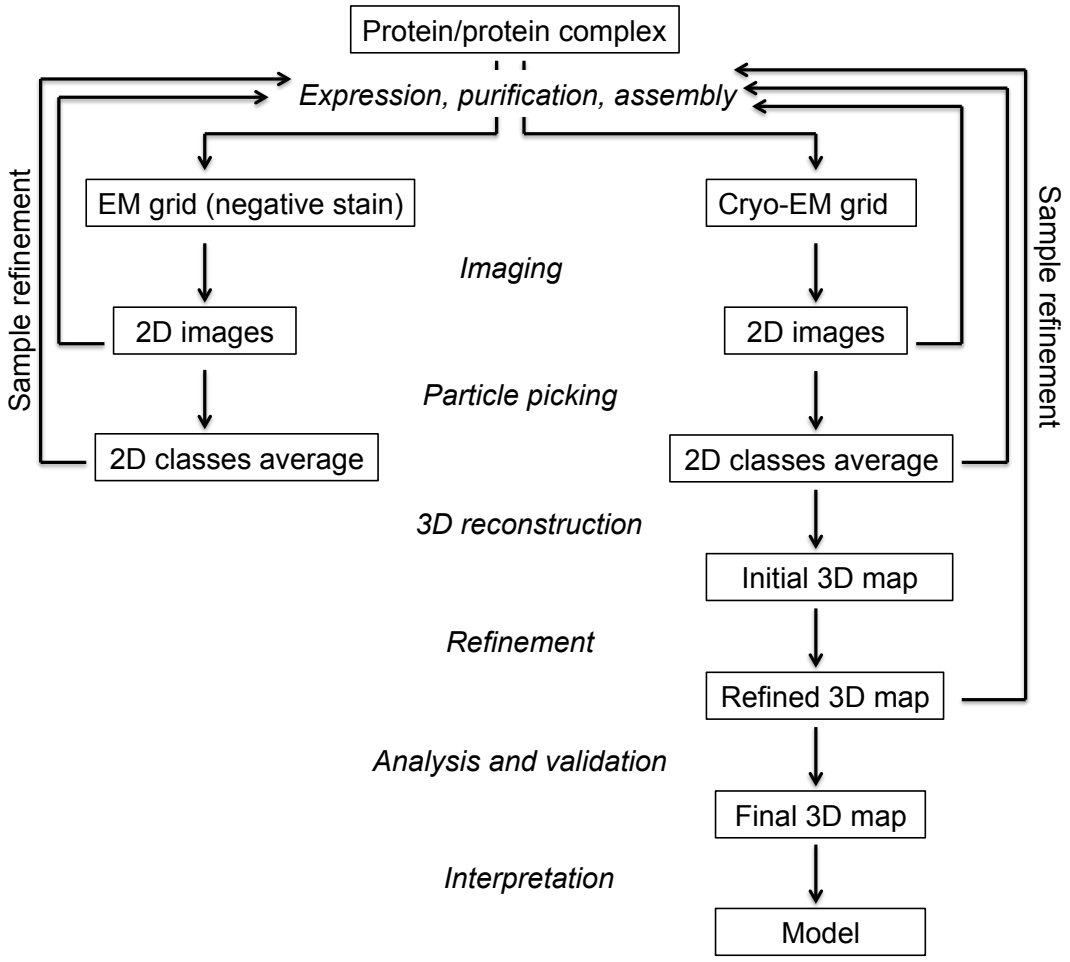


Figure 6.1. A schematic workflow of the structure determination using single-particle EM.

The purified protein or the assembled protein complex is applied onto a EM grid to be analysed and assessed though negative stain (left side of the flow). Only once images or 2D classification of the images are satisfactory (eg. Homogeneity and distribution of the particles), the sample is ready for cryo-EM analysis (right side of the workflow). 2D images and 2D classification of the initial dataset collected with am electron microscope are used to generate an initial 3D map. Subsequent rounds of particles alignment and classification are needed to refine the 3D map. Further improvements of the structures leads to the final map, which should be validated based on the resolution reached before deposited in the EM data bank (EMDB).

Single particle EM depends on averaging thousands of images of identical particles. Therefore, the ideal sample should be as homogenous as possible. Heterogeneity can result from conformational or compositional changes and should be minimised biochemically. Therefore, an optimisation

phase is essential for the final outcome. First of all, obtaining highly purified proteins is the first step towards this purpose. Second, buffer conditions have shown to help the stabilisation of the sample. Third, chemical cross-linking with glutaraldehyde is a useful tool for reducing sample heterogeneity when the sample becomes exposed to the cryo-grid or the air water interface. However, artefacts can be introduced by cross-linking such as trapping the complex in one particular state or in a non-functional conformation (Shukla et al., 2014). Finally, another way to reduce heterogeneity is to introduce a molecule (substrate, inhibitor) that could stabilise a certain conformation, an approach largely used in crystallography (Vedadi et al., 2006). Although the optimisation of the sample before imagining remains vital, two recent innovations made the technology much attractive - advanced direct electron detectors improved the images and novel image processing methods simplified the analysis, which both together started the cryo-EM resolution revolution (Kuhlbrandt, 2014). Importantly, these improvements can help with the processing of less homogenous samples (Thompson et al., 2016).

Negative staining is used as a tool to assess the quality of the sample, since it generates high contrast images of proteins. EM grids are usually made of copper, gold, nickel or rhodium. Continuous carbon films are used as a support in negative staining grids, depending on the affinity of the proteins for the carbon. The presence of a thin layer of carbon can improve the particle distribution, but needs to be pre-treated. Through glow-discharging, this surface is rendered hydrophilic, which allows the proteinaceous liquid to spread across the grid surface (Cheung et al., 2013; Grassucci et al., 2007). Few microliter of the sample is loaded on the grid, stained with 2% uranyl acetate and blotted to ensure a thin layer of stain. This process dehydrates the sample and fully envelops the molecule (Figure 6.2). Uranyl absorbs efficiently the electron beam efficiently, resulting in a black background. Proteins occlude the stain, the electron bean can pass through in this area, which allows their visualization (Thompson et al., 2016). Indeed the high contrast achieved by the stain and the speed of grid preparation technique allows a quick assessment of sample purity, concentration, heterogeneity, and conformational preference (Thompson et al., 2016). On the other hand, negative staining only produces limited resolution structures (>20 Å). Furthermore, staining artefacts and preferential

orientations of particles on the carbon support represent limiting factor in the use of negative staining. In addition, the stained sample is in a non-native environment and more prone to dehydration.

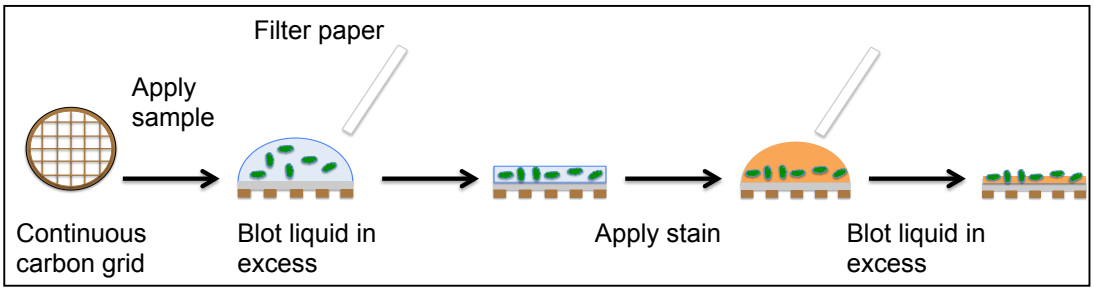


Figure 6.2. Negative stain grid preparation

Up to five microliters of sample are applied to a grid layered with a thin, continuous carbon film. After blotting away the excess liquid, the sample is stained with heavy metal (such as 2% uranyl acetate) and air-dried.

To overcome the limitations of negative staining, the hydrated sample can be preserved in the aqueous environment by cryo-immobilisation (Dubochet et al., 1988; McDowall et al., 1983) (Figure 6.3). The cryo-EM technique does not require staining of the sample and preserve it in its native environment. These characteristics allow achievement of high resolution structures. However, cryo-EM carries few disadvantages when compared to negative staining: (1) higher protein concentrations are required, (2) the contrast of the images is lower, (3) increased chances of radiation damage, and (4) possible denaturation at the air-water interface.

Few microliters of a concentrated sample (0.1-2 mg/ml depending on the molecular weight or on the use of carbon film) are embedded in ice. This is performed using automated blotting robot (e.g. FEI Vitrobot), which removes the excess of the liquid from the grid, while controlling the environmental parameters such as temperature and humidity before rapidly plunge-freezing in liquid ethane (Murata and Wolf, 2018). The grid with the frozen sample is then stored in liquid nitrogen. The ice layer should be as thin as possible in order to achieve high contrast between the molecules and the surrounding ice layer. A good vitrified sample generates cryo-EM images, where particles should be seen in high density and in different orientations (Cheng et al., 2015).

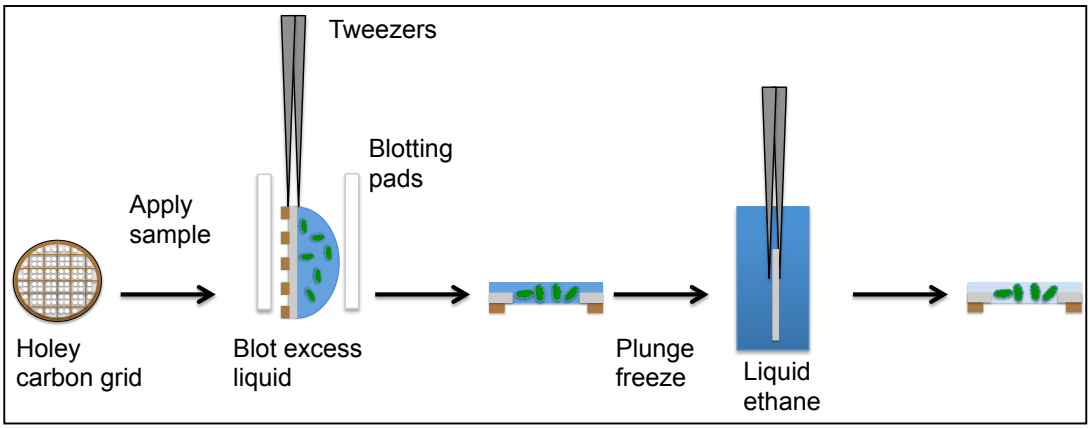


Figure 6.3. Cryo-EM grid preparation

Up to five microliters of sample are applied to a perforated carbon grid. The excess liquid is blotted and the sample is frozen by plunging into liquid ethane. The grid is stored in liquid nitrogen.

Cryo-EM images are recorded by exposing the sample to a low dose of electrons in order to minimise radiation damage of the proteins. Acquisition of high-quality images is essential to obtain high-resolution structures. This is achieved by using modern microscopes that have a very coherent electron beam, a very stable stage to minimize drift and detectors that produce images without losing the high-resolution information. A typical dataset consists of thousands of images each containing 100-1000 particles in different orientations. Once good micrographs have been selected, a few thousands of particles are picked in a manual manner, prior to fully automated particle picking. Particles are then sorted and averaged based on their similarity, a process called two-dimensional image classification. This step is essential for the identification of contaminants, the assessment of the data quality and the particle distribution (Cheng et al., 2015). Classified particles are used for an initial estimate of a 3D map, that is performed using a reference model or a map of an homolog (Beckmann et al., 1997). The principle of 3D reconstruction based on 2D projections is the Fourier central section theorem. It states that the 3D volume of any object can be reconstructed from its 2D projections. After the initial 3D map, the structure is refined to obtain a final map, which needs to be validated and interpreted (Cheng et al., 2015). The development of Relion, which employs Bayesian statistics, has reduced the need for user input and

resulted in general in much more robust 3D maps and higher resolution structures (Scheres, 2012).

6.2. Introduction

MCM2-7 double hexamer formation is a multi-step reaction in which two MCM2-7 helicases are recruited to replication origins and loaded in a head-to-head fashion on DNA (Evrin et al., 2009; Fernandez-Cid et al., 2013; Frigola et al., 2013; Remus et al., 2009). This reaction was reconstituted in 2009 and in the following years, the Speck lab and others have obtained much mechanistic insight. Furthermore, an increasing number of high resolution structures of key helicase loading intermediate complexes have been obtained. A current model of this reaction pathway is shown in Figure 6.4. The complexes that have been characterised by cryo-EM are represented in surface view (adapted from (Riera et al., 2017)). ORC/Cdc6 bound to DNA origins recruits MCM2-7/Cdt1 resulting in the formation of the OCCM complex (Figure 6.4 C). Upon ATP hydrolysis, Cdc6 and Cdt1 release and rebinding of Cdc6, an OCM is formed, which is competent to recruit a second hexamer. The final product of the reaction is the MCM2-7 DH (Figure 6.4 E). To date the only intermediate that lacks structural information is the OCM. Unlike the OCCM, the OCM is competent to recruit a second hexamer, and represents a transient and salt-sensitive intermediate (Fernandez-Cid et al., 2013). Two-dimensional class averages of negative stain and cryo-EM samples have been reported, comparing the OCM and the OCCM (Sun et al., 2014). However, due to the limitation of the sample reported in the paper, it has not been feasible in this instance to obtain a homogenous preparation for 3D reconstruction.

In this chapter, the experimental work performed in order to overcome the heterogeneity issues with this sample is reported, using a combination of biochemistry and EM approaches. Obtaining a high resolution structure of the OCM will be essential for understanding the consequences of ATP-hydrolysis and the structural features responsible for the recruitment of the second hexamer. It is possible that in the OCM conformation the C-termini of MCM2-7 engage more closely with ORC/Cdc6 than observed with the OCCM, revealing

potentially new protein-protein interactions important for double hexamer formation.

Due to the fact that this project is still at its early stage, the EM analysis presented here is mostly focussed on negative staining.

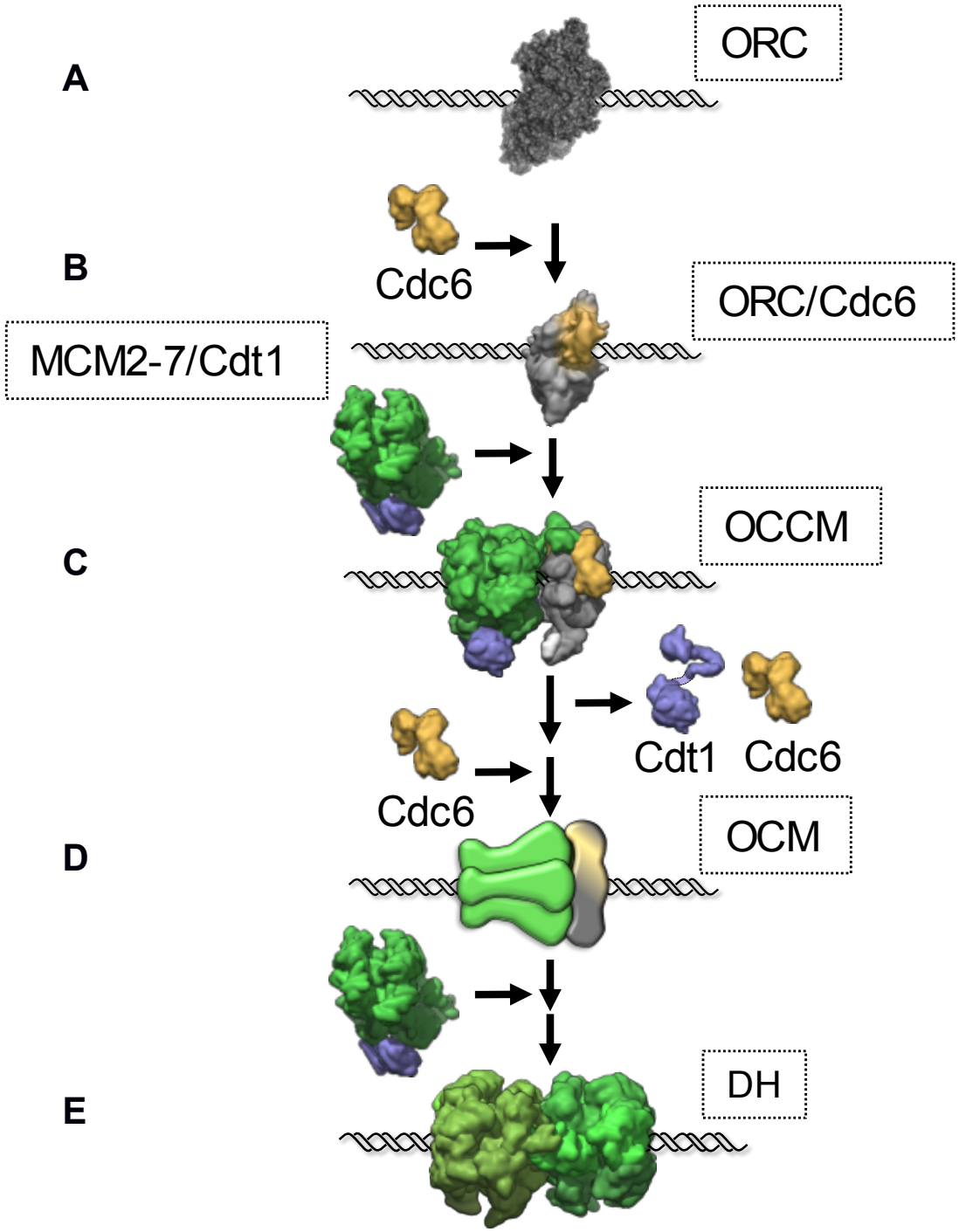


Figure 6.4. Eukaryotic initiation of DNA replication

The intermediate complexes that have been characterised by electron microscopy are shown in surface view. **A)** ORC bind on origins of replication (EMDB:6941). **B)** Cdc6 is recruited to form a complex with ORC (EMDB: 5381) which recruits MCM2-7/Cdt1 (EMDB: 6671). **C)** The resulting complex is called OCCM (EMDB: 8540) which encircles dsDNA. **D)** Upon ATP hydrolysis, Cdt1 and Cdc6 are released from the OCCM and after binding of a second Cdc6, the OCM is formed. This complex represents the platform for the recruitment of the second hexamer, but it has not been structurally characterised. **E)** The double hexamer (DH) (EMDB: 9400) formed around dsDNA represents the inactive helicase, which becomes activated in S phase. (Adapted from (Riera et al., 2017))

6.3. The OCM is a short-living intermediate

Previous attempts to isolate the OCM were described in (Sun et al., 2014). It was suggested that the OCM is a short lived intermediate that is rapidly formed on DNA containing origins of replication. However, at the time it was not possible to obtain a homogenous population of OCM particles. The reason for this is that the OCCM – OCM – DH transition includes many intermediates, particular during the OCCM to OCM transition (Ticau et al., 2017), and it is difficult to enrich for a single one of these. Moreover, all of these intermediates are less stable than the OCCM or double hexamer.

Multiple strategies were developed as part of this thesis. One of these considered pre-RC incubation time as a method to enrich for an OCM variant.

ORC, Cdc6, Cdt1 and MCM2-7 were incubated with DNA bound to beads for 7.5, 15 and 30 minutes, washed with low salt buffer and eluted from the beads with DNaseI. The sample was cross-linked with 0.1% glutaraldehyde and then the quality of the preparation was assessed by negative staining. Images were collected at the LMS EM facility and two-dimensional classification was performed in order to sort the different particles (Figure 6.5) (imaging and data analysis was performed by Dr. Ricardo Aramayo). The results showed that all analysed time-points were dominated by double hexamer particles with a reduced number of smaller ring-shaped particles that are ORC/Cdc6 and MCM2-7. A sample prepared at a shorter time-point remains to be analysed, and could potentially show a greater percentage of assembled OCM particles.

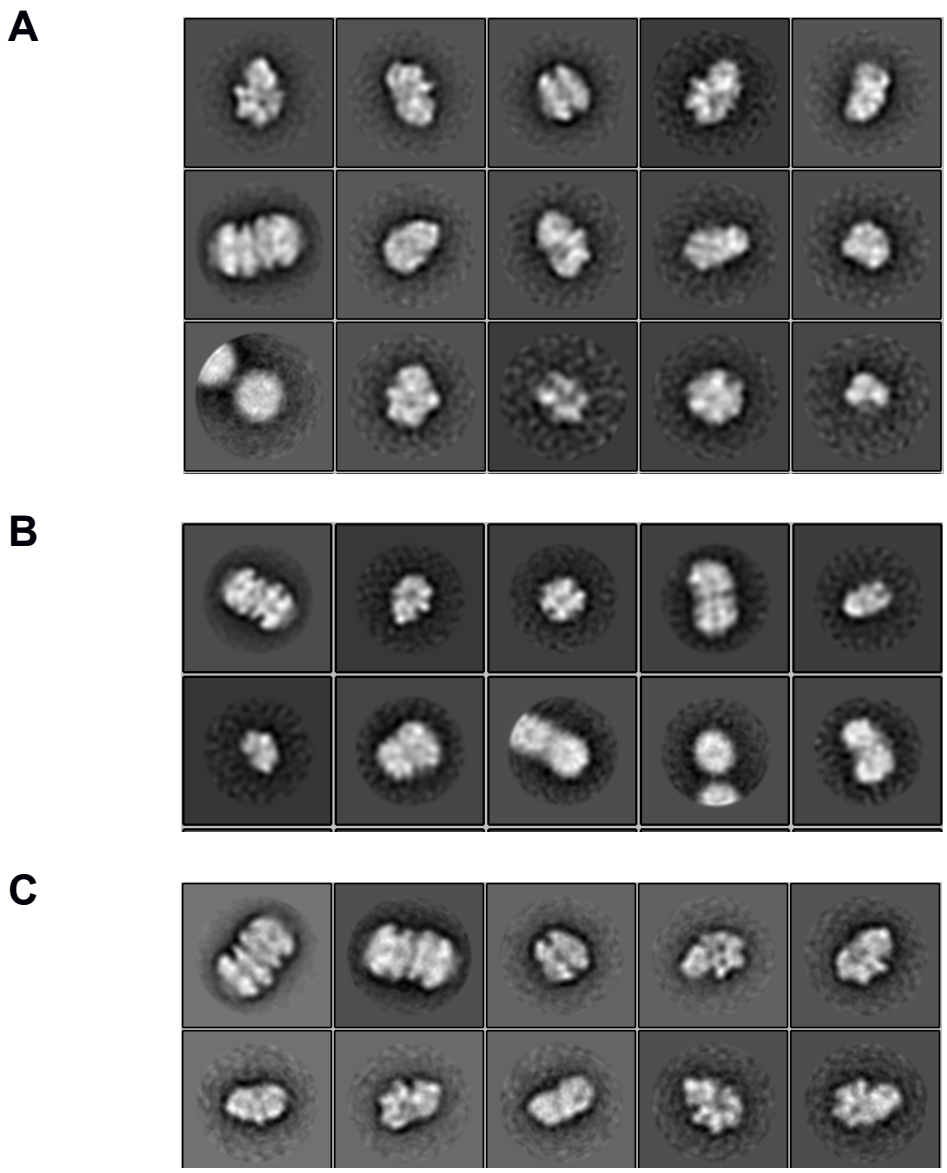


Figure 6.5. The OCM is a short-living intermediate.

Negative-stain EM analysis and 2D classes. ORC, Cdc6, Cdt1 and MCM2-7 were incubated with DNA containing the origin ARS1 for A) 7.5, B) 15 or C) 30 minutes. The complex was eluted from the beads with DNaseI and cross-linked with 0.1% glutaraldeide for 15 minutes at 4°C. In all of the three conditions, particles containing the double hexamer are the most abundant.

We considered whether the salt-sensitive OCM might become unstable during the washes or elution steps. It was previously observed (Yuan et al., 2017) that the DNaseI employed to elute the complex from the beads over-digests the DNA. It is possible that the DNA inserted inside the MCM2-7 ring

acts to keep the helicase stable. The over-digestion of DNA inside the MCM ring causes a conformational change in the MCM2-7 ring itself. In light with our finding described in the previous chapters, the opening of the ring could reposition the C-terminal domain of Mcm5 with consequent activation of the Cdc6 quality control pathway which leads to the complex disassembly. It is equally possible that the OCM complex assembled on DNA starts moving on DNA and slides off it (Tsakraklides and Bell, 2010).

One possible approach in order to stabilise the complex and prevent its disassembly could be to crosslink the OCM prior to elution, when the complex is still bound to DNA and attached to magnetic beads. This method has been successfully employed by a colleague (Yasunori Noguchi) for stabilising DNA replication intermediates in a different project. Therefore, we assembled the OCM on DNA for 15 minutes and cross-linked it using different glutaraldehyde concentration for 15 minutes at 4°C, followed by elution with DNaseI at 4°C. The samples were analysed by negative stain showing a large number of particles with the distinct four-tiered side view typical of the double hexamer (Figure 6.6 A). Indeed, a 2D classification confirmed the observation made by eye, that the most populated classes are formed by double hexamers (Figure 6.6 B, top panels). The first four classes (first row from left to right) represent more than 50% of the total particles identified. This result suggests that the OCM particles are not released from the beads once they are cross-linked suggesting that they become crosslinked to the beads. This appears possible, as only double hexamers were successfully released from the beads.

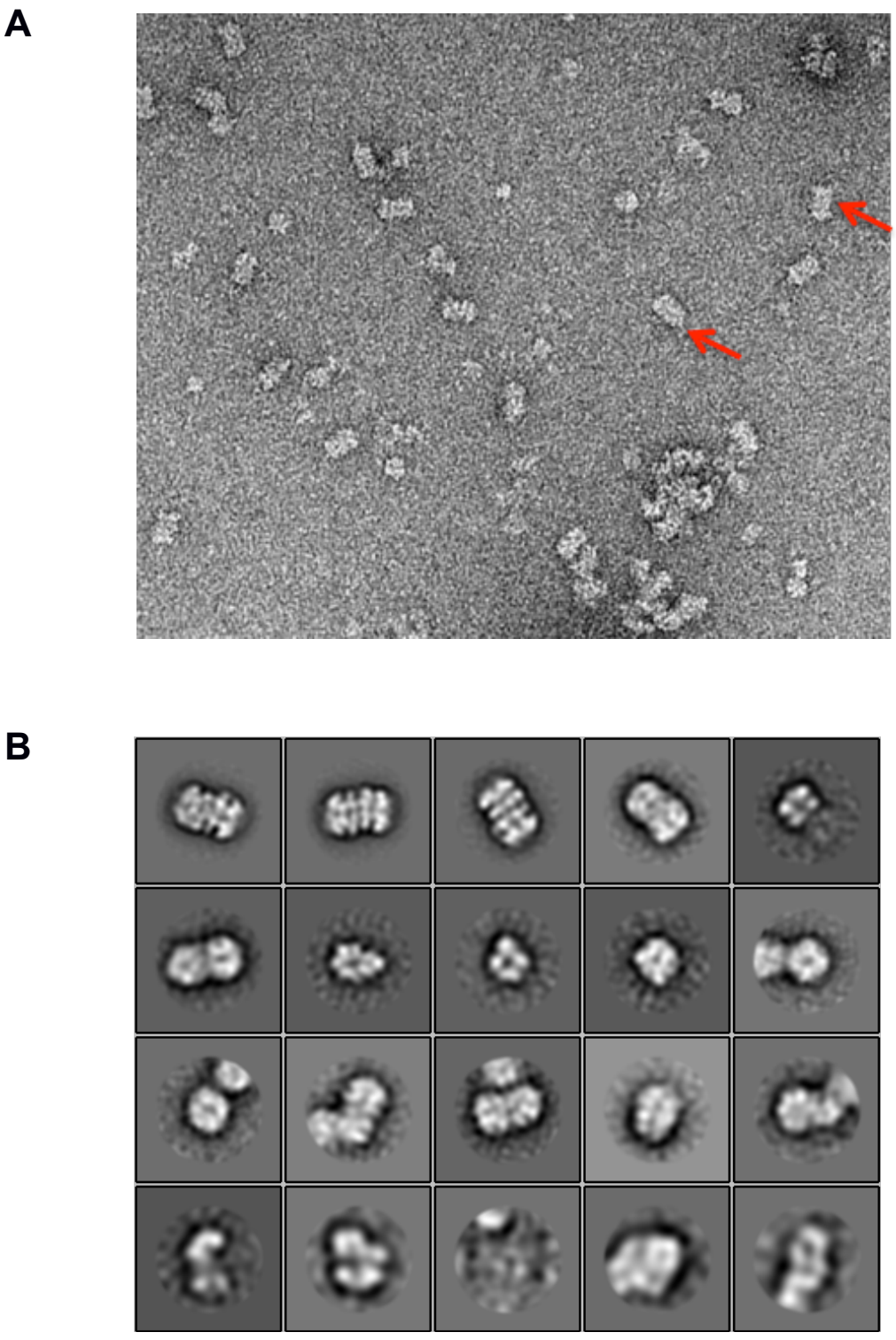


Figure 6.6: Cross-linked reaction before the elution from the beads

Pre-RC reactions were assembled with DNA containing ARS1 sequence and cross-linked on the beads with 0.1% glutaraldehyde for 15 minutes at 4°C. The cross-linked product were eluted with DNaseI and analysed by negative staining. **A)** A raw electron micrograph of the negative stained sample. Red arrows point at the big particles that have the size of double hexamer (around 20 nm). **B**) 2D class averages showing that the particles are double hexamers.

6.4. The OCM can be assembled at low temperatures

Reactions containing ORC, Cdc6, MCM2-7 and Cdt1 result in assembly of an OCCM on DNA, which can be trapped in this state by blocking or reducing ATP hydrolysis. When ATP hydrolysis is permitted, Cdt1 is released and an OCM complex is formed. From our previous experiments, it appeared that in the presence of ATP the OCM complex very quickly recruits the second hexamer (15 minutes), consistent with the transient nature of this intermediate complex.
We reasoned that another way to reduce the rate of ATP-hydrolysis-dependent reactions could be to assemble the complex at low temperatures. In this way a homogenous population of OCCM can be formed, which upon rapid warming would immediately release Cdt1 and form an OCM complex in a synchronous way. In order to minimise any further ATP hydrolysis once the OCM is formed, ATP can be replaced by its slowly hydrolysable analogue ATPγS, which would trap the complex in the intermediate configuration.

Initially it was investigated whether indeed an OCCM is formed at lower temperatures. To do so, the four proteins (ORC, Cdc6, MCM2-7, Cdt1) were incubated with bead-bound origin DNA for 20 minutes. A range of different temperatures were tested, from 4°C to 12°C. A silver stained SDS-PAGE gel of the fractions obtained during the experiment is shown in Figure 6.7. As a control, the standard reaction was assembled at 24°C (Figure 6.7 A, lane 5). While the amount of Cdt1 bound did not change at different temperatures, the ratio of MCM2-7 to Cdt1 did appear to be affected by the low temperatures. Indeed, at the lowest temperatures, a reduced amount of MCM2-7 is associated to ORC/Cdc6 (Figure 6.7 lanes 6 and 7). When the reaction was assembled at 8°C, 10°C or 12°C, the level of MCM2-7 appeared to be similar to the control reaction performed at 24°C (Figure 6.7 compare lanes 8, 9 and 10 with 5). We choose the 10°C reaction for the following experiments, since at this temperature the complex formation does not appear to be compromised compared to the control reaction.

Now, we wanted to test whether replacing ATP with ATPγS during the wash step would stabilise the OCM complex. The reactions were assembled at 10°C in the presence of ATP. After the initial assembly, washes in the presence

of ATPγS were performed and the complex was eluted. A standard reaction performed at 24°C in the presence of ATP was performed as a control (Figure 6.7 B). The silver stained gel showed that under these conditions (low temperature and ATPγS exchange), the resulting OCM complex appeared to be similar to the control reaction assembled at 24°C in ATP (Figure 6.7, compare lane 5 to 6).

From this experiment it was concluded that temperatures lower than 10°C compromise complex formation, but at 10°C complex assembly was improved. Most importantly, the exchange of ATP to ATPγS during the wash step seems to be effective in facilitating the generation of OCM complexes that may be amenable to downstream structural analysis.

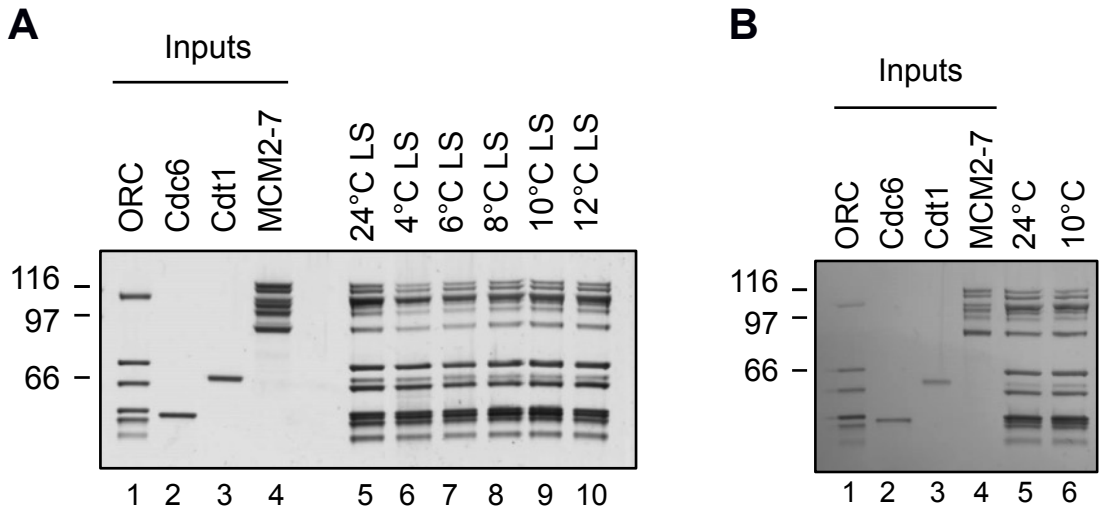


Figure 6.7. OCM is formed at low temperatures

A) ORC, Cdc6, Cdt1, MCM2-7 were assembled on DNA at different temperatures (from 4°C to 12°C), washed with low salt buffer and eluted with DNaseI. Silver stained gel showed the result of the elution (lanes 5-10). **B)** Silver stained gel showing the comparison between the control pre-RC reaction assembled on DNA at 24°C in ATP and a pre-RC reaction assembled at 10°C, followed by washes with buffer containing ATPγS. The experiment was performed twice.

Based on these promising results, the reaction products were cross-linked with 0.1% glutaraldehyde as described above, and analysed by negative

staining in order to evaluate the homogeneity of the sample (Figure 6.8). The sample appears to be more homogenous with particles that resemble the size of a complex containing ORC, Cdc6 and MCM2-7 (circled in black). However, several small size particles with a shape of ORC-Cdc6 are present (blue circles).

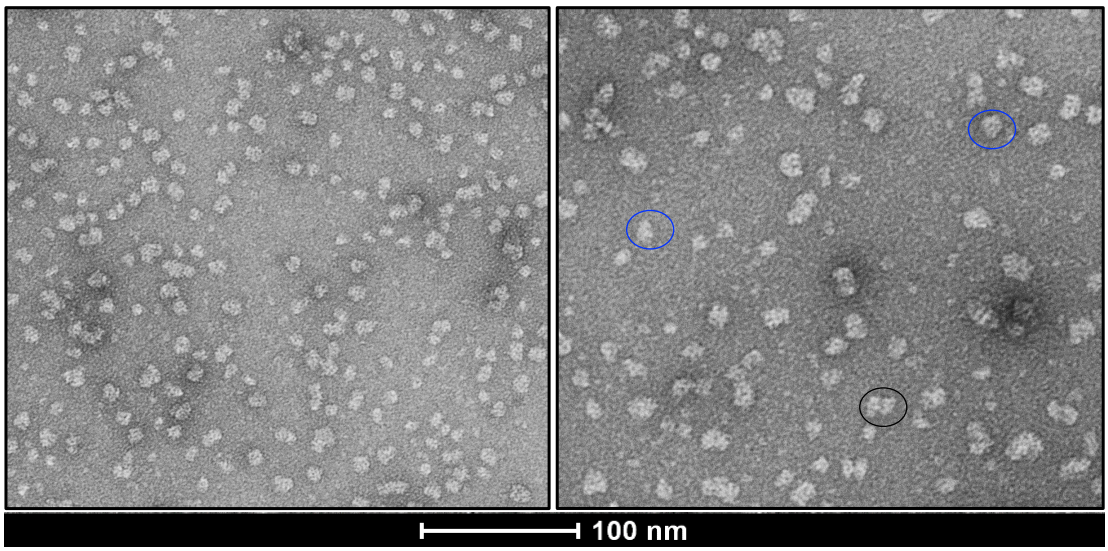


Figure 6.8 Temperature might help in increasing the homogeneity of the sample

Raw electron micrograph of negative stained sample. ORC, Cdc6, Cdt1 and MCM2-7 were assembled on DNA containing origin of replication (ARS1) at 10°C and washed with buffer containing ATPγS. The protein complex was eluted from the beads-bound DNA with DNaseI, cross-linked with 0.1% glutaraldeide and stained for EM analysis. Circled in blue the small particles containing ORC-Cdc6 complex. In black is highlighted an example of a bigger size particle containing ORC, Cdc6, MCM2-7.

Another issue that has compromised cryo-EM analysis of the OCCM in the past, was the absence of DNA within the distal N-terminal section of MCM2-7. This could be due to excessive DNaseI digestion, as seen by Yuan and colleagues (Yuan et al., 2017). The DNA over-digestion caused by the nuclease could be the reason why in the OCCM structure reported by Yuan et al, the MCM2-7 at the N-tier ring is partially open, which in turn might also affect the stability of the OCM complex.

In order to obtain a complex with a longer DNA fragment, it was considered using lower amounts of DNaseI. Since the OCM complexes result in more heterogenous complexes, it was decided to optimise this reaction in the context of the OCCM, as this complex is formed efficiently, more uniform and reproducibly. Consequently the complexes were assembled in ATPγS and samples were eluted from the beads using various concentrations of DNAseI (Figure 6.9, A to D from more concentrated to less concentrated). Because we are familiar with the size and shape of the OCCM, we could easily identify these particles, some of which are representatively highlighted by a red circle in Figure 6.8. Smaller particles that represent ORC/Cdc6 are marked by a blue square. As expected, reducing the amount of DNaseI resulted in reduced DNA digestion, which produced visible and longer DNA strands (indicated by the red arrows in Figure 6.9, panels C and D).

Indeed the availability of a structure in which DNA is visible at both ends of the OCCM would be helpful in understanding if the partial opening of ring in this intermediate is due to the nuclease digestion or if the closure of the ring is not completed at the stage of the OCCM.

In an alternative strategy to generate longer DNA fragments, the DNA could be cleaved using a restriction enzyme. Indeed, in the DNA construct employed specific AluI restriction sites are present in the origin flanking regions. For each sample presented in this chapter, an equivalent sample was also generated which was cleaved using AluI rather than DNaseI. This was performed in order to overcome potential over-digestion produced by DNaseI. Indeed, AluI generated longer DNA fragments that are visible in the EM micrograph; however, when compared to the results obtained with DNaseI, the resulting samples did not exhibit an appreciable improvement in sample homogeneity. Therefore, for simplicity, only the DNaseI digested samples are presented in this thesis.

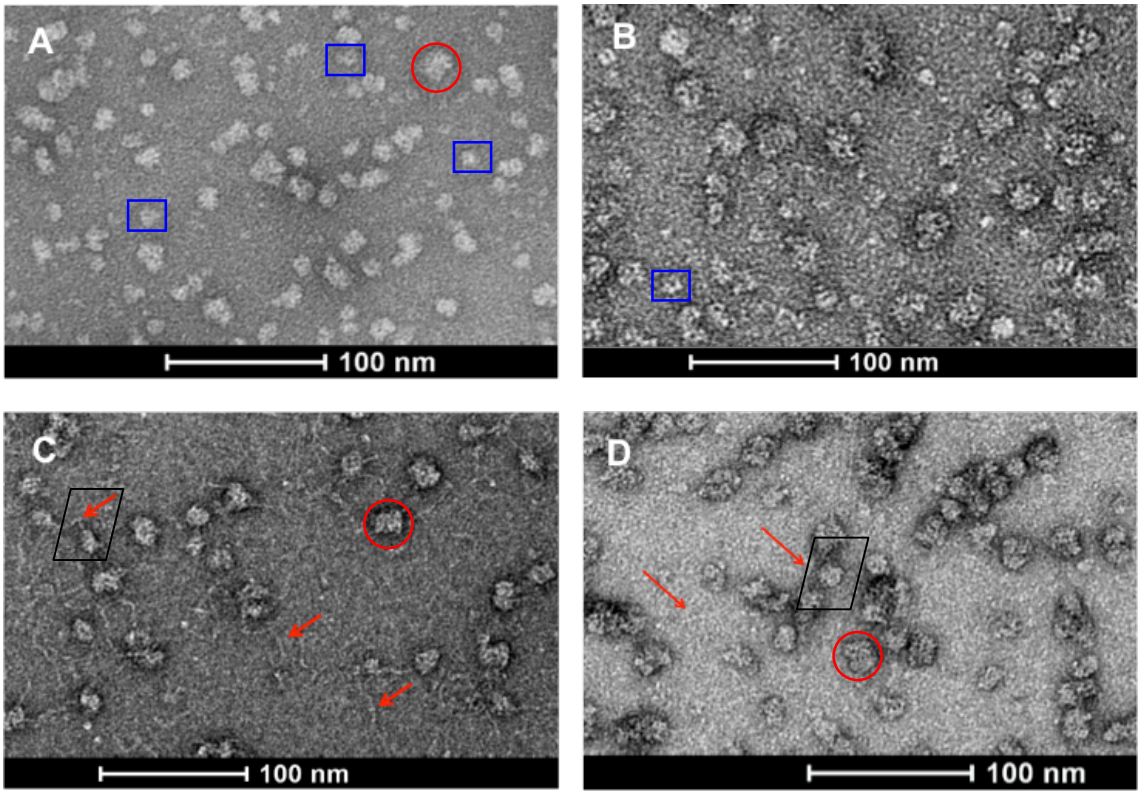


Figure 6.9. DNaseI dilutions affect the length of the exposed DNA

Raw electron micrograph of negative stained sample. ORC, Cdc6, Cdt1 and MCM2-7 were assembled on DNA containing origin of replication (ARS1), washed with buffer containing ATPγS. The protein complex were eluted from the beads-bound DNA with DNaseI, cross-linked with 0.1% glutaraldeide and stained for EM analysis. Different concentrations of DNaseI were used in order to maximise the length of DNA cleaved. Red arrows point to the DNA. Red circles indicate the OCCM complex, blue squares the ORC/Cdc6 complex, red arrows indicate the long undigested DNA, black rectangles show OCCM complexes on DNA. DNaseI dilutions: **A)** 1:10, **B)** 1.30, **C)** 1:100, **D)** 1:500.

6.5. An OCM can be assembled on short DNA

One major problem is the heterogeneity of the sample, due to the transient nature of the OCM. We observed that the double hexamer is formed in a rapid way and that even after 7.5 minutes of incubation with DNA, most of the particles are double hexamers. We reasoned that a modified DNA fragment containing only partial replication origins could prevent double hexamer formation and in this way generate a more homogeneous population of OCM. To facilitate this, a new DNA construct was engineered. The origin (ARS1)

contains three elements, A, B1, B2 which have been described in detail in the introduction (paragraph 1.9). The elements A and B1, but not B2, have been shown to be essential for ORC binding. B2 and further distal sequences are sought to promote recruitment of the second MCM2-7 hexamer. The newly designed DNA contains all the essential elements for the recruitment of the first MCM2-7 hexamer, required for the OCM formation, but should suppress double hexamer assembly. The total length of the combined DNA fragment containing A and B1 is 33bp (TTTTTTTATGTTTAGTTTCGCGGACGACGGTTT). This sequence is flanked by multiple AluI sites and a random GC rich spacer sequence to produce a DNA fragment of 145 bp in length (Figure 6.10). In order to maximise the number of complexes bound to DNA and increase the total protein concentration, this sequence is repeated 10 times generating a high number of replication origins available for OCM formation. All of the origins are orientated in the same direction, which further suppresses head-to-head double-hexamer formation (Zou and Stillman, 2000). From now I will refer to this DNA with the nomenclature “10X AB1”.

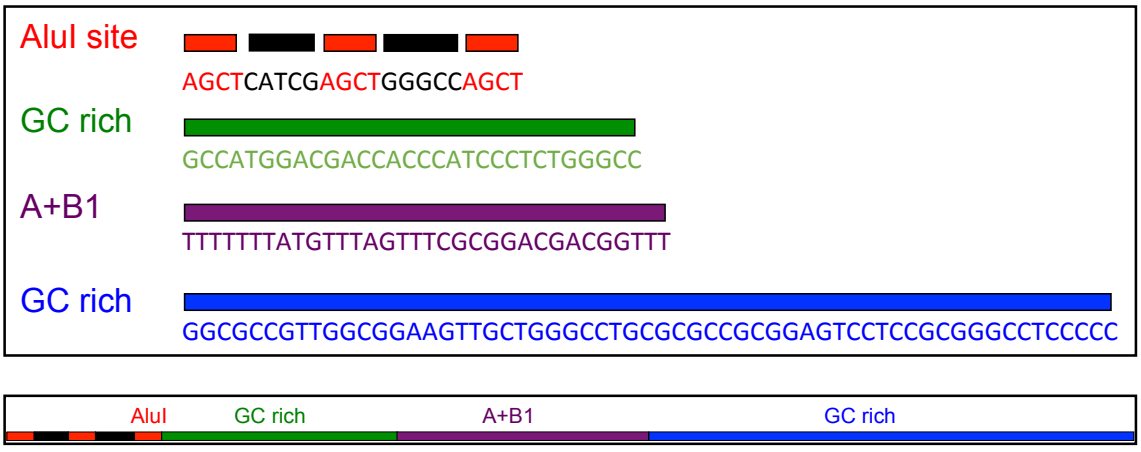


Figure 6.10. Design of a new DNA containing replication origin

DNA sequence containing the elements A and B1 of the ARS1 origin. In purple is the ORC consensus sequence containing A and B1 (33 bp); preceded by 30 bp of a GC-rich random sequence (green) and followed by 60 bp GC-rich random sequence (blue). The DNA region is flanked by three AluI restriction sites (red). The resulting DNA sequence is 145 bp long and is repeated 10 times.

The 10X AB1 DNA was bound to magnetic beads following the protocol described in the Materials and Methods (2.7.2). It was initially tested for its ability to support general complex formation and to suppress double hexamer formation. pre-RC reactions were assembled in ATPγS or ATP followed by low or high salt washes (standard protocol described in materials and methods 2.7.3). The 10X ARS1 full length was used as a comparison for testing the efficiency of complex assembly, since it fully supports the OCM and double hexamer formation. On the left hand side of Figure 6.11, the DNA-bound reactions were eluted from the beads using DNaseI whereas on the right hand side AluI was used. As expected, the 10X AB1 only supports low salt complex formation and is efficiently released by DNaseI (Figure 6.11 lane 8), whereas formation of high salt stable double hexamers was much reduced (Figure 6.11 lane 9). Surprisingly, the release of OCCM and OCM was less efficient with AluI (Figure 6.11 lanes 13 and 14). One hypothesis is that a protein complex could occupy the AluI restriction sites, reducing its accessibility by the enzyme. Based on these promising results complexes for electron microscopy analysis were performed. The newly generated DNA was employed here and complex formation was carried out for 20 minutes at 24°C in a buffer containing ATP. The washes were performed in the presence of ATPγS as previously described. The protein complexes were eluted with 1 U of DNaseI from the magnetic beads, cross-linked with 0.1% glutaraldehyde and applied to a cryo-grid. A representative picture acquired at the CM200 cryo-EM microscope by Dr. Ricardo Aramayo is shown in Figure 6.12 A, showing good ice quality, which is essential for achieving good contrast. The correct particle picking is an important step in order to isolate the real proteins from contaminants (Figure 6.12 B). All of the particles are then sorted according to their similarity to generate 2D classes (Figure 6.13 A). An initial 3D classification was generated based on the best three classes, giving a resolution of around 32 Å (Figure 6.13 B). Finally, a 3D refinement was carried out using the OCCM as a template, since we expected a similar structure, which gave a final resolution of about 30 Å (Figure 6.13 C). Surprisingly, the 3D model showed the presence of the Cdt1 density, similarly to the OCCM. This result suggested that the ATP/ATPγS exchange through the washes is preventing the complete Cdt1 release from the

OCCM complex, suggesting that this strategy is not suitable for the purpose of isolating an OCM.

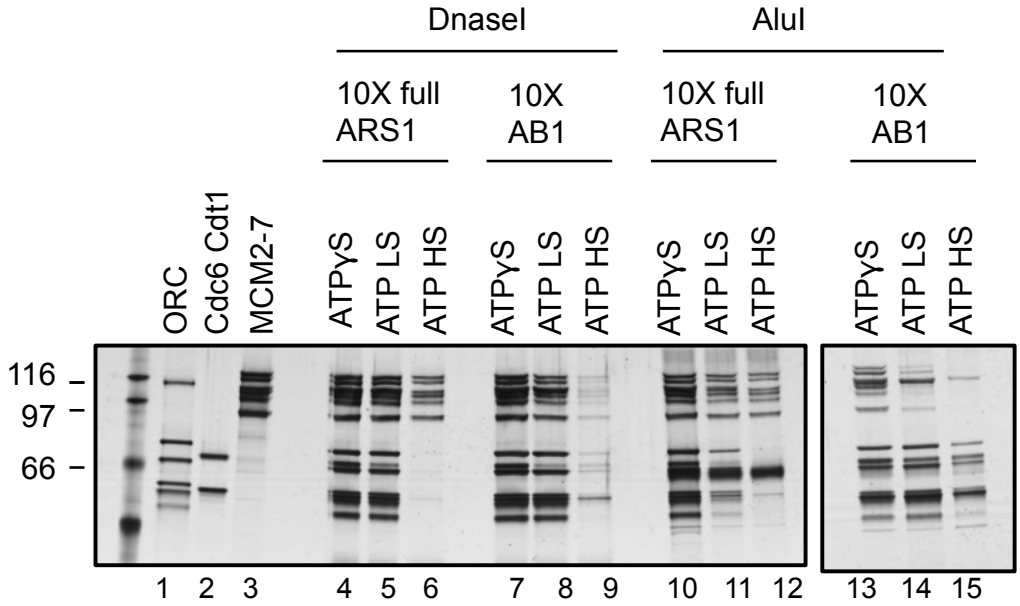
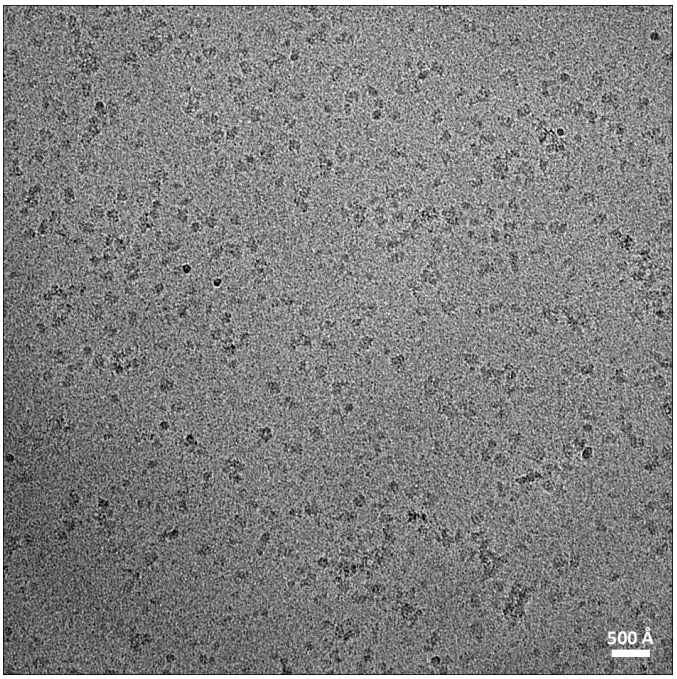


Figure 6.11. An OCM complex is formed on the 10XAB1 DNA

ORC, Cdc6, Cdt1 and MCM2-7 are assembled onto the 10XAB1 DNA bound to the beads, washed and eluted from the beads with DNaseI or AluI. The 10X ARS1 containing DNA is showed as a reference for complete complex formation. 20% of the proteins used in the assay are shown in lanes 1-3. All the conditions were tested in ATPγS for complex recruitment, ATP followed by low salt washes (LS) to test for proteins association or high salt washes with 300 mM potassium chloride (HS) for double hexamer formation. The experiment was performed three times.

A



B

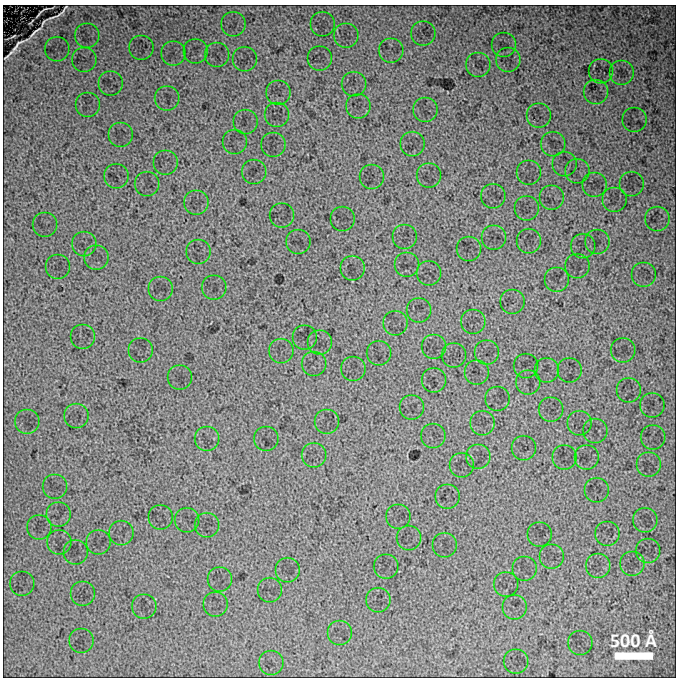


Figure 6.12. Cryo-EM analysis of OCM

ORC, Cdc6, Cdt1 and MCM2-7 were assembled on 10XAB1 containing DNA for 20 minutes at 24°C, followed by washes in buffer containing ATPγS. The protein complex was eluted from the beads using DNaseI, cross-linked with 0.1% glutaraldeide. **A)** A raw electron micrograph of the DNaseI treated sample embedded in vitreous ice. **B)** Representative particles picking procedure. Circled in green the particles that have been chosen for the following step of sorting.

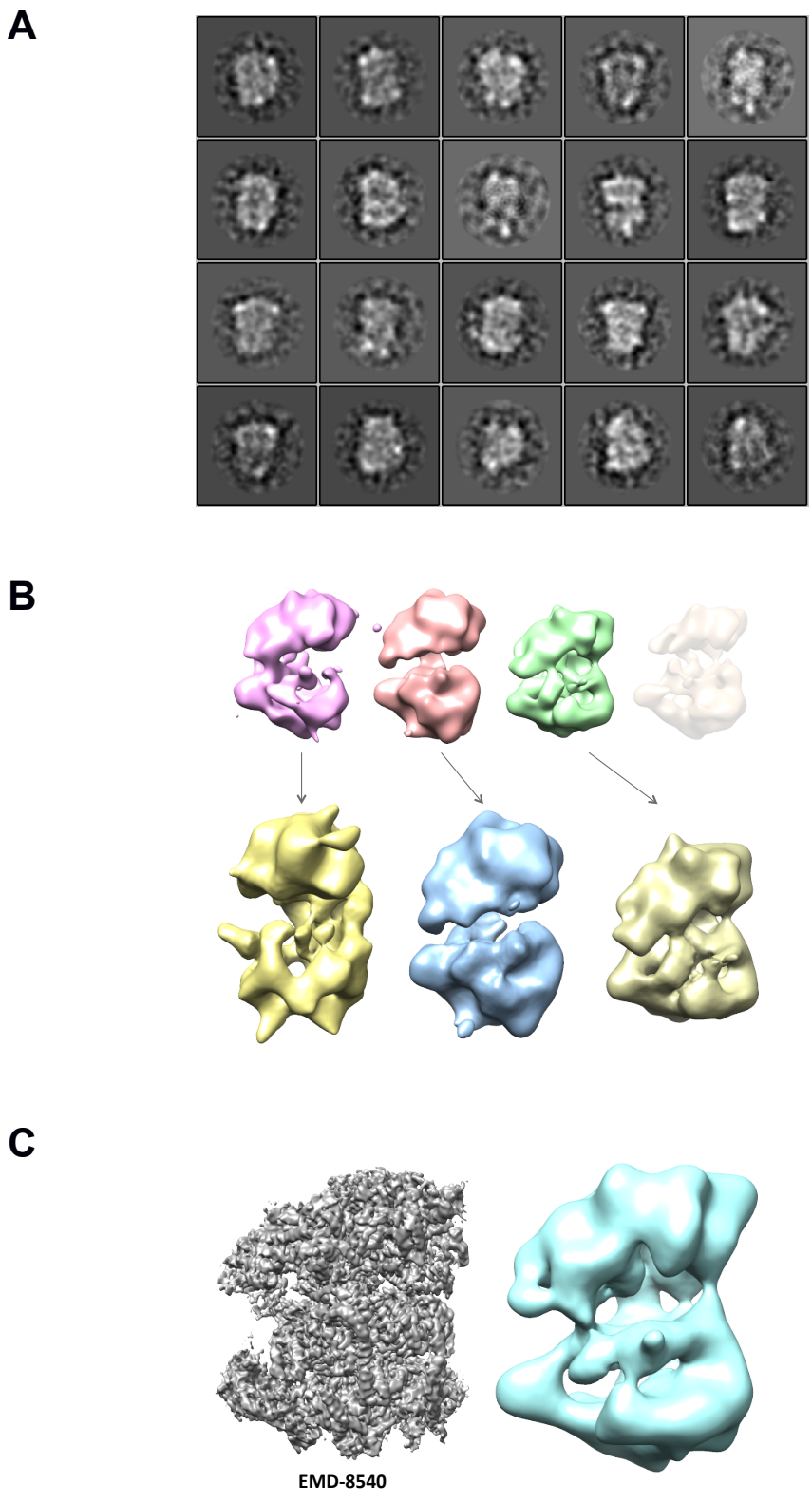


Figure 6.13. 3D classification procedure

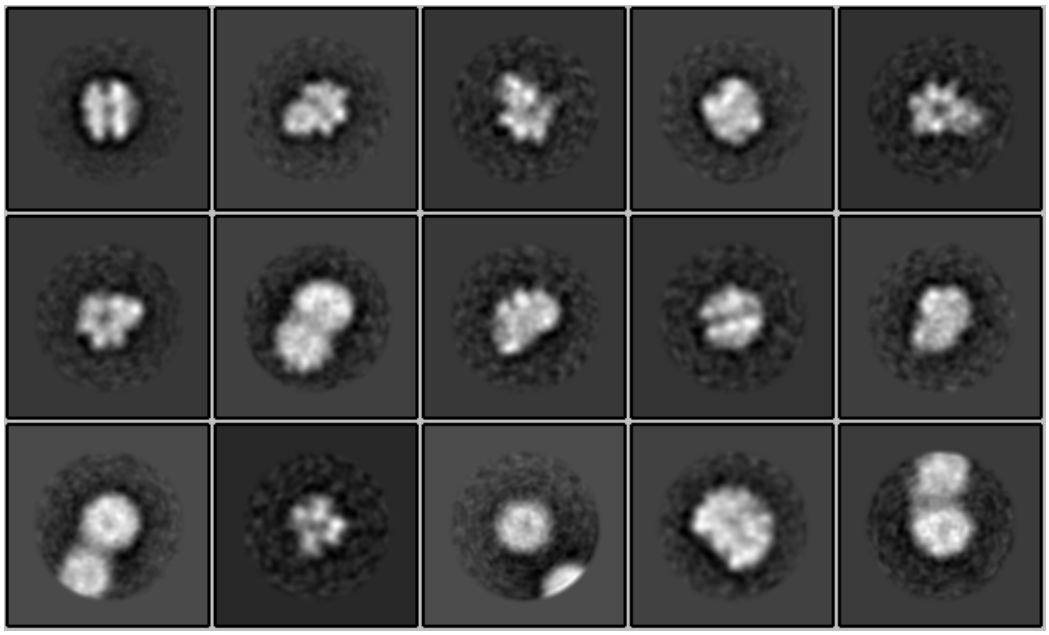
A) Selected 2D class averages from the best 10.000 particles. For scale the length of the particle is around 30 nm. **B)** 3D classification obtained from 17.000 particles (resolution around 30 Å). **C**) Separate refinement for the best three classes, each containing 4500 particles. The estimated resolution is around 32 Å. **D)** 3D refinement using the OCCM as a model (EMDB 8540), resolution around 30 Å.

6.6. Negative stain analysis of the OCM on a short DNA

Following the initial results obtained by cryo-EM, which suggested that Cdt1 was retained, the sample assembled on the 10X AB1 DNA was analysed. It was prepared as before but without the exchange of ATP to ATPγS during the wash step, in order to reduce/avoid OCCM formation. ORC, Cdc6, Cdt1 and MCM2-7 were incubated with DNA at 24°C for 30 minutes, washed and eluted with either AluI restriction enzyme or DNaseI. The samples were cross-linked and then analysed by negative staining. A 2D classification of the particles was generated for both samples. When the complex was released from the beads using AluI, two smaller sized ring-shaped complexes were predominantly observed in the 2D classes, likely corresponding to ORC/Cdc6 and MCM2-7 (Figure 6.14 A). This result is perhaps not surprising, as it is in line with the *in vitro* assay presented in Figure 6.11 (lane 14), which showed that the OCM is not released from the beads. This could suggest that MCM2-7 might bind on the regions of DNA containing the restriction sites for AluI limiting the accessibility of the enzyme. Interestingly, a high resolution structure of ORC/Cdc6 has not been obtained yet, due to stability issues related to this complex on the grid. However, in our preparation the complex appeared rather homogenous and stable, indicating a possible route to follow for the isolation of this protein complex.

The 2D analysis of the sample released from the beads using DNaseI showed a promising result, with significant decrease of double hexamer particles (Figure 6.14 B). It was found that the most populated class (10% of the particles picked) (first panel top left) showed a distinct three-tiered complex, which appeared to be different to the OCCM. Indeed, smaller complexes are abundant as well, suggesting a possible disassembly of the OCM complex upon a failed attempt to recruit the second hexamer, which is not supported by this short DNA (the class showed on the fourth panel on the first raw from left to right represents 7% of the total particles analysed).

A



B

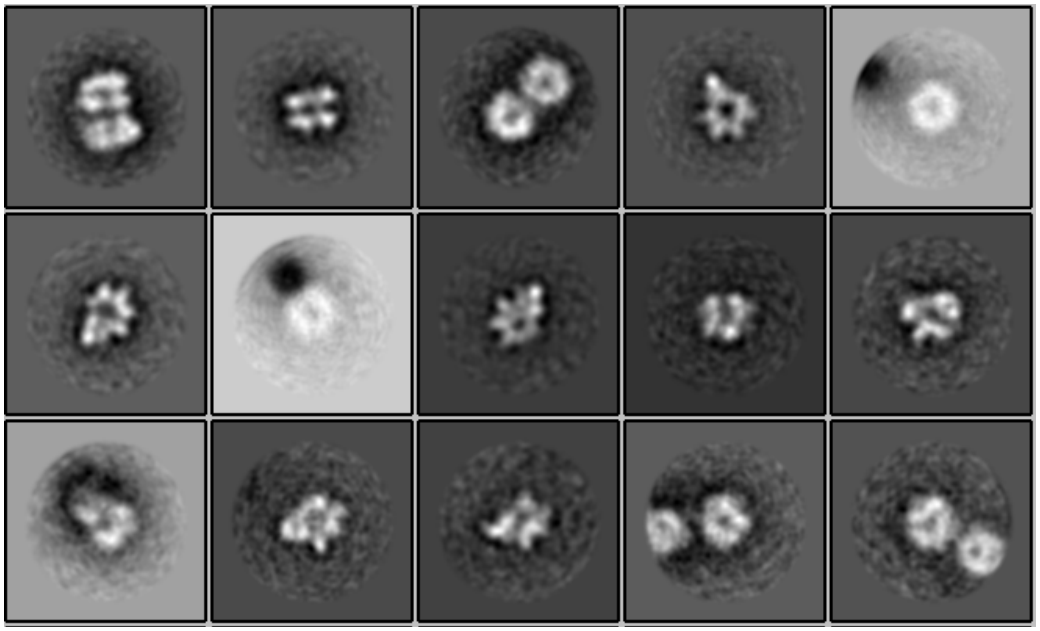


Figure 6.14 EM negative staining of the OCM complex assembled on 10XAB1 DNA

2D classifications of negative stained samples, analysed by electron microscope. Pre-RC reactions were assembled on 10XAB1-containing DNA for 30 minutes at 24C, followed by washes in buffer containing ATP. The eluted samples were cross-linked with 0.1% glutaraldeide and analysed by negative staining EM. **A)** The protein complexes were eluted from the beads using AluI. The most populated class contains 12% of the total particles (first panel, top left). **B)** The protein complexes were eluted from the beads using DnaseI at 4°C. 10% of particles belongs to the most populated class (first panel, top left).

Taken together the results obtained from this extensive optimisation of the sample preparation and their corresponding EM analysis highlight the difficulties in the isolation a pure and stable OCM complex. The design of a new short DNA construct proofed very promising, as it resulted in significantly decreased double-hexamer formation. However, still some sample heterogeneity was observed, with the presence of several particles of different sizes.

In order to try to trap the OCM complex before elution preventing its disassembly we attempted to cross-link the sample on beads. The protein complex was assembled on DNA and decreasing concentrations of glutaraldehyde were added (0.1%, 0.05% and 0.025%) prior elution with DNaseI. EM negative stained samples are shown in Figure 6.15. With highest concentration of cross-linker, the sample appeared aggregated (Figure 6.15 A). In the presence of less cross-linker (Figure 6.15 C), the sample appeared less aggregated and some particles could be identified. However, overall this strategy does not appear to be suitable, since particles appeared aggregated and therefore single particles cannot be observed in sufficient number. Lower glutaraldehyde concentrations have not been tried yet and could potentially help reducing the protein aggregation.

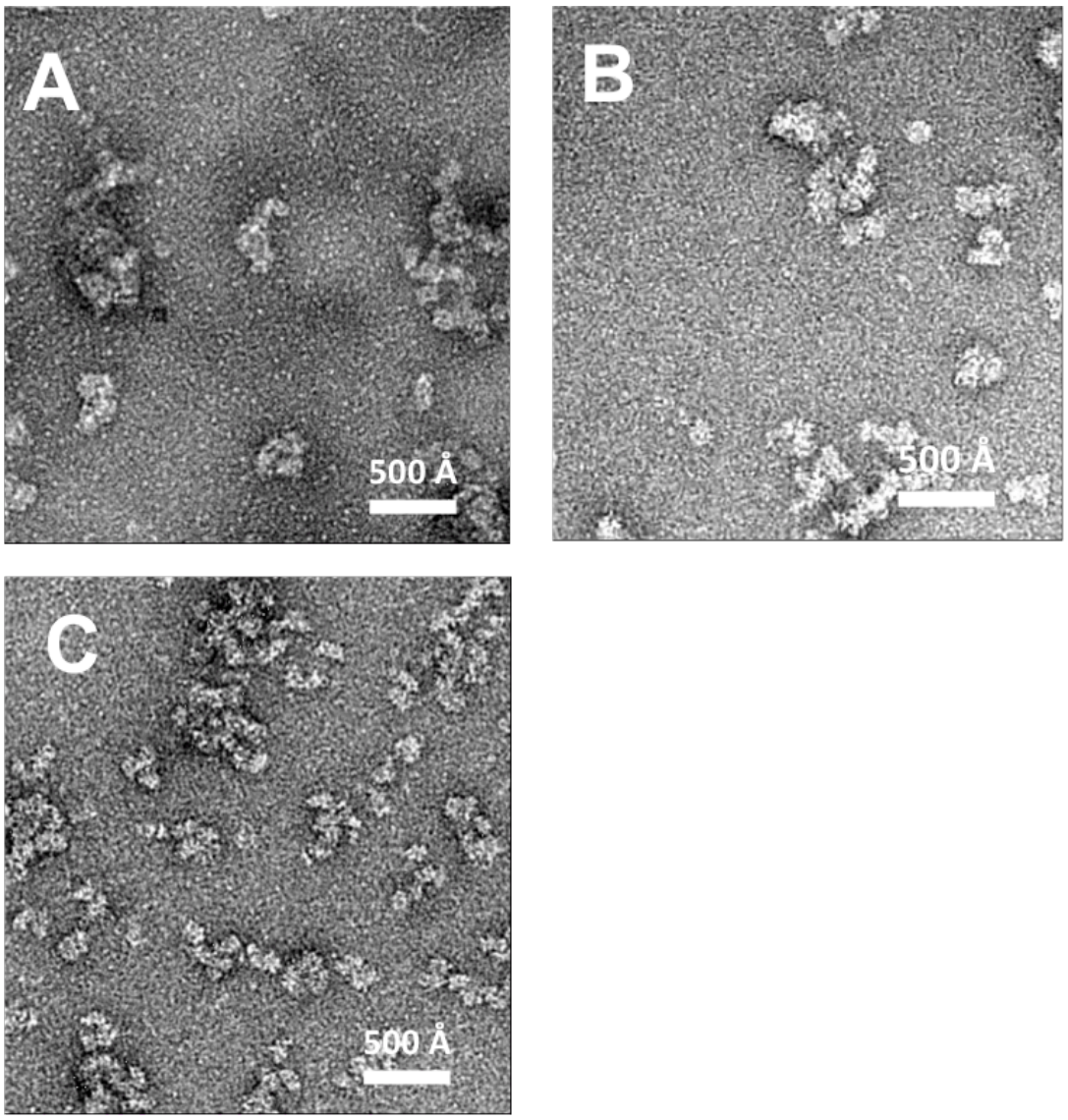


Figure 6.15. OCM in 10XAB1 cross-linked on beads

OCM complexes were assembled on 10XAB1-containing DNA for 30 minutes at 24C in pre-RC buffer containing ATP, cross-linked on top of the beads and eluted with DNaseI at 4°C. Raw images of negative stained samples cross-linked on beads with the following concentration of glutaraldehyde: **A)** 0.1%, **B)** 0.05%, **C)** 0.025% on top of beads.

6.7. Discussion

Key intermediates of the pre-RC assembly pathway have been recently isolated *in vitro* and visualised by cryo-EM (Figure 6.4). Important structural information have been revealed by the high resolution structure of the 16 proteins OCCM which is formed independently of ATP-hydrolysis, and can

therefore be captured in the presence of ATPγS (Yuan et al., 2017). This complex is not able to recruit a second hexamer that is required for ensuring bidirectional DNA replication. Upon ATP hydrolysis, Cdt1 is released from the OCCM forming the OCM, which is competent for double hexamer formation. However, this ATP-hydrolysis dependent intermediate has been challenging to study, because of its short-lived nature, various isoforms, low salt tolerance and general instability. Technical difficulties have been encountered in the isolation of the OCM due to its transient nature, as it was shown to quickly recruit the second hexamer (Fernandez-Cid et al., 2013). Our results, in agreement with a previous study (Sun et al., 2014), show that this complex does indeed rapidly recruit a second hexamer (Figure 6.5). Hence, the need for a protocol that is fast and able to prevent the double hexamer formation.

During this study, two different approaches were undertaken in order to isolate this complex. Initially, ATP was supplied to the reaction since it is required for Cdt1 release from the OCCM and subsequently it was washed out and replaced by ATPγS to prevent further ATP hydrolysis. However, our results showed that Cdt1 was not successfully released from the OCCM assembled in ATP, suggesting that the rapid exchange from ATP to ATPγS prevented ATP hydrolysis from occurring, trapping the majority of the particles at the OCCM stage (Figures 6.12). The second strategy involved the design of a shorter origin-containing DNA that possesses only the A, B1 elements that are essential for ORC/Cdc6 binding and helicase recruitment (Zou and Stillman, 2000). Indeed, this approach seemed to be effective in preventing the double hexamer formation, since this DNA is missing the specific origin DNA elements that support the formation of the double hexamer. Moreover, all the short origin fragments are aligned in the same direction, further suppressing the head-to-head double hexamer formation. Under these conditions, however, a heterogeneous population was generated with the presence of many small particles that were identified as being ORC/Cdc6 and MCM2-7. This might suggest that the OCM is formed but could undergo a disassembly process after the failed attempt of recruiting a second hexamer. Indeed, further options remain to be explored in the sample preparation, in order to stabilise the OCM and prevent its disassembly.

Visualising the OCM structure will represent an essential step towards understanding the as-yet unknown mechanisms of Cdt1 release and the recruitment of the second hexamer. As shown in this chapter, a variety of approaches have been explored that will hopefully lead to the production of a stable population of the OCM intermediate in the near future that will facilitate cryo-EM analysis of this so far elusive complex.

Chapter 7 - Discussion and conclusions

DNA replication is an essential step in the cell cycle, and must be performed correctly in order to maintain the integrity of the genome. Preserving genomic stability is crucial for the faithful transmission of genetic information from one generation to the next (Kolodner et al., 2002).

Eukaryotic cells duplicate their DNA from multiple regions called origins of replication during the S-phase of the cell cycle, enabling the replication of large genomes. Sophisticated mechanisms are in place to ensure that each origin is replicated only once per cell cycle. If re-replication occurs, the integrity of the genome is threatened resulting in unbalanced gene dosage which is a hallmark of tumorigenesis (Diffley, 2011). A two-step, temporally distinct, mechanism of DNA replication control exists in cells, which minimizes the chance for any re-replication to occur (Diffley et al., 1994).

In late mitosis and early G1 phase, ORC, Cdc6, Cdt1 and MCM2-7 act together to form the pre-RC complex at the origins of replication. The helicase MCM2-7 is loaded onto DNA in a step-wise process, which leads to assembly of two MCM2-7 hexamers on dsDNA in a head-to-head orientation facilitated by their N-terminal extensions; however, in this assembled form they are not active. In the case of eukaryotes, ORC/Cdc6 induce MCM ring closure around dsDNA. Interestingly, in the case of viral helicases, such as the Simian Virus helicase and the papillomavirus E1, the DNA is not inserted into the helicase by a loading complex analogous to ORC/Cdc6, but the helicase subunits oligomerise around origin DNA facilitated by specific dsDNA binding domains (Soultanas, 2012).

It is only during S-phase that the double hexamer becomes targeted by two serine-threonine kinases, CDK and DDK (Masai et al., 2005), resulting in the recruitment of other replicative factors and generating the active form of the helicase, called CMG. The helicase in the CMG complex catalyses DNA unwinding to generate ssDNA templates for DNA synthesis by polymerases. Once all of the DNA is replicated, the replicative machinery becomes inactivated and released until the next G1 (Ferreira et al., 2000).

In eukaryotes, pre-RC assembly is restricted to the G1 phase of the cell cycle by at least three different systems. These control mechanisms include 1) the inhibition of pre-RC factors through CDK phosphorylation in S-phase and 2) the PCNA-dependent degradation of Cdt1. Phosphorylation during the G2 phase, mediated by CDK, prevents re-association of MCM2-7 with chromatin. Mutations of different CDK sites in single ORC subunits is not sufficient, at least in yeast, to affect the replication control, suggesting the presence of multiple levels of control (Nguyen et al., 2001). In metazoans, Cdt1 is inactivated by the inhibitor geminin (Diffley, 2011).

The work reported in this thesis was conducted in order to contribute to the understanding of the mechanism of MCM helicase loading and its regulation during initiation of DNA replication, using a combination of biochemical and structural techniques. Specifically, the work presented here reveals new functions of the WHDs contained in the C-terminal region of MCM2-7 during pre-RC formation. Interestingly, all C-termini are highly variable in length and sequence, but each individual C-terminus is conserved from yeast to human. The new mechanisms will be discussed in the context of the current knowledge in the field.

7.1. The function of the Mcm5C during initiation of DNA replication

A large part of the work presented in this thesis aimed to elucidate the role of the Mcm C-terminal domains during the different stages of DNA replication initiation. In particular, extensive work was focused on Mcm5C as described in Chapters 3 and 4. In this section, a summary of these findings will be discussed in the context of the current literature. The conformational changes observed in Mcm5C in the available structures of DNA replication complexes will also be highlighted.

The OCCM intermediate, which traps these four multi-subunit factors together, has been isolated *in vitro* employing ATPγS, a slowly hydrolysable

ATP analogue. In this intermediate the WHDs of ORC/Cdc6 interact with the C-terminal domains of MCM2-7, while Cdt1 interacts with MCM2-7 (Sun et al., 2013). A high resolution structure of the complex was obtained by cryo-EM (Yuan et al., 2017), which revealed the location of four out of five C-terminal extensions of MCM2-7 and their interactions with the ORC subunits.

The WHD5 was not resolved in the OCCM, suggesting that it is not attached to the complex and adopts a flexible conformation, while the WHDs of the other Mcm subunits are visible and firmly latched onto ORC/Cdc6, generating a network of multiple weak interactions between MCM2-7 and ORC/Cdc6. The WHD5 was observed in the recent high resolution cryo-EM structure of *S. cerevisiae* MCM2-7 and in the MCM2-7/Cdt1 complex (Zhai et al., 2017a). In these two structures, the WHD5 appears to be located in a central position occluding the central pore of the hexameric ring (Zhai et al., 2017a). Here, the WHDs of Mcm4 and Mcm6 were stacked on top of WHD5, blocking the central channel. A new and unpublished structure of the OCCM is presented in chapter 4 (Yuan et al, 2018 unpublished), in which the WHD5 can be observed at the interface of the Mcm5 AAA+ domain, Orc3 and Orc2. In the new structure the Mcm2/5 ring is fully closed. It was reported that Cdt1 release and ring closure are concomitant events (Ticau et al., 2017) and that Cdt1 release is an ATP dependent process (Coster et al., 2014; Fernandez-Cid et al., 2013; Randell et al., 2006). However, in this new structure ATP hydrolysis was blocked by using ATPγS, suggesting that closure of the ring may be independent of ATP hydrolysis.

It was shown that intact Mcm3 C-termini are required for the loading of both hexamers of the double-hexamer (Frigola et al., 2013). Similarly, here it was shown that a functional Mcm5C is necessary in both MCMs. These results suggest that C5 is also involved in the loading of the first and second hexamer to ORC/Cdc6. In the double hexamer cryo-EM structures, the five WHDs of the yeast MCM2-7 are not longer visible, suggesting a high degree of flexibility (Abid Ali et al., 2017; Li et al., 2015; Noguchi et al., 2017).

In the active helicase, CMG, the C-termini of MCM2-7 are reorganised and the WHD5 is visible in the apo configuration (no DNA), again occluding the central channel of the helicase together with the WHD6 (Yuan et al., 2017). On the other hand, in the DNA bound CMG structure, WHD5 is not visible (Georgescu

et al., 2017). Here, the WHD4 is now partially occluding the central channel, in a similar position to that observed in the MCM2-7/Cdt1 structure (Zhai et al., 2017a), while the WHD6 moves backward.

Taken together, the changes in the positioning of WHD5 in the different protein complexes seem to suggest that this domain may act as a sensor of DNA insertion into the helicase ring. In the absence of DNA, it occludes the central pore, preventing the dsDNA access to the channel. When DNA is inserted, in the context of the OCCM formation, the helicase undergoes conformational changes that induce a repositioning of the WHD5, which is pushed away from the central channel. This allows DNA to enter the central channel of MCM2-7. This will be discussed in the next paragraph in more detail.

The work reported in this thesis discovered that Mcm5C has two clearly distinct functions in pre-RC formation – one in quality control and one in facilitating the OCM to double hexamer transition. In the following, several Mcm5C mutants will be discussed in the context of these novel functions.

Through biochemical and structural analysis, it was found that MCM2-7/Cdt1 lacking Mcm5C is competent for interaction with a DNA bound ORC/Cdc6 complex in the presence of ATPγS. This result is consistent with a recent study, which showed that only a small number of interactions involving Mcm3C with ORC/Cdc6 are required for the initial recruitment of MCM2-7 to the replication origin (Frigola et al., 2013). It was demonstrated that this mutant not only fully supports the OCCM formation, but also DNA insertion. However, Mcm5C is essential for the transition from the OCM to double hexamer, in particular for the successful recruitment of the second MCM2-7.

Interestingly, replacing the WHD5 with a structurally and functionally unrelated protein domain had no additional impact on the OCCM formation, further underscoring that this domain is not involved in the initial binding. Then again, replacing the WHD5 with a domain that is similar in sequence and structure, such as a different WHD, did not allow MCM2-7 regain double hexamer formation activity. All of these mutants hyperactivate the Cdc6 ATPase dependent quality control pathway, similar to MCM2-7ΔC5, and in turn promote the disassembly of incompletely loaded complexes. Interestingly, one mutant behaved differently in this respect. The human WHD5, which is most similar to

the yeast WHD5, displayed extremely low Cdc6 ATP-hydrolysis. This suggests that the human WHD5 is competent to suppress Cdc6 ATP hydrolysis, even more than the WT. Consequently, a more stable OCM is produced, but no double hexamer formation is achieved, indicating that the human Mcm5C does not support the OCM to double hexamer transition. In this way, this mutant represents a separation of function mutant, as it allows bypass of the quality control, but not of the double-hexamer formation.

The induction of ATP-hydrolysis is a key transition point during pre-RC formation. Here, two possibilities exist: 1) In the context of a non-functional complex, which fails to promote MCM2-7 ring closure, Cdc6 ATPase leads to complex disassembly in a quality control process. 2) In the context of functional DNA insertion and MCM2-7 ring closure, Orc1/MCM2-7 ATP hydrolysis leads to Cdt1 release, OCM formation and double-hexamer formation.

Importantly, in the case of the WT MCM, helicase loading is efficient, and therefore only limited Cdc6 ATP hydrolysis dependent quality control becomes induced and most complexes can progress to the double hexamer stage. However, mutants in Mcm5C can shift this balance, significantly upregulating the quality control pathway and reducing double hexamer formation.

Accordingly, some of the double, triple and multiple amino acids substitution mutants in Mcm5C generated during this study, showed medium to severe defects in salt-stable double hexamer formation *in vitro*. These defective mutants were seen to be associated with increased ATP hydrolysis. This would suggest that incompletely loaded helicases accumulate on DNA, possibly affecting interactions with ORC, and activating the quality control pathway for the disassembly of unproductive complexes.

In this work, it was suggested that the normal closure of the MCM2-7 ring will reposition the WHD5, and protein-protein interactions between this domain and Orc3 and/or Orc2 are involved in this process. These interactions in turn could cause structural rearrangements in ORC/Cdc6 that 1) block Cdc6 induced ATP hydrolysis and 2) activate Orc1/MCM2-7 ATP hydrolysis. The consequence of this is the release of Cdt1 from the OCCM and progression of OCM and double hexamer formation. Indeed, in the case of mutants that altered the network of interactions between Mcm5C, Orc2 and Orc3, the resulting complexes are unable to progress towards the double hexamer formation.

Instead, a quality control mechanism is activated, with Cdc6 induced ATP hydrolysis facilitating the complex disassembly.

It was shown that changing the characteristics, within reason, of the linker that precedes the WHD5 in Mcm5C did not affect the pre-RC formation *in vitro* but reduced the rate of pre-RC induced ATP hydrolysis, suggesting that the linker region might indirectly regulate the overall MCM2-7 ATP hydrolysis rate.

It is interesting to note that in the OCCM structure (Yuan et al., 2017), both the WHD5 and the N-terminal domain of Orc2 were not visible, suggesting a high degree of flexibility of these domains. In the unpublished OCCM structure, in which the gate is closed, the WHD5 becomes visible, and it can be seen in close proximity to Orc3. A future mutagenesis of the amino acids in Orc3, which are close to WHD5, could indeed confirm the role of the Mcm5C-Orc3 interaction in this process.

It has been proposed that Mcm5C has a twin role in the process: 1) via its interactions with the ORC proteins it seals off the MCM2-7 ring – forming a lock and 2) it acts as a MCM2-7 ring closure sensor, which directs the balance of Cdc6 and Orc1/MCM2-7 ATP-hydrolysis (Figure 7.1). In particular, the mutant Mcm5-3 illustrated this process very nicely. In this mutant nearly 100% of the ATP-hydrolysis is shifted in direction of Cdc6. Thus, the sensor is constitutively switched towards the quality control pathway, leading to a complete block in double hexamer formation. This result underscores the central role of Mcm5C in pre-RC formation. In the future, we plan to explore the role of Mcm5C as a *lock* and *sensor* by performing additional experiments. In the first instance, it requires linking specific MCM2-7 ring closure defects to induced Cdc6 ATP-hydrolysis and it is important to better characterise the network of Mcm5C interactions with ORC, e.g. by generating additional mutants in ORC subunits and by separating the Mcm5 double/triple mutants into single amino acid mutations.

Interestingly, point mutations in Mcm5C in human have not been described, although a few amino acids substitutions (missense) have been found in cancer samples from lung, pancreatic and breast cancer patients (Cosmic database). Similarly, a few missense point mutations in the N-terminal regions of Orc2 were found in patients affected by digestive tract cancers.

However, the low number of cases associated with these mutations makes it difficult to conclude specific associations between mutations in this domain and cancer. The small number of samples with MCM mutations in the Cosmic database might perhaps indicate that mutations in MCM subunits do not confer a survival advantage to cancer cells.

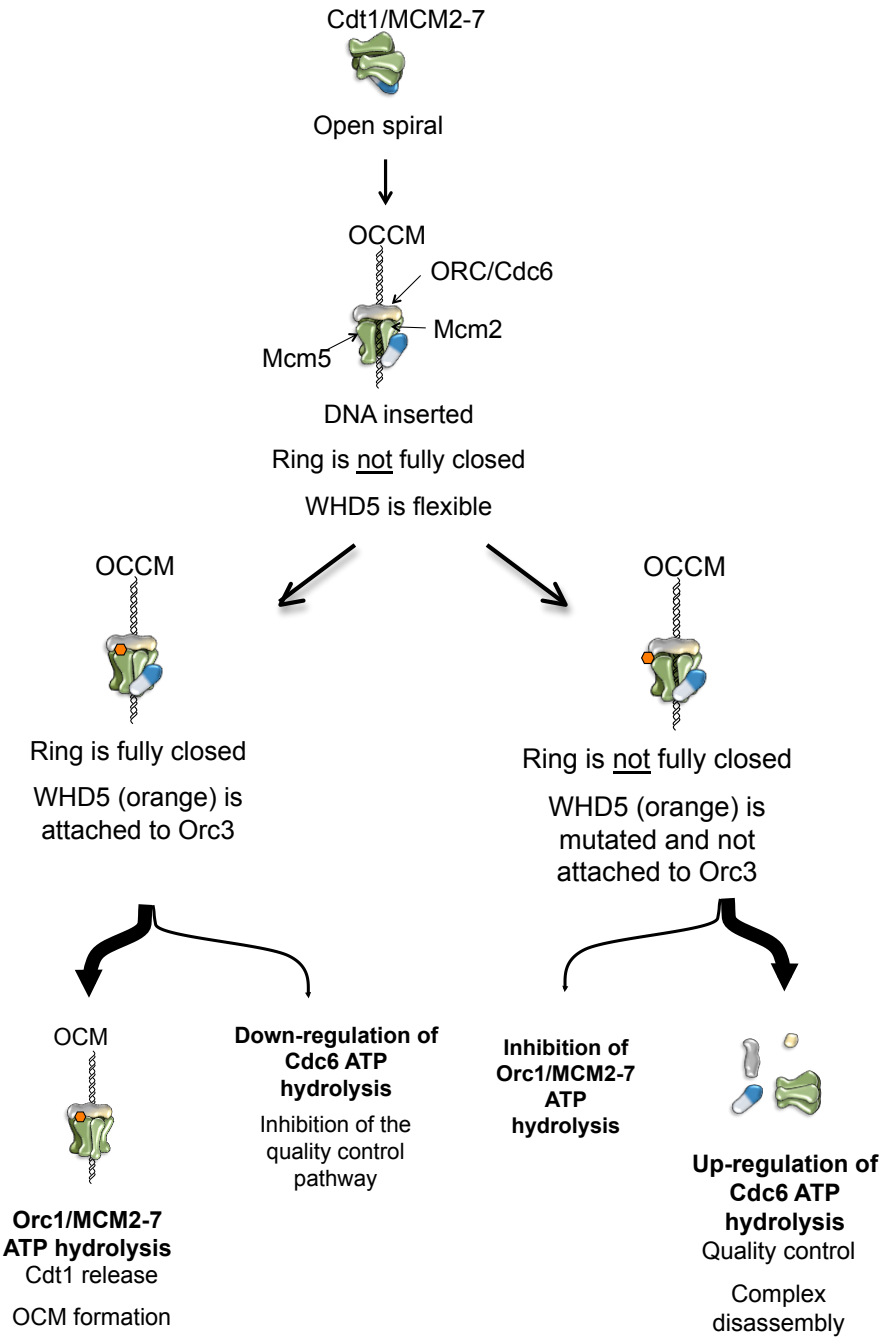


Figure 7.1. Model for Mcm5C-induced quality control pathway.

MCM2-7/Cdt1 is present in solution as an open ring, which is loaded on origin DNA by ORC/Cdc6. In the resulting complex (OCCM), dsDNA is inserted into the MCM2-7 ring which is partially closed. The closure of the ring induces a repositioning of the WHD5. Left hand side of the figure: When the WHD5 interacts with Orc3, this interaction induces a conformation change in ORC/Cdc6, which downregulates the quality control pathway and inhibits Cdc6-induced ATP hydrolysis. At the same time, it promotes ATP hydrolysis by Orc1 and Mcm2-7, which contributes to the pre-RC ATPase activity, leading to Cdt1 release and formation of the OCM. Right hand side of the figure: If the interaction WHD5-Orc3 cannot take place, for example as in Mcm5-3, the pathway is altered. As a consequence, the ATP-hydrolysis pathway is reconfigured towards the activation of the quality control. Orc1/MCM2-7 ATP hydrolysis is inhibited and Cdc6-induced ATP-hydrolysis is up-regulated with the release of Cdt1/MCM2-7 and complex disassembly.

7.2. The role of the other MCM2-7 C-termini

In this paragraph the new data described in this thesis that detail the mechanism and function of Mcm2C, Mcm4C and Mcm7C will be discussed.

Biochemistry experiments have shown that the WHDs of Mcm3 and Mcm6 are required for pre-RC formation, through interactions with Cdc6 and Cdt1 respectively. Mcm3C was found to be essential for the initial recruitment (Frigola et al., 2013) since an MCM2-7 mutant lacking this domain was unable to be recruited by a DNA bound ORC/Cdc6 complex. Mcm6C was described as being involved in the OCCM to OCM transition, inducing ATP hydrolysis and Cdt1 release (Fernandez-Cid et al., 2013).

No published data have reported to date on the functions of the other Mcm C-terminal regions during helicase loading (Mcm2C, Mcm4C, Mcm5C, Mcm7C). Protein constructs lacking Mcm2C, Mcm4C and Mcm7C named MCM2-7ΔC2, MCM2-7ΔC4 and MCM2-7ΔC7, respectively, were generated before the beginning of this study (Winker and Speck, unpublished). The function of the carboxyl terminal domains of these Mcm subunits during pre-RC formation was described assessing these deletion MCM2-7 mutants using a combination of biochemical, structural and *in vivo* techniques.

MCM2-7ΔC4 did not show defects in the formation of a salt-stable double hexamer *in vitro*. Although it forms interactions with Orc1, it seems that this domain does not have an evident role in pre-RC formation, but might be

involved in a later stage during helicase activation. Interestingly, in the CMG structure at the replication fork (Georgescu et al., 2017), the WHD4 is located in the central channel, partially occluding it and in close vicinity to the DNA. It might be possible that WHD4, similar to WHD5, is involved in a process of sensing DNA during CMG formation. Our data showed that the deletion of WHD4 in MCM2-7 did not cause dominant lethality upon overexpression *in vivo*. Similarly, a study in fission yeast showed that the deletion of Mcm4C did not cause apparent growth defects (Nitani et al., 2008). However, the authors suggested that Mcm4C becomes important when DNA replication is blocked by dNTP depletion, playing a role in recovering stalled replication forks after release from the replication block. Indeed, an interaction between MCM and replication checkpoint has been reported by several studies (Cortez et al., 2004; Ishimi et al., 2003). However whether Mcm4C plays a role in this mechanism has not been determined.

It is interesting that a short deletion of 20 amino acids (848-868) in Mcm2C produces a strong phenotype *in vivo* and *in vitro*, showing both dominant lethality and failure in double hexamer formation in the pre-RC assay. CLMS data in the context of OCCM suggest the presence of interactions between Mcm2C and Orc6 (Yuan et al., 2017). Orc6 is the smallest ORC subunit and in the OCCM structure it was not well resolved indicating high flexibility of this protein. Mcm2 has a key role in pre-RC formation, as it forms together with Mcm5 the “DNA entry gate” of the MCM2-7 helicase. Several cross-links between Mcm2C and Orc6 were found by a CLMS analysis (Yuan et al., 2017), suggesting that these two domain are in close proximity and they possibly interact with each other. As the deletion of the Mcm2 C-terminal extension affects the OCM to double hexamer transition, we propose that Mcm2 functions to stabilise the OCM or to facilitate the assembly of the two hexamers and the consequential ORC release. Unlike *S. cerevisiae* and *S. pombe,* higher eukaryotes have a WHD in Mcm2. These eukaryotes also have geminin, the main endogenous inhibitor of Cdt1. Interestingly, the N-terminal domain of human Cdt1 interacts with geminin (Lee et al., 2004). Due to this proximity, gemininis well placed to interact with the Mcm2C. It was suggested that the WHD of Mcm2 might have co-evolved as an anchoring site for geminin,

preventing in this way pre-RC formation (Riera et al., 2017). In the context of CMG, ssDNA is expelled from its channel at the C-terminal face of MCM2-7. Recently, polymerase ε was found to be localised in this position, contacting Mcm2C (together with the Mcm6C), ideally placed to carry out the synthesis of the leading strand (Sun et al., 2015).

The deletion of Mcm7C (727-845) did not affect double hexamer formation *in vitro,* but caused dominant lethality upon overexpression in yeast, suggesting that absence of this domain affects cell viability. Interestingly, Mcm7C was associated with a strong Cdt1 release defect. Since this defect did not affect double hexamer formation, we would like to suggest that Cdt1 release is probably not essential for pre-RC formation.

Previously it was shown that Cdt1 release and MCM2-7 ring closure are intimately linked or even interdependent (Ticau et al., 2017). Thus MCM2-7ΔC7 might represent a separation of function mutant, blocking Cdt1 release, but not affecting double-hexamer formation. This raises two questions: (1) what is the role of Cdt1 during pre-RC formation? and (2) what is the role of ATP hydrolysis during the OCCM-OCM transition?

The experiments conducted with MCM2-7ΔC7 suggest a specific and divergent function for this domain. Importantly, in addition to its role in Cdt1 release, the WHD7 has an additional role in initial ORC/Cdc6 – Cdt1/MCM2-7 complex formation. Indeed, the deletion of Mcm7C bypasses the initial Cdt1 requirement for helicase loading since MCM2-7ΔC7 can form a complex with ORC/Cdc6 in the absence of Cdt1. However, when Cdt1 is added to this ORC/Cdc6/MCM2-7ΔC7 complex, it does not support double hexamer formation. This is suggesting that Cdt1 is required at a very early stage of complex formation, when MCM2-7/Cdt1 makes the first contacts with ORC/Cdc6.

Previously it was assumed that ATP-hydrolysis is required for Cdt1 release or MCM2-7 ring closure. However, the MCM2-7ΔC7 experiments strongly suggest that Cdt1 release is not important for pre-RC formation. Indeed, the new OCCM cryo-EM structure, which was generated in the presence of ATPγS and displayed a fully closed MCM2-7 ring, indicates that ATP hydrolysis is not required for MCM2-7 ring closure. What is then the role of

ATP hydrolysis remains to be investigated. One hypothesis is that it might be involved in Cdc6 release. Indeed single molecule experiments suggested that ring closure occurs prior to Cdt1 release (Ticau et al., 2015). We propose that Mcm7C might be directly affected by Orc1/Cdc6 ATP hydrolysis and this way actively promotes Cdt1 release.

As part of this thesis a new model for ATPase dependent Cdt1 release has been proposed, which will be discussed in the following paragraph (Figure 7.2). In the OCCM, Mcm7C is located far away from Cdt1. As such it is initially difficult to reconcile how mutations in this protein could affect Cdt1 release. However, it was noted that the WHD7 lies directly at the interface between Orc1 and Cdc6, which are active ATPases. Based on this observation a new model was formed, which suggests that Orc1 ATP hydrolysis alter the Orc1/Cdc6 interface, which will affect the C-terminal section of Mcm7. Thus, a movement in the WHD7, via its connection to the AAA+ section of Mcm7, will restructure the associated Mcm subunits ultimately releasing Cdt1. It may be possible that Mcm7C blocks the Cdc6 ATP-hydrolysis dependent MCM2-7/Cdt1 release, which occurs for quality control, thus preventing the complex disassembly.

More subtle defects in Cdt1 release were previously observed in the MCM2-7 carrying mutations in either the Mcm2, Mcm3 or Mcm5 arginine fingers (Coster et al., 2014). These mutants did not support high salt stable double hexamer formation, suggesting that MCM2-7 ATP hydrolysis is required for Cdt1 release and OCM formation. In the case of the MCM2-7ΔC7, Cdt1 is not released, but the double hexamer is formed, indicating that this reaction follows a different mechanism to the MCM2-7 arginine finger mutants. However, from our current data, it is hard to judge whether Cdt1 release is completely blocked and even remains bound to the double hexamer upon completion of pre-RC formation. If this would be the case, negative stained EM samples of this complex would rapidly reveal the presence of the extra density on the sides of the two hexamers.

Overall, these are surprising results, since so far ATP hydrolysis was firmly associated with Cdt1 release prior to double hexamer formation. The role of Cdt1 has always been controversial. It was initially thought to be required for

helicase recruitment to ORC (Asano et al., 2007; Chen and Bell, 2011; Chen et al., 2007) but recent data suggest that MCM2-7 is recruited by direct interactions with ORC/Cdc6 (Fernandez-Cid et al., 2013; Frigola et al., 2013). Moreover, previously it was thought that Mcm6 is the preferred binding partner of Cdt1 (Ferenbach et al., 2005; Liu et al., 2012; Wei et al., 2010; Wu et al., 2012; Yanagi et al., 2002; Zhang et al., 2010), but then *in vitro* studies had suggested the existance of additional sites of interactions between MCM and Cdt1 (Fernandez-Cid et al., 2013). Finally, cryo-EM structures revealed that Cdt1 embraces Mcm2, Mcm6 and Mcm4, but not Mcm7 (Yuan et al., 2017; Zhai et al., 2017a). The proposed model tries to unify the different ideas and suggests a way to connect ATP hydrolysis dependent changes to Cdt1 release but further work is required to validate it.

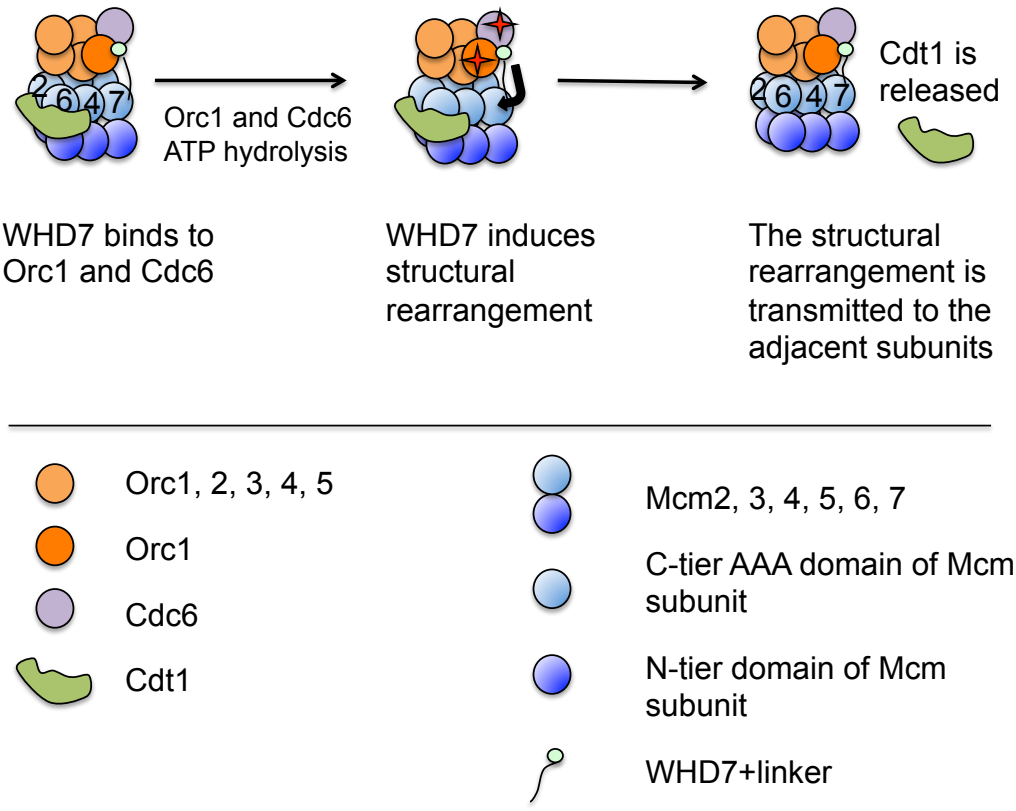


Figure 7.2. Model for Mcm7C-induced quality control pathway.

In the context of OCCM, the WHD7 is positioned between Orc1 and Cdc6, which are active ATPases. Upon Orc1 and/or Cdc6 dependent ATP hydrolysis, the interface between these proteins and WHD7 is altered. A movement in the WHD7 is reflected on the AAA+ domain of Mcm7 and a structural rearrangement is transmitted to the adjacent Mcm6, 4, 2 which interact with Cdt1 and ultimately induce the release of Cdt1.

7.3. The C-termini in S phase

The WHD5 can bind to ORC, but also binds to the central pore of the MCM2-7 helicase and therefore it appears very likely that the WHD5 potentially has multiple functions during DNA replication. In order to address roles of the WHD5 during distinct DNA replication processes we engineered an MCM2-7 construct with a PreScission protease cleavage site inserted into the flexible linker of Mcm5C. The addition of the site-specific protease to the OCCM or double hexamer resulted into the release of Mcm5C from the complex. This system allowed us to determine that Mcm5C is essential for the OCM to double hexamer transition but was not required for maintaining its stability. This cleavable MCM2-7 construct is a useful tool to study in the future the *in vitro* and *in vivo* roles of the Mcm5 C-terminal region. It would be interesting to ask whether the double hexamer missing Mcm5C is functional for CMG formation. For example, the construct could be used to form a reconstituted replisome *in vitro* and following its cleavage, one could address whether Mcm5C has a role during DNA synthesis or in forming interactions with other replication factors.

Similar investigation could be carried out with the Mcm5C point mutants that caused no phenotype in pre-RC formation, but caused dominant lethality in vivo, in order to investigate whether they are associated with other DNA replication defects. Also, the Mcm5C-linker mutants described in chapter 4 could be investigated in the context of the CMG. Their analysis *in vitro* showed that various linkers support pre-RC formation. However, reducing their length resulted in much less ATP hydrolysis, which could affect the CMG complex. Indeed, in the CMG, ATP hydrolysis is essential in the process of DNA unwinding, providing the energy to actively propel ssDNA through the helicase central channel (Moyer et al., 2006). How ATP hydrolysis in the context of the CMG is regulated is only partially understood. It appears possible that proteins binding to the C-terminal section of Mcm5 could alter the ATP hydrolysis rate of the helicase and as such the DNA unwinding rate of the CMG. Obviously, this is a simplification, but interestingly, electron microscopy data hint that polymerase ε can bind to the CMG while touching on the Mcm5 C-terminal region, which makes testing the model more attractive.

Finally, since MCM2-7ΔC7 supports double hexamer formation, but showed a dominant lethal phenotype when overexpressed, it would be interesting to ask whether Mcm7C has a specific role during CMG formation or replication fork function. Similar as for Mcm5C, one could ask whether this domain modulates the ATP hydrolysis rate of the active helicase.

7.4. A new concept for the MCM2-7 WHDs

Here a new concept is presented, explaining how distinct functions of the individual WHDs drive the multi-step pre-RC formation process. Importantly, 12 out of 14 OCCM proteins contain WHDs, underscoring the exceptional relevance of this domain in pre-RC formation. In the past, the canonical helix-turn-helix motif was typically described as a dsDNA-binding motif, present in a large number of DNA-binding proteins (Aravind et al., 2005). Interestingly, Orc4 and Cdc6 do not bind DNA through their wing-helix-wing motif, as seen in the case of the archaeal *Sulfolobus solfataricus* (Sso) WHD (Dueber et al., 2007), but the Orc4 WHD is interacting with the Mcm6 WHD, while the Cdc6 WHD is in proximity to Mcm3. Indeed, in the OCCM, the WHDs appears to be the main players in protein-protein interactions. The WHDs of MCM2-7 are latching onto WHDs of ORC/Cdc6, while Cdt1 possesses two WHDs that are involved in three interactions with Mcm subunits, particularly the Mcm6 WHD that is alleviating an auto-inhibitory conformation (Fernandez-Cid et al., 2013). In budding yeast five different MCM WHDs exist, with each one having a different role.

In archaea, Orc and Mcm proteins also carry WHDs, showing some similarities in the function with the eukaryotic ones. Interestingly, in the case of SsoMCM, the WHD can bind ssDNA weakly (Pucci et al., 2007). In SsoMCM (Barry et al., 2007) it was found that the WHD is most likely associated with initial assembly or activation of the helicase, which is reminiscent of its function in budding yeast. Recently, the WHD of the archaeal MCM was shown to be required for the helicase to be recruited to origins (Samson et al., 2016).
Furthermore, several studies reported that in archaea, the MCM WHDs allosterically modulate ATP hydrolysis of the AAA+domain (Barry et al., 2007; Jenkinson and Chong, 2006; Wiedemann et al., 2015). This is consistent with

our findings, since the deletion of Mcm2C, Mcm3C, Mcm7C strongly affect ATP hydrolysis, suggesting a conserved function of the C termini across kingdoms.
It is still poorly understood how ATP binding and hydrolysis by the Mcm subunits affects the structural reconfiguration of the helicase during DNA loading. The Mcm WHDs are in close proximity to their respective AAA+ domains, linked by a short flexible linker. Due to this physical proximity of the WHDs to the ATPase sites in the MCM subunits, it is possible that some of the Mcm C-termini may regulate ATP hydrolysis directly. Further investigation is required, with the use of linker mutants representing a sensible route.

In summary, the WHDs are conserved elements in archaeal and eukaryotic DNA replication, which mediate key protein-protein interactions that play a major role in helicase loading, but probably also influence helicase activation and DNA synthesis.

Based on the extensive characterisation of the WHDs in pre-RC formation, a new concept in helicase loading is proosed, which explains how distinct protein-protein interactions can drive a multi-step helicase loading process (Figure 7.3). In this model the Mcm C-termini have specific functions that occur in a temporal order. Some of the C-termini functions are overlapping, potentially acting together to drive the process forward. Mcm3C is starting the reaction cascade, as it is essential for the initial binding of the helicase to ORC/Cdc6 (Frigola et al., 2013). The deletion of Mcm3 completely blocks the process, illustrating it as a “all or nothing” reaction. Indeed, it was shown that Mcm3C binds directly to ORC/Cdc6, underscoring its role as the “initiator”. The second step in this process is Mcm6C. This WHD has a dual role, as it blocks in the absence of Cdt1 MCM2-7 interactions with ORC/Cdc6 (Fernandez-Cid et al., 2013), but it also forms a network of interactions with Cdt1 and Orc4 (Yuan et al., 2017). These interactions are essential for DNA insertion (Riera et al, in preparation) and to activate ATP hydrolysis (Fernandez-Cid et al., 2013). Thus, the WHD6 is the key player to drive “DNA loading”. The third step in this process is the WHD5, which partially overlaps with the previous step. Again, Mcm5C has multiple roles, as shown in this thesis. Once DNA is inserted, the Mcm2-7 ring will attempt to close around DNA. Here Mcm5C acts as a “lock”, initiating key protein-protein interactions with Orc3 and potentially others that

seal off the ring. Correct interactions will induce Orc1/MCM2-7 ATP hydrolysis to drive Cdt1 release. However, a failure in this process disrupts Mcm5 interactions with Orc3 and others, and strongly upregulates the quality control pathway, which then leads to Cdc6 ATP-hydrolysis and Cdt1/MCM2-7 release. As such, Mcm5C acts as a sensor, which directs ATP hydrolysis in two possible directions – driving either pre-RC assembly or disassembly. The second function of Mcm5C is at the stage of the OCM. Here it is required to facilitate the recruitment of the second MCM2-7 hexamer. As also described in this thesis, Mcm7C has a key function for Cdt1 release. The proposed mechanism involves an Orc1 ATP-hydrolysis driven structural change at the Orc1/Cdc6 interface, where Mcm7C is latched on, which in turn facilitates a structural change in Mcm7, which ultimately leads to Cdt1 release. Clearly, the full elucidation of this highly complex mechanism still requires more work, until it is complete. For example, one also has to consider the emergent CLMS data, which suggest that the Mcm7C is also involved in interactions with Orc2 (Yuan et al., 2017).

This thesis has contributed significantly to the concept that the different WHDs drive distinct functions for helicase loading. Interestingly, a study in the archaeal SsMCM showed that the WHD of this hexameric helicase is required for its recruitment to the replication origin (Samson et al., 2016). This is mediated by Orc1-1, a protein containing sequences that appear to be ancestors of both Orc1 and Cdc6. While Orc1-1 contains a WHD in its C-terminal region, it was found that the recruitment of MCM is mediated by the AAA+ domain of Orc1-1 (Samson et al., 2016). Furthermore, as archaea use homo-hexameric Mcm proteins, these cannot accomplish the same level of control that are achievable with six different proteins.

In bacteria, a different scenario is observed. Here, origin melting precedes helicase loading. DnaC is the helicase loader, a monomer in solution, which uses its AAA+ domains to oligomerise forming a hexamer. DnaC binds the helicase DnaB inducing the opening of the ring for DNA insertion. This process is highly analogous to how clamp loaders open a sliding clamp, which are proteins that encircle dsDNA and act as replication processivity factors by tethering the polymerases to the DNA template (Moldovan et al., 2007). However, differently from the MCM interactions with ORC, the C-terminal

extensions of the clamp are interacting with the N-terminal extensions of the loader. The clamp loader consists of five subunits which oligomerise together in a ring-like shape via their C-terminal extensions to form a “collar”. The N-terminal domains adopt an open conformation below the C-terminal collar and bind the sliding clamp. Six domains assemble in a circle to form the clamp and their C-terminal extensions interact with the loader and other proteins such as polymerases (Hedglin et al., 2013). Extensive interactions between the sliding clamp and the loader ATPase domains induce conformational changes in the clamp converting it into an open state that is competent for binding primer-template DNA substrates (Miyata et al., 2005).

Although the DnaC loading mechanism is globally similar to that of the clamp loader, there also are key differences. DnaC uses a dedicated N-terminal domain to associate with its target (Ioannou et al., 2006; Ludlam et al., 2001; Tsai et al., 2009), rather than the AAA+ region employed by clamp loaders (Bowman et al., 2004). Furthermore, in bacteria helicase ring opening is induced by the binding with the loader. However, a similar mechanism is not observed in eukaryotes where MCM2-7/Cdt1 is found as an open spiral in solution (Zhai et al., 2017a). It is possible that the WHDs play a role in keeping the spiral stable. In conclusion, the work in this thesis highlights that helicase loading in eukaryotes is conceptual different to any other system, with the archaea the closest match. Nevertheless, very important differences remain, since only a single archaeal Mcm subunit is unlikely to facilitate the highly complex helicase loading process observed in eukaryotes.

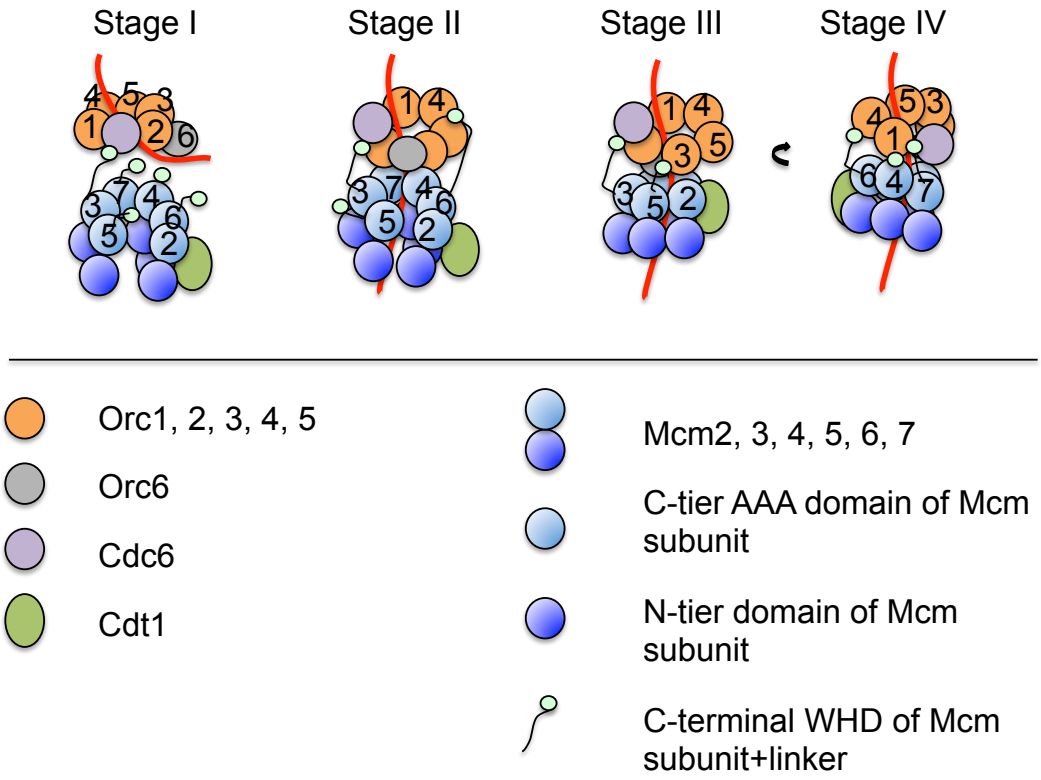


Figure 7.3. Molecular events mediated by the Mcm C-termini during the loading of the first Cdt1-bound Mcm2-7 hexamer by the ORC-Cdc6.

During the loading of the MCM2-7 helicase to ORC/Cdc6, the first contact between the helicase and the helicase loader is made by the Mcm3C (stage I). The second step is Mcm6C, which forms interactions with Cdt1 and Orc4 (stage II). The Mcm5C (stage III) acts as a "lock" of DNA inside the helicase ring, promoting interactions with Orc3. It also acts as a "sensor" of correct DNA insertion, regulating ATP hydrolysis. Finally, the Mcm4C binds Orc1 and Mcm7C interacts with both Orc1 and Cdc6 (stage IV).

7.5. CDK as a negative regulator of DNA replication

Helicase loading occurs efficiently in the G1 phase of the cell cycle, but in S phase re-loading of the replicative helicase on DNA is prohibited, guaranteeing that every piece of DNA becomes only replicated once (Arias and Walter, 2007). In budding yeast the main negative regulator of DNA replication is the kinase CDK, which blocks pre-RC assembly in multiple ways. CDK dependent phosphorylation of Cdc6 leads to its ubiquitination and degradation (Drury et al., 2000). CDK dependent phosphorylation of Mcm3 results in the nuclear export of the MCM2-7 complex (Nguyen et al., 2000). Finally,

phosphorylation of ORC on Orc2 and Orc6 directly interferes with helicase loading (Chen and Bell, 2011; Fernandez-Cid et al., 2013). How CDK phosphorylation of ORC affects pre-RC formation is only partially understood.

Chen and Bell used cell extracts containing ORC and they showed that CDK dependent phosphorylation of Orc6 inhibits the Orc6-Cdt1 interaction and as a result strongly blocked helicase recruitment, suggesting that the main level of regulation occurs at the level of initial recruitment (Chen and Bell, 2011). Then, Frigola et al, 2013 and Fernandez-Cid et al, 2013 showed using purified proteins that initial MCM2-7/Cdt1 recruitment by phosphorylated ORC was similar to that of unphosphorylated ORC (Fernandez-Cid et al., 2013; Frigola et al., 2013). However, ATP-hydrolysis dependent OCM formation was severely impaired by CDK phosphorylated ORC.

In this thesis, this process was looked in more detail and it was identified that CDK regulates pre-RC formation in three different ways:

1.) The first level of control occurs at the stage of the OCCM formation. Phosphorylated ORC is less efficient in OCCM formation than non-phosphorylated ORC, which is different to previous observations; Chen and Bell was showing a much stronger effect and both Frigola and colleagues and Fernandez and colleagues were showing no effect at all (Chen and Bell, 2011; Fernandez-Cid et al., 2013; Frigola et al., 2013). Very interestingly, the CDK dependent effect on OCCM formation was completely dependent on Mcm5C. Using MCM2-7 lacking Mcm5C we observed that initial recruitment of the helicase by phosphorylated ORC was very efficient. Similar result were obtained when WHD5 was replaced with the human WHD5, suggesting that the mechanism of sensing ORC phosphorylation by Mcm5C in not conserved between yeast and human. On the other hand, the point mutants in Mcm5C generated during this study did not show the same effect suggesting that they do not bypass the initial recruitment inhibition. This indicates that the inhibition of the helicase recruitment by CDK phosphorylated ORC can only be bypassed by removal of the entire WHD5 or mutations in several regions of this domain.

2.) Both Frigola et al and Fernadez-Cid et al showed that P-ORC negatively regulates pre-RC formation during the OCCM to OCM transition by activating the Cdc6 dependent ATP hydrolysis quality control pathway, which leads to disassembly of incomplete loaded MCM2-7.

3.) Here a further level of CDK control was observed. This occurs at the OCM level. We found that an OCM formed with P-ORC is not able to support double hexamer formation. The mechanism for this defect in OCM function is currently not clear.

These are interesting observations, and no other studies have looked in detail on how CDK regulates the pre-RC formation. From these results, it appears that Mcm5C is involved in the mechanism of sensing P-ORC. The position of the phosphorylated Orc amino acids relative to the WHD5 is not known. Previous work showed that Thr-116 and Thr-226 in the Orc2 N-terminal region are CDK target sites (Nguyen et al., 2001), while CLMS data indicated that K750 of Mcm5C and K226 in the N-terminus of Orc2 are in proximity (Yuan et al., 2017). Unfortunately, in the OCCM structure, the N-terminus of Orc2 is not visible and therefore it is not possible to precisely locate it relatively to Mcm5C. To understand this process in more detail it would be necessary to mutate CDK target sites in Orc2, which could abolish an interaction with Mcm5C, and possibly alleviate the initial inhibition in recruitment.

The control of DNA replication in higher eukaryotes has been studied as well and seems to work differently than to budding yeast. In *Xenopus* egg extract, CDK activity dissociates ORC, Cdc6, MCM2-7 from chromatin (Findeisen et al., 1999; Sun et al., 2002). In *Drosophila*, *in vitro* phosphorylation of Orc1 and Orc2 results in inhibition of ORC binding to DNA and ATP hydrolysis (Remus et al., 2005). In human cells, Orc2 phosphorylation was found to be linked to ORC dissociation from chromatin with consequent block of DNA replication initiation (Lee et al., 2012). In higher eukaryotes, phosphorylated ORC appears to be regulated at the level of DNA binding. It would require a full reconstituted system to address the different levels of CDK control during pre-RC formation.

7.6. The role of MCM C-termini beyond DNA replication

The MCM2-7 C-termini contain folded domains (WHDs) that are connected to the core of the MCM2-7 complex via a flexible linker. As such, these WHDs are ideally suited as attachment sites for a number of protein factors. In this way, the C-termini can regulate DNA replication, but equally they could influence non-canonical processes unrelated to DNA replication. Although this concept has not yet been discussed in the literature, several pieces of data fit with this idea. For example, from a yeast two-hybrid screen, it was found that in particular human Mcm7C interacts with the amino-terminal of the retinoblastoma (Rb) protein (Sterner et al., 1998), suggesting a possible negative regulation of DNA replication by the Rb. The authors also showed that binding of human Rb to *Xenopus* MCM7 inhibits DNA replication *in vitro*, suggesting that Mcm7C plays a regulatory role during licensing. A different study showed that the human Mcm7C forms a complex with the oncoprotein E6 of the human papillomavirus associated with cervical cancer (Kukimoto et al., 1998). Moreover, another yeast two-hybrid screen identified an interaction between the human Rad17 checkpoint protein and the human Mcm7C (Tsao et al., 2004) while a study with human cells found a direct connection with ATM and ATR checkpoint signalling to three MCM subunit (Cortez et al., 2004). This would suggest that MCM proteins could be involved in S-phase DNA damage checkpoint activation, signalling fork stalling.

Two residues in the human Mcm5C (R732 and K734) were identified as binding sites for the transcription factor Stat1 (DaFonseca et al., 2001). Mcm5 R732 is a highly conserved residue from yeast to human and it is located in the terminal alpha-helix of the WHD, fitting with the concept that the WHD serves as a protein-protein interaction domain.

In summary, there is good evidence from the literature for a potential role of the Mcm C-termini in non-canonical processes, in particular for Mcm7C. Whether other phosphorylation sites on the C-termini of the MCM subunits are present and targeted by other kinases during replication, transcriptions or checkpoint regulation is not reported in literature. Due to the presence of a number of serines and threonines in the C-terminal domains of Mcm subunits,

bioinformatics tools (NetPhos) predicted some PKA/PKC phosphorylation sites in human MCM2-7. However, no published studies have experimentally confirmed these predictions.

7.7. The OCM

At the time when this project was started very little was known about the structural organisation of the key DNA replication initiation intermediates, since high-resolution structures had not yet been published. In the last few years, an increasing number of high resolution structures of helicase loading intermediates have been obtained. The only intermediate that lacks structural information is the OCM. Using a combination of biochemistry and EM approaches, efforts towards obtaining a high resolution structure of the OCM have been described (Chapter 6).

The OCM was first described by Fernandez-Cid et al, 2013 and was found to consist of one copy of ORC, Cdc6 and MCM2-7. *In vitro* data showed that this complex forms within seconds, whilst formation of the salt-stable double hexamer requires several minutes. In addition, the OCM serves as a platform for the recruitment of the second helicase and appears to be salt-sensitive if compared to the double hexamer, which is stabilised by inter-hexameric interactions. Attempts to obtain a structure by cryo-EM of the OCM were previously made (Sun et al., 2014), but only a two-dimensional classification was obtained, revealing the general shape of this complex through comparison with the already known OCCM. The most evident feature was the absence of Cdt1. However, the heterogeneity of the sample and the technical limitations associated with this did not allow any further progress. With the advent of the so-called “resolution revolution” of the recent years, technical advances have allowed the high resolution analysis of complicated samples. Therefore, preliminary work towards the structural characterisation of the OCM is described in Chapter 6.

This study highlighted the difficulties that can be encountered during a cryo-EM analysis of a heterogeneous and meta-stable complex. However, important technical achievements have been made providing essential preliminary data for the future experiments. In summary, we have learnt that: (1)

a short incubation time with origin DNA is essential to prevent double hexamer formation and to enrich for the OCM, (2) a DNA lacking specific origin DNA elements for the recruitment of the second hexamer is better suitable for OCM isolation, (3) after release from the beads, the OCM becomes rapidly unstable, suggesting that it is a short-lived intermediate. In the near future, further investigation will be carried out taking into account these consideration during the sample preparation.

The structural characterisation of this complex would be essential to map the protein-protein interactions between ORC/Cdc6 and MCM2-7. It would be interesting to see how protein interactions become rewired during the OCCM to OCM transition. In particular, it would be informative to get more information on the WHD5, as it is essential during the OCM to double hexamer transition. It appears possible that the WHDs of MCM engage more closely with ORC/Cdc6 than observed in the OCCM, revealing potentially new interactions important for double hexamer formation.

7.8. Final remarks

Biochemical studies over the last 20 years have shed light onto the critical steps of helicase loading on DNA, identifying key intermediate complexes and novel mechanisms. Recent structural advancements have contributed to the field through the visualisation of these protein complexes at high resolution. However, we still lack a fundamental understanding on how structural changes drive complex processes, such as helicase loading and some of the key regulatory mechanisms remain to be described.

Due to the conservative nature of the main processes in DNA replication, studies obtained in yeast are relevant for any organisms, and can be in large parts translated to human. Defects in DNA replication have been implicated with genome instability, cancer and other human diseases. Indeed, targeting MCM2-7, the core of the replicative helicase, could be essential for developing new therapeutics against cancers. For this purpose, we may need more understanding of the diverse features of MCM2-7, including the fine mapping of its interactions with other proteins, during pre-RC formation and in the active CMG. Indeed, a combination of structural aspects together with specific assays

for assessing each step of DNA replication will be required for a complete understanding of the mechanism of action. High-yield purification of MCM and factors associated to it (CMG) combined with high throughput assays would enable the screening of small molecules targeting the replicative helicase, potentially contributing to development of therapeutics for human cancers in which replicative factors have found to be involved. However, selectivity over normal cells might be difficult to achieve.

Although *in vitro* and structural studies have contributed to the understanding of the general process of DNA replication, the precise mechanistic roles of the various protein components have not been fully clarified. We provide here a number of new concepts describing the function of the MCM2-7 WHDs in the initiation of DNA replication, in particular the role of WHD5 in sensing MCM2-7 ring closure and regulating the ATP-hydrolysis pathway choice. Moreover, the discovery that Mcm7C is essential for Cdt1 release, that Cdt1 release is not required for pre-RC formation, that Cdt1 functions early in the pre-RC cycle and that CDK dependent regulation of pre-RC formation depends on WHD5 were exciting findings.

References

Abid Ali, F., Douglas, M.E., Locke, J., Pye, V.E., Nans, A., Diffley, J.F.X., and Costa, A. (2017). Cryo-EM structure of a licensed DNA replication origin. Nat Commun *8*, 2241.

Abid Ali, F., Renault, L., Gannon, J., Gahlon, H.L., Kotecha, A., Zhou, J.C., Rueda, D., and Costa, A. (2016). Cryo-EM structures of the eukaryotic replicative helicase bound to a translocation substrate. Nat Commun *7*, 10708.

Aravind, L., Anantharaman, V., Balaji, S., Babu, M.M., and Iyer, L.M. (2005). The many faces of the helix-turn-helix domain: transcription regulation and beyond. FEMS Microbiol Rev *29*, 231-262.

Argos, P. (1990). An investigation of oligopeptides linking domains in protein tertiary structures and possible candidates for general gene fusion. J Mol Biol *211*, 943-958.

Arias, E.E., and Walter, J.C. (2007). Strength in numbers: preventing rereplication via multiple mechanisms in eukaryotic cells. Genes Dev *21*, 497-518.

Asano, T., Makise, M., Takehara, M., and Mizushima, T. (2007). Interaction between ORC and Cdt1p of Saccharomyces cerevisiae. FEMS Yeast Res *7*, 1256-1262.

Baldwin, P., Laskey, R., and Coleman, N. (2003). Translational approaches to improving cervical screening. Nat Rev Cancer *3*, 217-226.

Barry, E.R., McGeoch, A.T., Kelman, Z., and Bell, S.D. (2007). Archaeal MCM has separable processivity, substrate choice and helicase domains. Nucleic Acids Res *35*, 988-998.

Beckmann, R., Bubeck, D., Grassucci, R., Penczek, P., Verschoor, A., Blobel, G., and Frank, J. (1997). Alignment of conduits for the nascent polypeptide chain in the ribosome-Sec61 complex. Science *278*, 2123-2126.

Bell, S.P. (2014). DNA Replication. Terminating the replisome. Science *346*, 418-419.

Bell, S.P., and Dutta, A. (2002). DNA replication in eukaryotic cells. Annu Rev Biochem *71*, 333-374.

Bell, S.P., Mitchell, J., Leber, J., Kobayashi, R., and Stillman, B. (1995). The multidomain structure of Orc1p reveals similarity to regulators of DNA replication and transcriptional silencing. Cell *83*, 563-568.

Bell, S.P., and Stillman, B. (1992). ATP-dependent recognition of eukaryotic origins of DNA replication by a multiprotein complex. Nature *357*, 128-134.

Bicknell, L.S., Bongers, E.M., Leitch, A., Brown, S., Schoots, J., Harley, M.E., Aftimos, S., Al-Aama, J.Y., Bober, M., Brown, P.A.*, et al.* (2011a). Mutations in the pre-replication complex cause Meier-Gorlin syndrome. Nat Genet *43*, 356-359.

Bicknell, L.S., Walker, S., Klingseisen, A., Stiff, T., Leitch, A., Kerzendorfer, C., Martin, C.A., Yeyati, P., Al Sanna, N., Bober, M.*, et al.* (2011b). Mutations in ORC1, encoding the largest subunit of the origin recognition complex, cause microcephalic primordial dwarfism resembling Meier-Gorlin syndrome. Nat Genet *43*, 350-355.

Bleichert, F., Balasov, M., Chesnokov, I., Nogales, E., Botchan, M.R., and Berger, J.M. (2013). A Meier-Gorlin syndrome mutation in a conserved C-terminal helix of Orc6 impedes origin recognition complex formation. Elife *2*, e00882.

Bleichert, F., Botchan, M.R., and Berger, J.M. (2015). Crystal structure of the eukaryotic origin recognition complex. Nature *519*, 321-326.

Bleichert, F., Botchan, M.R., and Berger, J.M. (2017). Mechanisms for initiating cellular DNA replication. Science *355*.

Bleichert, F., Leitner, A., Aebersold, R., Botchan, M.R., and Berger, J.M. (2018). Conformational control and DNA-binding mechanism of the metazoan origin recognition complex. Proc Natl Acad Sci U S A *115*, E5906-E5915.

Blow, J.J., and Laskey, R.A. (1988). A role for the nuclear envelope in controlling DNA replication within the cell cycle. Nature *332*, 546-548.

Bochman, M.L., and Schwacha, A. (2007). Differences in the single-stranded DNA binding activities of MCM2-7 and MCM467: MCM2 and MCM5 define a slow ATP-dependent step. J Biol Chem *282*, 33795-33804.

Bochman, M.L., and Schwacha, A. (2008). The Mcm2-7 complex has in vitro helicase activity. Mol Cell *31*, 287-293.

Bochman, M.L., and Schwacha, A. (2009). The Mcm complex: unwinding the mechanism of a replicative helicase. Microbiol Mol Biol Rev *73*, 652-683.

Bochman, M.L., and Schwacha, A. (2010). The Saccharomyces cerevisiae Mcm6/2 and Mcm5/3 ATPase active sites contribute to the function of the putative Mcm2-7 'gate'. Nucleic Acids Res *38*, 6078-6088.

Bongers, E.M., Opitz, J.M., Fryer, A., Sarda, P., Hennekam, R.C., Hall, B.D., Superneau, D.W., Harbison, M., Poss, A., van Bokhoven, H.*, et al.* (2001). Meier-Gorlin syndrome: report of eight additional cases and review. Am J Med Genet *102*, 115-124.

Bowers, J.L., Randell, J.C., Chen, S., and Bell, S.P. (2004). ATP hydrolysis by ORC catalyzes reiterative Mcm2-7 assembly at a defined origin of replication. Mol Cell *16*, 967-978.

Bowman, G.D., O'Donnell, M., and Kuriyan, J. (2004). Structural analysis of a eukaryotic sliding DNA clamp-clamp loader complex. Nature *429*, 724-730.

Brennan, R.G., and Matthews, B.W. (1989). The helix-turn-helix DNA binding motif. J Biol Chem *264*, 1903-1906.

Bruck, I., and Kaplan, D.L. (2015). Conserved mechanism for coordinating replication fork helicase assembly with phosphorylation of the helicase. Proc Natl Acad Sci U S A *112*, 11223-11228.

Buchan, D.W., Minneci, F., Nugent, T.C., Bryson, K., and Jones, D.T. (2013). Scalable web services for the PSIPRED Protein Analysis Workbench. Nucleic Acids Res *41*, W349-357.

Burgers, P.M.J., Gordenin, D., and Kunkel, T.A. (2016). Who Is Leading the Replication Fork, Pol epsilon or Pol delta? Mol Cell *61*, 492-493.

Cairns, J. (1966). The bacterial chromosome. Sci Am *214*, 36-44.

Callebaut, I., Courvalin, J.C., and Mornon, J.P. (1999). The BAH (bromo-adjacent homology) domain: a link between DNA methylation, replication and transcriptional regulation. FEBS Lett *446*, 189-193.

Cayrou, C., Coulombe, P., Puy, A., Rialle, S., Kaplan, N., Segal, E., and Mechali, M. (2012a). New insights into replication origin characteristics in metazoans. Cell Cycle *11*, 658-667.

Cayrou, C., Coulombe, P., Vigneron, A., Stanojcic, S., Ganier, O., Peiffer, I., Rivals, E., Puy, A., Laurent-Chabalier, S., Desprat, R.*, et al.* (2011). Genome-scale analysis of metazoan replication origins reveals their organization in specific but flexible sites defined by conserved features. Genome Res *21*, 1438-1449.

Cayrou, C., Gregoire, D., Coulombe, P., Danis, E., and Mechali, M. (2012b). Genome-scale identification of active DNA replication origins. Methods *57*, 158-164.

Chan, C.S., and Tye, B.K. (1980). Autonomously replicating sequences in Saccharomyces cerevisiae. Proc Natl Acad Sci U S A *77*, 6329-6333.

Chang, F., Riera, A., Evrin, C., Sun, J., Li, H., Speck, C., and Weinreich, M. (2015). Cdc6 ATPase activity disengages Cdc6 from the pre-replicative complex to promote DNA replication. Elife *4*.

Chen, S., and Bell, S.P. (2011). CDK prevents Mcm2-7 helicase loading by inhibiting Cdt1 interaction with Orc6. Genes Dev *25*, 363-372.

Chen, S., de Vries, M.A., and Bell, S.P. (2007). Orc6 is required for dynamic recruitment of Cdt1 during repeated Mcm2-7 loading. Genes Dev *21*, 2897-2907.

Chen, X., Zaro, J.L., and Shen, W.C. (2013). Fusion protein linkers: property, design and functionality. Adv Drug Deliv Rev *65*, 1357-1369.

Chen, Z., Speck, C., Wendel, P., Tang, C., Stillman, B., and Li, H. (2008). The architecture of the DNA replication origin recognition complex in Saccharomyces cerevisiae. Proc Natl Acad Sci U S A *105*, 10326-10331.

Cheng, Y., Grigorieff, N., Penczek, P.A., and Walz, T. (2015). A primer to single-particle cryo-electron microscopy. Cell *161*, 438-449.

Chesnokov, I., Remus, D., and Botchan, M. (2001). Functional analysis of mutant and wild-type Drosophila origin recognition complex. Proc Natl Acad Sci U S A *98*, 11997-12002.

Cheung, M., Kajimura, N., Makino, F., Ashihara, M., Miyata, T., Kato, T., Namba, K., and Blocker, A.J. (2013). A method to achieve homogeneous dispersion of large transmembrane complexes within the holes of carbon films for electron cryomicroscopy. J Struct Biol *182*, 51-56.

Clarey, M.G., Erzberger, J.P., Grob, P., Leschziner, A.E., Berger, J.M., Nogales, E., and Botchan, M. (2006). Nucleotide-dependent conformational changes in the DnaA-like core of the origin recognition complex. Nat Struct Mol Biol *13*, 684-690.

Cocker, J.H., Piatti, S., Santocanale, C., Nasmyth, K., and Diffley, J.F. (1996). An essential role for the Cdc6 protein in forming the pre-replicative complexes of budding yeast. Nature *379*, 180-182.

Cohen, B., Temple, I.K., Symons, J.C., Hall, C.M., Shaw, D.G., Bhamra, M., Jackson, A.M., and Pembrey, M.E. (1991). Microtia and short stature: a new syndrome. J Med Genet *28*, 786-790.

Cordingley, M.G., Callahan, P.L., Sardana, V.V., Garsky, V.M., and Colonno, R.J. (1990). Substrate requirements of human rhinovirus 3C protease for peptide cleavage in vitro. J Biol Chem *265*, 9062-9065.

Cortez, D., Glick, G., and Elledge, S.J. (2004). Minichromosome maintenance proteins are direct targets of the ATM and ATR checkpoint kinases. Proc Natl Acad Sci U S A *101*, 10078-10083.

Costa, A., Ilves, I., Tamberg, N., Petojevic, T., Nogales, E., Botchan, M.R., and Berger, J.M. (2011). The structural basis for MCM2-7 helicase activation by GINS and Cdc45. Nat Struct Mol Biol *18*, 471-477.

Costa, A., and Onesti, S. (2009). Structural biology of MCM helicases. Crit Rev Biochem Mol Biol *44*, 326-342.

Coster, G., and Diffley, J.F.X. (2017). Bidirectional eukaryotic DNA replication is established by quasi-symmetrical helicase loading. Science *357*, 314-318.

Coster, G., Frigola, J., Beuron, F., Morris, E.P., and Diffley, J.F. (2014). Origin licensing requires ATP binding and hydrolysis by the MCM replicative helicase. Mol Cell *55*, 666-677.

DaFonseca, C.J., Shu, F., and Zhang, J.J. (2001). Identification of two residues in MCM5 critical for the assembly of MCM complexes and Stat1-mediated transcription activation in response to IFN-gamma. Proc Natl Acad Sci U S A *98*, 3034-3039.

Davey, M.J., Indiani, C., and O'Donnell, M. (2003). Reconstitution of the Mcm2-7p heterohexamer, subunit arrangement, and ATP site architecture. J Biol Chem *278*, 4491-4499.

de Munnik, S.A., Bicknell, L.S., Aftimos, S., Al-Aama, J.Y., van Bever, Y., Bober, M.B., Clayton-Smith, J., Edrees, A.Y., Feingold, M., Fryer, A.*, et al.* (2012). Meier-Gorlin syndrome genotype-phenotype studies: 35 individuals with pre-replication complex gene mutations and 10 without molecular diagnosis. Eur J Hum Genet *20*, 598-606.

Deegan, T.D., and Diffley, J.F. (2016). MCM: one ring to rule them all. Curr Opin Struct Biol *37*, 145-151.

Deegan, T.D., Yeeles, J.T., and Diffley, J.F. (2016). Phosphopeptide binding by Sld3 links Dbf4-dependent kinase to MCM replicative helicase activation. EMBO J *35*, 961-973.

Dewar, J.M., Budzowska, M., and Walter, J.C. (2015). The mechanism of DNA replication termination in vertebrates. Nature *525*, 345-350.

Diffley, J.F. (2011). Quality control in the initiation of eukaryotic DNA replication. Philos Trans R Soc Lond B Biol Sci *366*, 3545-3553.

Diffley, J.F., Cocker, J.H., Dowell, S.J., and Rowley, A. (1994). Two steps in the assembly of complexes at yeast replication origins in vivo. Cell *78*, 303-316.

Diffley, J.F., and Stillman, B. (1988). Purification of a yeast protein that binds to origins of DNA replication and a transcriptional silencer. Proc Natl Acad Sci U S A *85*, 2120-2124.

Donovan, S., Harwood, J., Drury, L.S., and Diffley, J.F. (1997). Cdc6p-dependent loading of Mcm proteins onto pre-replicative chromatin in budding yeast. Proc Natl Acad Sci U S A *94*, 5611-5616.

Douglas, M.E., Ali, F.A., Costa, A., and Diffley, J.F.X. (2018). The mechanism of eukaryotic CMG helicase activation. Nature *555*, 265-268.

Drury, L.S., Perkins, G., and Diffley, J.F. (2000). The cyclin-dependent kinase Cdc28p regulates distinct modes of Cdc6p proteolysis during the budding yeast cell cycle. Curr Biol *10*, 231-240.

Dubochet, J., Adrian, M., Chang, J.J., Homo, J.C., Lepault, J., McDowall, A.W., and Schultz, P. (1988). Cryo-electron microscopy of vitrified specimens. Q Rev Biophys *21*, 129-228.

Dueber, E.L., Corn, J.E., Bell, S.D., and Berger, J.M. (2007). Replication origin recognition and deformation by a heterodimeric archaeal Orc1 complex. Science *317*, 1210-1213.

Duncker, B.P., Chesnokov, I.N., and McConkey, B.J. (2009). The origin recognition complex protein family. Genome Biol *10*, 214.

Duzdevich, D., Warner, M.D., Ticau, S., Ivica, N.A., Bell, S.P., and Greene, E.C. (2015). The dynamics of eukaryotic replication initiation: origin specificity, licensing, and firing at the single-molecule level. Mol Cell *58*, 483-494.

Edwards, M.C., Tutter, A.V., Cvetic, C., Gilbert, C.H., Prokhorova, T.A., and Walter, J.C. (2002). MCM2-7 complexes bind chromatin in a distributed pattern surrounding the origin recognition complex in Xenopus egg extracts. J Biol Chem *277*, 33049-33057.

Enemark, E.J., and Joshua-Tor, L. (2008). On helicases and other motor proteins. Curr Opin Struct Biol *18*, 243-257.

Erzberger, J.P., Mott, M.L., and Berger, J.M. (2006). Structural basis for ATP-dependent DnaA assembly and replication-origin remodeling. Nat Struct Mol Biol *13*, 676-683.

Evrin, C., Clarke, P., Zech, J., Lurz, R., Sun, J., Uhle, S., Li, H., Stillman, B., and Speck, C. (2009). A double-hexameric MCM2-7 complex is loaded onto origin DNA during licensing of eukaryotic DNA replication. Proc Natl Acad Sci U S A *106*, 20240-20245.

Evrin, C., Fernandez-Cid, A., Zech, J., Herrera, M.C., Riera, A., Clarke, P., Brill, S., Lurz, R., and Speck, C. (2013). In the absence of ATPase activity, pre-RC formation is blocked prior to MCM2-7 hexamer dimerization. Nucleic Acids Res *41*, 3162-3172.

Fang, D., Cao, Q., and Lou, H. (2016). Sld3-MCM Interaction Facilitated by Dbf4-Dependent Kinase Defines an Essential Step in Eukaryotic DNA Replication Initiation. Front Microbiol *7*, 885.

Ferenbach, A., Li, A., Brito-Martins, M., and Blow, J.J. (2005). Functional domains of the Xenopus replication licensing factor Cdt1. Nucleic Acids Res *33*, 316-324.

Fernandez-Cid, A., Riera, A., Tognetti, S., Herrera, M.C., Samel, S., Evrin, C., Winkler, C., Gardenal, E., Uhle, S., and Speck, C. (2013). An ORC/Cdc6/MCM2-7 complex is formed in a multistep reaction to serve as a platform for MCM double-hexamer assembly. Mol Cell *50*, 577-588.

Ferreira, M.F., Santocanale, C., Drury, L.S., and Diffley, J.F. (2000). Dbf4p, an essential S phase-promoting factor, is targeted for degradation by the anaphase-promoting complex. Mol Cell Biol *20*, 242-248.

Findeisen, M., El-Denary, M., Kapitza, T., Graf, R., and Strausfeld, U. (1999). Cyclin A-dependent kinase activity affects chromatin binding of ORC, Cdc6, and MCM in egg extracts of Xenopus laevis. Eur J Biochem *264*, 415-426.

Forsburg, S.L. (2004). Eukaryotic MCM proteins: beyond replication initiation. Microbiol Mol Biol Rev *68*, 109-131.

Francis, L.I., Randell, J.C., Takara, T.J., Uchima, L., and Bell, S.P. (2009). Incorporation into the prereplicative complex activates the Mcm2-7 helicase for Cdc7-Dbf4 phosphorylation. Genes Dev *23*, 643-654.

Frigola, J., Remus, D., Mehanna, A., and Diffley, J.F. (2013). ATPase-dependent quality control of DNA replication origin licensing. Nature *495*, 339-343.

Froelich, C.A., Kang, S., Epling, L.B., Bell, S.P., and Enemark, E.J. (2014). A conserved MCM single-stranded DNA binding element is essential for replication initiation. Elife *3*, e01993.

Frolova, N.S., Schek, N., Tikhmyanova, N., and Coleman, T.R. (2002). Xenopus Cdc6 performs separate functions in initiating DNA replication. Mol Biol Cell *13*, 1298-1312.

Fujita, M. (2006). Cdt1 revisited: complex and tight regulation during the cell cycle and consequences of deregulation in mammalian cells. Cell Div *1*, 22.

Gajiwala, K.S., and Burley, S.K. (2000). Winged helix proteins. Curr Opin Struct Biol *10*, 110-116.

Gambus, A., Jones, R.C., Sanchez-Diaz, A., Kanemaki, M., van Deursen, F., Edmondson, R.D., and Labib, K. (2006). GINS maintains association of Cdc45 with MCM in replisome progression complexes at eukaryotic DNA replication forks. Nat Cell Biol *8*, 358-366.

Gambus, A., Khoudoli, G.A., Jones, R.C., and Blow, J.J. (2011). MCM2-7 form double hexamers at licensed origins in Xenopus egg extract. J Biol Chem *286*, 11855-11864.

Georgescu, R., Yuan, Z., Bai, L., de Luna Almeida Santos, R., Sun, J., Zhang, D., Yurieva, O., Li, H., and O'Donnell, M.E. (2017). Structure of eukaryotic CMG helicase at a replication fork and implications to replisome architecture and origin initiation. Proc Natl Acad Sci U S A *114*, E697-E706.

Gillespie, P.J., and Blow, J.J. (2000). Nucleoplasmin-mediated chromatin remodelling is required for Xenopus sperm nuclei to become licensed for DNA replication. Nucleic Acids Res *28*, 472-480.

Gillespie, P.J., Li, A., and Blow, J.J. (2001). Reconstitution of licensed replication origins on Xenopus sperm nuclei using purified proteins. BMC Biochem *2*, 15.

Giordano-Coltart, J., Ying, C.Y., Gautier, J., and Hurwitz, J. (2005). Studies of the properties of human origin recognition complex and its Walker A motif mutants. Proc Natl Acad Sci U S A *102*, 69-74.

Gonzalez, M.A., Tachibana, K.E., Laskey, R.A., and Coleman, N. (2005). Control of DNA replication and its potential clinical exploitation. Nat Rev Cancer *5*, 135-141.

Goujon, M., McWilliam, H., Li, W., Valentin, F., Squizzato, S., Paern, J., and Lopez, R. (2010). A new bioinformatics analysis tools framework at EMBL-EBI. Nucleic Acids Res *38*, W695-699.

Grassucci, R.A., Taylor, D.J., and Frank, J. (2007). Preparation of macromolecular complexes for cryo-electron microscopy. Nat Protoc *2*, 3239-3246.

Green, B.M., Finn, K.J., and Li, J.J. (2010). Loss of DNA replication control is a potent inducer of gene amplification. Science *329*, 943-946.

Harami, G.M., Gyimesi, M., and Kovacs, M. (2013). From keys to bulldozers: expanding roles for winged helix domains in nucleic-acid-binding proteins. Trends Biochem Sci *38*, 364-371.

Hartwell, L.H. (1973). Three additional genes required for deoxyribonucleic acid synthesis in Saccharomyces cerevisiae. J Bacteriol *115*, 966-974.

Head, B.M., Rubinstein, E., and Meyers, A.F. (2016). Alternative pre-approved and novel therapies for the treatment of anthrax. BMC Infect Dis *16*, 621.

Hedglin, M., Kumar, R., and Benkovic, S.J. (2013). Replication clamps and clamp loaders. Cold Spring Harb Perspect Biol *5*, a010165.

Heller, R.C., Kang, S., Lam, W.M., Chen, S., Chan, C.S., and Bell, S.P. (2011). Eukaryotic origin-dependent DNA replication in vitro reveals sequential action of DDK and S-CDK kinases. Cell *146*, 80-91.

Hemerly, A.S., Prasanth, S.G., Siddiqui, K., and Stillman, B. (2009). Orc1 controls centriole and centrosome copy number in human cells. Science *323*, 789-793.

Herbig, U., Marlar, C.A., and Fanning, E. (1999). The Cdc6 nucleotide-binding site regulates its activity in DNA replication in human cells. Mol Biol Cell *10*, 2631-2645.

Herrera, M.C., Tognetti, S., Riera, A., Zech, J., Clarke, P., Fernandez-Cid, A., and Speck, C. (2015). A reconstituted system reveals how activating and inhibitory interactions control DDK dependent assembly of the eukaryotic replicative helicase. Nucleic Acids Res *43*, 10238-10250.

Hiraiwa, A., Fujita, M., Nagasaka, T., Adachi, A., Ohashi, M., and Ishibashi, M. (1997). Immunolocalization of hCDC47 protein in normal and neoplastic human tissues and its relation to growth. Int J Cancer *74*, 180-184.

Hofmann, J.F., and Beach, D. (1994). cdt1 is an essential target of the Cdc10/Sct1 transcription factor: requirement for DNA replication and inhibition of mitosis. EMBO J *13*, 425-434.

Hoggard, T., Shor, E., Muller, C.A., Nieduszynski, C.A., and Fox, C.A. (2013). A Link between ORC-origin binding mechanisms and origin activation time revealed in budding yeast. PLoS Genet *9*, e1003798.

Honeycutt, K.A., Chen, Z., Koster, M.I., Miers, M., Nuchtern, J., Hicks, J., Roop, D.R., and Shohet, J.M. (2006). Deregulated minichromosomal maintenance

protein MCM7 contributes to oncogene driven tumorigenesis. Oncogene *25*, 4027-4032.

Hoshina, S., Yura, K., Teranishi, H., Kiyasu, N., Tominaga, A., Kadoma, H., Nakatsuka, A., Kunichika, T., Obuse, C., and Waga, S. (2013). Human origin recognition complex binds preferentially to G-quadruplex-preferable RNA and single-stranded DNA. J Biol Chem *288*, 30161-30171.

Hsiao, C.L., and Carbon, J. (1979). High-frequency transformation of yeast by plasmids containing the cloned yeast ARG4 gene. Proc Natl Acad Sci U S A *76*, 3829-3833.

Huang, H., Stromme, C.B., Saredi, G., Hodl, M., Strandsby, A., Gonzalez-Aguilera, C., Chen, S., Groth, A., and Patel, D.J. (2015). A unique binding mode enables MCM2 to chaperone histones H3-H4 at replication forks. Nat Struct Mol Biol *22*, 618-626.

Huberman, J.A., and Riggs, A.D. (1966). Autoradiography of chromosomal DNA fibers from Chinese hamster cells. Proc Natl Acad Sci U S A *55*, 599-606.

Huberman, J.A., and Riggs, A.D. (1968). On the mechanism of DNA replication in mammalian chromosomes. J Mol Biol *32*, 327-341.

Hyrien, O., and Mechali, M. (1993). Chromosomal replication initiates and terminates at random sequences but at regular intervals in the ribosomal DNA of Xenopus early embryos. EMBO J *12*, 4511-4520.

Ibarra, A., Schwob, E., and Mendez, J. (2008). Excess MCM proteins protect human cells from replicative stress by licensing backup origins of replication. Proc Natl Acad Sci U S A *105*, 8956-8961.

Ilves, I., Petojevic, T., Pesavento, J.J., and Botchan, M.R. (2010). Activation of the MCM2-7 helicase by association with Cdc45 and GINS proteins. Mol Cell *37*, 247-258.

Ioannou, C., Schaeffer, P.M., Dixon, N.E., and Soultanas, P. (2006). Helicase binding to DnaI exposes a cryptic DNA-binding site during helicase loading in Bacillus subtilis. Nucleic Acids Res *34*, 5247-5258.

Ishimi, Y., Komamura-Kohno, Y., Kwon, H.J., Yamada, K., and Nakanishi, M. (2003). Identification of MCM4 as a target of the DNA replication block checkpoint system. J Biol Chem *278*, 24644-24650.

Iyer, L.M., Leipe, D.D., Koonin, E.V., and Aravind, L. (2004). Evolutionary history and higher order classification of AAA+ ATPases. J Struct Biol *146*, 11-31.

Jackson, A.P., Laskey, R.A., and Coleman, N. (2014). Replication proteins and human disease. Cold Spring Harb Perspect Biol *6*.

Jacob, F., and Brenner, S. (1963). [On the regulation of DNA synthesis in bacteria: the hypothesis of the replicon]. C R Hebd Seances Acad Sci *256*, 298-300.

Jee, J., Mizuno, T., Kamada, K., Tochio, H., Chiba, Y., Yanagi, K., Yasuda, G., Hiroaki, H., Hanaoka, F., and Shirakawa, M. (2010). Structure and mutagenesis studies of the C-terminal region of licensing factor Cdt1 enable the identification of key residues for binding to replicative helicase Mcm proteins. J Biol Chem *285*, 15931-15940.

Jenkinson, E.R., and Chong, J.P. (2006). Minichromosome maintenance helicase activity is controlled by N- and C-terminal motifs and requires the ATPase domain helix-2 insert. Proc Natl Acad Sci U S A *103*, 7613-7618.

Johnson, R.E., Klassen, R., Prakash, L., and Prakash, S. (2015). A Major Role of DNA Polymerase delta in Replication of Both the Leading and Lagging DNA Strands. Mol Cell *59*, 163-175.

Kaguni, J.M. (2011). Replication initiation at the Escherichia coli chromosomal origin. Curr Opin Chem Biol *15*, 606-613.

Kanemaki, M., and Labib, K. (2006). Distinct roles for Sld3 and GINS during establishment and progression of eukaryotic DNA replication forks. EMBO J *25*, 1753-1763.

Kang, H.Y., Choi, E., Bae, S.H., Lee, K.H., Gim, B.S., Kim, H.D., Park, C., MacNeill, S.A., and Seo, Y.S. (2000). Genetic analyses of Schizosaccharomyces pombe dna2(+) reveal that dna2 plays an essential role in Okazaki fragment metabolism. Genetics *155*, 1055-1067.

Kang, S., Kang, M.S., Ryu, E., and Myung, K. (2018). Eukaryotic DNA replication: Orchestrated action of multi-subunit protein complexes. Mutat Res *809*, 58-69.

Kang, S., Warner, M.D., and Bell, S.P. (2014). Multiple functions for Mcm2-7 ATPase motifs during replication initiation. Mol Cell *55*, 655-665.

Karata, K., Inagawa, T., Wilkinson, A.J., Tatsuta, T., and Ogura, T. (1999). Dissecting the role of a conserved motif (the second region of homology) in the AAA family of ATPases. Site-directed mutagenesis of the ATP-dependent protease FtsH. J Biol Chem *274*, 26225-26232.

Katayama, T., Kubota, T., Kurokawa, K., Crooke, E., and Sekimizu, K. (1998). The initiator function of DnaA protein is negatively regulated by the sliding clamp of the E. coli chromosomal replicase. Cell *94*, 61-71.

Khayrutdinov, B.I., Bae, W.J., Yun, Y.M., Lee, J.H., Tsuyama, T., Kim, J.J., Hwang, E., Ryu, K.S., Cheong, H.K., Cheong, C.*, et al.* (2009). Structure of the Cdt1 C-terminal domain: conservation of the winged helix fold in replication licensing factors. Protein Sci *18*, 2252-2264.

Kim, J., and Kipreos, E.T. (2008). Control of the Cdc6 replication licensing factor in metazoa: the role of nuclear export and the CUL4 ubiquitin ligase. Cell Cycle *7*, 146-150.

Klemm, R.D., Austin, R.J., and Bell, S.P. (1997). Coordinate binding of ATP and origin DNA regulates the ATPase activity of the origin recognition complex. Cell *88*, 493-502.

Klemm, R.D., and Bell, S.P. (2001). ATP bound to the origin recognition complex is important for preRC formation. Proc Natl Acad Sci U S A *98*, 8361-8367.

Kolodner, R.D., Putnam, C.D., and Myung, K. (2002). Maintenance of genome stability in Saccharomyces cerevisiae. Science *297*, 552-557.

Kuhlbrandt, W. (2014). Cryo-EM enters a new era. Elife *3*, e03678.

Kukimoto, I., Aihara, S., Yoshiike, K., and Kanda, T. (1998). Human papillomavirus oncoprotein E6 binds to the C-terminal region of human minichromosome maintenance 7 protein. Biochem Biophys Res Commun *249*, 258-262.

Kuo, A.J., Song, J., Cheung, P., Ishibe-Murakami, S., Yamazoe, S., Chen, J.K., Patel, D.J., and Gozani, O. (2012). The BAH domain of ORC1 links H4K20me2 to DNA replication licensing and Meier-Gorlin syndrome. Nature *484*, 115-119.

Labib, K., Diffley, J.F., and Kearsey, S.E. (1999). G1-phase and B-type cyclins exclude the DNA-replication factor Mcm4 from the nucleus. Nat Cell Biol *1*, 415-422.

Larkin, M.A., Blackshields, G., Brown, N.P., Chenna, R., McGettigan, P.A., McWilliam, H., Valentin, F., Wallace, I.M., Wilm, A., Lopez, R.*, et al.* (2007). Clustal W and Clustal X version 2.0. Bioinformatics *23*, 2947-2948.

Lee, C., Hong, B., Choi, J.M., Kim, Y., Watanabe, S., Ishimi, Y., Enomoto, T., Tada, S., Kim, Y., and Cho, Y. (2004). Structural basis for inhibition of the replication licensing factor Cdt1 by geminin. Nature *430*, 913-917.

Lee, D.G., and Bell, S.P. (1997). Architecture of the yeast origin recognition complex bound to origins of DNA replication. Mol Cell Biol *17*, 7159-7168.

Lee, K.Y., Bang, S.W., Yoon, S.W., Lee, S.H., Yoon, J.B., and Hwang, D.S. (2012). Phosphorylation of ORC2 protein dissociates origin recognition complex from chromatin and replication origins. J Biol Chem *287*, 11891-11898.

Leonard, A.C., and Mechali, M. (2013). DNA replication origins. Cold Spring Harb Perspect Biol *5*, a010116.

Li, H., and Stillman, B. (2012). The origin recognition complex: a biochemical and structural view. Subcell Biochem *62*, 37-58.

Li, N., Lam, W.H., Zhai, Y., Cheng, J., Cheng, E., Zhao, Y., Gao, N., and Tye, B.K. (2018). Structure of the origin recognition complex bound to DNA replication origin. Nature *559*, 217-222.

Li, N., Zhai, Y., Zhang, Y., Li, W., Yang, M., Lei, J., Tye, B.K., and Gao, N. (2015). Structure of the eukaryotic MCM complex at 3.8 A. Nature *524*, 186-191.

Liang, C., and Stillman, B. (1997). Persistent initiation of DNA replication and chromatin-bound MCM proteins during the cell cycle in cdc6 mutants. Genes Dev *11*, 3375-3386.

Liku, M.E., Nguyen, V.Q., Rosales, A.W., Irie, K., and Li, J.J. (2005). CDK phosphorylation of a novel NLS-NES module distributed between two subunits of the Mcm2-7 complex prevents chromosomal rereplication. Mol Biol Cell *16*, 5026-5039.

Linskens, M.H., and Huberman, J.A. (1988). Organization of replication of ribosomal DNA in Saccharomyces cerevisiae. Mol Cell Biol *8*, 4927-4935.

Lipford, J.R., and Bell, S.P. (2001). Nucleosomes positioned by ORC facilitate the initiation of DNA replication. Mol Cell *7*, 21-30.

Liu, C., Wu, R., Zhou, B., Wang, J., Wei, Z., Tye, B.K., Liang, C., and Zhu, G. (2012). Structural insights into the Cdt1-mediated MCM2-7 chromatin loading. Nucleic Acids Res *40*, 3208-3217.

Liu, E., Lee, A.Y., Chiba, T., Olson, E., Sun, P., and Wu, X. (2007). The ATR-mediated S phase checkpoint prevents rereplication in mammalian cells when licensing control is disrupted. J Cell Biol *179*, 643-657.

Liu, J., Smith, C.L., DeRyckere, D., DeAngelis, K., Martin, G.S., and Berger, J.M. (2000). Structure and function of Cdc6/Cdc18: implications for origin recognition and checkpoint control. Mol Cell *6*, 637-648.

Liu, S., Balasov, M., Wang, H., Wu, L., Chesnokov, I.N., and Liu, Y. (2011). Structural analysis of human Orc6 protein reveals a homology with transcription factor TFIIB. Proc Natl Acad Sci U S A *108*, 7373-7378.

Looke, M., Maloney, M.F., and Bell, S.P. (2017). Mcm10 regulates DNA replication elongation by stimulating the CMG replicative helicase. Genes Dev *31*, 291-305.

Ludlam, A.V., McNatt, M.W., Carr, K.M., and Kaguni, J.M. (2001). Essential amino acids of Escherichia coli DnaC protein in an N-terminal domain interact with DnaB helicase. J Biol Chem *276*, 27345-27353.

Lyubimov, A.Y., Costa, A., Bleichert, F., Botchan, M.R., and Berger, J.M. (2012). ATP-dependent conformational dynamics underlie the functional asymmetry of the replicative helicase from a minimalist eukaryote. Proc Natl Acad Sci U S A *109*, 11999-12004.

Madine, M.A., Swietlik, M., Pelizon, C., Romanowski, P., Mills, A.D., and Laskey, R.A. (2000). The roles of the MCM, ORC, and Cdc6 proteins in determining the replication competence of chromatin in quiescent cells. J Struct Biol *129*, 198-210.

Maine, G.T., Sinha, P., and Tye, B.K. (1984). Mutants of S. cerevisiae defective in the maintenance of minichromosomes. Genetics *106*, 365-385.

Maiorano, D., Moreau, J., and Mechali, M. (2000). XCDT1 is required for the assembly of pre-replicative complexes in Xenopus laevis. Nature *404*, 622-625.

Marahrens, Y., and Stillman, B. (1992). A yeast chromosomal origin of DNA replication defined by multiple functional elements. Science *255*, 817-823.

Maric, M., Maculins, T., De Piccoli, G., and Labib, K. (2014). Cdc48 and a ubiquitin ligase drive disassembly of the CMG helicase at the end of DNA replication. Science *346*, 1253596.

Masai, H., Matsumoto, S., You, Z., Yoshizawa-Sugata, N., and Oda, M. (2010). Eukaryotic chromosome DNA replication: where, when, and how? Annu Rev Biochem *79*, 89-130.

Masai, H., You, Z., and Arai, K. (2005). Control of DNA replication: regulation and activation of eukaryotic replicative helicase, MCM. IUBMB Life *57*, 323-335.

McDowall, A.W., Chang, J.J., Freeman, R., Lepault, J., Walter, C.A., and Dubochet, J. (1983). Electron microscopy of frozen hydrated sections of vitreous ice and vitrified biological samples. J Microsc *131*, 1-9.

McIntosh, D., and Blow, J.J. (2012). Dormant origins, the licensing checkpoint, and the response to replicative stresses. Cold Spring Harb Perspect Biol *4*.

Mechali, M. (2001). DNA replication origins: from sequence specificity to epigenetics. Nat Rev Genet *2*, 640-645.

Mechali, M., and Kearsey, S. (1984). Lack of specific sequence requirement for DNA replication in Xenopus eggs compared with high sequence specificity in yeast. Cell *38*, 55-64.

Mendez, J., and Stillman, B. (2000). Chromatin association of human origin recognition complex, cdc6, and minichromosome maintenance proteins during the cell cycle: assembly of prereplication complexes in late mitosis. Mol Cell Biol *20*, 8602-8612.

Miller, J.M., Arachea, B.T., Epling, L.B., and Enemark, E.J. (2014). Analysis of the crystal structure of an active MCM hexamer. Elife *3*, e03433.

Miyata, T., Suzuki, H., Oyama, T., Mayanagi, K., Ishino, Y., and Morikawa, K. (2005). Open clamp structure in the clamp-loading complex visualized by electron microscopic image analysis. Proc Natl Acad Sci U S A *102*, 13795-13800.

Moldovan, G.L., Pfander, B., and Jentsch, S. (2007). PCNA, the maestro of the replication fork. Cell *129*, 665-679.

Moreno, S.P., Bailey, R., Campion, N., Herron, S., and Gambus, A. (2014). Polyubiquitylation drives replisome disassembly at the termination of DNA replication. Science *346*, 477-481.

Moyer, S.E., Lewis, P.W., and Botchan, M.R. (2006). Isolation of the Cdc45/Mcm2-7/GINS (CMG) complex, a candidate for the eukaryotic DNA replication fork helicase. Proc Natl Acad Sci U S A *103*, 10236-10241.

Murata, K., and Wolf, M. (2018). Cryo-electron microscopy for structural analysis of dynamic biological macromolecules. Biochim Biophys Acta *1862*, 324-334.

Muzi-Falconi, M., and Kelly, T.J. (1995). Orp1, a member of the Cdc18/Cdc6 family of S-phase regulators, is homologous to a component of the origin recognition complex. Proc Natl Acad Sci U S A *92*, 12475-12479.

Neuwald, A.F., Aravind, L., Spouge, J.L., and Koonin, E.V. (1999). AAA+: A class of chaperone-like ATPases associated with the assembly, operation, and disassembly of protein complexes. Genome Res *9*, 27-43.

Nguyen, V.Q., Co, C., Irie, K., and Li, J.J. (2000). Clb/Cdc28 kinases promote nuclear export of the replication initiator proteins Mcm2-7. Curr Biol *10*, 195-205.

Nguyen, V.Q., Co, C., and Li, J.J. (2001). Cyclin-dependent kinases prevent DNA re-replication through multiple mechanisms. Nature *411*, 1068-1073.

Nick McElhinny, S.A., Gordenin, D.A., Stith, C.M., Burgers, P.M., and Kunkel, T.A. (2008). Division of labor at the eukaryotic replication fork. Mol Cell *30*, 137-144.

Nieduszynski, C.A., Knox, Y., and Donaldson, A.D. (2006). Genome-wide identification of replication origins in yeast by comparative genomics. Genes Dev *20*, 1874-1879.

Nishitani, H., Lygerou, Z., Nishimoto, T., and Nurse, P. (2000). The Cdt1 protein is required to license DNA for replication in fission yeast. Nature *404*, 625-628.

Nitani, N., Yadani, C., Yabuuchi, H., Masukata, H., and Nakagawa, T. (2008). Mcm4 C-terminal domain of MCM helicase prevents excessive formation of single-stranded DNA at stalled replication forks. Proc Natl Acad Sci U S A *105*, 12973-12978.

Noguchi, Y., Yuan, Z., Bai, L., Schneider, S., Zhao, G., Stillman, B., Speck, C., and Li, H. (2017). Cryo-EM structure of Mcm2-7 double hexamer on DNA suggests a lagging-strand DNA extrusion model. Proc Natl Acad Sci U S A *114*, E9529-E9538.

O'Donnell, M., Langston, L., and Stillman, B. (2013). Principles and concepts of DNA replication in bacteria, archaea, and eukarya. Cold Spring Harb Perspect Biol *5*.

Ogura, T., Whiteheart, S.W., and Wilkinson, A.J. (2004). Conserved arginine residues implicated in ATP hydrolysis, nucleotide-sensing, and inter-subunit interactions in AAA and AAA+ ATPases. J Struct Biol *146*, 106-112.

Pavlov, Y.I., Shcherbakova, P.V., and Kunkel, T.A. (2001). In vivo consequences of putative active site mutations in yeast DNA polymerases alpha, epsilon, delta, and zeta. Genetics *159*, 47-64.

Perkins, G., and Diffley, J.F. (1998). Nucleotide-dependent prereplicative complex assembly by Cdc6p, a homolog of eukaryotic and prokaryotic clamp-loaders. Mol Cell *2*, 23-32.

Perkins, G., Drury, L.S., and Diffley, J.F. (2001). Separate SCF(CDC4) recognition elements target Cdc6 for proteolysis in S phase and mitosis. EMBO J *20*, 4836-4845.

Prasanth, S.G., Shen, Z., Prasanth, K.V., and Stillman, B. (2010). Human origin recognition complex is essential for HP1 binding to chromatin and heterochromatin organization. Proc Natl Acad Sci U S A *107*, 15093-15098.

Pucci, B., De Felice, M., Rocco, M., Esposito, F., De Falco, M., Esposito, L., Rossi, M., and Pisani, F.M. (2007). Modular organization of the Sulfolobus solfataricus mini-chromosome maintenance protein. J Biol Chem *282*, 12574-12582.

Pursell, Z.F., Isoz, I., Lundstrom, E.B., Johansson, E., and Kunkel, T.A. (2007). Yeast DNA polymerase epsilon participates in leading-strand DNA replication. Science *317*, 127-130.

Randell, J.C., Bowers, J.L., Rodriguez, H.K., and Bell, S.P. (2006). Sequential ATP hydrolysis by Cdc6 and ORC directs loading of the Mcm2-7 helicase. Mol Cell *21*, 29-39.

Randell, J.C., Fan, A., Chan, C., Francis, L.I., Heller, R.C., Galani, K., and Bell, S.P. (2010). Mec1 is one of multiple kinases that prime the Mcm2-7 helicase for phosphorylation by Cdc7. Mol Cell *40*, 353-363.

Rao, H., and Stillman, B. (1995). The origin recognition complex interacts with a bipartite DNA binding site within yeast replicators. Proc Natl Acad Sci U S A *92*, 2224-2228.

Remus, D., Beall, E.L., and Botchan, M.R. (2004). DNA topology, not DNA sequence, is a critical determinant for Drosophila ORC-DNA binding. EMBO J *23*, 897-907.

Remus, D., Beuron, F., Tolun, G., Griffith, J.D., Morris, E.P., and Diffley, J.F. (2009). Concerted loading of Mcm2-7 double hexamers around DNA during DNA replication origin licensing. Cell *139*, 719-730.

Remus, D., Blanchette, M., Rio, D.C., and Botchan, M.R. (2005). CDK phosphorylation inhibits the DNA-binding and ATP-hydrolysis activities of the Drosophila origin recognition complex. J Biol Chem *280*, 39740-39751.

Rialland, M., Sola, F., and Santocanale, C. (2002). Essential role of human CDT1 in DNA replication and chromatin licensing. J Cell Sci *115*, 1435-1440.

Richet, N., Liu, D., Legrand, P., Velours, C., Corpet, A., Gaubert, A., Bakail, M., Moal-Raisin, G., Guerois, R., Compper, C.*, et al.* (2015). Structural insight into how the human helicase subunit MCM2 may act as a histone chaperone together with ASF1 at the replication fork. Nucleic Acids Res *43*, 1905-1917.

Riera, A., Barbon, M., Noguchi, Y., Reuter, L.M., Schneider, S., and Speck, C. (2017). From structure to mechanism-understanding initiation of DNA replication. Genes Dev *31*, 1073-1088.

Riera, A., Tognetti, S., and Speck, C. (2014). Helicase loading: how to build a MCM2-7 double-hexamer. Semin Cell Dev Biol *30*, 104-109.

Romanowski, P., Madine, M.A., Rowles, A., Blow, J.J., and Laskey, R.A. (1996). The Xenopus origin recognition complex is essential for DNA replication and MCM binding to chromatin. Curr Biol *6*, 1416-1425.

Rowley, A., Cocker, J.H., Harwood, J., and Diffley, J.F. (1995). Initiation complex assembly at budding yeast replication origins begins with the recognition of a bipartite sequence by limiting amounts of the initiator, ORC. EMBO J *14*, 2631-2641.

Saha, P., Chen, J., Thome, K.C., Lawlis, S.J., Hou, Z.H., Hendricks, M., Parvin, J.D., and Dutta, A. (1998). Human CDC6/Cdc18 associates with Orc1 and cyclin-cdk and is selectively eliminated from the nucleus at the onset of S phase. Mol Cell Biol *18*, 2758-2767.

Samel, S.A., Fernandez-Cid, A., Sun, J., Riera, A., Tognetti, S., Herrera, M.C., Li, H., and Speck, C. (2014). A unique DNA entry gate serves for regulated loading of the eukaryotic replicative helicase MCM2-7 onto DNA. Genes Dev *28*, 1653-1666.

Samson, R.Y., Abeyrathne, P.D., and Bell, S.D. (2016). Mechanism of Archaeal MCM Helicase Recruitment to DNA Replication Origins. Mol Cell *61*, 287-296.

Scheffzek, K., Ahmadian, M.R., Kabsch, W., Wiesmuller, L., Lautwein, A., Schmitz, F., and Wittinghofer, A. (1997). The Ras-RasGAP complex: structural basis for GTPase activation and its loss in oncogenic Ras mutants. Science *277*, 333-338.

Schepers, A., and Diffley, J.F. (2001). Mutational analysis of conserved sequence motifs in the budding yeast Cdc6 protein. J Mol Biol *308*, 597-608.

Scheres, S.H. (2012). RELION: implementation of a Bayesian approach to cryo-EM structure determination. J Struct Biol *180*, 519-530.

Schwacha, A., and Bell, S.P. (2001). Interactions between two catalytically distinct MCM subgroups are essential for coordinated ATP hydrolysis and DNA replication. Mol Cell *8*, 1093-1104.

Seo, Y.S., and Kang, Y.H. (2018). The Human Replicative Helicase, the CMG Complex, as a Target for Anti-cancer Therapy. Front Mol Biosci *5*, 26.

Sheu, Y.J., and Stillman, B. (2006). Cdc7-Dbf4 phosphorylates MCM proteins via a docking site-mediated mechanism to promote S phase progression. Mol Cell *24*, 101-113.

Sheu, Y.J., and Stillman, B. (2010). The Dbf4-Cdc7 kinase promotes S phase by alleviating an inhibitory activity in Mcm4. Nature *463*, 113-117.

Shima, N., Alcaraz, A., Liachko, I., Buske, T.R., Andrews, C.A., Munroe, R.J., Hartford, S.A., Tye, B.K., and Schimenti, J.C. (2007a). A viable allele of Mcm4 causes chromosome instability and mammary adenocarcinomas in mice. Nat Genet *39*, 93-98.

Shima, N., Buske, T.R., and Schimenti, J.C. (2007b). Genetic screen for chromosome instability in mice: Mcm4 and breast cancer. Cell Cycle *6*, 1135-1140.

Shukla, A.K., Westfield, G.H., Xiao, K., Reis, R.I., Huang, L.Y., Tripathi-Shukla, P., Qian, J., Li, S., Blanc, A., Oleskie, A.N.*, et al.* (2014). Visualization of arrestin recruitment by a G-protein-coupled receptor. Nature *512*, 218-222.

Siddiqui, K., On, K.F., and Diffley, J.F. (2013). Regulating DNA replication in eukarya. Cold Spring Harb Perspect Biol *5*.

Simon, N.E., and Schwacha, A. (2014). The Mcm2-7 replicative helicase: a promising chemotherapeutic target. Biomed Res Int *2014*, 549719.

Soultanas, P. (2012). Loading mechanisms of ring helicases at replication origins. Mol Microbiol *84*, 6-16.

Speck, C., Chen, Z., Li, H., and Stillman, B. (2005). ATPase-dependent cooperative binding of ORC and Cdc6 to origin DNA. Nat Struct Mol Biol *12*, 965-971.

Speck, C., and Stillman, B. (2007). Cdc6 ATPase activity regulates ORC x Cdc6 stability and the selection of specific DNA sequences as origins of DNA replication. J Biol Chem *282*, 11705-11714.

Sterner, J.M., Dew-Knight, S., Musahl, C., Kornbluth, S., and Horowitz, J.M. (1998). Negative regulation of DNA replication by the retinoblastoma protein is mediated by its association with MCM7. Mol Cell Biol *18*, 2748-2757.

Stinchcomb, D.T., Struhl, K., and Davis, R.W. (1979). Isolation and characterisation of a yeast chromosomal replicator. Nature *282*, 39-43.

Stinchcomb, D.T., Thomas, M., Kelly, J., Selker, E., and Davis, R.W. (1980). Eukaryotic DNA segments capable of autonomous replication in yeast. Proc Natl Acad Sci U S A *77*, 4559-4563.

Stoeber, K., Swinn, R., Prevost, A.T., de Clive-Lowe, P., Halsall, I., Dilworth, S.M., Marr, J., Turner, W.H., Bullock, N., Doble, A.*, et al.* (2002). Diagnosis of

genito-urinary tract cancer by detection of minichromosome maintenance 5 protein in urine sediments. J Natl Cancer Inst *94*, 1071-1079.

Stoeber, K., Tlsty, T.D., Happerfield, L., Thomas, G.A., Romanov, S., Bobrow, L., Williams, E.D., and Williams, G.H. (2001). DNA replication licensing and human cell proliferation. J Cell Sci *114*, 2027-2041.

Struhl, K., Stinchcomb, D.T., Scherer, S., and Davis, R.W. (1979). High-frequency transformation of yeast: autonomous replication of hybrid DNA molecules. Proc Natl Acad Sci U S A *76*, 1035-1039.

Sun, J., Evrin, C., Samel, S.A., Fernandez-Cid, A., Riera, A., Kawakami, H., Stillman, B., Speck, C., and Li, H. (2013). Cryo-EM structure of a helicase loading intermediate containing ORC-Cdc6-Cdt1-MCM2-7 bound to DNA. Nat Struct Mol Biol *20*, 944-951.

Sun, J., Fernandez-Cid, A., Riera, A., Tognetti, S., Yuan, Z., Stillman, B., Speck, C., and Li, H. (2014). Structural and mechanistic insights into Mcm2-7 double-hexamer assembly and function. Genes Dev *28*, 2291-2303.

Sun, J., Kawakami, H., Zech, J., Speck, C., Stillman, B., and Li, H. (2012). Cdc6-induced conformational changes in ORC bound to origin DNA revealed by cryo-electron microscopy. Structure *20*, 534-544.

Sun, J., Shi, Y., Georgescu, R.E., Yuan, Z., Chait, B.T., Li, H., and O'Donnell, M.E. (2015). The architecture of a eukaryotic replisome. Nat Struct Mol Biol *22*, 976-982.

Sun, W.H., Coleman, T.R., and DePamphilis, M.L. (2002). Cell cycle-dependent regulation of the association between origin recognition proteins and somatic cell chromatin. EMBO J *21*, 1437-1446.

Symeonidou, I.E., Taraviras, S., and Lygerou, Z. (2012). Control over DNA replication in time and space. FEBS Lett *586*, 2803-2812.

Tada, S., Li, A., Maiorano, D., Mechali, M., and Blow, J.J. (2001). Repression of origin assembly in metaphase depends on inhibition of RLF-B/Cdt1 by geminin. Nat Cell Biol *3*, 107-113.

Takahashi, N., Tsutsumi, S., Tsuchiya, T., Stillman, B., and Mizushima, T. (2002). Functions of sensor 1 and sensor 2 regions of Saccharomyces cerevisiae Cdc6p in vivo and in vitro. J Biol Chem *277*, 16033-16040.

Takara, T.J., and Bell, S.P. (2011). Multiple Cdt1 molecules act at each origin to load replication-competent Mcm2-7 helicases. EMBO J *30*, 4885-4896.

Tanaka, S., and Araki, H. (2010). Regulation of the initiation step of DNA replication by cyclin-dependent kinases. Chromosoma *119*, 565-574.

Tanaka, S., and Diffley, J.F. (2002). Interdependent nuclear accumulation of budding yeast Cdt1 and Mcm2-7 during G1 phase. Nat Cell Biol *4*, 198-207.

Tanaka, S., Umemori, T., Hirai, K., Muramatsu, S., Kamimura, Y., and Araki, H. (2007). CDK-dependent phosphorylation of Sld2 and Sld3 initiates DNA replication in budding yeast. Nature *445*, 328-332.

Tanaka, T., Knapp, D., and Nasmyth, K. (1997). Loading of an Mcm protein onto DNA replication origins is regulated by Cdc6p and CDKs. Cell *90*, 649-660.

Tanaka, T., Umemori, T., Endo, S., Muramatsu, S., Kanemaki, M., Kamimura, Y., Obuse, C., and Araki, H. (2011). Sld7, an Sld3-associated protein required for efficient chromosomal DNA replication in budding yeast. EMBO J *30*, 2019-2030.

Thomae, A.W., Baltin, J., Pich, D., Deutsch, M.J., Ravasz, M., Zeller, K., Gossen, M., Hammerschmidt, W., and Schepers, A. (2011). Different roles of the human Orc6 protein in the replication initiation process. Cell Mol Life Sci *68*, 3741-3756.

Thompson, R.F., Walker, M., Siebert, C.A., Muench, S.P., and Ranson, N.A. (2016). An introduction to sample preparation and imaging by cryo-electron microscopy for structural biology. Methods *100*, 3-15.

Ticau, S., Friedman, L.J., Champasa, K., Correa, I.R., Jr., Gelles, J., and Bell, S.P. (2017). Mechanism and timing of Mcm2-7 ring closure during DNA replication origin licensing. Nat Struct Mol Biol *24*, 309-315.

Ticau, S., Friedman, L.J., Ivica, N.A., Gelles, J., and Bell, S.P. (2015). Single-molecule studies of origin licensing reveal mechanisms ensuring bidirectional helicase loading. Cell *161*, 513-525.

Tocilj, A., On, K.F., Yuan, Z., Sun, J., Elkayam, E., Li, H., Stillman, B., and Joshua-Tor, L. (2017). Structure of the active form of human origin recognition complex and its ATPase motor module. Elife *6*.

Todorov, I.T., Werness, B.A., Wang, H.Q., Buddharaju, L.N., Todorova, P.D., Slocum, H.K., Brooks, J.S., and Huberman, J.A. (1998). HsMCM2/BM28: a novel proliferation marker for human tumors and normal tissues. Lab Invest *78*, 73-78.

Tsai, K.L., Lo, Y.H., Sun, Y.J., and Hsiao, C.D. (2009). Molecular interplay between the replicative helicase DnaC and its loader protein DnaI from Geobacillus kaustophilus. J Mol Biol *393*, 1056-1069.

Tsakraklides, V., and Bell, S.P. (2010). Dynamics of pre-replicative complex assembly. J Biol Chem *285*, 9437-9443.

Tsao, C.C., Geisen, C., and Abraham, R.T. (2004). Interaction between human MCM7 and Rad17 proteins is required for replication checkpoint signaling. EMBO J *23*, 4660-4669.

Tye, B.K. (1999). Minichromosome maintenance as a genetic assay for defects in DNA replication. Methods *18*, 329-334.

Ullah, R., Shah, M.A., Tufail, S., Ismat, F., Imran, M., Iqbal, M., Mirza, O., and Rhaman, M. (2016). Activity of the Human Rhinovirus 3C Protease Studied in Various Buffers, Additives and Detergents Solutions for Recombinant Protein Production. PLoS One *11*, e0153436.

Vedadi, M., Niesen, F.H., Allali-Hassani, A., Fedorov, O.Y., Finerty, P.J., Jr., Wasney, G.A., Yeung, R., Arrowsmith, C., Ball, L.J., Berglund, H.*, et al.* (2006). Chemical screening methods to identify ligands that promote protein stability, protein crystallization, and structure determination. Proc Natl Acad Sci U S A *103*, 15835-15840.

Wang, B., Feng, L., Hu, Y., Huang, S.H., Reynolds, C.P., Wu, L., and Jong, A.Y. (1999). The essential role of Saccharomyces cerevisiae CDC6 nucleotide-binding site in cell growth, DNA synthesis, and Orc1 association. J Biol Chem *274*, 8291-8298.

Waugh, D.S. (2011). An overview of enzymatic reagents for the removal of affinity tags. Protein Expr Purif *80*, 283-293.

Wei, Z., Liu, C., Wu, X., Xu, N., Zhou, B., Liang, C., and Zhu, G. (2010). Characterization and structure determination of the Cdt1 binding domain of human minichromosome maintenance (Mcm) 6. J Biol Chem *285*, 12469-12473.

Weinreich, M., and Stillman, B. (1999). Cdc7p-Dbf4p kinase binds to chromatin during S phase and is regulated by both the APC and the RAD53 checkpoint pathway. EMBO J *18*, 5334-5346.

Wiedemann, C., Szambowska, A., Hafner, S., Ohlenschlager, O., Guhrs, K.H., and Gorlach, M. (2015). Structure and regulatory role of the C-terminal winged helix domain of the archaeal minichromosome maintenance complex. Nucleic Acids Res *43*, 2958-2967.

Wohlschlegel, J.A., Dwyer, B.T., Dhar, S.K., Cvetic, C., Walter, J.C., and Dutta, A. (2000). Inhibition of eukaryotic DNA replication by geminin binding to Cdt1. Science *290*, 2309-2312.

Woodward, A.M., Gohler, T., Luciani, M.G., Oehlmann, M., Ge, X., Gartner, A., Jackson, D.A., and Blow, J.J. (2006). Excess Mcm2-7 license dormant origins of replication that can be used under conditions of replicative stress. J Cell Biol *173*, 673-683.

Wu, R., Wang, J., and Liang, C. (2012). Cdt1p, through its interaction with Mcm6p, is required for the formation, nuclear accumulation and chromatin loading of the MCM complex. J Cell Sci *125*, 209-219.

Wyrick, J.J., Aparicio, J.G., Chen, T., Barnett, J.D., Jennings, E.G., Young, R.A., Bell, S.P., and Aparicio, O.M. (2001). Genome-wide distribution of ORC and MCM proteins in S. cerevisiae: high-resolution mapping of replication origins. Science *294*, 2357-2360.

Yanagi, K., Mizuno, T., You, Z., and Hanaoka, F. (2002). Mouse geminin inhibits not only Cdt1-MCM6 interactions but also a novel intrinsic Cdt1 DNA binding activity. J Biol Chem *277*, 40871-40880.

Yao, N.Y., and O'Donnell, M. (2012). The RFC clamp loader: structure and function. Subcell Biochem *62*, 259-279.

Yeeles, J.T., Deegan, T.D., Janska, A., Early, A., and Diffley, J.F. (2015). Regulated eukaryotic DNA replication origin firing with purified proteins. Nature *519*, 431-435.

Yeeles, J.T.P., Janska, A., Early, A., and Diffley, J.F.X. (2017). How the Eukaryotic Replisome Achieves Rapid and Efficient DNA Replication. Mol Cell *65*, 105-116.

Young, C.L., Britton, Z.T., and Robinson, A.S. (2012). Recombinant protein expression and purification: a comprehensive review of affinity tags and microbial applications. Biotechnol J *7*, 620-634.

Yuan, Z., Bai, L., Sun, J., Georgescu, R., Liu, J., O'Donnell, M.E., and Li, H. (2016). Structure of the eukaryotic replicative CMG helicase suggests a pumpjack motion for translocation. Nat Struct Mol Biol *23*, 217-224.

Yuan, Z., Riera, A., Bai, L., Sun, J., Nandi, S., Spanos, C., Chen, Z.A., Barbon, M., Rappsilber, J., Stillman, B.*, et al.* (2017). Structural basis of Mcm2-7 replicative helicase loading by ORC-Cdc6 and Cdt1. Nat Struct Mol Biol *24*, 316-324.

Zegerman, P., and Diffley, J.F. (2007). Phosphorylation of Sld2 and Sld3 by cyclin-dependent kinases promotes DNA replication in budding yeast. Nature *445*, 281-285.

Zellner, E., Herrmann, T., Schulz, C., and Grummt, F. (2007). Site-specific interaction of the murine pre-replicative complex with origin DNA: assembly and

disassembly during cell cycle transit and differentiation. Nucleic Acids Res *35*, 6701-6713.

Zhai, Y., Cheng, E., Wu, H., Li, N., Yung, P.Y., Gao, N., and Tye, B.K. (2017a). Open-ringed structure of the Cdt1-Mcm2-7 complex as a precursor of the MCM double hexamer. Nat Struct Mol Biol *24*, 300-308.

Zhai, Y., Li, N., Jiang, H., Huang, X., Gao, N., and Tye, B.K. (2017b). Unique Roles of the Non-identical MCM Subunits in DNA Replication Licensing. Mol Cell *67*, 168-179.

Zhang, J., Yu, L., Wu, X., Zou, L., Sou, K.K., Wei, Z., Cheng, X., Zhu, G., and Liang, C. (2010). The interacting domains of hCdt1 and hMcm6 involved in the chromatin loading of the MCM complex in human cells. Cell Cycle *9*, 4848-4857.

Zou, L., and Stillman, B. (2000). Assembly of a complex containing Cdc45p, replication protein A, and Mcm2p at replication origins controlled by S-phase cyclin-dependent kinases and Cdc7p-Dbf4p kinase. Mol Cell Biol *20*, 3086-3096.